

# **CHARACTERISATION OF INFLAMMATORY RESPONSES IN TWO MODELS OF EXPERIMENTAL ISCHAEMIA**

Louise Marks, April 2001

A thesis submitted for the degree of Doctor of Philosophy to the Faculty  
of Medicine, University of Glasgow.

Wellcome Surgical Institute and Hugh Fraser Neuroscience Laboratories, University  
of Glasgow, Bearsden Road, Glasgow, G61 1QH.



**UNIVERSITY**  
*of*  
**GLASGOW**

ProQuest Number: 13833994

All rights reserved

INFORMATION TO ALL USERS

The quality of this reproduction is dependent upon the quality of the copy submitted.

In the unlikely event that the author did not send a complete manuscript and there are missing pages, these will be noted. Also, if material had to be removed, a note will indicate the deletion.



ProQuest 13833994

Published by ProQuest LLC (2019). Copyright of the Dissertation is held by the Author.

All rights reserved.

This work is protected against unauthorized copying under Title 17, United States Code  
Microform Edition © ProQuest LLC.

ProQuest LLC.  
789 East Eisenhower Parkway  
P.O. Box 1346  
Ann Arbor, MI 48106 – 1346

GLASGOW  
UNIVERSITY  
LIBRARY:

12372

COPY 1

## **Contents**

<b>Title page</b>	<b>page I</b>
<b>Contents</b>	<b>page II</b>
<b>List of tables</b>	<b>page VIII</b>
<b>List of figures</b>	<b>page IX</b>
<b>Abbreviations</b>	<b>page XIV</b>
<b>Acknowledgements</b>	<b>page XVI</b>
<b>Authors declaration</b>	<b>page XVII</b>
<b>Summary</b>	<b>page XVIII</b>
<b>Chapter 1. Introduction</b>	<b>page 1</b>
1.1 Stroke Background	page 1
1.1.1 Stroke facts and figures	page 1
1.1.2 Ischaemia and stroke	page 1
<b>1.2 Classification of stroke</b>	<b>page 2</b>
1.2.1 Haemorrhagic stroke	page 3
1.2.2 Ischaemic stroke	page 3
<b>1.3 Models of cerebral ischaemia</b>	<b>page 4</b>
1.3.1 Use of the rat as a model of cerebral ischaemia	page 4
1.3.2 Rat models of experimental ischaemia	page 7
1.3.3 Models of permanent middle cerebral artery occlusion	page 9
1.3.4 Models of transient focal ischaemia	page 12

1.3.5 Models of global ischaemia	page 16
1.3.6 The spontaneously hypertensive stroke prone rat as a model of cerebrovascular disease	page 18
<b>1.4 Ischaemic events</b>	<b>page 19</b>
1.4.1 Reperfusion injury	page 21
1.4.2 Excitotoxicity and ischaemia	page 22
1.4.3 Inflammation and ischaemia	page 23
1.4.3.1 Neutrophils	page 26
1.4.3.2 Microglia	page 31
1.4.3.3 Matrix metalloproteinases	page 48
1.4.3.4 Free radicals	page 72
1.4.3.5 Calcium	page 79
<b>Chapter 2 Materials and methods</b>	<b>page 81</b>
<b>2.1 Surgical procedures</b>	<b>page 81</b>
2.1.1 Preparation of animals for surgery	page 81
2.1.2 Intraluminal thread model of ischaemia	page 82
2.1.3 Permanent ischaemia by electrocoagulation	page 85
2.1.4 LPS stereotaxic injections	page 86
2.1.5 Recovery of animals following surgery	page 87
2.2 Processing of tissue for H&E and immunohistochemistry	page 88
2.2.1 Fixation	page 88
2.2.2 Post fixation	page 90

2.2.3 Cutting cryostat sections	page 90
2.2.4 Paraffin processing	page 91
2.2.5 Infarct determination	page 91
2.2.5.1 Haematoxylin & eosin	page 91
2.2.5.2 Detection of ischaemic neurons	page 92
2.2.5.3 Measuring of infarct size	page 94
2.2.6 Immunohistochemistry	page 96
2.2.6.1 On cryostat cut sections	page 96
2.2.6.2 Dehydration and counterstaining	page 98
2.2.6.3 On paraffin sections	page 98
2.2.6.4 Double label immunohistochemistry	page 99
2.2.6.5 Fluorescence labelling	page 101
2.2.7 Controls for immunohistochemistry	page 102
2.3 Western blotting	page 102
2.3.1 Mini gels	page 102
2.3.2 Protein determination	page 103
2.3.3 Running of gels	page 104
2.3.4 Optical density measurements	page 106
2.4 Scanning Electron Microscopy	page 106
2.4.1 Fixation	page 106
2.4.2 Processing of tissue	page 107
2.4.3 Developing of films	page 109

<b>Results : Chapter 3. Microvilli/ Neutrophil Study</b>	<b>page 110</b>
3.1 Introduction	page 110
<b>3.2 Materials and Methods</b>	<b>page 112</b>
3.2.1 Surgical procedures	page 112
3.2.2 Neutrophil adherence/ accumulation	page 113
3.2.3 Ultrastructural changes	page 113
3.2.4 Statistical analysis	page 114
<b>3.3 Results</b>	<b>page 114</b>
3.3.1 Physiological variables	page 114
3.3.2 Extent of ischaemic damage	page 116
3.3.3 Neutrophil adhesion	page 117
3.3.4 Microvilli counts	page 118
3.3.5 Ultrastructural changes to MCA	page 124
<b>3.4 Discussion</b>	<b>page 125</b>
<b>Results: Chapter 4. Matrix Metalloproteinase Study</b>	<b>page 136</b>
<b>4.1 Introduction</b>	<b>page 136</b>
<b>4.2 Materials and methods</b>	<b>page 138</b>
4.2.1 Surgical procedures	page 138
4.2.2 Infarct determination	page 139
4.2.3 Western blotting	page 139
4.2.4 Immunohistochemistry	page 139
4.2.5 Double label immunohistochemistry	page 140
4.2.6 Blocking peptide control	page 141

4.2.7 Distribution and quantification of staining	page 141
4.2.8 Statistical analysis	page 142
<b>4.3 Results</b>	<b>page 143</b>
4.3.1 Physiological variables	page 143
4.3.2 Infarct size	page 143
4.3.3 Western blotting- mini gels	page 145
4.3.4 Distribution and cellular location of MMP-9	page 149
4.3.5 Distribution and cellular location of MMP-8	page 156
4.3.6 Specificity of neuronal staining	page 159
4.3.7 BBB permeability and MMP staining	page 161
<b>4.4 Discussion</b>	<b>page 163</b>
<b>Results: Chapter 5. SHRSP / WKY Microglial Study</b>	<b>page 173</b>
<b>5.1 Introduction</b>	<b>page 173</b>
<b>5.2 Materials and methods</b>	<b>page 176</b>
5.2.1 Surgical procedures	page 177
5.2.2 Infarct determination	page 177
5.2.3 Neutrophil counts	page 178
5.2.4 Immunohistochemistry	page 179
5.2.5 Quantification of staining	page 179
5.2.6 Statistical analysis	page 181
<b>5.3 Results</b>	<b>page 182</b>
5.3.1 Physiological parameters	page 182
5.3.2 Infarct size	page 182

5.3.3 Neutrophil counts	page 186
5.3.4 Characterisation of microglial activation	page 186
5.3.5 Distribution of microglia	page 187
5.3.6 Microglial counts	page 189
5.3.7 Strain differences	page 189
5.3.8 Correlation graphs	page 197
5.3.8 naïve controls	page 197
<b>5.4 Discussion</b>	<b>page 201</b>
<b>Results: Chapter 6 SHRSP/WKY Time Course Study</b>	<b>page 208</b>
<b>6.1 Introduction</b>	<b>page 208</b>
<b>6.2 Materials and methods</b>	<b>page 209</b>
6.2.1 Assessment of brain swelling	page 209
<b>6.3 Results</b>	<b>page 210</b>
6.3.1 Physiological variables	page 210
6.3.2 Evolution of infarct over 72-hour time course	page 210
6.3.3 Tissue Swelling	page 213
6.3.4 Microglial counts in brain regions	page 215
6.3.5 Characterisation of microglial response	page 225
6.3.6 Microglial distribution maps	page 228
6.3.7 Characterisation of MMP-8 /MMP-9 staining	page 232
6.3.8 Distribution maps for MMP staining	page 239
6.3.9 Characterisation of IL-1 $\beta$ staining	page 244
<b>6.4 Discussion</b>	<b>page 246</b>

<b>Chapter 7 General Discussion</b>	<b>page 257</b>
7.1 Introduction	page 257
7.2 Microvilli and neutrophils in ischaemic damage	page 258
7.3 Microglia in inflammatory mediated ischaemic damage	page 261
7.4 MMP-8 and MMP-9 in ischaemic damage	page 264
7.5 General conclusions	page 265
<b>References</b>	<b>page 267</b>
<b>Publications</b>	<b>page 299</b>
<b>Appendices</b>	<b>page I-VII</b>

**List of tables**

1. Role of cytokines in the proliferation of microglia	page 38
2. Involvement of microglia in other pathological conditions	page 46
3. Antibodies against microglia	page 47
4. The matrix metalloproteinases family	page 51
5. MMP localisation within cell types	page 58
6. MMP studies using various animal models of experimental ischaemia	page 63
7. Physiological variables for scanning electron microscopy	page 114
8. Number of microvilli per $25\mu\text{m}^2$ in ILT induced ischaemia	page 121
9. Physiological variables for 24 hour ILT induced ischaemia	page 144
10. Physiological variables for 24 hour permanent MCAO	page 183
11. Physiological variables for time course study of permanent MCAO	page 211

## List of Figures

1. Arrangement of the blood vessels in the Circle of Willis	page 5
2. Infarction rate is determined by the site and location of the area of electrocoagulation	page 10
3. Intraluminal thread induced ischaemia	page 13
4. Events following ischaemia	page 20
5. Inflammatory time scale following ischaemia	page 25
6. Steps of neutrophil migration	page 27
7. Stages of microglial activation	page 34
8. The migration of cells	page 39
9. Structure of the extracellular matrix	page 50
10. MMP structure	page 53
11. Activation of MMPs	page 56
12. Free radical involvement in ischaemia and reperfusion	page 74
13. a. Haber Weiss reaction, b. iron catalyses OH production, c. Fenton reaction.	page 75
14. Involvement of calcium in reperfusion injury	page 80
15. Intraluminal thread model of ischaemia	page 83
16. Permanent middle cerebral artery occlusion by electrocoagulation	page 85
17. Haematoxylin and eosin staining	page 92
18. Morphology of ischaemic neurons	page 93
19. Line diagram representing the eight coronal levels	page 95
20. Processing of tissue for Scanning Electron Microscopy	page 108
21. Microvilli in a control non-ischaemic vessel in the cortex	page 111
22. Volume of ischaemic damage for intraluminal thread induced ischaemia.	page 116
23. Lack of neutrophil accumulation in parenchymal vessels or MCAs	page 117
24. Microvilli in parenchymal cortical vessels	page 118
25. Number of microvilli per $25\mu\text{m}^2$ in cortical parenchymal blood vessels	page 119
26. Number of microvilli in small and large vessels	page 120
27. Microvilli distribution and number in parenchymal cortical vessels	page 122

28. Correlation between the number of microvilli in parenchymal cortical vessels and infarct size	page 123
29. Ultrastructural changes to ipsilateral MCA	page 124
30. Extent of ischaemic damage following 24 -hour transient intraluminal thread induced ischaemia	page 145
31. Graph for Lowry protein assay	page 146
32. Western blots for MMP-9 antibody AB805	page 147
33. Optical density graphs for western blots	page 148
34. Distribution of MMP-9 staining	page 149
35. Photographs representing cellular staining of MMP-9	page 151
36. Representative MMP-9 cytosolic staining as present in the contralateral hemisphere of occluded animals and throughout sham sections	page 150
37. Double labelling with DAB/SG	page 153
38. Confocal images representing microglial staining observed with MMP-9	page 154
39. MMP expression in oligodendrocytes	page 155
40. Distribution of MMP-8 staining	page 156
41. Photographs representing cellular staining of MMP-8	page 158
42. Double labelling with DAB/SG	page 157
43. MMP-9 Santa Cruz antibody staining with blocking peptide	page 160
44. PAP immunoreactivity following ILT induced ischaemia	page 161
45. Staining of extravasated serum proteins following ILT induced ischaemia	page 162
46. Characteristic neutrophil morphology	page 178
47. Regions of interest for microglial counts	page 180
48. Microglial phenotype	page 180
49. Ischaemic damage following 24 hour permanent MCAO	page 184
50. Composite line diagrams of topography of the infarct and of activated microglial densities	page 185
51. Distribution and morphology of microglial cells in grey and white matter of both hemispheres of SHRSP following distal electrocoagulation of the MCA	page 188

52. Mean counts of activated microglia per mm<sup>2</sup> in the brain regions examined page 190
53. Activated microglial numbers for peri-infarct region in the ipsilateral and equivalent region in the contralateral hemisphere page 191
54. Activated microglial numbers for cingulate cortex region in ipsilateral and contralateral hemispheres page 192
55. Activated microglial numbers for infarct core in ipsilateral equivalent region in the contralateral hemisphere page 193
56. Activated microglial numbers for external capsule region in ipsilateral and contralateral hemispheres page 194
57. Activated microglial numbers for genu corpus callosum in ipsilateral and contralateral hemispheres page 195
58. Strain differences between microglial numbers in SHRSP Vs WKY page 196
59. Correlation graphs for SHRSP and WKY – ischaemic damage Vs number of activated microglia at the level of the lateral septal nucleus in the peri-infarct and core regions page 198
60. Mean counts of microglia per mm<sup>2</sup> in naïve animals page 199
61. Representative images of activated and resting microglia in grey and white matter of a naïve SHRSP rat page 200
62. Evolution of the infarct over 72 hours in SHRSP and WKY page 212
63. Tissue swelling in SHRSP and WKY over 72 hours page 214
64. Counts of activated microglia in WKY and SHRSP over 72 hours page 219
65. Microglial counts in WKY Vs SHRSP in the infarct core following permanent MCAO page 220
66. Microglial counts in WKY Vs SHRSP in the cingulate cortex following permanent MCAO page 221
67. Microglial counts in WKY Vs SHRSP in the external capsule following permanent MCAO page 222
68. Microglial counts in WKY Vs SHRSP in the peri-infarct region following permanent MCAO page 223
69. Microglial counts in WKY Vs SHRSP in the infarct core following

permanent MCAO	page 224
70. Microglia in the peri-infarct region following 4 hours permanent MCAO	page 225
71. Microglia in the peri-infarct region following 24 hours permanent MCAO	page 226
72. Microglia in the peri-infarct region following 48 hours permanent MCAO	page 227
73. Microglia in the peri-infarct region following 72 hours permanent MCAO	page 228
74. Microglial distribution maps for SHRSP 4- 72 hours	page 230
75. Microglial distribution maps for WKY 4- 72 hours	page 231
76. Activated microglial and phagocytic microglia forming a boundary around the infarct core	page 229
77. MMP-8 staining 4 hours following permanent MCAO within the region of ischaemic damage	page 232
78. MMP-8 staining 24 hours following permanent MCAO within the infarct core	page 234
79. MMP-8 staining 48 hours following permanent MCAO within the infarct core	page 235
80. MMP-8 staining in neurons within the peri-infarct region at 48 hours following permanent MCAO	page 236
81. MMP-8 staining 72 hours following permanent MCAO within the infarct core	page 237
82. Lack of MMP-9 staining in astrocytes and evidence of staining in oligodendrocytes at 24 hours following permanent MCAO	page 238
83. MMP distribution in SHRSP and WKY at 4 hours following permanent MCAO	page 240
84. MMP distribution in SHRSP and WKY at 24 hours following permanent MCAO	page 241
85. MMP distribution in SHRSP and WKY at 48 hours following permanent MCAO	page 242
86. MMP distribution in SHRSP and WKY at 72 hours following permanent MCAO	page 243

87. IL-1 $\beta$  staining

page 244

88. Lack of IL-1 $\beta$  staining in WKY and SHRSP following MCAO

page 245

## Abbreviations

ACA	Anterior Cerebral Artery
AD	Alzheimer's Disease
AIDS	Acquired Autoimmune Deficiency Syndrome
AMPA	Alpha amino-3-hydroxy-5 methyl-4 isoxazole propionic acid
APP	Amyloid Precursor Protein
BBB	Blood Brain Barrier
BSA	Bovine Serum Albumin
CCA	Common Carotid Artery
CNS	Central Nervous System
ECA	External Carotid Artery
ECM	Extracellular Matrix
FGF	Fibroblast Growth Factor
GMCSF	Granulocyte- Macrophage Colony Stimulating Factor
HMDS	Hexamethyldisilazane
ICA	Internal Carotid Artery
ICV	Inferior Cerebral Vein
IL-1-8	Interleukin 1-8
LPS	Lipopolysaccharide
LTB4	Leukotriene B4
MCA	Middle Cerebral Artery
MCAO	Middle Cerebral Artery Occlusion
MCSF	Microglial Colony Stimulating Factor

MHC	Major Histocompatibility Complex
MMP	Matrix Metalloproteinase
MRF-1	Microglial Response Factor
MS	Multiple Sclerosis
NMDA	N-methyl D-aspartate
NO	Nitric Oxide
OD	Optical Density
PBS	Phosphate Buffered Saline
PCA	Posterior Cerebral Artery
PCR	Polymerase Chain Reaction
PNS	Peripheral Nervous System
QTL	Quantitative Trait Loci
RA	Rheumatoid Arthritis
SEM	Scanning Electron Microscope
SHR	Spontaneously Hypertensive Rat
SHRSP	Spontaneously Hypertensive Stroke Prone Rat
TBS	Tris-Base Buffer
TGF	Transforming Growth Factor
TIMP	Tissue Inhibitor of Matrix Metalloproteinase
TNF- $\alpha$	Tumour Necrosis Factor- alpha
TPA	Tissue Plasminogen Activator
T-TBS	Tris buffered saline + 0.1% Tween 20.
T-TBS-M	Tris buffered saline + 0.1% Tween 20 + 0.5% defatted milk.
WKY	Wistar Kyoto Rat

## Acknowledgements

I would like to thank everyone at the Wellcome Surgical Institute, past and present, for their help, support and friendship over the last three years. In particular I would like to thank my supervisor Dr Mhairi Macrae for her continued support and words of wisdom and Dr Hilary Carswell for her guidance and teaching throughout my PhD. I would like to thank Dr Elaine Peters for her patience and for guiding me through many complicated procedures with ease and a sense of humour! I'd also like to thank the technicians at the Wellcome again for their patience in helping me in my times of need especially Mrs Lindsay Gallacher whose help in theatre was invaluable; British Biotech for their generous gift of MMP antibodies and funding over my three years and lastly Fiona White, Jill Fowler, Dr Eileen McCracken and all the new recruits in the PhD office for their support and for many a laugh. Thanks to Craig for all his support, even when I was being unbearably neurotic and for his computing knowledge, which got me out of a number of scary situations!

Lastly I would like to take this opportunity to thank my parents for their support and for their unfaltering faith in me throughout my time at University. I greatly appreciate everything they have done for me and would like to dedicate this thesis to them.

## **Declaration**

This thesis comprises my own work, unless otherwise acknowledged, and has not previously been presented for a degree in any other form.

Louise Marks April 2001.

## Summary

Stroke is one of the leading causes of death and disability throughout the world with limited effective therapies currently available. It is therefore an important and deserving area for experimental research. The mechanisms underlying the damage associated with stroke are very complex and include excitotoxicity and oxidative stress as well as a number of inflammatory mediated mechanisms which ultimately leads to both necrotic and apoptotic cell death.

An inflammatory response can occur within minutes of an ischaemic insult and has been well documented. The response is proposed to involve resident inflammatory cells of the brain such as microglia and circulating inflammatory cells such as macrophages and neutrophils. Although numbers of inflammatory cells have been reported to increase under ischaemic conditions, opinion remains divided as to what the exact role of these cells are in ischaemic damage and whether these roles are beneficial or detrimental.

This thesis examined the role of the circulating inflammatory cell the neutrophil, the brain's resident inflammatory cell the microglia and the inflammatory mediators IL-1 $\beta$ , rat neutrophil collagenase (MMP-8) and gelatinase B (MMP-9) in experimental models of middle cerebral artery occlusion in the rat to gain a better understanding of their roles in ischaemic damage.

The role of the neutrophil in inflammatory mediated ischaemic damage was examined in two models of focal ischaemia- 1) the intraluminal thread model of transient middle cerebral artery occlusion (2 hours occlusion + 2 or 22 hours

reperfusion ) and 2) the diathermy model of permanent middle cerebral artery occlusion (4-72 hours).

This study found no evidence for significant neutrophil accumulation in the parenchyma or adherence to cerebral blood vessels in acute focal cerebral ischaemia using scanning electron microscopy and light microscopy in either Sprague Dawley rats (intraluminal thread) or Spontaneously Hypertensive Stroke Prone Rats (SHRSP) (diathermy model) up to 72 hours post ischaemia.

It has been reported that neutrophil accumulation following ischaemia can result in the impairment of blood flow and damage via the release of cytotoxic substances.

Some groups have reported significant neutrophil accumulation in models of experimental ischaemia and have demonstrated significant reductions in ischaemic damage upon administration of antibodies designed to prevent neutrophil adhesion to the endothelium of blood vessels. However in accordance with the findings of this study, some groups have also failed to show significant neutrophil accumulation in the same models of experimental ischaemia, suggesting that they may not be major contributors to acute ischaemic damage.

In addition to neutrophil accumulation, this thesis also considered the possible pathogenic role of microglia in ischaemic damage. Microglial activation was examined in the diathermy model of permanent middle cerebral artery occlusion in the SHRSP and their normotensive reference strain the Wistar Kyoto (WKY).

Quantitative analysis of the microglial response to focal cerebral ischaemia in the SHRSP and WKY revealed three major points: 1) SHRSP displayed increases in the numbers of activated microglia associated with the site of injury compared to the

WKY reference strain between 4 and 72 hours. These differences were most significant at 24 hours post ischaemia and within the peri-infarct zone. At 24 hours the infarct is still evolving and so the presence of activated microglia in the peri-infarct region may suggest a role for the cells in the expansion of the infarct; 2) activated microglia were found to express MMP-8 and MMP-9, known contributors to the pathology of a number of inflammatory conditions and 3) under normal, non-ischaemic conditions, SHRSP also displayed a greater density of microglia, especially in the white matter tracts compared to WKY rats.

This is an important study as it is the first to measure the evolution of the infarct in the SHRSP and investigate the inflammatory response over 72 hours. The greater degree of microglial activation in the SHRSP may be representative of the enhanced inflammatory response to ischaemia previously reported in this strain with the increased microglial activation possibly contributing to the genetically determined stroke sensitivity of the SHRSP.

Microglia are known to become activated in conditions of ischaemia and have been reported to either contribute to ischaemic damage via the release of cytotoxic substances or to promote recovery and prevent further damage by inducing re-growth and repair via phagocytosis and the release of growth factors.

Therefore, the findings of this study are important both in terms of improving our understanding of genetically determined stroke sensitivity and of the role of inflammatory cells in focal cerebral ischaemia, two research areas associated with many unresolved questions and opposing views.

In addition to the role of inflammatory cells in ischaemic damage, this thesis also examined other possible contributors to inflammatory mediated ischaemic damage. This included examining ultrastructural changes to the vasculature of parenchymal blood vessels to determine whether any changes were apparent which may be contributing to ischaemic damage.

Scanning electron microscopy was used to examine the ultrastructure of the vasculature following 2 hours intraluminal thread induced ischaemia plus 2 hours of reperfusion in Sprague Dawley rats. Increased endothelial microvilli numbers (previously reported to increase in conditions of brain trauma and ischaemia) were observed in the blood vessels of the parenchyma following intraluminal thread induced ischaemia. However similar changes were also observed in sham animals suggesting that microvilli formation may be primarily due to the trauma associated with the induction of ischaemia, rather than to the ischaemia *per se*.

Levels of IL-1 $\beta$  and matrix metalloproteinases (MMP-8 and MMP-9), believed to be contributors to ischaemic damage were also examined to map their distribution and cellular location and gain a better understanding of their role in inflammatory mediated ischaemic damage. This study found no evidence for IL-1 $\beta$  expression following either intraluminal thread induced ischaemia (24 hours) or following diathermy induced permanent ischaemia (up to 72 hours). MMP-8 and MMP-9 were found to be expressed by activated microglia in both models of ischaemia from 4-72 hours, in oligodendrocytes (4-72 hours) and in neurons (24-72 hours). No MMP expression was found in astrocytes at any of the time points studied.

The presence of MMP-8 and MMP-9 in activated microglia suggests a role for the MMPs in mediating the microglial response to ischaemia be it beneficial or detrimental.

# Chapter 1. Introduction

## 1.1 Stroke Background

### 1.1.1 Stroke facts and figures

Stroke is one of the largest causes of death in the world, with the loss of brain function from stroke being the primary cause of adult disability in the United States and accounting for 12% of deaths in the United Kingdom (Bamford *et al.*, 1988). Around three million Americans are currently disabled as a result of an ischaemic insult to the brain and 500,000 patients in the United Kingdom are being cared for in acute National Health Service and long term beds (Forbes, 1993). Despite the severity of the problem and the drain on health resources, no therapy is currently licensed in the UK and other than thrombolytic agents (T-PA), no existing therapy has the ability to significantly reduce neurological disability. Therefore experimental research in the field of stroke is widespread and focuses on gaining a better understanding of the complicated mechanisms behind this debilitating disorder in order to identify potential therapies.

### 1.1.2 Ischaemia and stroke

The brain requires a constant supply of blood to meet its high metabolic demands and allow normal healthy function, in turn allowing proper control and regulation of the whole body. Severe reductions in the flow of blood within the brain, ischaemia,

are very poorly tolerated and if maintained give rise to the symptoms of clinical stroke. The reduced blood flow to the brain during ischaemia results in an insufficient supply of nutrients for cell survival.

Cerebral ischaemia can be divided into global and focal ischaemia. In global ischaemia, the blood supply to the entire brain is reduced, normally as a result of complete cardiac arrest or severe peripheral haemorrhage, whilst in focal ischaemia blood supply is reduced in a particular region of the brain due to the blockade of a blood vessel supplying that brain region.

Cerebral ischaemia can be defined as complete or incomplete depending on the severity of the reduction in blood flow. Complete ischaemia is defined as a total absence of cerebral blood flow to either the entire brain or a particular brain region. Incomplete ischaemia is defined as a drastic reduction in cerebral blood flow in either a global or focal pattern (Siegel *et al.*, 1976 ).

## **1.2 Classification of Stroke**

Stroke can be classed as either ischaemic or haemorrhagic depending on the mechanism by which blood flow to the brain is reduced.

Ischaemic stroke can be further subdivided into embolic and thrombotic stroke while haemorrhagic stroke occurs as either an intracerebral haemorrhage or a subarachnoid haemorrhage.

Ischaemic stroke is more prevalent than haemorrhagic stroke, accounting for around 80% of stroke occurrences in the USA while haemorrhagic stroke constitutes around 15-20% of stroke cases (McAuley, 1995).

### **1.2.1 Haemorrhagic stroke**

Haemorrhagic stroke occurs when a blood vessel within the cerebral vasculature ruptures, normally as a result of recurring high blood pressure or due to the presence of an aneurysm or weakening of the blood vessel wall. There are different types of haemorrhagic stroke- an intracerebral haemorrhage normally results from hypertension mediated bleeding from blood vessels within the brain, and subarachnoid or subdural haemorrhage which are normally caused by the rupture of an aneurysm (often congenital) resulting in blood collecting under the arachnoid membrane (subarachnoid) or under the dural membrane (subdural).

### **1.2.2 Ischaemic stroke**

In ischaemic stroke, the blood supply to a particular part of the brain is reduced (focal ischaemia) by the presence of a blood clot or embolus in the cerebral vasculature supplying that particular region. If the clot has its origins out with the brain, and travels to the cerebral vessel via the bloodstream, this is classed as an embolic stroke. If however the blood supply to the brain is impaired due to narrowing and occlusion of the blood vessel calibre by thrombus formation in

arteries supplying the brain, then this is classed as a thrombotic stroke. A thrombus is an unwanted formation consisting of a 'head' of platelets and leukocytes in a fibrin mesh and a 'tail' consisting of a diffuse fibrin network capable of trapping blood cells. A thrombus can form in an artery or a vein and can break up, dispersing fragments of thrombus which can travel in the bloodstream to the brain where they may occlude cerebral blood vessels resulting in ischaemia.

### **1.3 Models of Cerebral Ischaemia**

#### **1.3.1 Use of the rat as a model of cerebral ischaemia**

Although many different species have been used to develop animal models of experimental ischaemia, the rat is the most frequently used.

Similarities between rat and human cerebrovasculature make the rat model of ischaemia an important research tool.

In both rat and man, the brain is supplied by the internal carotid and vertebral arteries.

The internal carotid arteries supply the cerebrum, while the vertebral arteries and basilar artery supply the rest of the brain and part of the cerebrum (Lee, 1995)

The main arteries connect at the base of the brain to form the Circle of Willis, with the paired anterior, middle and posterior cerebral arteries branching off from the Circle of Willis (Lee *et al.*, 1995) (Figure 1).

The arrangement of the vessels in the Circle of Willis can vary between species and even within members of the same species. In humans the Circle of Willis is primarily comprised of the anterior cerebral arteries, posterior communicating and posterior cerebral arteries. However in the rat, in addition to the above, the internal carotid arteries form part of the circle (Lee, 1995)

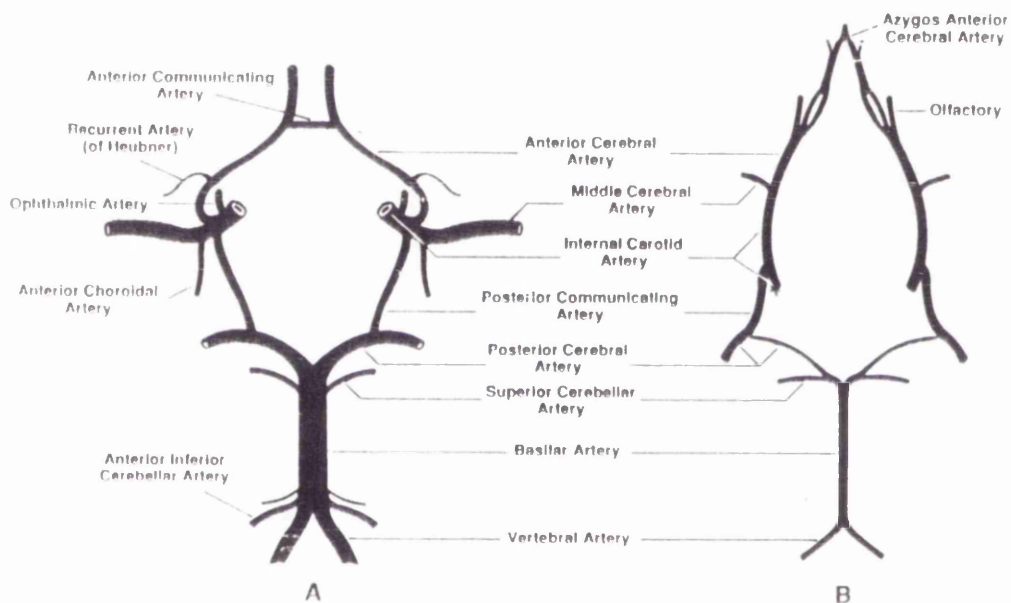


Figure 1. Arrangement of the blood vessels in the Circle of Willis in A. Human and B. Rat. From Lee *et al.*, 1995.

Collateral circulation is present in both rodents and man which allows re-routing of blood flow between the main cerebral arteries through the circle of Willis and

connecting anastomoses. In humans there are eight possible collateral pathways capable of supplying the cerebral cortex with blood should the blood supply through the internal carotid or vertebral arteries become blocked. In the rat, there are four to five times as many collateral supplies. With respect to the MCA, anastomoses are present between the anterior cerebral artery and MCA and between the posterior cerebral artery and the MCA.

While the rat system can be said to be similar to the human system in some ways, in that they both possess a Circle of Willis and internal and vertebral arteries providing the brain with blood, there are also important variations.

The human, in common with the bird, cat, sheep, swine and dog, possesses a network of branching blood vessels called the carotid rete mirabilis which connects arteries and veins. The rat however does not possess such a system. Whereas in most species arteries and veins run together in pairs, in rats the vessels do not run in pairs but are connected by a complex capillary network. Rats also lack connections between arteries and veins (A-V shunts in humans).

Despite these differences, the cerebral anatomy of the rat is similar enough to man to allow it to be used in experimental models of ischaemia. The size of the rat makes it a more economical choice than the cat, dog or guinea pig which are also used in experimental stroke research and it also seems to be more acceptable in terms of ethical considerations than the primate, cat or the dog.

### 1.3.2 Rat models of experimental cerebral ischaemia

Models of experimental ischaemia have been developed to investigate the complex mechanisms of damage and to develop potential therapeutic strategies.

Most studies designed to replicate human stroke use models of focal ischaemia where the infarct (the region of irreversible brain damage affecting all cell types) is localised to a particular brain region. This type of ischaemia can be produced in a number of different ways, each of which offers its own advantages and disadvantages.

Most of the models developed have concentrated on the occlusion of the middle cerebral artery (MCA) as this is the vessel most commonly occluded in human stroke, the MCA being occluded in at least 25% of ischaemic incidents (Bamford *et al.*, 1987). This figure may be even higher with some groups suggesting a role for the MCA in up to 80% of infarcts (Derosne *et al.*, 1993).

The first rodent model of ischaemia was developed in the 1930s by Peterson and Evans and subsequent modifications and improvements have since been introduced. Models are commonly modified to increase reproducibility, reduce mortality and reduce the difficulty of the surgery (McAuley *et al.*, 1995). No one model can be said to be the ideal choice for the study of stroke and although compounds may prove successful in animal models of ischaemia when they are then moved to clinical trials many prove unsuccessful in ameliorating stroke damage in humans (LASA report, 1999).

Models of focal ischaemia can involve either permanent or transient occlusion of the MCA, the latter allows a period of reperfusion following a defined period of

vessel occlusion. It has been suggested that permanent models of ischaemia are most valuable in drug evaluation studies as they produce more consistent and definite infarcts (STAIR report, 1999) with transient models being used as a follow up to study the drug in more detail.

If the period of focal ischaemia is short enough, it may result in reversible cell injury from which the brain tissue can recover. In patients presenting with stroke symptoms this is known as a transient ischaemic attack (TIA) which resolves with no lasting neurological deficit. If the period of ischaemia is prolonged and of sufficient severity it will result in irreversible cell injury with the formation of a volume of necrotic tissue known as the infarct (McGee *et al.*, 1992).

The degree and type of disability seen in humans following a period of cerebral ischaemia depends on the region of the brain affected, the size of the region affected and the severity and duration of the ischaemia.

Common disabilities associated with stroke include paralysis, aphasia and/or memory loss. Neurological deficits are also seen in animals and include cognitive and sensorimotor deficits (Hunter *et al.*, 1998).

In some cases, collateral circulation can provide a salvaging supply of blood to the regions directly surrounding the infarct “core” through anastomoses which connect up the most distal of the major cerebral vessels (Coyle *et al.*, 1991). This surrounding region is known as the peri-infarct region or the penumbra and if it receives a large enough collateral blood supply can recover from ischaemia.

### 1.3.3 Models of permanent middle cerebral artery occlusion

**Electrocoagulation of the MCA** is a common method of permanent MCA occlusion. The model involves the surgical exposure of the MCA via a craniectomy and the opening of the dura. The electrocoagulation or diathermy occlusion of the MCA is produced either distal or proximal to the origin of the lateral lenticulostriate branches of the artery. A proximal occlusion increases the size of the lesion produced and increasing the length of vessel occluded results in larger and more consistent lesions (Bederson *et al.*, 1986).

MCA occlusion proximal to the lenticulostriate branches will produce both striatal and cortical damage within the MCA territory. Diathermy occlusion has the advantage of a low mortality rate, good reproducibility of infarct volume and relatively few complications on recovery from surgery.

The position and extent of vessel electrocoagulation has an impact on the localisation and the probability of infarction rates in a study. Bederson *et al.*, 1986 found that when carrying out a distal occlusion of the MCA (distal to the Inferior Cerebral Vein, ICV), the infarction rate varied from as much as 13%- 100% depending on the location and size of the region of electrocoagulation (Figure 2)

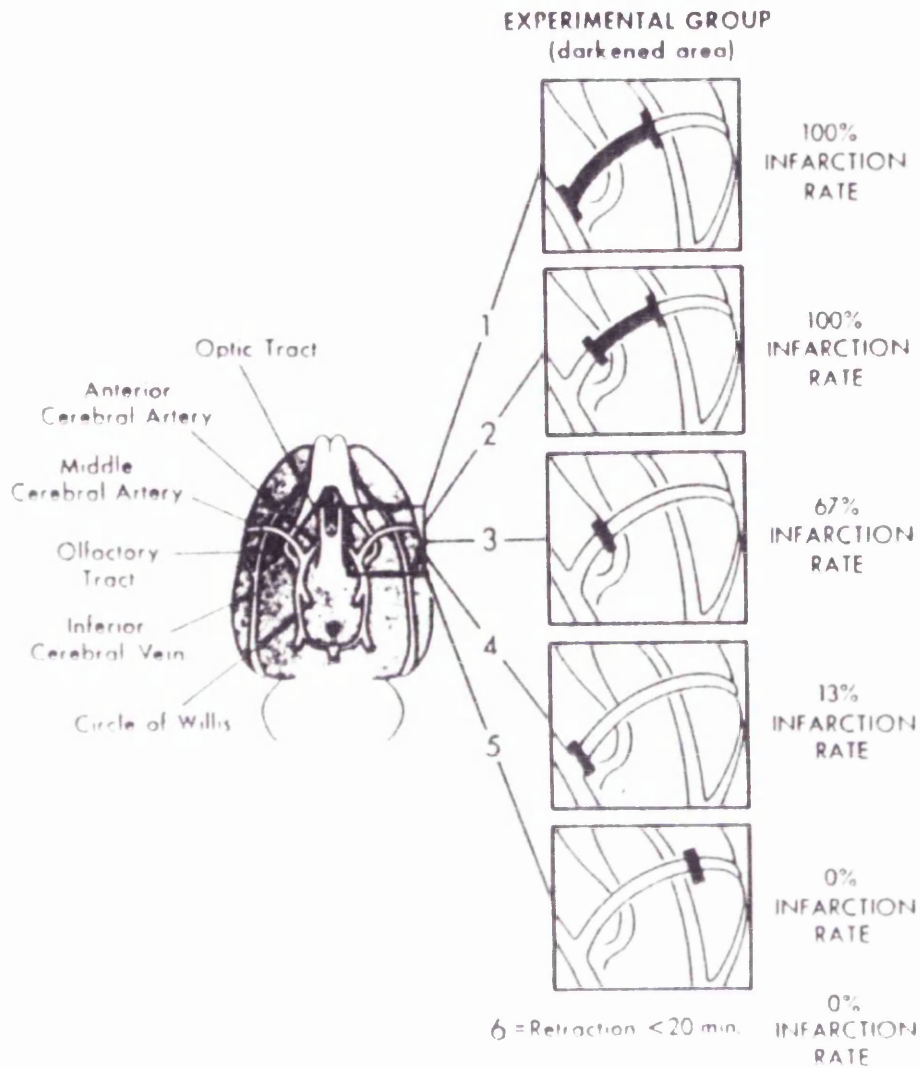


Figure 2. Infarction rate is determined by the size and location of the area of electrocoagulation. From Bederson *et al.*, 1986.

The electrocoagulation model does have some disadvantages due to the possibility of direct tissue damage and the need for a craniectomy. The electrocoagulation model was originally described by Robinson and colleagues, 1975 but was later modified by Tamura and co-workers, in an attempt to produce more reproducible infarct sizes.

**Two Vessel Occlusion Model-** this model of permanent MCA occlusion involves the ligation of the ipsilateral common carotid artery along with electrocoagulation of the MCA. This model again produces reproducible infarct sizes which can incorporate both cortical and striatal damage.

In an attempt to reduce direct tissue damage associated with the electrocoagulation procedure, models of permanent MCA occlusion have been developed where a ligature or a clip is applied to the MCA, blocking blood flow by a method other than electrocoagulation. With models using a clip or ligature the volume of infarction is influenced by the position and number of clip/ligatures involved (Bederson *et al.*, 1986).

As with the diathermy occlusion of the MCA, in clip/ligature models, applying occlusive pressure below the lenticulostriate branches has been shown to produce a greater degree of ischaemic damage with a striatal involvement.

The introduction of a reperfusion phase with this model is relatively easy due to the ability to remove the clip /ligature from the occluded vessel as required. Therefore unlike with the electrocoagulation model of MCA occlusion which is purely a permanent MCA occlusion model, models using clips or ligatures can produce permanent or transient vessel occlusion depending on whether the clip is removed or kept in place.

### **1.3.4 Models of transient focal ischaemia**

Transient focal ischaemia involves vessel occlusion followed by a period of reperfusion. Reperfusion is believed to play a role in human stroke as in many cases a degree of reperfusion is likely within the first few days following vessel occlusion. Various models of transient focal ischaemia exist and each model has its own advantages and disadvantages.

**Intraluminal Thread Model of Focal Ischaemia-** this is a popular model and was first introduced by Koizumi and colleagues, in 1986. The technique involves the insertion of a filament, normally a nylon suture of a diameter wide enough to block the distal portion of the internal carotid artery (ICA) , into the external carotid artery (ECA) and then into the internal carotid artery until in a position to block the origin of the MCA at the Circle of Willis (Figure 3)

Reperfusion is induced by retraction and removal of the filament. The original Koizumi method has since been modified by Longa ZE and co-workers , to produce more reproducible infarcts.

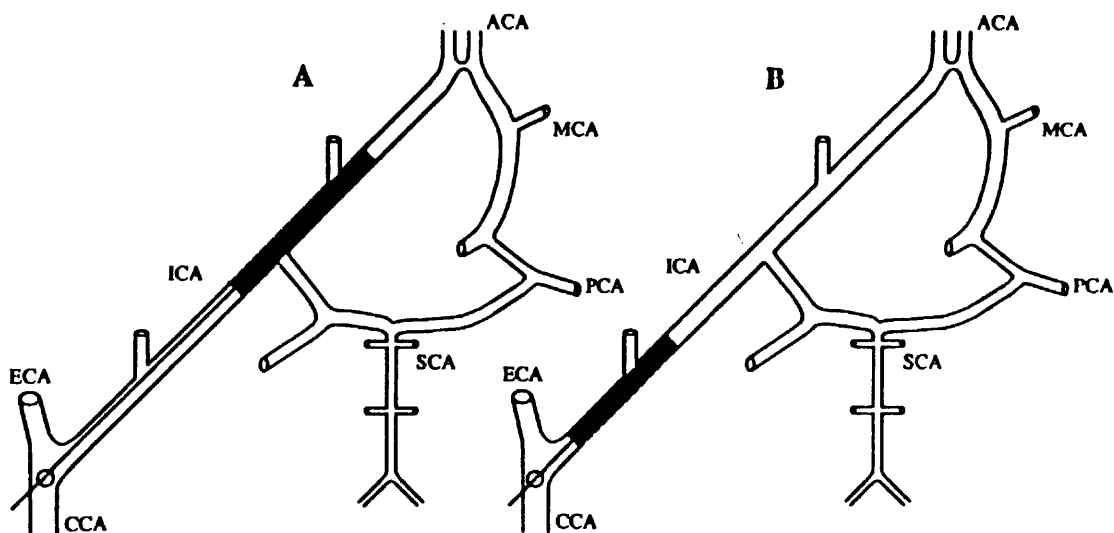


Figure 3. Intraluminal thread induced ischaemia. From McAuley, 1995.

ICA- internal carotid artery, ECA- external carotid artery, CCA- common carotid artery, ACA- anterior cerebral artery, MCA-middle cerebral artery, PCA- posterior cerebral artery, SCA- superior cerebellar artery

The intraluminal thread model can also be used as a model of permanent vessel occlusion when the filament is kept in place throughout the surgical procedure and /or recovery period, therefore not introducing a period of reperfusion.

A distinct advantage of this model is that no craniectomy is required although mechanical damage to the endothelium of the internal carotid can be expected due to the insertion and advancement of the filament. Preparation of the animal for insertion of the filament is less technically demanding and can be accomplished in a shorter time than that needed for models involving the exposure of the MCA for direct occlusion of the vessel.

Disadvantages of the intraluminal thread model include a risk of subarachnoid haemorrhage due to the piercing of the vessel wall while the filament is being advanced, failure to induce damage due to a residual flow supplying the MCA territory whilst the filament is in place and an increased mortality rate for permanent intraluminal thread due to large infarcts and potentially damaging rises in intracranial pressure not relieved due to the absence of a craniectomy.

**Endothelin-1 models of MCA Occlusion-** Two methods of Endothelin –1 MCA occlusion exist. The first method involves surgical exposure of the MCA with a lesser degree of mechanical damage than methods using electrocoagulation or application of a clip/ ligature to a vessel and pharmacologically induced occlusion of the vessel.

Following opening of the dura and puncturing of the arachnoid membrane the potent vasoconstrictor peptide endothelin-1 (ET-1) is applied topically to the MCA. Severe constriction leading to complete occlusion of the MCA occurs within seconds, significantly reducing cerebral blood flow within the MCA territory (Macrae *et al.*, 1993). The severity and duration of ischaemia can be modulated by altering the dose of ET-1 administered. As the effects of the ET-1 wear off ( $t_{1/2}$  is between 45 and 60 minutes in studies in cat pial arterioles, Robinson & McCulloch, 1990) the MCA returns to its normal calibre resulting in reperfusion of blood into the MCA territory (Macrae *et al.*, 1993). Reperfusion levels of approximately 50% can be seen at 4 hours post ET-1 application.

The second ET-1 model of MCA occlusion is the Sharkey model (Sharkey *et al.*, 1993) and is an alternative to the ET-1 model described above. A lower dose of ET-1 is used (0.12nmol when compared to 2.5nmol) and the vasoconstrictor is stereotaxically injected into parenchymal tissue adjacent to the MCA in conscious animals via a previously implanted cannula. In this model the ischaemia is more prolonged than in the Macrae model with no evidence of reperfusion for the first 3-4 hours.

The intraluminal thread model and the diathermy model of MCA occlusion are the most widely used of the models of focal experimental ischaemia. Other available but less common models of focal MCA occlusion include the introduction of a catheter containing **blood clot fragments** into the common carotid artery (CCA) and/or ICA, branches of the ECA. The catheter is advanced into the ECA following the ligation of one or more of the following - the ICA, CCA or branches of the ECA, and is advanced to the origin of the ICA where blood clot fragments were injected (Penar, 1987).

**Microspheres** can also be injected into the CCA following ligation of the extra cranial branches of the ECA providing an alternative method of occlusion of the MCA (Zivin *et al.*, 1987).

**Photothrombosis-** this method uses photoactive agents (for example Rose Bengal a photosensitive dye) to occlude vessels on the surface of the cortex (Dietrich *et al.*, 1989). The dye is administered intravenously and the skull is exposed to light of a specific wavelength which irradiates the skull and results in thrombus formation. The thrombus is formed as a result of irradiation of the Rose Bengal dye which produces singlet oxygen capable of peroxidizing lipids present within the vascular endothelium and among constituents of the blood. An argon laser is also used to induce thrombolysis in large arteries such as the CCA (Watson *et al.*, 1987).

### **1.3.5 Models of global ischaemia**

Although the studies in this thesis exclusively used models of focal ischaemia, the commonly used models of global ischaemia will be briefly described.

Global ischaemia involves cutting off the blood supply to the whole brain rather than a defined region of the brain. As with focal ischaemia, global ischaemia can be either permanent or non-permanent (complete or incomplete).

#### **Complete Global Ischaemia**

**Decapitation ischaemia-** this is perhaps the most simple of all the experimental models of ischaemia and will produce complete ischaemia. This model has been used to study the biochemistry of cerebral ischaemia (Ross *et al.*, 1993)

**Application of a neck tourniquet** – blood supply to the brain is halted by the application of a pressure cuff to the blood vessels in the neck. The method was first introduced by Levine and Marvine in the 1960's and causes not only ischaemia but also cardiovascular failure. It is not therefore exclusively a model of cerebral ischaemia. The model has a high mortality rate and is now rarely used as a model of experimental ischaemia.

### **Incomplete Global Ischaemia**

Models of incomplete global ischaemia do not completely block the blood supply to the entire brain and so cardiovascular function is less affected. Vessels leading to the brain are occluded outside of the skull and as a result models of incomplete ischaemia will cause less indirect damage and are surgically easier to perform than some of the models of focal ischaemia previously described. The most commonly used models of incomplete global ischaemia are:

**Bilateral occlusion of the common carotid arteries**- this model was first introduced in the 1970's by Elkof and Siesjo and involves the clipping or ligation of the common carotid arteries. This can be either permanent or transient with the clips/ligature being removed to allow reperfusion. This model is usually combined with hypotension to improve reproducibility.

**Four vessel occlusion-** this model involves the prior permanent occlusion of both the vertebral arteries with recovery followed later by the application of clips /ligature to the common carotid arteries to induce a defined period of ischaemia. This model was first introduced by Pulsinelli and Brierly in 1979 and is still widely used.

In models of global ischaemia there is selective neuronal vulnerability. Neurons in certain regions of the brain have a greater vulnerability to ischaemic damage than those in other regions. For example in models of global ischaemia, the neurons in the CA1, CA3 and CA4 regions of the hippocampus, regions in the caudate and the cerebellum and layers 3,5 and 6 of the neocortex are particularly sensitive to ischaemia (Siegel *et al.*, 1976).

### **1.3.6 The Spontaneously Hypertensive Stroke Prone Rat as a model of cerebrovascular disease**

The Spontaneously Hypertensive Stroke Prone Rat (SHRSP) is classed as an '*inbred animal model of cerebrovascular disease*' (Okamoto *et al.*, 1974) with a pathology of hypertension similar to that in humans.

SHRSPs develop a rapid onset of hypertension following birth with a typical mean arterial blood pressure of around 190mmHg at age 3 months compared to around 130 mmHg in its normotensive reference strain the Wistar Kyoto (WKY). Hypertension remains a trait of the SHRSP throughout its life (Fredriksson *et al.*, 1985).

The SHRSP is often used to study stroke as the strain has a high incidence of spontaneous stroke and an increased sensitivity to an induced experimental stroke.

This is illustrated by an increased volume of infarction following MCA occlusion when compared to their normotensive reference strain the WKY. This increased stroke sensitivity is reported to be independent of high blood pressure and controlled by a gene or genes within a quantitative trait loci (QTL) on rat chromosome 5 (Jeffs *et al.*, 1997). Although the gene(s) responsible has not yet been identified various factors have been proposed to contribute to this increased stroke sensitivity. These include a reduced internal diameter and impaired function of cerebral anastomoses leading to a reduced collateral blood supply (Coyle *et al.*, 1991; Carswell *et al.*, 2000). Other possible contributory factors include an increased release in glutamate following ischaemia (Gemba *et al.*, 1992) and an increased inflammatory response to ischaemia (Hallenbeck *et al.*, 1991).

SHRSPs and the genetically related spontaneously hypertensive rat strain (SHR) have been used in experimental stroke studies because of the reproducibility of the infarct size produced (Duverger and Mackenzie, 1988; Sauter *et al.*, 1995 ) and to investigate genetically determined factors contributing to sensitivity to ischaemia.

Although SHRs and SHRSPs have a similar pathology to humans they may not be ideal as models to study neuroprotection as they tend to possess less salvageable tissue available for drug intervention compared to normotensive strains.

## **1.4 Ischaemic Events**

The focal ischaemia associated with a stroke deprives brain tissue of both oxygen and glucose resulting in rapid energy loss with resultant impairment in energy

dependent ion and neurotransmitter pumps which maintain normal cellular homeostasis. Neurons consequently depolarise and release their neurotransmitter content. The neurotransmitter glutamate is particularly toxic when levels are not strictly controlled in the extracellular space and this can lead to excitotoxicity via receptor mediated and non-receptor mediated events (Figure 4- From Koroshetz *et al.*, 1996). These events culminate in the swelling and infarction of the brain tissue (Koroshetz & Moskowitz , 1996).

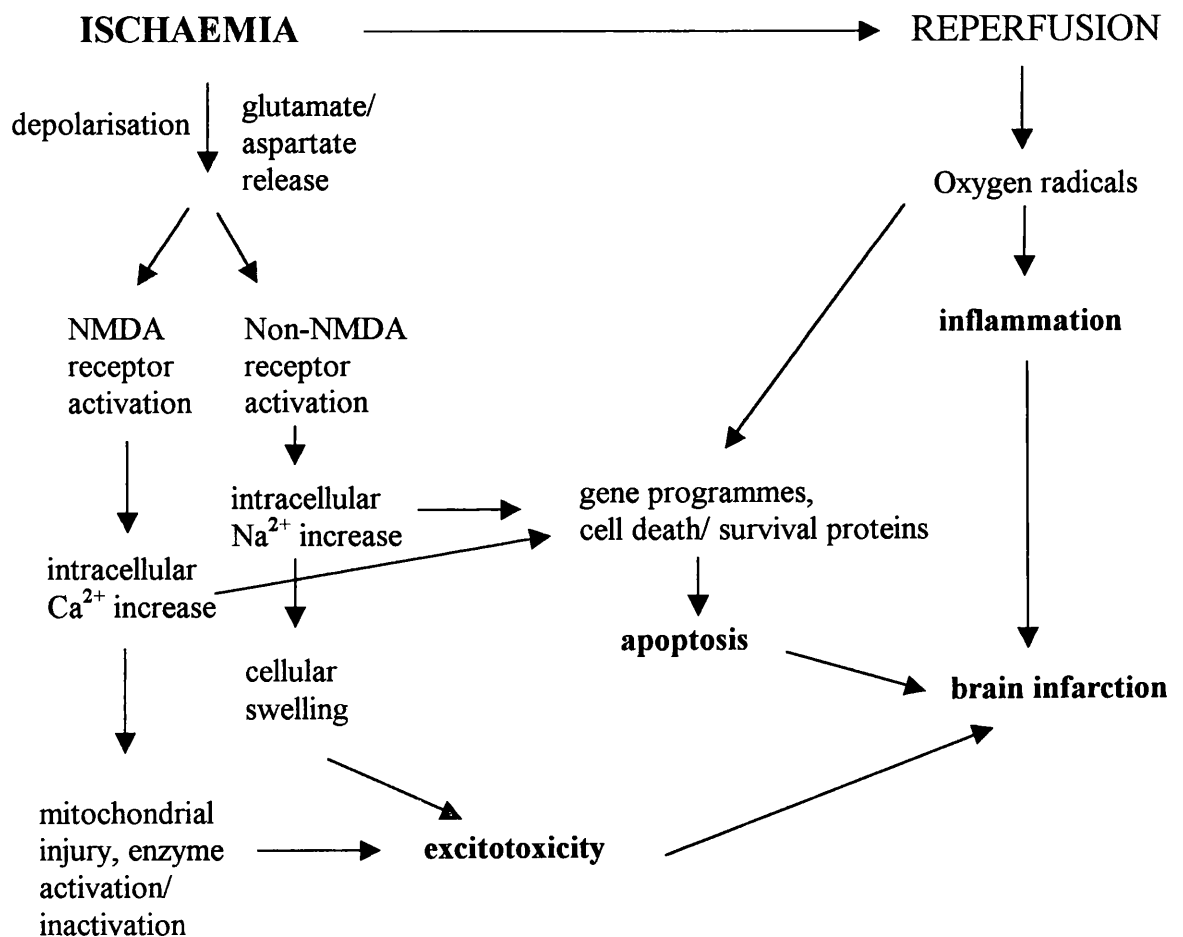


Figure 4. Events following ischaemia. Modified from Koroshetz, 1996.

### 1.4.1 Reperfusion Injury

In addition to the brain damage caused during the ischaemic period, recent evidence would suggest that on reperfusion of the cerebral tissue after a significant period of ischaemia (1-2 hours in rat), further damage can occur as a result of returning oxygen and glucose to ischaemically challenged tissue and as a result of interactions between components of the blood and the damaged/ischaemic tissue (Hallenbeck & Dutka , 1990; Aronowski *et al.*, 1997; Sharkey *et al.*, 1996).

Reperfusion has the potential to salvage tissue in the peri-infarct area- the area between the densely ischaemic core and the normally perfused brain. During reperfusion of the brain there is resumption of oxygen delivery, provision of substrates for metabolism and clearance of metabolic waste in an attempt to return tissue function to normal (Hallenbeck & Dutka, 1990).

The first indications of reperfusion injury were observed in relation to myocardial ischaemia but it is now widely accepted that following ischaemia, restoration of blood flow in many tissues, including the brain, can result in further damage (Hallenbeck & Dutka, 1991; Traytsman *et al.*, 1991; Yang *et al.*, 1994).

Although early reperfusion aids tissue recovery, delayed reperfusion may induce deleterious mechanisms in injured tissue leading to further damage to the brain tissue and provide a route for inflammatory cells in the bloodstream to the tissue.

### 1.4.2 Excitotoxicity and ischaemia

Glutamate mediated excitotoxicity is perhaps one of the most important acute mechanisms of ischaemic damage following a period of neuronal oxygen deprivation.

High concentrations of glutamate are capable of triggering neuronal death and are suspected to play a role in the pathogenesis of a number of CNS diseases including stroke.

Three mechanisms give rise to high glutamate concentrations in synaptic clefts during ischaemia. 1) glutamate released from synapses in response to the depolarisation of ischaemic neurons; 2) glutamate released from depolarised astrocytes and 3) failure of glutamate uptake into neurons or glia because of loss of ATP. The consequence is over stimulation of NMDA and AMPA receptors. This over stimulation of receptors leads to a massive influx of  $\text{Na}^+$ ,  $\text{Ca}^{2+}$  and  $\text{Zn}^{2+}$  ions and loss of  $\text{K}^+$  ions through ion channels associated with the NMDA and AMPA receptors. It is the increase in these ion concentrations which leads to metabolic disruption and neuronal cell death (Lee J.M., 1999). Other problems associated with the excitotoxicity include the rapid influx of water leading to dendritic swelling and plasma membrane failure.

NMDA antagonists such as MK801 and AMPA antagonists such as NBQX attenuate excitotoxic mediated neuronal cell death following ischaemia and reduce the amount of brain damage in experimental models of global and focal ischaemia (Wieloch T., 1985, Simon R.P. *et al.*, 1984).

While NMDA receptor antagonists appear more effective in reducing focal ischaemic damage, evidence would seem to suggest that AMPA receptors play a significant role in excitotoxicity following global ischaemia (Yin *et al.*, 1994; McDonald *et al.*, 1998)

There are several endogenous factors which may reduce the role of NMDA receptors in the excitotoxic process. Following ischaemia there is an increase in free radicals,  $Zn^{2+}$  and protons all of which have been reported to reduce the activation of the NMDA receptors (Lee *et al.*, 1999). This inhibition of the NMDA receptors may be complemented by the direct inhibition of NMDA receptors by intracellular calmodulin (Lee *et al.*, 1999). These occurrences may put more emphasis on the role of AMPA mediated excitotoxicity.

### **1.4.3 Inflammation and ischaemia**

Although the brain has been described as immunologically deprived due to its lack of a lymphoid system and dendritic antigen presenting cells (Schwartz *et al.*, 1999), an inflammatory response to ischaemia can clearly be seen spanning the period from minutes to weeks after the ischaemic insult.

The brain's inflammatory response to ischaemia is a complicated one with many instances of overlap and feedback. It involves not only resident inflammatory cells such as microglia but also circulating peripheral inflammatory cells such as the neutrophils and macrophages. Circulating inflammatory cells can exacerbate ischaemic damage by adhering to the walls of injured blood vessels promoting blood

cell aggregation and physically blocking the lumen. These cells are also capable of becoming activated and crossing into the brain releasing cytotoxic substances such as interleukins, free radicals, proteases and cytotoxins, further contributing to inflammatory mediated damage and increased blood brain barrier permeability.

Mediators of the inflammatory response to ischaemia are thought to include free radicals, inflammatory cells such as neutrophils and microglia, cytokines, proteases and protease inhibitors.

These mediators are all part of the general inflammatory response which occurs in response to cerebral ischaemia (Figure 5- From Sharkey *et al.*, 1996).

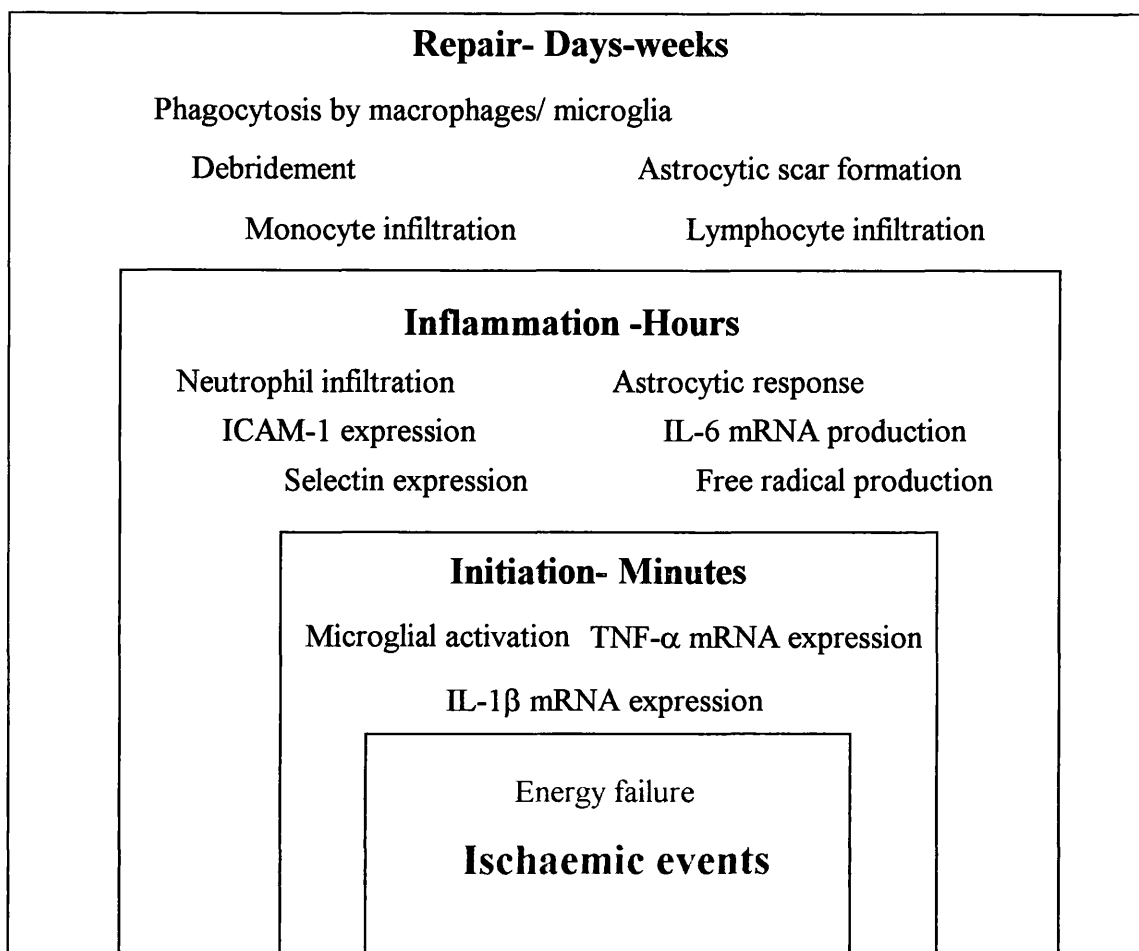


Figure 5. Inflammatory timescale following ischaemia. Modified from Sharkey *et al.*, 1996.

### 1.4.3.1 Neutrophils

The accumulation and adherence of inflammatory cells and their migration into the brain has been reported to contribute to ischaemic damage.

Neutrophils are important inflammatory cells which have been proposed to contribute to ischaemic damage. Neutrophils form an important part of the immune system, which involves recognition and elimination of potentially pathogenic molecules from the body (Male *et al.*, 1996). Neutrophil migration to sites of damage and infection helps to combat pathogenic invasion and inflammatory damage.

However, in addition to playing a beneficial role in the host defences, neutrophil accumulation would seem to accompany various pathological conditions. Perhaps most importantly, global and focal ischaemia. Since the late 1960's, the possible contribution of neutrophils to ischaemic damage has been investigated (Sornas *et al.*, 1972; Garcia *et al.*, 1974). It is now widely believed that neutrophil accumulation and aggregation resulting in the blocking of blood vessels, brain infiltration and the release of cytotoxic substances is likely to contribute to ischaemic damage (Groggaard *et al.*, 1989; Hallenbeck *et al.*, 1986; Pozzilli *et al.*, 1985).

Neutrophils are peripheral inflammatory cells which have to travel from the periphery to the brain in order to contribute to inflammatory mediated ischaemic damage. This process is collectively known as neutrophil extravasation and constitutes the following steps- capture, tethering/rolling, activation, adhesion and then migration (Figure 6).

Once the neutrophils have reached cerebral blood vessels the blood flow to an ischaemic area can be hindered due to the ability of the neutrophils to accumulate

and adhere to the endothelium of the blood vessel walls, resulting in a plugging of the vessels.

This hindrance of blood flow has been termed “no-reflow” and has been demonstrated in various animal models. For example in a baboon model of 3 hour MCA occlusion, the no-reflow phenomenon was reported in >60% of capillaries within 1 hour of reperfusion (Del Zoppo *et al.*, 1991).

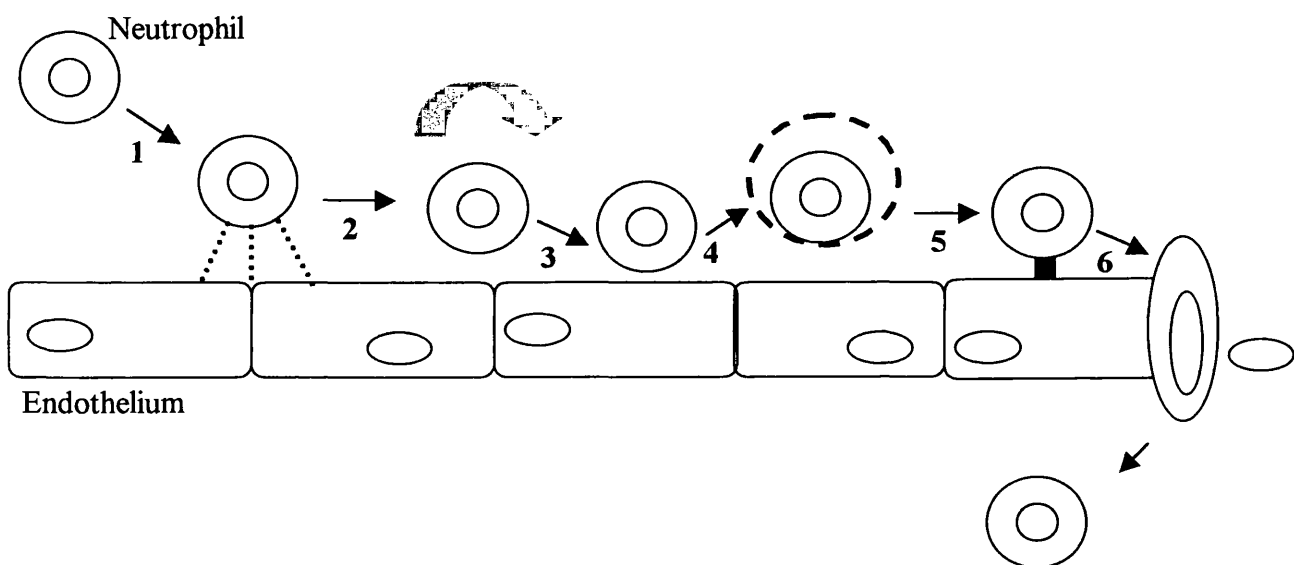


Figure 6. Steps of Neutrophil Migration. (Modified from Rothlin., 1977)

**1** – Circulating neutrophil attracted to endothelial surface, **2 + 3** – slowing, tethering and rolling, **4** – Activation, **5** – Adhesion, **6** – Passage of neutrophil through endothelium.

Neutrophils can also transmigrate into surrounding tissue causing damage by a variety of mechanisms including the release of free radicals, cytotoxic substances and activation of proteinases.

For neutrophil adherence to occur, the expression of adhesion receptors is required. The two classes of adhesion molecules which play the greatest role in neutrophil adhesion are 1) The Selectins (P and E) recognising carbohydrate ligands and 2) members of the Immunoglobulin Super family (including the intercellular adhesion molecules-1 and 2- ICAM-1 and ICAM-2 and VCAM) which recognise integrins. Various studies have shown that these adhesion molecules are up regulated during cerebral ischaemia (Okada *et al.*, 1994; Pantani *et al.*, 1998; Soriano *et al.*, 1996) and antibodies which block these adhesion sites have been reported to reduce ischaemic damage.

Various mediators are responsible for the expression of receptors on the neutrophils and the endothelium. These include N-formyl-methionyl-leucyl-phenylalanine and platelet activating factor in the case of neutrophils and interleukin-1 (IL-1) in the case of the endothelium adhesion molecule expression. Tumour necrosis factor (TNF), lipopolysaccharide (LPS) and leukotriene B4 stimulate both selectins and adhesion molecules.

Evidence for the early accumulation of neutrophils in ischaemic damage comes from histopathological, biochemical and iodine labelled neutrophil studies. The actual significance of such accumulation is unclear, although there is a suggestion that it may represent a "homeostatic" response to scavenge debris and re-seal damaged tissue.

The time course of neutrophil accumulation after stroke in humans (Pozzilli *et al.*, 1985) and after permanent MCA occlusion in animal models (Garcia & Kamijyo, 1974) has been reviewed. It has been reported that maximal neutrophil infiltration around the ischaemic core occurred between 48 and 72 hours with further infiltration into the core by 7 days post occlusion. Neutrophil accumulation is greater in animal models of transient focal cerebral ischaemia with reperfusion than in permanent occlusion models. A greater number of neutrophils are most probably present in reperfusion models compared to permanent models due to the fact that reperfusion provides a route into ischaemic territory. Reperfusion may also promote earlier cellular migration into parenchyma than permanent MCAO due to blood / vessel interactions.

Other than the plugging of vessels, neutrophils can also cause ischaemic damage and damage during reperfusion via the release of cytotoxic substances such as free radicals. A certain degree of positive feedback can occur at this point as free radicals are able to stimulate further neutrophil adherence and accumulation.

The release of free radicals by neutrophils and other cell types during reperfusion has been studied and a time course of free radical production has been suggested (Matsuo *et al.*, 1995). A biphasic profile exists, with an increase in free radicals occurring immediately after reperfusion, continuing for around an hour and then falling to basal levels with a further increase occurring after 24 hours reperfusion.

Based on these observations and the fact that neutrophil infiltration usually occurs between 6 and 12 hours after reperfusion in the MCA model, it has been hypothesised that the initial rise in free radical levels may be due in part to

circulating neutrophils while the subsequent rise is more likely to be due to infiltrating neutrophils and macrophages.

Although numerous studies looking for elevated neutrophil accumulation and studies investigating the effect of antibodies against adhesion molecules have been carried out in different animal models of ischaemia (Chopp *et al.*, 1994; Zhang *et al.*, 1994; Clark *et al.*, 1991; Zhang *et al.*, 1995), opinion still remains divided as to the significance of their role in reperfusion injury.

In the dog, indium 111 labelled granulocytes have been shown to accumulate as early as one hour after a sixty minute period of brain ischaemia in an air embolism model (Hallenbeck *et al.*, 1986). This accumulation occurred in the injured hemisphere of the ischaemic animals. Using autoradiography the clustering of punctate granulocyte images was detected in regions of low blood flow in half of the animals at both 60 minutes and two hundred and forty minutes after ischaemia with no clustering occurring in non-ischaemic animals.

As previously mentioned, to further investigate the role of neutrophils in reperfusion injury, studies have been carried out to determine the effect of antibodies to neutrophil adhesion molecules and integrins on brain damage in models of transient MCA occlusion.

Administration of antibodies against endothelial adhesion molecules would be expected to ameliorate damage caused during reperfusion if these molecules played a significant role in this damage.

A number of studies have demonstrated attenuation of ischaemic damage by anti-adhesion molecule antibodies. In a rabbit embolic model of stroke (Helps & Gorman,

1991), anti-ICAM-1 antibody was shown to increase the amount of clot necessary to produce permanent damage.

In rat models of MCA occlusion with forty-six hour reperfusion, administration of anti-CD11b integrin, anti-MAC-1 or anti ICAM-1 monoclonal antibodies administered either at the time of ischaemia, within an hour of reperfusion or twenty two hours after reperfusion attenuated ischaemic damage (Zhang *et al.*, 1995, Chopp *et al.*, 1994).

Although it would seem feasible that neutrophils play a part in ischaemic damage, various studies have reported no evidence of neutrophil accumulation following experimental cerebral ischaemia (Hayward *et al.*, 1996; Peters *et al.*, 1998; Oruckaptan *et al.*, 2000). In addition to negative studies, some groups have found that neutrophil accumulation and contribution to ischaemic damage would seem to be dependent on the duration of ischaemia with neutrophils contributing to damage in transient but not permanent models of middle cerebral artery occlusion (Zhang *et al.*, 1995; Prestigiacomo *et al.*, 1999).

#### **1.4.3.2 Microglia**

In previous studies from our laboratories, little evidence has been found for a significant recruitment of inflammatory cells from the circulation during the time of maximal infarct growth. Consequently this thesis has concentrated on the microglial cells which are present and activated within the brain during the time of infarct maturation.

Microglia are inflammatory cells thought to play a role in Central Nervous System (CNS) pathology. They constitute 5-20% of the total glial cell population in the CNS (Gehrmann, 1996) and have been shown to become activated in conditions of brain injury, neurodegeneration, inflammation and ischaemia. Whilst their purpose is primarily to remove debris and dead cells and limit further damage by promoting neural regeneration and tissue repair, it is proposed that their activation may also prove detrimental in certain disorders (Nakajima *et al.*, 1998; Moore & Thanos, 1996; Nakajima *et al.*, 1993).

As mentioned previously, ischaemia and brain trauma are commonly associated with the expression of inflammatory cytokines (IL-1, TNF- $\alpha$ , IL-8, LTB<sub>4</sub>) and the up regulation of adhesion molecules which play a vital role in neutrophil adherence to cerebral blood vessel endothelium. Microglia have been shown to secrete inflammatory cytokines, glutamate, free radicals and proteases and have also been reported to show up regulation of adhesion molecule expression. It is possible therefore that they may be involved in the pathology of conditions such as ischaemia and brain trauma.

In terms of the origin of brain microglia, various theories have been formed. Microglia could be of monocytic, mesodermal or neuroectodermal origin.

The monocytic theory of origin is the most widely believed and it is generally accepted that monocytes are capable of crossing the blood brain barrier in the early embryonic stages. They are then capable of transforming into ameboid microglia and then into ramified, resting microglia following completion of brain development.

Various pieces of evidence would seem to support this theory. For example, studies have shown that the injection of carbon labelled monocytes can lead to the

production of carbon labelled mature microglia within the brain (Perry *et al.*, 1985).

A monocytic origin would also seem to be likely due to the fact that isolectin  $\beta$  4 binds to both microglia and monocytes and that microglia are recognised by many macrophage markers (For example antibodies to Fc receptors and major histocompatibility complexes (MHC) ).

Microglia appear in the CNS from early in development in the postembryonic period (Barron, 1995). At this stage microglial cells have the appearance of macrophages, possessing a large cell body and very short projections. They also undertake the role of a macrophage by removing cellular debris, engulfing dead neurons and oligodendrocytes and playing a role in the remodelling and reabsorption of brain fibre tracts. These functions justify the microglial cell being given the name “brain macrophage” in the early stages of brain development.

As the brain matures, the appearance and the role of the microglial cell changes and the number of ameboid microglia decrease. They are replaced by ramified (or resting) microglia which have small cell bodies and long spindly processes. In the ameboid form, microglia can be said to be in an active form and are able to revert from activated to resting and vice versa in response to different stimuli throughout their lifetime (Figure 7).



Figure 7. Stages of microglial activation. A. resting microglia, B. activated microglia, C. phagocytic microglia.

In the normal CNS, microglia are present in a resting state, with their morphology being dependent on their location in the brain (Keane & Hickey, 1997). For example in the white matter, microglia possess a bipolar morphology while in the grey matter they possess a stellate morphology. The spiny appearance of microglia was first described by Rio- Hortega in the 1930's (1932) with the use of silver carbonate staining and has further been shown with fluorescent labels. Scanning electron microscope images have shown that the whole of the microglial surface is covered in spines between 2 and 4 $\mu\text{m}$  in length and 0.1 $\mu\text{m}$  in diameter (Giulian *et al.*, 1995). These are long when compared to the size of the cell body- 5-10 $\mu\text{m}$ . Microglia have been shown to have an average of 20 spines per cell and this spiny appearance distinguishes the microglial cell from peripheral blood borne macrophages as they do not possess this feature. The spines are believed to play a role in the migration of the microglia.

With the onset of CNS injury or potentially damaging changes in the microenvironment, microglia are able to undergo a series of changes and become activated (Davis *et al.*, 1994) within a matter of minutes to hours in the case of cerebral ischaemia.

Microglial activation is not a single step and microglia undergo several changes in morphology until they resemble a phagocytic cell such as the macrophage.

In the activated state microglia develop more pronounced but shorter projections and their nucleus becomes more defined. They also undergo up regulation of cell surface antigen receptor expression. Examples of antigens up regulated include MHC class 1 and class 11 antigens. Other antigens thought to be expressed by microglial cells during activation include ED1, CR3, EBM11, Fc receptors and plasminogen activator inhibitor (Kato *et al.*, 1995; Gehrman *et al.*, 1992; Morioka *et al.*, 1991).

The development of a phagocytic phenotype is normally the last step in the activation process and not all microglia will reach it. When in the phagocytic form, the microglial cells perform the beneficial role of removing debris including necrotic neurons and damaged tissue to allow remodelling and glial scar formation (Abraham and Lazar, 2000; Mabuchi *et al.*, 2000).

The mechanisms by which the microglial cell becomes activated are not entirely understood but are believed to involve changes in calcium and potassium levels in the microenvironment, with microglia being particularly sensitive to changes in the outward potassium currents.

The following factors have been suggested as potential mediators of microglial activation in ischaemia: activation due to the energy depletion accompanying ischaemia; activation by exposure to neuronal distress factors; activation by exposure

to astrocytic secretory products (unlikely as the astrocytic response occurs later than the microglial response- Kato & Waltz, 2000); spreading depression induced changes and activation by exposure to blood borne elements as a result of the breakdown of the blood brain barrier.

Kato and Waltz (2000) set out to investigate energy depletion and spreading depression as potential contributors to microglial activation following in vitro chemical ischaemia (depriving cells of glucose and applying an inhibitor of the electron transport chain). The study found that energy depletion was unlikely to be the stimulus for microglial activation as the depletion caused irreversible damage in the form of changes in membrane current and in morphology and did not cause an increase in the outward potassium current implicated in microglial activation. Spreading depression on the other hand, was found to elicit changes to the microenvironment conducive to microglial activation. An increase in ATP and potassium in microglial cells during spreading depression was found to enhance the calcium response to ischaemia. This calcium response is thought to enable the microglial cell to translate external factors into a signal code alerting the cell to the presence of damage. The intensity of the signal allows the microglial cell to determine the severity of the ischaemic damage and to mount an appropriate graded response.

It is still relatively unclear what the main signalling molecules involved in the microglial cellular response during activation are, although microglial mitogens are thought to play a role in initiating such a response. These include macrophage colony stimulating factor (MCSF) and IL-6.

Prior to the changes in morphology described above, the microglia normally undergo a certain degree of proliferation and migrate towards the site of damage, for example towards the site of ischaemia.

Proliferation and migration are thought to be induced by a number of inflammatory mediators including those belonging to the cytokine family (Table 1) (Rauvich *et al.*, 1996).

One of the main ways in which microglia are thought to be able to migrate towards the site of damage is via a process known as chemotaxis. Different types of microglia migrate towards different chemoattractants. In the case of rat microglia they have been shown to migrate towards the chemoattractant C5a.

For such an attraction to take place, a soluble chemoattractant gradient must exist down which cells are able to move from low to high concentration.

CYTOKINE	ROLE IN INFLAMMATION
I gamma - IFN	MHC class 11 (MHC2) expression, antigen presentation.
IL-1	induction of urokinase-type PA (UPA)
LPS	NGF,MCSF and IL-2 receptor induction, inhibition of UPA.
TPA	delayed microglial proliferation in vitro
FGF	indirect effect on microglial proliferation, UPA induction in vitro
IL-2	LPS-dependent microglial survival and proliferation in vitro
IL-3	microglial proliferation in vitro/in vivo, activation of phagocytosis, MHC2 expression
IL-4	microglial proliferation in vitro, inhibition of MHC2
MCSF	microglial proliferation in vitro, superoxide ion formation, acid phosphatase, inhibition of MHC2 expression
GMcsf	microglial proliferation in vitro/in vivo, activation of phagocytosis

Table 1. Role of cytokines in proliferation of microglia and the microglial mediated inflammatory response. From Rauvitch *et al.*, 1996.

During migration the microglial cell undergoes structural changes which allows the cell to physically move. These changes involve alterations to actin polymerisation and distribution which can lead to elongation of projections/pseudopodia etc. allowing the cells to advance (Figure 8, Lauffenburger and Horwitz, 1996).

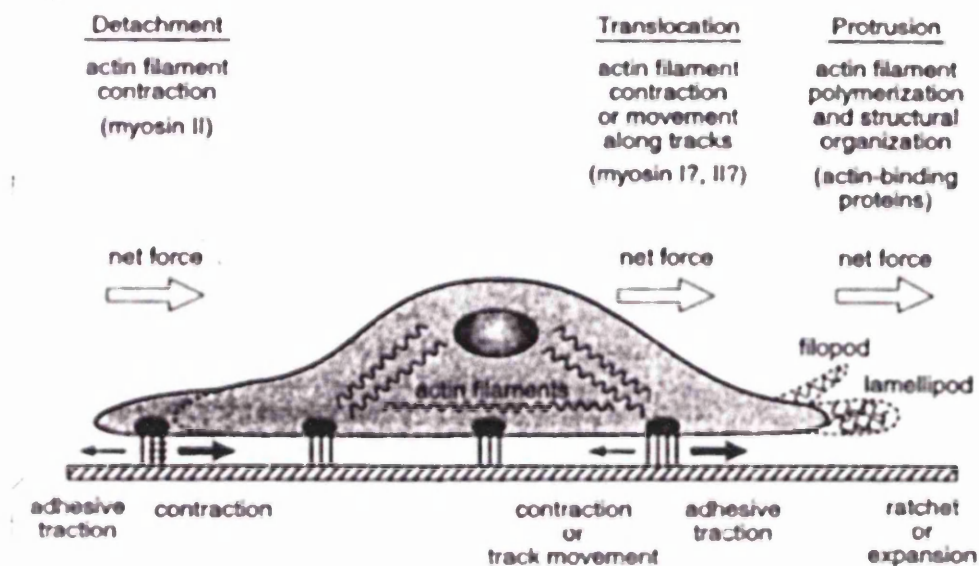


Figure 8. The migration of Cells. (From Lauffenburger and Horwitz, 1996)

Various chemokines have been shown to induce migration of microglia. These include IL-8, macrophages inflammatory protein 1 $\alpha$  and 1 $\beta$ , RANTES and interferon gamma inducible protein 10.

When the microglia proliferate and migrate to the site of damage they become activated. Once activated the microglia are capable of secreting a number of damaging substances such as NO, oxygen free radicals, proteases, glutamate and cytokines (Banati *et al.*, 1993). This release of cytotoxic agents can be modulated by inflammatory mediators and certain neurotransmitters. Either the microglia can be

stimulated to secrete cytotoxic substances, (for example by IFN- $\gamma$ ) or the cytotoxic properties of microglia can actually be reduced by cytokines such as IL-4 or TGF- $\beta$ 1.

A rise in cytokine levels occurring 1-2 days following ischaemia as reported by Baback *et al.*, 1996, would seem to correlate well with the timescale for microglia activation.

### **Microglia and ischaemia**

Various studies have been carried out looking at microglia numbers and activity following ischaemia (Abraham and Lazar, 2000; Zhang *et al.*, 1997; Moore and Thanos, 1996; Gehrmann, 1992) when increased proliferation, migration and activation of microglia can occur.

Microglia have the potential to play a double role following an ischaemic insult. On the one hand as a contributor to ischaemic damage, and on the other hand promoting the recovery and survival of nerve cells.

Microglial mediated neuronal damage is thought to primarily occur due to the release of cytotoxic substances such as glutamate, nitric oxide and a host of cytokines while the salvaging of recoverable neurons is thought to rely on the release of another group of substances including IL-1, TGF-beta1 and other growth factors.

Although many studies support a deleterious role for microglia following ischaemia, microglia are also capable of beneficial effects following both PNS and CNS injury. Microglia are known to be involved in phagocytosis and following injury can clear

away debris, for example from permanently degenerated neurons, allowing wound healing and neuronal regrowth ( Zeev-Brann *et al.*, 1998; Chen *et al.*, 1995).

Indeed, clusters of phagocytic microglia are often seen accumulating around dying neurons. Microglia also have the ability to secrete substances which can aid neuronal regeneration by stimulating the migration of scar forming and wound healing astrocytes to the site of damage (Faber-Elman *et al.*, 1996). These substances include IL-1 beta, TNF-alpha and the growth factors- TGF-beta, TGF-alpha, bFGF, EGF and IGF. The growth factors released can also inhibit or activate many of the activities involved in neuronal regrowth. For example they may stimulate cell migration and or proliferation, increase protease activity or alter the expression of extracellular matrix components.

While the major role of microglia is to perform a phagocytic role in most forms of PNS and CNS neuronal damage, there is evidence to suggest a pathological role in cerebral ischaemia (Moore & Thanos, 1996) and it is widely accepted that an increased presence of activated microglia following an ischaemic insult may contribute to the pathology of the condition.

As mentioned previously the microglia can cause damage directly and indirectly.

Indirect mechanisms include the release of cytokines- IL-1, IL-6, TNF- $\alpha$ , M-csf, prostaglandins and leukotrienes, reactive oxygen intermediates ( $O_2^-$ ,  $H_2O_2$ , ONOO-) matrix metalloproteinases, enzymes (hydrolases, cathepsins, plasminogen activator) and enzyme inhibitors (Tissue Inhibitors of MMPs).

These substances can cause damage through a variety of mechanisms including direct tissue injury, lipid peroxidation, release of neurotransmitters, vascular leakage, edema, necrosis and changes in ion flow and hormone release.

In terms of neurotoxicity associated with transmitter release, microglial induced toxicity is thought to be partially due to increased glutamate release (Banati *et al.*, 1993) since microglia have been shown to be capable of secreting glutamate in vitro. This increased glutamate increases NMDA receptor activity and so increases NMDA mediated toxicity and neuronal cell death.

The release of glutamate from microglia would seem to occur most often in conditions of high extracellular potassium levels. Microglial cells are particularly sensitive to changes in extracellular potassium levels due to their lack of a substantial potassium outward current.

Microglial cells can also cause damage directly via their ability to strip synapses and carry out neurophagia.

The presence of activated microglia following ischaemic insults has been reported by a number of groups.

In general it would seem that certain brain regions produce a faster inflammatory response to ischaemia than others explaining why certain areas produce a more pronounced increase in activated microglia early after ischaemia while in others the microglial response is not apparent until days after the insult. For example, in the hippocampus, especially the CA1 cell layer, microglia appear particularly susceptible to ischaemic damage responding within hours, while in white matter microglial responses tend to require days to develop. Studies have shown that following 30 minutes of global forebrain ischaemia, a microglial reaction can be seen after 24 hours in the striatum and the CA1 and CA4 of the hippocampus (Gehrmann *et al.*, 1992). After 72 hrs activated microglia have been shown to spread to other regions

including the thalamus, substantia nigra and the white matter (Gehrmann *et al.*, 1992).

A rapid activation of microglial cells following focal cerebral ischaemia has been observed following 1 hour of intraluminal filament occlusion of the right middle cerebral artery. Microglial activation was seen over 4hrs- 7 days (Kato *et al.*, 1994 ).

An elevated microglial response in the cortex has also been observed within 18 hrs of an occlusion of the middle cerebral artery in the rat in alternative models of experimental ischaemia (Morioka *et al.*, 1991).

The involvement of microglial cells in the development of the infarct was examined by Mabuchi *et al.*, 2000. They found that following intraluminal thread occlusion of the left MCA in the rat, the infarct was still developing from 16 to 48 hours after the induction of ischaemia. During the acute stages of ischaemia (up to 16 hours), they found little evidence for inflammatory cell contribution to ischaemic neuronal damage and postulated that spreading depression and increased glutamate toxicity were the main drivers for the progression of the ischaemic lesion. From 16 hours to 48 hours an expansion of the ischaemic lesion could be seen and it was during this period that activated microglia numbers increased in areas which were subsequently to become infarcted. From this observation Mabuchi and colleagues proposed that microglia and macrophages producing cytotoxic substances including IL-1 beta, were capable of contributing to the expansion of the ischaemic lesion after the early ischaemic period.

### **Role of microglia in other pathological conditions**

In addition to a possible role in the pathology of cerebral ischaemia, microglia are also thought to contribute to the pathology of a number of other CNS conditions and become activated in states of inflammation and in response to brain injury. (Table 2 modified from Nakajima and Kohsaka, 1993).

In Alzheimers Disease,  $\beta$ -amyloid depositions within the brain can lead to memory loss, confusion and mental instability. Activated microglial cells are observed in and around almost all  $\beta$ - amyloid plaques and would appear to be in the activated state expressing MHC class I and or class II antigens (Dickson *et al.*, 1993; Mattiace *et al.*, 1990).

There are various explanations given for microglial plaque association in Alzheimer's disease although no one explanation has been totally accepted.

There is speculation that the microglia may be directly involved in deposition of  $\beta$ -amyloid and that microglial cells may possess proteases capable of processing amyloid precursor protein (APP) (Moore & Thanos , 1996). The other train of thought is that the microglia perform a phagocytic role or that they congregate round degenerating neurons releasing cytokines and proteases which may cause neurons to produce more amyloid precursor protein.

In Multiple Sclerosis (MS), as in Alzheimers Disease, microglia are seen to accumulate in and around MS plaques. Plaques are widely distributed in spinal cord and intracerebral white matter tracts which are normally the primary sites of demyelination and inflammation. Microglia are proposed to contribute to the pathology of the condition due to their ability to secrete cytotoxic substances and through direct disruption of myelin (Moore & Thanos 1996; Cattieri *et al.*, 1994).

Microglia are also thought to be involved in the pathology of acquired immunodeficiency syndrome (AIDS) as microglial cells are among the CNS cells which become infected with the HIV retrovirus (Dickson *et al.*, 1991)

The primary importance of this infection of microglial cells is the appearance of a dementia like syndrome which could be due in part to a loss of neurons caused by the release of neurotoxic substances from recruited microglia or directly due to the infection and debilitation of the microglia themselves (Nakajima & Kohsaka , 1993).

INJURY OR DISEASE	REACTION OF MICROGLIA	POSSIBLE FUNCTION
Injury (Giulian <i>et al.</i> , 1987)	proliferation and migration to injury site.	defence, phagocytosis, gliosis and repair
Axotomy of facial nerve (Graeber <i>et al.</i> , 1988; Rieske <i>et al.</i> , 1989)	activation expression of CR3	regeneration
Alzheimers Disease (McGeer <i>et al.</i> , 1988; Frackowiak <i>et al.</i> , 1992)	accumulation around senile plaques	phagocytosis, amyloid formation, APP processing
AIDS-DC (Navia <i>et al.</i> , 1986; Dickson <i>et al.</i> , 1991; Watkins <i>et al.</i> , 1990)	Host for HIV-1 infection	alteration of function
MS (EAE,EAN) (Anthony <i>et al.</i> , 1991)	accumulation in or around plaque	phagocytosis, degeneration of myelin, antigen presentation

Table 2- The involvement of microglia in other pathological conditions. Modified from Nakajima & Kohsaka, 1993.

### Antibodies specific for microglia

Antibodies to microglia are widely available and are a very useful tool in the identification of both resting and activated microglia in cerebral ischaemia (Gehrmann , 1992).

Different antibodies are currently available which can distinguish between microglia in different species and in different stages of activation (Table 3).

ANTIBODY	REACTIVITY	REFERENCE
F4/80	mouse microglia	Perry <i>et al.</i> , 1995
<b>MAC-1,</b> <b>Ox-42,</b> <b>MRF-1,</b> <b>Isolectin <math>\beta</math>4</b> <b>ED-1</b>	rat microglia	Htain <i>et al.</i> , 1994  Robinson <i>et al.</i> , 1986  Tanaka <i>et al.</i> , 1999  Boya <i>et al.</i> , 1991  Damoiseaux <i>et al.</i> , 1994
EBM11, Ki-M1P	human microglia	Esiri and McGeer, 1986

Table 3- Antibodies against microglia. Modified from Gehrmann , 1992.

These antibodies are cell specific for microglia and will not stain any other cell type in the brain. The problem is however that they are capable of staining peripheral macrophages - which may migrate into the brain during ischaemia. Microglia can be distinguished from peripheral macrophages at the ultrastructural level as the

macrophages do not possess spines characteristic of microglia (Ulvestad *et al.*, 1994; Giulian *et al.*, 1995).

#### **1.4.3.3 Matrix metalloproteinases (MMPs)**

As previously discussed, upon activation, microglia are capable of secreting a number of cytotoxic substances capable of contributing to ischaemic damage.

Among these substances are the matrix metalloproteinases (MMPs) and a number of groups have shown that MMP levels are increased following ischaemia and that administration of inhibitors of MMPs can reduce ischaemic damage and oedema.

The MMPs are a family of zinc dependent endopeptidases which are capable of degrading all of the components of the extracellular matrix (ECM) which maintains the viability of cells.

MMPs were first discovered in the 1960's by Cross and Lapiere (1962) who realised that an enzyme on the tail of the metamorphosing frog had the ability to degrade collagen. This enzyme has since been identified as MMP-13. Since the discovery of this first MMP over 40 years ago, over 20 have now been identified.

MMPs are distributed throughout the body and are involved in both beneficial and detrimental processes. Beneficial effects include the regeneration of tissue in wound healing and scar formation, while detrimental effects include an involvement in the pathology of conditions such as rheumatoid arthritis, cancer (where they would seem to have a role in the promotion of tumour growth and metastasis), neurodegenerative

disorders and ischaemia. In the central nervous system MMPs have also been implicated in the pathogenesis of neoplastic, degenerative and inflammatory/demyelinating diseases including multiple sclerosis.

### **The Extracellular Matrix.**

An extracellular matrix (ECM) is found in all organs, and is located in the interstitial space. The ECM can be defined as the naturally occurring extracellular substance upon which cells migrate, proliferate and differentiate in vivo (Rutka *et al.*, 1988). Any substance with the ability to degrade the ECM therefore has the potential to disrupt normal physiological function. The ECM is normally composed of collagen, non-collagenous glycoproteins, glycosaminoglycans and proteoglycans which are all substrates for the MMPs. In the brain, the ECM is not well defined in all areas, however a well defined ECM can be found surrounding cerebral blood vessels. The extracellular matrix takes the form of a true basement membrane involving interactions between the glial limitans externa, pial cells, astrocytes, capillaries and neurons of the grey matter and also incorporating oligodendrocytes in the white matter (Figure 9).

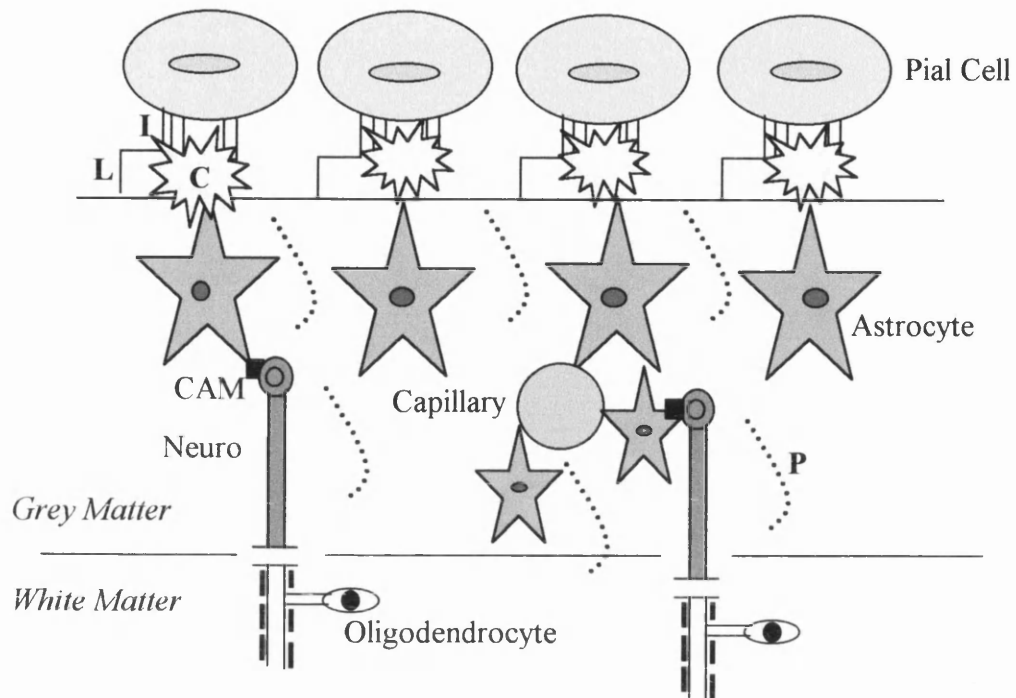


Figure 9. Structure of the Extracellular Matrix. Modified from Rutka et al 1988.

L – Laminin, C – Collagen, I – Integrin, P- Proteoglycan, CAM- Cell Adhesion Molecule.

### Classes of MMPs.

Matrix metalloproteinases can be divided into 3 classes - the collagenases, stromelysins and gelatinases. Each of these classes contains a number of different MMPs capable of degrading certain components of the extracellular matrix (Table 4).

MMP No.	Name	Mr latent/active	Other names
MMP-1	Collagenase1	52 000/43 000	Interstitial Collagenase
MMP-2	Gelatinase A	71 000/62 000	72 kDa collagenase
MMP-3	Stromelysin1	52 000/43 000	Transin, Proteoglycanase, CAP
MMP-4	Procollagen peptidase		Not available
MMP-5	<sup>3</sup> / <sub>4</sub> Collagenase		“
MMP-6	Acid metalloproteinase		“
MMP-7	Matrilysin	28 000/19 000	Pump-1
MMP-8	Collagenase-2	51 000/42 000	Neutrophil Collagenase
MMP-9	Gelatinase B	76 000/67 000	92 kDa collagenase, Type V collagenase
MMP-10	Stromelysin2	52 000/44 000	Transin 2
MMP-11	Stromelysin 3	51 000/46 000	Furin motif
MMP-12	Macrophage elastase	52 000/20 000	Metalloelastase
MMP-13	Collagenase 3	52 000/42 000	Rat interstitial collagenase
MMP-14	Membrane type matrix Metalloproteinase1	64 000/54 000	MT1-MMP, furin motif
MMP-15	Membrane type matrix Metalloproteinase2	71 000/61 000	MT2-MMP, furin motif
MMP-16	Membrane type matrix Metalloproteinase3	66 000/56 000	MT3-MMP, furin motif
MMP-17	Membrane type matrix Metalloproteinase 4	62 000/51 000	MT4-MMP, furin motif
MMP-18	Collagenase 4	53 000/42 000	<i>Xenopus</i>
MMP-19	No trivial name	54 000/45 000	RAS-1
MMP-20	Enamelysin	54 000/22 000	
MMP-21	XMMP	70 000/53 000	<i>Xenopus</i> , furin motif
MMP-22	CMMP	51 000/42 000	Chick embryo
	MMPC31		<i>Caenorhabditis elegans</i>
	MMPH19		<i>C.elegans</i> , furin motif
	MMPY19		<i>C.elegans</i> , furin motif
	Envelysin		Sea Urchin
	Soybean MMP		<i>Glycine max</i>
	Fragilysin		<i>Bacteroides fragilis</i>

Table 4 The Matrix Metalloproteinase family. Modified from Woessner and Nagase, 2000.

## Structure and activity

MMPs share a number of structural and functional properties. Most members can be organised into three basic distinctive and well-conserved domains based on structural considerations (Massova , 1998). These are an amino acid terminal propeptide, a catalytic domain (consisting of a conserved sequence in which 3 histidine residues form a complex with a catalytic zinc ion) and a Hemopexin-like domain at the carboxy –terminal end. Different members of the MMP family have different structures (Figure 10). Of all the members of the MMP family, MMP-7 has the simplest structure and MMP-9 the most complex.

Different parts or domains of the MMP structure have different roles. The first component of the basic MMP structure is the signal peptide comprising of 18-30 amino acid residues. The signal peptide is cut from the MMP when it is secreted from its cellular source and so plays no role in the activation of the enzyme or the binding of the enzyme to its substrate. Lying next to the signal peptide is the propeptide domain which extends from the N-terminus (created after the removal of the signal peptide) to the catalytic domain and consists of around 80 amino acids. Within the propeptide domain, the cysteine residue plays an important role in the activation of the MMP. The cysteine residue is located opposite a zinc atom which is part of the active centre of the enzyme which allows the MMP to bind to its substrates (Springman EB et al., 1990). When the cysteine residue is displaced, by gold compounds, mercurials, proteolytic cleavage or oxidation, this exposes the zinc atom, therefore exposing the active site of the enzyme.

Matrilysin (MMP-7)



Collagenase (MMP-1, MMP-8, MMP-13, MMP-18)

Stromelysins (MMP-3, MMP-10)

Metalloelastase (MMP-12)

Enamelysin (MMP-20)

MMP-19



### Gelatinases

MMP-2



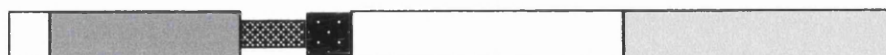
MMP-9



Stromelysin 3 (MMP-11)



Xenopus XMMP (MMP-21)



Membrane-type MMPs (MMP-14, MMP-15, MMP-16, MMP-17)

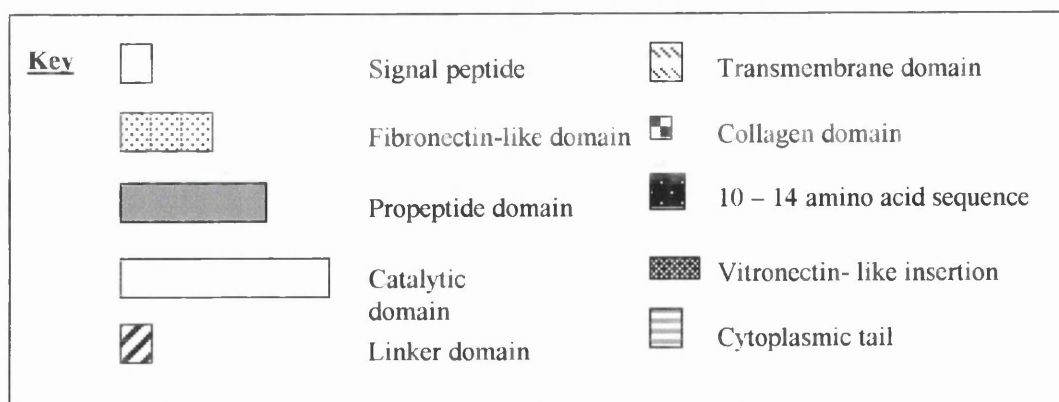


Figure 10. MMP structure

The catalytic domain lies between the propeptide domain and the hemopexin like domain in all MMPs with the exception of matrilysin. It constitutes 160-170 amino acid residues with the catalytic activity being centred around amino acids at positions 50-54. Fibronectin inserts divide the catalytic domain, separating the last 50 residues from the others. The catalytic zinc atom is found in the C-terminal portion of the domain bound by three histidine residues. The catalytic domain is believed to contain two ions of  $Zn^{2+}$  and one  $Ca^{2+}$  ion (Lovejoy B *et al.*, 1994). The fibronectin domains which divide the catalytic domain are found in gelatinase A and B. It is possible that fibronectin may aid with the binding process and certainly in the case of MMP-2 each of the units binds to the MMP-2 substrate gelatin (Banyai L *et al.*, 1994). Between the end of the catalytic domain and the start of the hemopexin domain lies a series of amino acid residues known as the hinge region or linker region. This region can vary in length from 2-72 amino acids and may play a role in destabilising substrates allowing part of their structure to interact with the active binding site.

The hemopexin domain is believed to play a role in binding and is around 200 amino acid residues in length. The domain is thought to be particularly important in collagenase activity. Clark and co-workers (1989) found that MMP-1 lacking the hemopexin domain was unable to digest collagen even though it still retained its catalytic activity. The hemopexin domain also binds heparin which is believed to accelerate activation rate when bound to the pro-enzyme (Crabbe *et al.*, 1993). The domain is also involved in the binding of MMPs to their naturally occurring inhibitors the Tissue Inhibitors of MMPs (TIMPs). The transmembrane domain is

found in the membrane inserted MMPs- MT1-MMP and MMP-14. At the end of the hemopexin domain lies an extension of 74 residues which includes a highly hydrophobic span suggested to be a transmembrane domain. This domain is believed to have a role in cleavage of the pro form of the enzyme to the active form.

All MMPs are produced in the latent form and must undergo proteolysis before becoming activated. The activation process involves the removal of the propeptide region of the molecule consisting of around 80-90 amino acids and including a cysteine residue which is capable of interacting with the catalytic zinc atom in the molecule via its thiol group. This proteolytic cleavage of the propeptide domain can be carried out by other proteolytic enzymes including other MMPs, mercurial compounds, thiol reactive agents and reactive oxygens.

In 1990, it was suggested by Van Wart and co-workers that the mechanism by which MMPs are activated involves the removal of a cysteine residue in the pro-peptide domain. Under normal circumstances the cysteine residue interacts with the catalytic zinc atom and prevents it from becoming associated with a water molecule allowing hydrolysis of the peptide. When the peptide becomes activated the cysteine residue is removed from the structure, and this exposes the catalytic zinc allowing hydrolysis and cleavage of the active form of the enzyme. (Figure 11)

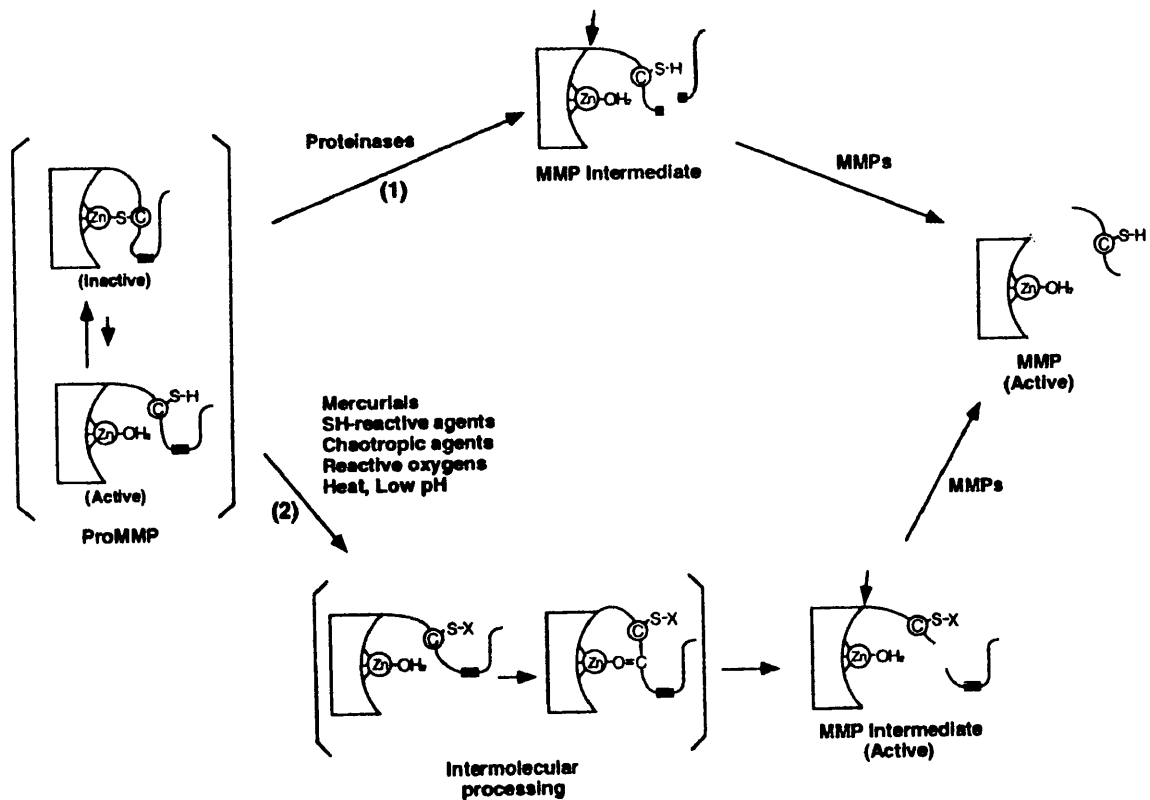


Figure 11. Activation of MMPs, from Woessner & Nagase, 2000

Different members of the MMP family are cleaved at slightly different points by different substances.

The MMPs are capable of degrading a number of different substrates. MMPs have their own specific cleavage sequences. For example MMP-9 can cleave substances from collagen, myelin basic protein to substance P.

It is the absence or presence of certain structural and functional domains which give the different members of the metalloproteinase family specificity for different matrix

components. For example, MMP-2 and MMP-9, otherwise known as the gelatinases, possess the domain which enables them to bind to the denatured collagen or gelatin. MMP-11 contains a transmembrane domain at the end of the carboxy terminus, which allows recognition of furin-like convertases.

### **Distribution of MMPs in the CNS.**

Matrix metalloproteinases are present within the normal central nervous system (CNS) as well as in conditions of inflammation and damage to the CNS. Studies have been carried out to determine the cellular localisation and levels.

CNS MMPs are present in small amounts in the latent form in a number of different cell types (Table 5). It is only in response to inflammatory stimuli or brain damage that the enzyme will be become activated. Inflammatory cytokines such as IL-1 and TNF-alpha, growth factors such as TGF-beta and noxious stimuli are capable of initiating transcription of the MMPs.

CELL TYPE	MMP PRESENT
Astrocyte	72 kDa and 92kDa gelatinase, stromelysin-1, stromelysin-2, collagenase-3
Schwann cells	72kDa gelatinase, stromelysin
Neurons	72kDa and 92kDa gelatinase
Microglia	Stromelysin-1, 92kDa gelatinase, collagenase-3
Endothelial cells, Vascular smooth muscle cells, Ependymal cells	Various MMPs

Table 5- MMP Localisation Within Cell Types- modified from Mun-Bryce, 1998.

The presence of MMPs within the CNS as previously mentioned, is extremely important, as they are known to contribute to inflammatory disorders. It is important therefore that the cellular localisation of the MMPs is known to enable a better understanding of the role of the MMPs in these disorders. In a study looking at the cellular localisation of MMPs in control and multiple sclerosis human CNS tissue (Maeda & Schobel , 1996) the greatest number of positively stained cells were found to be microglial cells and the staining pattern was reasonably consistent among the different MMPs. A range of microglia with different morphologies were immunoreactive for the MMPs and reactive cells were found in both grey and white matter. MMP-1, MMP-2, MMP-3 and MMP-9 were found expressed in microglial cells but MMP-1 and MMP-2 would seem to be the MMPs which are most likely only to be found within microglia. MMP positive macrophages were found in the MS

material but not the control tissue. MMP reactivity has also been seen in endothelial cells, vascular smooth muscle cells and ependymal cells. In terms of the possible presence of MMPs on the endothelium there is evidence that they may play a role in adhesion and migration of inflammatory cells. The wide number of immunoreactive cells in control tissue would seem to suggest that a high basal level of MMPs is present within the human CNS and that these MMPs could be rapidly mobilised and activated in pathological conditions.

### **CNS effects of MMPs**

MMP presence is essential for wound healing and scar formation (Slavomir *et al.*, 1997; Trengove *et al.*, 1999; Wysocki *et al.*, 1999). Following a surgical procedure such as a mastectomy MMP levels in serum are shown to be increased by a factor of at least 5 to 10 fold increase (Tarlton *et al.*, 1997). It is the presence of these enzymes, which allows the rapid healing of the wound.

MMPs are also thought to play a role in bone formation during development with MMP-9 especially being found in osteoblasts and being involved in bone remodelling (Wee Yong *et al.*, 1998).

Although there are more disorders where MMPs are reported to play a detrimental role it is thought that there could be a link between lack of MMPs and the development of  $\beta$  amyloid plaques in Alzheimers Disease.

Alzheimer's disease involves the deposition and accumulation of insoluble  $\beta$  amyloid plaques in certain regions of the brain leading to neuronal degeneration and memory loss. It has been shown that MMP levels are increased in Alzheimer's disease, in particular MMP-9/ gelatinase B. Based on results from human and canine studies (Backstrom, 1996; Linn *et al.*, 1997; Backstrom *et al.*, 1992), it is believed that this and possibly other MMPs may be involved in the breakdown of the insoluble  $\beta$  amyloid plaques and so a lack of MMP activation could actually result in the accumulation of insoluble peptides within the plaques worsening the condition.

However it is the detrimental role of MMPs in pathological conditions which is the focus of this thesis, laying foundation research that is important in terms of the development of therapeutic agents.

Multiple Sclerosis (MS), is a serious inflammatory disorder of the central nervous system (CNS) where inflammatory cells such as T-cells, macrophages and microglia are involved in widespread myelin destruction and axonal damage within regions of the brain and the spinal cord.

From the studies on the pathology of MS there is evidence to suggest the involvement of proteinase activity leading to myelin destruction. It is thought that this proteinase activity could be that of the MMPs.

Studies using animal models of MS, such as Experimental Autoimmune Neuritis, have shown that the MMPs are indeed up regulated in conditions of MS. It has been consistently demonstrated using techniques such as PCR, immunohistochemistry and zymography that matrilysin, macrophage metalloelastase and 92kDa gelatinase are up regulated in the MS lesion (Maeda & Sobue, 1996). These findings have also been confirmed to be true in human brain sections (Anthony *et al.*, 1997).

The involvement of MMPs in MS has been further confirmed by the fact that administration of certain broad spectrum MMP inhibitors such as GM-6001 ameliorates the symptoms of MS and reduces the increase in blood brain barrier permeability often associated with the disease (Slavomir *et al.*, 1997). Another MMP inhibitor BB-1101 has also been shown to reduce MS symptoms by inhibiting the release of the pro-inflammatory cytokine- tumour necrosis factor (TNF) which is believed to play a role in MS pathology.

MMPs are also linked to the pathology of Rheumatoid Arthritis (RA) and Osteoarthritis (OA) (Slavomir *et al.*, 1997; Wee Yong *et al.*, 1998; Gomez *et al.*, 1994) due to their ability to destroy connective tissue. MMP-3 expression is significantly increased in these disorders and this increase was found to correlate with traditional markers of inflammation for RA. MMP-9/ gelatinase B has an important role in bone remodelling. In pathologic conditions such as RA and OA, MMP-9 levels in the joints of patients were found to be elevated and correlated with MMP-3 levels (Slavomir *et al.*, 1997). This increase in MMP-9 is likely to cause pathologic bone resorption.

Perhaps the most important pathological condition where MMPs play a vital role is in cancer where they promote both tumour growth and metastasis.

Metastasis is a very important component of the pathology of cancer. A many step process it involves proliferation and spread of cancer cells from the primary site of invasion to multiple sites throughout the body. This requires movement of tumour cells across the extracellular matrix, which in turn requires attachment to and degradation of the ECM allowing the cells to pass through the ECM and reach sites

where they can divide and grow. MMPs are thought to be involved in the series of steps allowing metastasis to occur by their degradation of the extracellular matrix.

MMP-2 / gelatinase A and MMP-9/ gelatinase B have been specifically implicated in metastasis associated with lung, breast and colorectal carcinomas (Slavomir *et al.*, 1997; Wee Yong *et al.*, 1998). Levels of these two MMPs have been found to be significantly higher in tissue specimens and there would seem to be a definite correlation between MMP levels and the extent of tumour spread.

It is probable that MMP inhibitors may have therapeutic value in reducing the spread of cancer and making therapies such as surgery and chemotherapy more successful.

### **MMPs and Cerebral Ischaemia**

In addition to a role in the pathology of the above mentioned conditions , the matrix metalloproteinases are believed to contribute to the damage caused by cerebral ischaemia and increased MMP levels have been found in different models including thromboembolic and haemorrhagic stroke (Table 6).

MMPs have been associated with the inflammatory cells involved in the ischaemic cascade and levels of these enzymes have been shown to be increased in various studies using models of experimental stroke.

In most studies the main technique used is zymography (Rosenberg *et al.*, 1994) a form of gel electrophoresis which can detect and quantify the active form of MMPs.

Group	Species	Findings	Technique
Permanent MCAO. <i>Rosenberg et al., 1996</i>	Rat(SHR)	Increased MMP-9 at 12-24 hrs, increased MMP-2 at 5 days	Zymography
Permanent MCAO. <i>Romanic et al., 1998</i>	Rat	Increased MMP-9 at 12-24 hrs, increased MMP-2 at 24 hrs- 5 days	Zymography Immunohistochemistry
Haemorrhagic stroke. <i>Mun-Bryce et al., 1998</i>	Rat	Increased MMP-9 and MMP-2 at site of injection.	Zymography
Permanent intraluminal thread MCAO. <i>Gasche et al., 1999</i>	Mouse	Increased MMP-9 at 4 hours	Zymography Immunohistochemistry.
Transient MCAO MCA Balloon. <i>Heo et al., 1999</i>	Non- human primates	Increased latent MMP-2 and MMP-9 after 1 hr. Increased active MMP-2	Zymography on brain tissue and plasma.

Table 6 MMP studies using various animal models of ischaemia.

A few studies have identified MMPs using immunohistochemical techniques with antibodies directed against specific MMPs however immunohistochemical markers

for MMPs cannot differentiate between the latent and the active forms of the enzyme.

In a study involving permanent middle cerebral artery occlusion in spontaneously hypertensive rats (Rosenberg *et al.*, 1994), MMP-9/ gelatinase B was found to be elevated in the ipsilateral hemisphere of the brain after 12-24 hours. MMP-2/ gelatinase A was found to be elevated at 5 days after the occlusion. A correlation between MMP levels and cytokine levels was investigated and TNF-alpha and IL-1beta in particular were found to be significantly increased. The elevation in levels occurred from as early as 3-6 hours and peaked at 12 hours. These results may suggest a link between elevation of cytokine levels and the subsequent increase in MMP levels.

In another study using immunohistochemistry after permanent MCAO in the rat (Romanic *et al.*, 1998), the results were consistent with Rosenberg *et al.*, 1996. MMP-9 levels were found to be elevated after 12 hours and enzymatic activity reached maximum levels by 24 hours. MMP-2 levels were increased by 24 hours and reached its maximum levels by 5 days. MMP-9 was found within endothelial cells and neutrophils in and around the periphery of the infarct at the early stages of its activation. After 5 days it was also found within macrophages in the infarct. MMP-2 was present within macrophages in the infarcted area. This study also reported a significant decrease in infarct volume on administration of the MMP-9 antibody BB1101 (Romanic *et al.*, 1998).

In a model of haemorrhagic stroke, MMP-9 was found to be elevated after 16-24 hours of permanent MCAO (identified by zymography) and MMP-2 and MMP-9 both elevated at the site of the blood injection (Mun-Bryce *et al.*, 1998).

Due to the high probability of a contribution of MMPs to the pathology of stroke various MMP inhibitors have been tested in experimental models of stroke and BB-1101 has been shown to reduce the secondary brain oedema occurring after haemorrhage (Mun-Bryce *et al.*, 1998).

MMPs could contribute to damage following ischaemia by a number of mechanisms:

- 1) degradation of the blood brain barrier causing oedema. MMPs have been shown to contribute to the breakdown of the BBB directly due to its matrix degrading properties and indirectly due to its ability to stimulate cytokine production.
- 2) degradation of the extracellular matrix allowing migration of inflammatory cells to the site of the region of ischaemic injury.
- 3) increasing or decreasing the release of cytokines and growth factors from inflammatory cells. For example MMPs are involved in the cleavage of the latent form of TNF to produce the active form.

In response to injury or an inflammatory stimulus, the CNS will respond with an immune response, which causes the release of inflammatory cytokines, leading to the recruitment of lymphocytes and neutrophils, activation of microglia, the release of TNF- $\alpha$  and IL-1 $\beta$ , with the consequent breakdown of the BBB.

The contribution of MMPs to BBB breakdown has been examined. In one such study (Mun-Bryce *et al.*, 1998), brains injected with lipopolysaccharide (LPS, a potent inflammatory stimulus) showed a rise in active gelatinase B production after 24 hours and found latent gelatinase B at 4,8 and 24 hours. BB-1101, an MMP inhibitor was found to reduce levels of gelatinase A and B in LPS injected brains and also reduced the uptake of  $^{14}$  C sucrose, which would suggest reduced BBB breakdown.

The fact that CNS cells known to be involved in inflammatory processes such as microglia, astrocytes and macrophages express MMPs, would seem to support the idea that these cells are using the MMP's matrix degrading properties to allow them to migrate to the area of damage within the brain following ischaemia.

An indication that this indeed might be the case comes from the fact that MMPs have been shown to be expressed when inflammatory cells such as T-cells adhere to endothelial cells (Romanic & Madri, 1994; Aoudjit *et al.*, 1998) and that this expression might be to allow the T-cells to use the degrading properties of the MMPs to migrate to sites of damage or inflammation.

The induction of MMPs especially MMP-2 in T cells would seem to rely on the expression of one particular cell adhesion molecule- vascular adhesion molecule-1 or VCAM-1. It has been shown that T-cells only express MMP-2 activity when they adhered to VCAM-1 positive cells (Romanic & Madri, 1994). Adhesion to VCAM-1 negative cells did occur but was not induced by MMP-2.

The same process would also seem to occur for MMP-9 and the cell adhesion molecule ICAM-1 or intercellular adhesion molecule-1 when lymphoma cells bind to endothelial cells (Aoudjit *et al.*, 1998).

Adhesion of the T-lymphoma cell to the endothelium induces de novo expression of MMP-9 and enzymatic activity by both cell types. This expression of MMP-9 allows the migration of the T-lymphoma cells to surrounding tissue.

These cells seem capable of releasing and using MMPs to migrate and therefore it would seem plausible that inflammatory cells involved in ischaemic damage could do the same allowing them to break through the extracellular matrix and reach the area of infarction and the surrounding tissue in the peri-infarct region. MMPs both

stimulate and are capable of inactivating cytokines. TNF-alpha and the pro-inflammatory cytokine IL-1-beta can be cleaved and inactivated by MMP-1,2,3 and 9. Cytokines also have the ability to interfere with the MMP network and increased cytokine levels can lead to increased activation of the latent forms of the MMPs.

The ability of the MMPs to increase MMP levels may be due to their involvement in the cleavage of the pro peptide TNF-alpha to the active form. It has been shown in studies that MMP inhibitors such as BB-1101 were not only capable of reducing MMP activity but also that of the cytokine TNF-alpha.

### **Regulation of MMP activity- Inhibition**

Due to the ability of MMPs to cause widespread tissue damage their regulation is under strict control.

The activity of the MMPs can be regulated at various points including transcription, secretion and activation which is almost certainly advantageous in terms of reducing MMP levels in conditions where they are thought to contribute greatly towards the pathology of the disorder. Various control mechanisms are in place to prevent uncontrollable degradation by MMPs once they have been secreted from their site of synthesis. MMPs are only secreted from their cellular source in response to well defined signals which arise when MMP degradation is essential, for example in wound healing and scar formation. Once secreted from a cell, the MMP commonly remains associated with the cell either by remaining bound to the cell surface or matrix components or by remaining in close proximity to the cell. Another important

control mechanism is the fact that most MMPs are secreted in the latent form and so require activation before being capable of degradation.

Inhibition of MMPs allows the control of MMP levels. An imbalance can result in the development of pathological conditions and it is thought that metastasis can occur at a faster rate if naturally occurring inhibitor activity is in some way reduced. It can also lead to profound effects on the composition and the adhesion, migration and differentiation of cells at the ECM.

Under physiological conditions within the body, inhibition of MMPs is primarily carried out by the naturally occurring inhibitors of metalloproteinases including the tissue inhibitors of metalloproteinases or TIMPs (Beckett *et al.*, 1998) and the large alpha 2-macroglobulin produced by the liver. Synthetic MMP inhibitors are also available such as barimastat (BB-94) and marimastat (BB-2516) which are potent and specific inhibitors of the metalloproteinases.

### **Naturally Occurring Inhibitors of MMPs**

Various naturally occurring inhibitors of MMPs exist. One of the most important members of this group is the Tissue Inhibitor of Metalloproteinases (TIMP) family of enzymes. The TIMP family was first identified in 1975 and four members of the family have been identified to date- TIMP-1, -2, -3, -4 ranging in molecular weight from 20.6-22.3 kDa. TIMP-1, -2 and -3 are capable of inhibiting most members of the MMP family while TIMP-4 specifically inhibits MMP-1, -2, -3, -7 and -9.

TIMP-1 (28 kDa) is perhaps the most important of the TIMPs and its activity was first reported in 1975 in the medium of cultured human fibroblasts (Bauer *et al.*,

1975). It is thought that invasion and metastasis could be inhibited by transfection of malignant cells with TIMP-1. But in some forms of cancer (e.g. bladder cancer) there was a higher degree of invasion and metastasis with increased levels of TIMP-1 and TIMP-2 suggesting a beneficial response is dependent on the type of cancer and the MMPs involved.

TIMP-2 (20 kDa) was discovered when reverse zymography was developed and 2 TIMP forms were identified, one at 28 kDa (TIMP-1) and another at 20 kDa which was later named TIMP-2 (Raynes et al., 1988). TIMP-2 has about a 40% homology with TIMP-1. It has the ability to down regulate the activity of MMP-1, MMP-2 and MMP-9. TIMP-2 is also believed to play a role in metastasis and tumour invasion with TIMP-2 expression possibly denoting a stromal response to tumour invasion especially in breast carcinoma.

TIMP-3 (21 kDa) has a similar structure to TIMP-1 and TIMP-2 in terms of amino acid sequences. High levels of TIMP-3 are found in kidneys, lungs and brain where it is thought to play a large part in tissue remodelling.

TIMP-4 has recently been identified by molecular cloning (Greene *at al.*, 1996) with the highest levels found in the heart and lower levels in the colon, kidney and placenta. TIMP-4 has been shown to inhibit MMP-1, -2, -3, -7 and -9.

In addition to the ability of the TIMPs to inhibit MMPs they are also believed to play a role in growth factor activity, steroidogenesis and cell morphology modulation.

In terms of which domains of the TIMP molecule are involved in the MMP inhibition, the most important domain is the N-terminus domain which consists of 1-126 amino acid residues and can bind tightly to MMP-1, -2, -3, -7 and -9. TIMP-1 and TIMP-2 particularly rely on the N-terminus domain for their main inhibitory

action. The C terminus domain of the TIMP also plays an important role in inhibition of MMPs. Although the C-terminus domain doesn't bind tightly to MMPs it associates with the hemopexin domain on the MMP which allows proper alignment of the TIMP at the active site of the MMP.

TIMP-1 has been shown to be co-ordinately regulated with MMPs and in some situations reciprocally regulated. For example, TIMP expression can be regulated by substances such as phorbol esters and interleukin-1 beta which are capable of stimulating both TIMPs and MMPs and TGF- beta1 which is capable of up regulating TIMP-1 and down regulating MMPs. TIMP-1 production can be stimulated and or suppressed by TNF-alpha depending on the concentration i.e. stimulation of TIMP-1 at lower concentrations and suppression at higher concentrations (Woessner, and Nagase, 2000) There is also a possibility that there may be some hormonal control of TIMPs with regard to their role in cancer. One study has shown that treatment with progestin either alone or in combination with estradiol, down regulates TIMP-2 production by 50% (Woessner, and Nagase, 2000) In addition to TIMPS other MMP inhibitors include antibiotics (erythromycin, rifamycin); tetracyclines (minocycline, doxycycline); propeptides of MMPs (pro-MMP-2, pro-MMP-3) and macroglobulins ( $\alpha$ -macroglobulin).

Naturally occurring antibiotics which inhibit MMPs act by a chelation mechanism of the active zinc atom at the MMP active site, which is then removed from the MMP and the enzyme is joined with a second molecule of chelator.

Members of the tetracycline group of antibiotics also have chelating properties which may help to explain their inhibition of MMPs. *In vitro*, minocycline has been shown

to reduce the activity of collagenase (MMP-8) in periodontal disease by up to 90% at a concentration of 20 $\mu$ g/ $\mu$ l (40 $\mu$ M) (Golub *et al.*, 1983). Although the actions of tetracyclines is clearly inhibitory in vitro, in vivo the inhibition is more of a down regulation rather than chelation of the MMP.

Another naturally occurring inhibitor of the MMPs is  $\alpha$ -macroglobulin.  $\alpha$ -macroglobulin is a compound found in human serum. It has a molecular mass of 725kDa. The  $\alpha$ -macroglobulin is capable of binding to all of the MMPs regardless of their substrate specificity. The binding and inhibition of the MMP is initiated by proteolysis of the 'bait' region located near the middle of the subunit. This binding causes conformational changes in the  $\alpha$ -macroglobulin and entraps the proteinase. Although the entrapment doesn't completely block the active site of the MMP, it prevents the MMP from binding to large substrates.

### **Synthetic inhibitors of MMPs**

Synthetic inhibitors have been tested in experimental stroke models and have been shown to significantly ameliorate ischaemic damage. It is therefore possible that these drugs may prove valuable as part of the therapeutic strategy against stroke. Batimastat is a low molecular weight inhibitor of MMPs. Its ability to inhibit the MMPs comes from its collagen like backbone, which facilitates binding to the active site of the MMP. It also has the ability to chelate the zinc ion in the active site due to its hydroxamate structure.

Studies so far have shown that there are virtually no toxic side effects of Batimastat in animals with prolonged survival times in some models of carcinoma. For example Batimastat prolongs survival time several fold and suppressed malignant ascites formation in human ovarian carcinoma xenograft in athymic nude mice. Similar results have been shown with the synthetic inhibitor marimastat.

These drugs are capable of binding to the catalytic domain of the metalloproteinases and rendering them incapable of enzymatic activity.

It is therefore apparent that inhibitors of MMPs, be they synthetic or naturally occurring, may also prove useful as a therapeutic tool against cerebral ischaemia.

#### **1.4.3.4 Free radicals**

Free radical production is believed to contribute to ischaemic damage and or reperfusion injury mediated damage (Figure 12 ).

Free radicals are produced as part of the inflammatory response and can also contribute to the inflammatory process causing further stimulation of inflammatory cells.

Brain cells produce significant amounts of free radicals as by-products of the mitochondrial respiratory chain, from which they derive a large fraction of their total energy supply, and as by-products of enzymatic reactions (eg lipo-oxygenase, cyclo-oxygenase)

The brain is particularly sensitive to free radical mediated damage following ischaemia due to its high lipid content and to a loss in the normal equilibrium between anti-oxidants and free radicals. Under normal circumstances in the brain

there are sufficient levels of anti-oxidants to mop up free radicals. However as a result of damage resulting from ischaemia low levels of anti-oxidant enzymes including catalase, superoxide dismutase and glutathione peroxidase which normally act to neutralise free radicals produced by the electron transport chain and are unable to cope with the increased free radical production (Siddiqi *et al.*, 1996). As well as low levels of these neutralising enzymes following ischaemia, the brain possesses a large amount of iron which can catalyse free radical production and large amounts of polyunsaturated fats such as arachidonate which can undergo free radical mediated lipid peroxidation (Siddiqi *et al.*, 1996).

During a stroke, damage caused by the initial ischaemic insult can lead to uncontrolled free radical production. Oedema and increased BBB permeability resulting from ischaemia can cause the movement of red blood cells into extracellular spaces. As these red blood cells along with neurons and glial cells in the infarcted area disintegrate and die, iron and copper complexes are formed and released into the tissue spaces. Normally radicals such as the hydroxyl radical ( $\text{OH}^\bullet$ ) are produced by superoxide generating systems such as the Haber-Weiss reaction (Figure 13a). The Haber Weiss reaction produces hydroxyl radicals in the presence of hydrogen peroxide but the reaction will not have much biological significance in the absence of a catalyst. It is only when a catalyst such as iron is present that the reaction proceeds at a fast enough rate to produce significant and potentially damaging levels of hydroxyl radicals. The iron and copper complexes released during ischaemia therefore act as catalysts to increase free radical levels and subsequently increase cellular damage (Figure 13b).

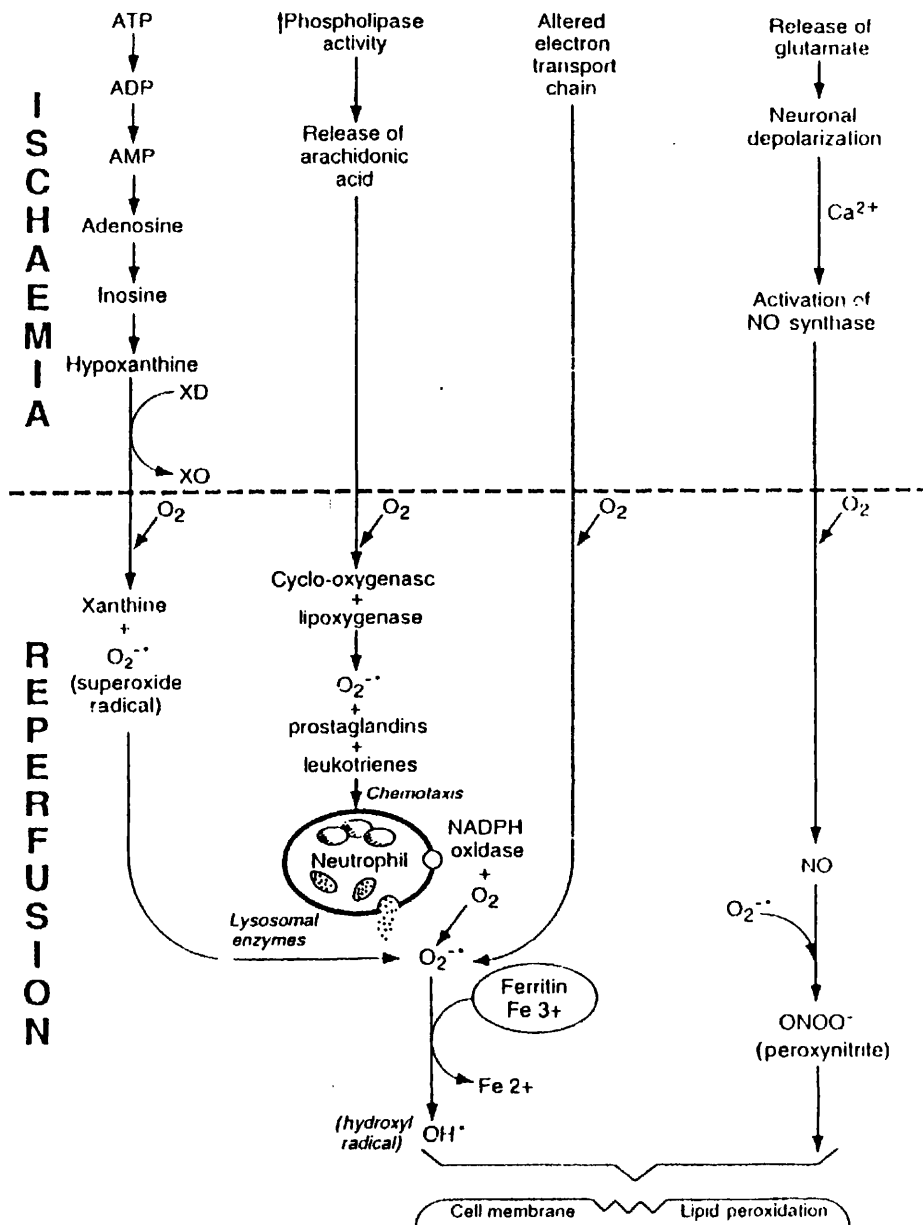


Figure 12 Free Radical Involvement in Ischaemia and Reperfusion. From Siddiqi *et al.*, 1996.

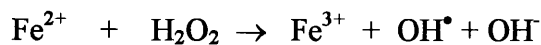
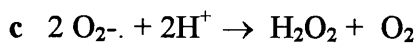
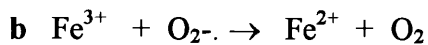
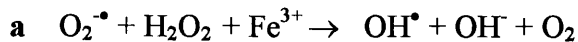


Figure 13a - Haber Weiss reaction 13b- Iron catalyses  $\text{OH}^{\bullet}$  production, 13c-Fenton reaction. (Siddiqi *et al.*, 1996) .

The damage caused by free radicals includes alteration in membrane fluidity and permeability, disruption of cellular and membrane function and integrity, an increase in blood brain barrier permeability, DNA damage, destruction of essential enzymes, activation of latent enzymes such as the calpains, necrosis and oedema. All of these actions also contribute to the intensification of the inflammatory response following ischaemia.

The most damaging oxidant species tend to be those generated from molecular oxygen (Butterfield & McGraw , 1978). These include the superoxide anion ( $\text{O}_2^{\bullet-}$ ), hydrogen peroxide ( $\text{H}_2\text{O}_2$ ) and the hydroxyl radical ( $\text{OH}^{\bullet}$ ). Of these, the hydrogen peroxide and the hydroxyl radicals are the most potent and the most damaging to brain tissues when produced in levels exceeding those that the endogenous neutralising enzymes can normally cope with .

Various studies support a role for  $\text{OH}^{\bullet}$  in ischaemic damage (Nakashima *et al.*, 1999; Mori *et al.*, 1999; Takamatsu *et al.*, 1998). These studies have demonstrated elevated levels of free radicals following ischaemia and have shown that the

administration of OH<sup>\*</sup> scavengers such as mannitol and dimethylsulphoxide (DMSO) can ameliorate ischaemic damage (Halliwell & Gutteridge, 1995).

Elevation of superoxide free radicals have also been demonstrated in a number of studies of ischaemic damage and reperfusion injury (Beetsch *et al.*, 1998; Fabian & Kent, 1999). The studies would suggest that during ischaemia and reperfusion, activation of some of the enzyme systems responsible for the conversion of oxygen to the superoxide radical occurs and contributes to membrane damage to cerebral vessel walls (Siddiqi *et al.*, 1996).

Two enzyme systems which have been suggested to contribute to such damage are the xanthine oxidase system and the nicotamide- adenine nucleotide phosphate with the reduced form NADP(H), NADH(H) oxidase system which is associated with free radical production in neutrophils.

The xanthine oxidase system has been investigated most in terms of its potential contribution of free radical mediated ischaemic damage. Recent studies have reported increased levels of xanthine oxidase in the ischaemic brain, which may lead to the subsequent generation of free radical species (Linas *et al.*, 1990; Nishino, 1994).

Xanthine Oxidase, an enzyme with the ability to produce oxidising agents such as the superoxide free radical and hydrogen peroxide exists in two forms: a nicotamide dinucleotide (NAD) dependent dehydrogenase (Type D) and an oxygen dependent superoxide-producing oxidase (Type O). The type D form appears to predominate in most tissues (Mori *et al.*, 1998).

Studies investigating the effect of xanthine oxidase activity on ischaemic damage (Patt, *et al.*, 1988 ) have shown that xanthine oxidase inhibitors such as tungsten and dimethyl urea are capable of reducing brain XO activity, or reducing brain  $H_2O_2$  and subsequently reducing cerebral oedema. These observations would suggest that  $H_2O_2$  formed by XO contributes to ischaemia and reperfusion mediated oedema in brains subjected to temporary ischaemia.

As well as free radical generation occurring from altered xanthine oxidase activity, experimental evidence would seem to suggest that increased superoxide free radical generation could also occur as a result of an increase in the activity of the cyclooxygenase pathway in the walls of damaged vessels (Hallenbeck & Dutka, 1990). The sequence of events involves an increase in phospholipase activation, leading to an increase in arachidonate and a subsequent increase in the generation of free radicals (Abe *et al.*, 1993; Yashuda *et al.*, 1999).

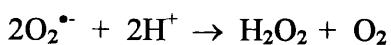
The endogenous inflammatory cells, the microglia, also provide a potential source of free radicals and cause cell damage by releasing free radicals (Sharkey *et al.*, 1996).

Regardless of the origin of free radical production, they potentiate ischaemic damage by a number of different mechanisms. These include causing membrane damage to cerebral vessel walls, leading to fluid leakage and oedema, damage to DNA, carbohydrates, proteins and enzymes, cause inactivation of ion pumps, impairment of receptor function and excitotoxic neuronal cell death (Siddiqi *et al.*, 1996).

Free radical scavengers and inhibitors have been shown to reduce brain damage following ischaemia and this is particularly true for damage occurring during reperfusion (Schmid-Elsaesser *et al.*, 1999; Phillis *et al.*, 1998).

Free radical scavengers such as the endogenous neutralising enzymes superoxide dismutase (SOD), catalase and glutathione peroxidase have been used experimentally to reduce ischaemic damage.

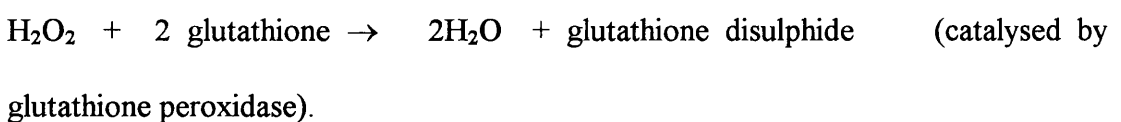
SOD enzymes Mn-SOD and CuZn-SOD found in the mitochondria and the cytosol, respectively, catalyse the reaction in which superoxide ions are converted to hydrogen peroxide:



In the second step of the process catalase and glutathione peroxidase convert the  $\text{H}_2\text{O}_2$  to water:



or



Transgenic mice over-expressing SOD have been shown to exhibit reduced cerebral infarct size after MCAO compared to wild-type compared to wild-type mice (Sheng *et al.*, 1999; Nikawa *et al.*, 1995; Kinouchi *et al.*, 1991). Studies administering PEG-SOD, and the glutathione peroxidase mimic, ebselen (Dawson, 1993; Tasksgo *et al.*, 1997) have also shown reduced ischaemic damage (Repine, 1990; Beetsch *et al.*, 1998).

### 1.4.3.5 Calcium

An alteration in the level of intracellular calcium following ischaemia was first suggested as a possible contributory factor to ischaemia by Siesjo and co-workers .

Under normal conditions, the intracellular calcium concentration is  $10^{-7}$  M compared to an extracellular concentration of  $10^{-3}$  M (Hallenbeck and Dutka, 1990)). These concentrations are kept stable by the presence of ion pumps such as the  $\text{Ca}^{2+}$  extruding pump ( $\text{Ca}^{2+}$  ATP ase) and an electrogenic  $\text{Na}^{+} / \text{Ca}^{2+}$  exchanger and pumps that sequester  $\text{Ca}^{2+}$  into intracellular stores with concomitant loss of ATP cell depolarisation and excess activation of ionotropic receptors which allow  $\text{Ca}^{2+}$  influx (e.g. NMDA) and voltage gated  $\text{Ca}^{2+}$  (Hallenbeck and Dutka, 1990)

channels. During ischaemia, failure and reversal of ion pumps and membrane leakage leads to increases in intracellular calcium concentration with further increases during reperfusion.

A rise in intracellular calcium levels can lead to damage caused by increased free radical production , tissue disruption , latent enzyme activation and release, reduction of high energy phosphate stores, neurotransmitter release and activation of second messenger systems leading to neuronal excitability (Figure 14).

Reperfusion mediated damage to cell membranes can also lead to a rise in calcium due to substances released during reperfusion directly damaging cell membranes. Other ways in which calcium levels can be elevated include interference with the sodium adenosine triphosphate pump function normally responsible for the exchange of sodium into and calcium out of the cell.

Various studies looking into the benefits of calcium channel blockers have been carried out with mixed results (Nakayami *et al.*, 1988; Grotta *et al.*, 1988). Early studies blocked the L-type calcium channels found in blood vessels which produced the unwanted side effect of hypotension.

This haemodynamic effect often counteracted any beneficial effect of calcium channel blockade in the CNS. More recent studies have concentrated on using N-type (neuronal) calcium channel blockers which offer greater selectivity for neurons over the vasculature.

It is also generally accepted that rises in intracellular calcium can occur without resultant permanent cellular damage and so the role of altered calcium homeostasis in reperfusion injury remains a possibility requiring further investigation.

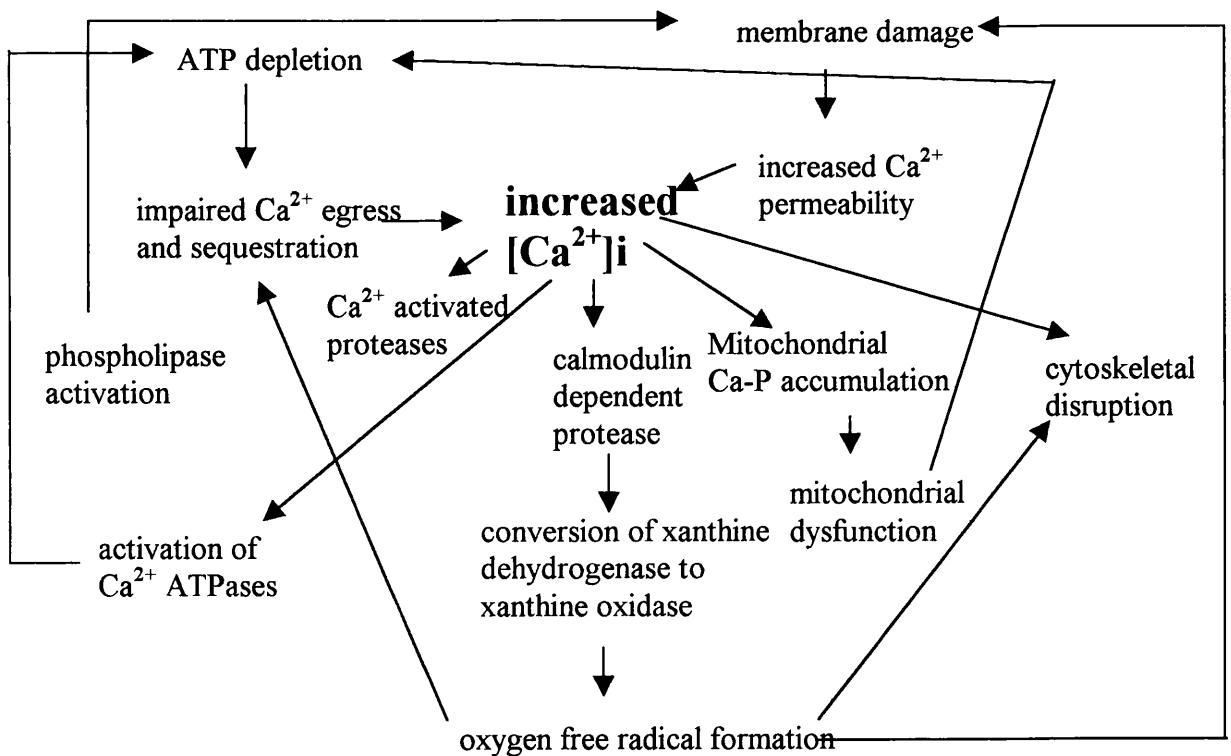


Figure 14. Involvement of calcium in reperfusion injury.

## **Chapter 2. Methods**

### **2.1 Surgical Procedures**

#### **2.1.1 Preparation of Animals for surgery**

Animals undergoing middle cerebral artery occlusion were housed under a 12 hour light-dark cycle and were given free access to food and water.

Animals were placed in a perspex chamber and anaesthetised with 5% halothane (30:70 oxygen, nitrous oxide mix) for 3-4 minutes then intubated with a 16-gauge cannula (the stainless steel guide needle inside the cannula was blunted before use). Intubation involved suspending the animal from a silk thread loop around the top teeth, on a corkboard propped up between two lead blocks. The animals tongue was gently held to the side and the intubation tube slowly inserted into the trachea with the aid of a fibre optic light to visualise the opening to the trachea. The intubation tube was attached to a ventilation pump and the animal mechanically ventilated with anaesthetic gases for the remainder of the surgical procedure. For recovery procedure (AB) the pump was set at 60 cycles per minute, for acute procedures (AC) the pump was set at 42 cycles per minute. The stroke volume was adjusted according to the weight. Following intubation, halothane level was dropped to 1.5%-2% and maintained at this lower level throughout the subsequent surgical procedure. A rectal probe was used to monitor body temperature within normal limits (36.7-37.2°C) in

order to prevent the effects of hypothermia or hyperthermia on the infarct size (Corbett and Thornhill, 2000). Measurement of blood gases (278 Blood Gas System, CIBA Corning, UK), blood glucose (Glucose Analyser 2, Beckman, UK) and blood pressure (Biopac) were made via cannulation of the femoral artery using a polythene cannula (0.58mm ID, 0.96mm OD). The cannula, containing heparinised saline, was inserted for a distance of around 1 cm and tied in place with 4/0 silk suture. A small amount of Xylocaine anaesthetic gel was applied to the wound and superglue was used to secure the cannula in place. The wound was sutured with 4/0 silk following the completion of the surgical procedure. For recovery animals the cannula was externalised at the nape of the neck and at the end of the experimental procedure, filled with heparinised polyvinylpyrrolidone (PVP, Appendix A) to maintain a patent line. For the externalisation a small incision was made in the nape of the neck and a stainless steel guide cannula (International Market Supply, UK) was used to pass the cannula subcutaneously to the exit point.

### **2.1.2 Intraluminal Thread model of ischaemia**

Method used was Longa et al., 1989. (Figure 15)

A midline incision was made in the neck of the animal to expose the underlying muscle covering the trachea and surrounding blood vessels. The muscles were carefully teased apart, retractors inserted and connective tissue cleared to expose the

external and common carotid arteries. These were carefully separated from surrounding nerves and fascia and occipital branches of the external

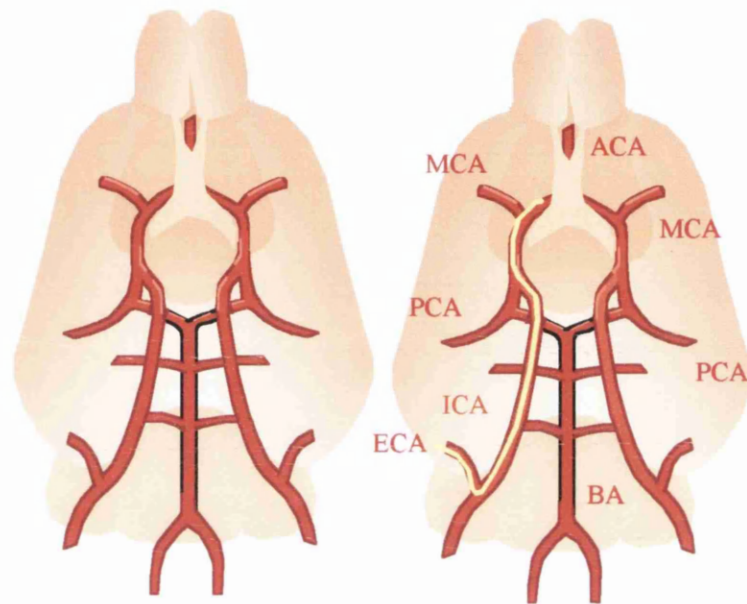


Figure 15. Intraluminal thread model of ischaemia, modified version of Longa *et al.*, 1989.

— Filament inserted for a distance of around 22mm to block the origin of the MCA at the circle of Willis.

MCA- Middle Cerebral Artery, ACA- Anterior Cerebral Artery

PCA- Posterior Cerebral Artery, ECA- External Carotid Artery

BA- Basilar Artery.

carotid coagulated and cut. The maxillary and lingual artery branches were dissected and coagulated. The internal carotid, after being freed from occipital branches, was separated from the vagus nerve and the pterygopalatine artery exposed and ligated with a 6/0 suture at the bifurcation with the internal carotid. A 6mm micro-clip (Johnson & Johnson) was applied to the internal carotid at the bifurcation with the pterygopalatine and a second clip applied at the bifurcation between the internal and the external carotid. A loose tie (6/0 suture) was placed on the external carotid above the bifurcation and the maxillary and lingual branches cut. The external branch was held and an incision made in the vessel. A 3/0 nylon mono-filament with rounded tip (0.28-0.3mm OD for rats 300-350g) was inserted into the external and advanced to the clip on the internal carotid artery. The tie around the external was tightened to hold the filament in place and the clip removed to allow the filament to be advanced beyond the origin of the posterior cerebral artery and past the origin of the middle cerebral artery (approximately 22mm in animals within the weight range 270-320gms). All direct sources of perfusion from the ICA, ACA and PCA to the MCA are now blocked. The tie was then tightened to secure the filament in place.

To induce reperfusion, the filament was gently removed, the hole in the external carotid coagulated and clips and ties removed.

Sham animals had the filament inserted and then removed immediately to simulate possible mechanical damage associated with the filament.

### 2.1.3 Permanent ischaemia by electrocoagulation

Method used was a modified version of Tamura *et al.*, 1981. (Figure 16)

Surgery was carried out with the aid of an operating microscope. The animal was placed on its side and a 1.5-2 cm incision made between the left orbit and the left auditory canal. The underlying temporalis muscle was divided along its fibre bundles and retractors inserted to expose the zygomatic arch (Unlike previous methods, the zygomatic arch remains intact throughout the surgical procedure to facilitate recovery). A dental drill was used to shave away bone from under the zygomatic arch and a craniectomy made to expose the distal MCA. The craniectomy site and the drill tip were kept cool using sterile saline to prevent heating artefacts and damage. A sterile 30 gauge dental needle was used to firstly pierce and then pull back the dura to expose the middle cerebral artery running over the ICV. The MCA was electrocoagulated by diathermy, distally, for a distance of around 1-1.5mm just distal to the ICV and proximal to the first major bifurcation of the MCA (Figure 16).

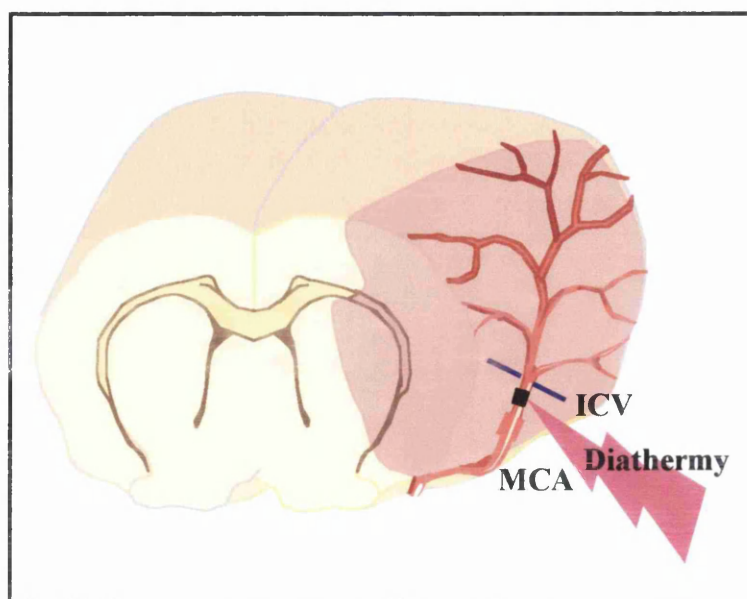


Figure 16. Permanent MCAO by diathermy

Following electrocoagulation, the MCA was cut using micro scissors to ensure complete occlusion. Retractors were then removed and muscle allowed to fall back into place after which the muscle and skin were sutured and the animal allowed to recover for 4, 24, 48 or 72 hours before being transcardially perfused with 4% paraformaldehyde in PBS (Appendix A).

#### **2.1.4 LPS stereotaxic injections (for generation of positive control material for immunohistochemistry)**

The stereotaxic frame was set up before the animal was put in place, the side arm was aligned, the Hamilton syringe attached to the suspended arm and screwed into place. The dorsal surface of the head was shaved, swabbed with alcohol and the animal placed into the frame with the tooth bar set at  $-3.5\text{mm}$ . A special nose cone allowed the anaesthetic gases to be delivered to the animal. A midline incision (1-1.5cm) was made in the scalp and skin and muscle retracted to expose the skull. Any remaining muscle and connective tissue was scraped away to reveal bregma. The co-ordinates for the LPS needle placement (RC 0.26mm, L2mm, V2mm) were identified in relation to bregma and a fine ink mark made on the skull. A saline cooled dental drill was used to make a small craniectomy and the dura pierced with a sterile 30 gauge dental needle. A 10 $\mu\text{l}$  Hamilton syringe attached to the stereotaxic frame was gently lowered according to the co-ordinates and 2 $\mu\text{l}$  of lipopolysaccharide (*Escherichia Coli*, serotype 055-B5, Sigma, UK) slowly injected over 2 minutes. The

needle was kept in place for 10 minutes before being slowly retracted. The muscle and skin were then sutured and the animal allowed to recover for 24 hours.

### **2.1.5 Recovery of animals following surgery**

Following induction of middle cerebral artery occlusion wounds were sutured with 4/0 silk. A subcutaneous injection of 3 mls of sterile saline was given to prevent dehydration due to loss of body fluids during surgery and recovery. In intraluminal thread animals where there is the possibility of Vagus nerve stimulation, 0.3-0.5 mls of atropine (0.1mgs/Kg; Atropine sulphate, Phoenix Pharmaceuticals Ltd., UK) was administered to prevent the build up of mucus and subsequent breathing difficulties. Halothane was discontinued and oxygen administered until the animal showed signs of consciousness. When the animal started to breathe spontaneously, the intubation tube was removed and when fully conscious, and the animal moved to a recovery room and monitored throughout the recovery period. Soft diet was provided to encourage eating.

## **2.2 Processing of Tissue for H&E and for Immunohistochemistry**

### **2.2.1 Fixation**

Once a piece of tissue has been removed from an organism it will lose all of its microscopic features and structure unless the tissue is preserved. Non preserved tissue faces potential damage from osmotic swelling or shrinkage, attack from bacteria, autolysis and evaporation. To prevent the above from happening, tissues can be preserved using solutions which allow the tissue to be kept for long periods of time and also to undergo treatments or processes without damaging the original state of the tissue (common processes leading to damage include embedding, sectioning and mounting). Fixation can be either chemical or heat based. Chemical fixation is favoured today and results in less distortion than heat fixing material.

Fixatives can be divided into two groups- coagulating (methanol, ethanol, HCl and picric acid) and non-coagulating (formaldehyde, paraformaldehyde, acetic acid, potassium dichromate). Coagulating fixatives like methanol create protoplasm networks while non- coagulating fixatives like paraformaldehyde do not. The choice of fixative for individual experiments depends on what the material is to be used for and how long the material has to be preserved for. In most of the studies in this thesis the fixative of choice was paraformaldehyde.

For acute experiments: Following the surgical procedure, the percentage of halothane was increased to 3% for a period of around 5 minutes to deepen anaesthesia. An incision was made below the sternum to expose the rib cage. The diaphragm was cut

away from the rib cage and the rib cage cut at either side to expose the heart. A 12 gauge needle attached to the perfusion apparatus was inserted into the apex of the heart and advanced into the aorta until visible. The needle was clamped in place and the right atrium punctured. A constant pressure (equivalent to the average blood pressure of the anaesthetised animal during the surgical procedure) was applied to allow the perfusion of 300-350mls of heparinised saline. When saline outflow from the atrium was bloodless, 300-400mls of fixative (4% paraformaldehyde in PBS, Sigma, UK) was perfused until the animal was drained of colour and rigid to the touch. The perfusion needle was removed, the animal decapitated and the head placed in 4% paraformaldehyde for 24-48 hours which allows a more rapid penetration of the tissue. The length of time tissue should be left in fixative is debatable as the minimum length of time required depends on the rate of penetration of the fixative used. Fixatives such as formaldehyde/ paraformaldehyde continue to act progressively on tissue after it has penetrated the tissue. Periods of 24-48 hours seem to be commonly used but prolonged fixation is rarely detrimental to the condition of the tissue (Baker, 1968).

For chronic experiments: Animals were placed in a perspex box and anaesthetised with 5% halothane in a 30:70 oxygen: nitrous oxide mix for 3-5 minutes. Anaesthesia was then delivered via a facemask, halothane dropped to 3% and the fixation procedure carried out as above.

### **2.2.2 Post fixation**

Following 24-48 hours post-fixation in 4% paraformaldehyde in PBS, the brain was removed from the skull and placed in 4% paraformaldehyde for 24 hours. For cryostat cut sections, the brain was removed from the skull and placed in 30% sucrose solution (cryoprotectant) for 3-5 days or until sunk. For paraffin processing, the brain was removed and kept in fixative before processing.

### **2.2.3 Cutting cryostat sections for immunohistochemistry**

Brains were removed from 30% sucrose and frozen for 5 minutes at -42°C in isopentane (Fischer Chemicals, UK). The brain was then mounted using OPC (Sigma, UK) and 20µm coronal sections cut at -22 °C to provide sections throughout the eight coronal levels used to cover the MCA territory (Osborne *at al.*, 1987), picked up on poly-l-lysine coated slides (Appendix A) or collected in cryoprotectant in cell wells for mounting on poly-lysine slides at a later date. Sections on poly-lysine slides were left overnight at room temperature to dry and then stored at -80°C until used for immunohistochemistry or traditional histology.

## **2.2.4 Paraffin processing**

Brains were passed through a graded series of alcohols, then into xylene and finally into wax over a period of 3 days. (Appendix A).

Following processing and paraffin embedding, the brains were re-embedded and mounted onto wooden chucks for microtome cutting of 6 $\mu$ m thick coronal sections.

Paraffin processing is a common method of preparing sections for immunohistochemistry as multiple sections can be obtained and stored easily. However at various points throughout the paraffin processing procedure the tissue may be subject to shrinkage. The fixation procedure itself doesn't usually cause shrinkage (it may indeed lead to swelling) but dehydration and embedding can lead to substantial shrinkage.

## **2.2.5 Infarct determination**

### **2.2.5.1 Haematoxylin & Eosin staining for determination of infarct**

Sections were washed in running water for 3 minutes. They were then passed through graded alcohols (70%, 90% and 100 % alcohol) for 2 minutes each then washed again in running water. Sections were placed in haematoxylin for 1-2 minutes and then washed. At this point the sections were examined under the light microscope to check for degree of haematoxylin staining. It is preferable to have only nuclear staining with a very faint background. If the staining is too intense the

sections can be differentiated in acid alcohol and washed to remove excess haematoxylin. When the desired level of staining had been achieved, sections were placed in Scots Tap Water Substrate for 2 minutes, washed in running water for two minutes and placed into aqueous eosin for 3 minutes. Following another wash, sections were passed through the graded alcohols for 2 minutes each and then placed in histoclear for 2-4 minutes prior to being mounted on coverslips using DPX (RA. Lamb Ltd.UK).

#### 2.2.5.2 Detection of ischaemic neurons for infarct determination

H&E staining allows the area of infarct to be clearly seen on a brain section at low magnification. The damaged area appears as an area of pallor on a darker stained background (Figure 17)

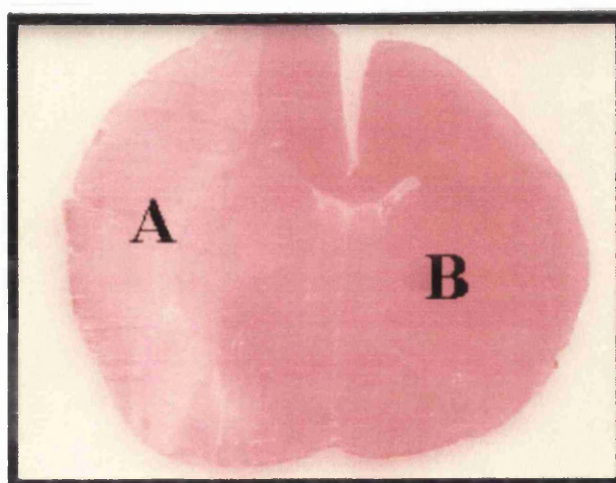


Figure 17. Haematoxylin and eosin staining of A. damaged hemisphere and B. contralateral hemisphere.

Focal ischaemia, leads to morphological changes in neurons and the presence of certain characteristics which make it possible to distinguish between a healthy neuron and an ischaemic neuron at the light microscopic level (Figure 18).

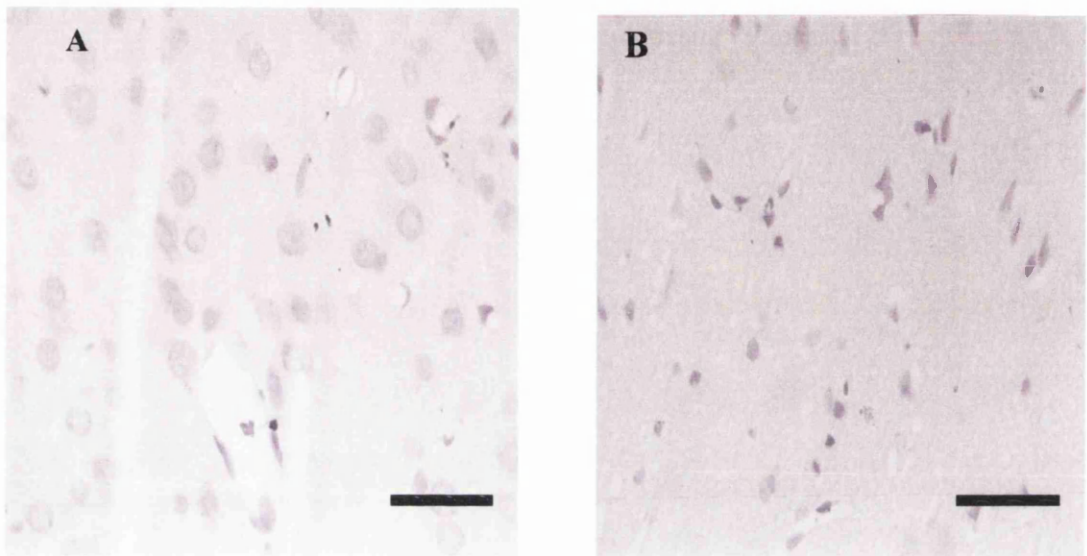


Figure 18. Morphology of neurons: A. healthy neurons and B. ischaemic neurons.

Ischaemic neurons undergo a series of changes termed the ischaemic cell process which normally starts with the formation of small circular/ oval spaces in the cytoplasm known as microvacuoles. These are swollen mitochondria and endoplasmic reticulum. Then a visible change in cell shape occurs with the cell body and the nucleus becoming shrunken and triangular in shape. The nucleus also becomes densely stained and the cytoplasm becomes eosinophilic. The next stage involves the formation of inclusions caused by the shrinking of the cytoplasm and the nucleus. Small densely stained circular bodies appear caused by the compression

of the cytoplasm by astrocytic processes. The process normally culminates in the neuronal cell taking on a pale and homogenous appearance and it is at this point that the cell can be said to be irreversibly damaged (Greenfield, 1992)

It is sometimes possible to mistake fixation artefacts for the above changes and for this reason it is important to achieve a good perfusion fixation at all times and to leave the brain within the skull in fixative for 24 hours before removing for processing. Changes such as dark cell change, hydropic cell change and the presence of peri-neuronal and vascular spaces can occur as a result of improper control of perfusion pressure or due to an inadequate volume of fixative being passed through the animal.

By identifying the characteristics of ischaemic neurons, the area of infarction can be identified to allow the mapping of the boundary of ischaemic damage for infarct size determination and for mapping of immunohistochemical staining.

### **2.2.5.3 Measuring Infarct Size.**

The light microscope was used to identify ischaemic neurons and mark the boundary of the infarct onto a line diagram consisting of eight coronal brain levels (Figure 19)

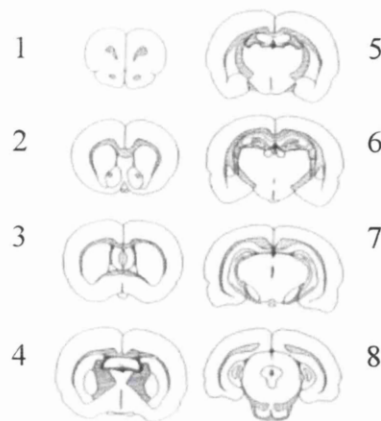


Figure 19. Line diagram representing the eight coronal levels, as described by Osborne *et al.*, 1987). Level of the: 1. Anterior Commissure; 2. Nucleus Accumbens; 3. Lateral Septal Nucleus; 4. Globus Pallidus; 5. Dorsal Hippocampus; 6. Lateral Habenular Nucleus; 7. Substantia Nigra; 8. Cerebral Aqueduct.

The area of the infarct at each of the eight levels was outlined and measured using a computer based imaging analysis system (MCID, Imaging Research Inc.). The system allows the counting of the number of pixels which constitute the outlined image, to give an area measurement. To allow expression of the data in units of area, the system was calibrated using a graticule of 40mm to allow the pixels to be calibrated with a spatial reference scale. The line diagram from each animal was placed under a video camera and the area of the infarct drawn round. The MCID was then able to count the number of pixels within the outline of the infarct and the mean area calculated by repeating the measurement three times and taking the average value for each coronal level. The volume of ischaemic damage in the ipsilateral hemisphere was calculated by integration of the 8 coronal areas ( $\text{mm}^2$ ) with the known distance between the stereotaxic co-ordinates of the levels.

## **2.2.6 Immunohistochemistry**

Immunohistochemistry was employed to identify different cell types and their contents within the brain. An antigen on the cell can be labelled in a series of steps culminating in the visualisation of the antigen at the light microscope level.

The first step in the process involves the application of a primary antibody which has the ability to bind to one (monoclonal) or more than one (polyclonal) antigenic sites. A secondary antibody, which is normally biotinylated, is then applied to bind to the primary antibody. The signal is amplified with the addition of an avidin-biotin complex (ABC) which binds to the biotin on the secondary antibody. In the final step in the immunohistochemical process, a visualisation substance, commonly diaminobenzidine (DAB), is used which reacts with the ABC to produce a visible brown deposit representing labelled cells or areas containing the substance of interest

### **2.2.6.1 Immunohistochemistry on cryostat cut sections**

The following immunohistochemical technique was used for the staining of microglial cells with monoclonal antibodies for the staining of microglia : Ox-42 antibody (1:1000, Serotec, UK); staining of astrocytes with GFAP (1:1000, Dako, UK); oligodendrocytes with tau-1 (1:1000, Dr D Hanger, Institute Psychiatry, University of London); and polyclonal antibodies for MMP-9: AB805 (1:100, Chemicon , UK) and C-20 (1:100, Santa Cruz, USA); MMP-8 antibody Se594

(1:100, British Biotech, UK); microglial marker mrf-1 (1:100, gift from Dr S Tanaka, Hokaido University, Japan) ; IL-1 $\beta$  antibody S328 (1:100, NIBSC, UK).

As a general rule, monoclonal antibodies used in this thesis were blocked with normal horse serum and an anti-mouse raised in horse secondary applied. For polyclonal antibodies, a normal goat serum was used followed by an anti-rabbit raised in goat secondary. The only exception to this was the IL-1 $\beta$  antibody which was blocked using normal donkey serum and an anti- sheep secondary raised in donkey used.

Immunohistochemistry was carried out over two days. Day 1: Sections were circled with a hydrophobic pen (DAKO) and the following steps carried out – sections were washed with 50mM PBS for 2 x 5 minutes, Triton X100 (30 $\mu$ l in 15 mls PBS, Sigma, UK) for 30 minutes, 2 x 5 minute wash with PBS, 10% H<sub>2</sub>O<sub>2</sub> in PBS for 20 minutes to quench endogenous peroxidase activity. After 2 x 5minute washes with PBS, sections were blocked with 10% normal horse/goat serum (or 20% normal donkey serum for IL-1 $\beta$ ) for 1 hour to suppress non-specific binding of the immunoglobulin then incubated with primary antibody at 4°C overnight.

Day 2: following a 2 x 5 minute wash with PBS, sections were incubated with the secondary antibody (1:100; biotinylated anti-mouse IgG raised in horse/ anti rabbit raised in goat or anti sheep raised in donkey, Vector, UK) for 1 hour (1hr 30 mins for mrf-1). After another 2 x 5 minute washes with PBS, sections were incubated with avidin biotin peroxidase complex (ABC reagent, Vector, UK) for 1 hour to enable visualisation of the immunoreactivity. Following ABC, diaminobenzidine

tetrahydrochloride (DAB, Vector, UK) was applied for 5-7 minutes or until colour had developed to enable positive staining to be visualised. Sections were then placed in distilled water for 20 minutes and counterstained with haematoxylin.

#### **2.2.6.2 Method for dehydration of sections and counterstaining with haematoxylin.**

Sections were washed in running water for 10 minutes then rehydrated by passing them through graded alcohols: 2 minutes in 70%, 90%, absolute alcohol and then 2 minutes in absolute, 90%, 70% alcohol. Sections were then washed in running water for 2 minutes. After 6 dips in haematoxylin, sections were washed in tap water (if

required sections can be differentiated in acid alcohol at this point), then were passed through graded alcohols for 2 minutes: 70%, 90%, absolute alcohol, 4 minutes in histoclear, mount using DPX (R. A. Lamb Ltd. UK).

#### **2.2.6.3 Immunohistochemistry on paraffin sections.**

Pre-treatment for paraffin sections: Sections were placed in histoclear for 10 minutes, then placed in absolute alcohol for 10 minutes then a further 5 minutes. After 30 minutes in 0.3% H<sub>2</sub>O<sub>2</sub> in methanol, sections were washed in distilled water for 20 minutes.

Pre-treatment to maximise staining: The fixation procedure and the paraffin embedding can mask some antigenic determinants. Treatment with heat (e.g. microwaving), enzymes and detergents can help to reveal the masked antigens.

**Microwaving with citric acid buffer:** Sections were placed in a citric acid buffer (1.05g of citric acid in 500mls of distilled water, pH 6.0), and microwaved on high for 5 minutes. The solution was topped up and reheated for a further 5 minutes and allowed to cool for twenty minutes before proceeding with the immunohistochemistry protocol- otherwise the steps for the paraffin treated sections were the same as laid out in section 2.2.6.1.

#### **2.2.6.4 Double label immunohistochemistry**

Double label immunohistochemistry was carried out for the following combinations of antibodies:

<b>1<sup>st</sup> DAB</b>	<b>2<sup>nd</sup> SG</b>
AB805 (MMP-9) + Mrf-1 (microglia)	
Se594 (MMP-8) + Mrf-1 (microglia)	
AB805 (MMP-9) + GFAP (astrocytes)	
Se594 (MMP-8) + GFAP (astrocytes)	
AB805 (MMP-9) + Tau-1 (oligodendrocytes)	
Se594 (MMP-8) + Tau-1 (oligodendrocytes)	

For paraffin sections dewaxing and pre-treatment was carried out as in section 2.2.6.3.

Immunohistochemistry was carried out over three days. Day 1: Following a 2 x 5 minute washes with PBS, sections were blocked with 10% normal goat /normal horse serum (Vector, UK) for 1 hour then incubated with the first primary antibody overnight at 4°C. Day 2: Following a 2 x 5 minute wash with PBS, secondary antibody (1:100, monoclonal anti-mouse IgG/polyclonal anti-rabbit IgG, vector, UK) was applied for 1 hour, following another 2 x 5 minute washes with PBS, ABC reagent was applied for 1 hour. 2 x 5 minute washes with PBS preceded VIP/DAB (Vector, UK) for 3-4 minutes or until pink colour develops.

A 2 x 5 minute wash with PBS was carried out prior to blocking with 10% normal horse serum/normal goat serum for 1 hour. Sections were then incubated with the second primary antibody overnight at 4°C. Day 3: Following 2 x 5 minute washes with PBS, sections were incubated with the second secondary antibody (1:100, monoclonal anti-mouse IgG or polyclonal anti-rabbit IgG, Vector, UK). Sections were washed with PBS and ABC reagent applied for 1 hour. Another 2 x 5 minute washes with PBS were carried out prior to application of SG (Vector, UK) for 3-4 minutes or until grey colour develops. Sections were then placed in running water for 20 minutes then rehydrated and mounted using DPX (R. A. Lamb Ltd. UK).

### **2.2.6.5 Fluorescence double labelling.**

For paraffin sections dewaxing and pre-treatment was carried out as in section 2.2.6.3. Immunohistochemistry was carried out over 3 days.

Day 1: Following 2 x 5 minute washes with PBS, sections were blocked with 10% normal horse serum/normal goat serum for 1 hour. They were then incubated with primary antibody at 4°C overnight.

Day 2: Following 2 x 5 minute washes with PBS sections were incubated with the secondary antibody (1:100, monoclonal anti-mouse IgG Texas Red labelled or polyclonal anti-rabbit IgG fluorescein labelled, Vector, UK) for 1 hour (sections should be kept covered and protected from light from this point on). After 2 x 5 minute washes with PBS sections were blocked with 10% normal horse serum/normal goat serum for 1 hour and incubated with the second primary antibody overnight at 4°C. Day 3: Sections were washed with PBS and the second secondary antibody (1:100, monoclonal anti-mouse IgG, fluorescein or polyclonal anti-rabbit IgG Texas\_Red, Vector, UK) applied for 1 hour. Sections were then mounted with special aqueous mounting media.

### **2.2.7 Controls for immunohistochemistry**

To ensure the efficacy and specificity of the stain obtained with an antibody, negative and positive control material was included in every immunohistochemistry run.

Negative controls followed the same protocol as standard sections but the primary antibody was omitted. Instead sections were incubated with blocker or PBS. The negative control should give an indication of the levels of non-specific background staining.

For the immunohistochemistry studies in this thesis, positive control material used had expression of inflammatory mediators to confirm positive staining with the inflammatory markers. Rat ischaemic tissue with either the presence of an abscess or meningitis as identified by a neuropathologist (Professor D.I. Graham, Southern General Hospital, Glasgow) was used to test the efficacy of the antibodies. Tissue injected with the inflammatory stimulus LPS was also used to test antibody efficacy.

## **2.3 Western Blotting**

### **2.3.1 Mini Gels**

Antibody specificity was checked with Western blotting to ensure that the band detected by the antibody on the gel was consistent with the molecular weight of the protein concerned.

For example, western blots were run to determine if antibody (AB805/ anti-MMP-9) was detecting the correct band in rat tissue.

### **2.3.2 Protein concentration determination**

After a recovery period of 24 hours, animals having undergone 24 hours intraluminal thread induced middle cerebral artery occlusion were re-anaesthetised, decapitated and the brains rapidly removed. Tissue from the MCA territory and from the cingulate cortex was dissected from both the ipsilateral and the contralateral hemispheres and snap frozen in liquid nitrogen and stored at - 80°C until required for Western Blotting.

Brain samples were homogenised 1:10 (weight to volume ratio) in Hepes buffer using a glass homogeniser. Samples were then homogenised for five minutes at 13000 rpm using a Beckman Microfuge E and the supernatant stored at -80°C until required. Supernatant samples were used to run protein assays (Lowry et al., 1951).

This involved diluting samples in homogenisation buffer (1:5 & 1:10) and vortexing. Samples were allowed to stand for 20-30 minutes at room temperature following vortexing. A standard curve using bovine serum albumin (BSA, Sigma, UK) was then prepared to allow determination of the protein concentration of the unknown samples. The Bio-Rad protein assay was the method used to determine the protein concentration of the samples. The following concentrations of BSA standards were prepared: 0.2,0.4,0.6,0.8 and 1.0mg.ml in homogenisation buffer. The absorbance of the BSA standards and samples were measured at 680nm using a spectrophotometer

(Pharmacia LKB, Ultrospec III) and a standard curve obtained. The absorbance of unknown samples protein concentrations were determined from the known protein concentration samples on the standard curve. Following the calculation of the protein content in the brain homogenates, samples were prepared in Laemmli buffer (1  $\mu$ l = 1  $\mu$ g protein).

### **2.3.3 Running of gels**

SDS Polyacrylamide Gel electrophoresis (SDS-Page).

Prior to the loading of the gel, glass plates were cleared with distilled water followed by alcohol. The plates were assembled and distilled water used to check for leaks. A mark was made on the plate 1 cm below the comb position. Resolving gel (Appendix A) was added to the plates up to the mark avoiding air bubbles and the gel overlaid with 0.1% SDS (Appendix A). The gel was allowed to set for 15-30 minutes after which time the SDS was poured off and stacking gel prepared (Appendix A). Stacking gel was poured into the apparatus and the comb inserted at an angle to avoid bubbles. The gel was allowed to set for 45 minutes. A gel loading pattern was constructed and a running buffer prepared. Prestained and biotinylated standards (Bio-Rad, UK) were defrosted and 5  $\mu$ l of stock added to 10  $\mu$ l of laemmli buffer (Appendix A). Standards and samples were boiled for 5 minutes and spun in a microfuge. Running buffer was poured into the inner reservoir and the outer reservoir of the electrophoresis tank. The combs were removed from the gel and samples and standards (10  $\mu$ l) injected into the relevant lanes using a Hamilton syringe. The power

pack was switched on and set to run at 200V until the proteins had run 1cm from the bottom of the gel. The gels were then prepared for transferring. Prior to transferring, 2 pieces of nitrocellulose (8.5cm x 6cm) were soaked in distilled water for 30 minutes and 24 pieces of filter paper (8.5cm x 6cm) in transfer buffer for 30 minutes. The platinum transfer plates were wiped with distilled water prior to transfer. After the gels had been removed from the electrophoresis apparatus and the SDS gel cut away and discarded, they were placed between 6 sheets of filter paper and a sheet of nitrocellulose placed on top. 6 sheets of filter paper were placed on top of the nitrocellulose and the process repeated for the second gel. The sheets were flattened between stages to remove air bubbles and excess liquid wiped from the transfer plates. The gels were transferred for 15 minutes at 15V.

Following the transfer step, the blots were incubated with T-TBS-M (5% Marvel, Appendix A) for 1 hour on a shaker. Blots were then washed for 3 x 10 minutes with T-TBS and then incubated with primary antibody (diluted in T-TBS) overnight at 4°C.

For the immunodetection step, blots were washed with T-TBS for 3 x 10 minutes then incubated with biotinylated secondary antibody (1:500, diluted in T-TBS) for 1 hour on a shaker. Blots were washed for 3 x 10 minutes in T-TBS then incubated with SAP (1:500, diluted in T-TBS-M) for 1 hour at room temperature. Following another 3 x 10 minutes wash with T-TBS blots were developed with AP substrate kit, washed in distilled water and air dried on filter paper.

### **2.3.4 Optical density measurements**

The optical densities of the bands were measured using the MCID image analysis program. The blots were placed onto a light box and the image enlarged and captured on the computer screen. Three optical density readings were then taken from each separate band and averaged. A background reading was also taken and this value subtracted from the band readings to remove any variation associated with background differences. Values were then analysed and graphed.

## **2.4 Scanning Electron Microscopy (SEM)**

### **2.4.1 Fixation**

Animals in the group for SEM were fixed with non-heparinised Karnovsky's fixative (2% formaldehyde, 2% gluteraldehyde). Karnovsky's fixative achieves a more rapid overall penetration of tissue than with formaldehyde or gluteraldehyde alone (Karnovsky, 1971) and is the fixative of choice for SEM studies. Heads were removed and placed in fixative for 24-48 hours, and the brains post fixed for 24 hours. Following the fixation procedure, middle cerebral arteries were dissected from the brains and placed in 200mM phosphate buffer (pH 7.4) and kept for processing.

#### 2.4.2 Processing of tissue for SEM

The sequence of steps involved in processing tissue for SEM is illustrated in Figure 20. 300µm brain slices were required for SEM examination and were cut using a vibrotome. Prior to vibrotoming brains were placed in phosphate buffer overnight. After cutting the slices were transferred to pH 7.4 phosphate buffer for 1 hour then post fixed with buffered 1% osmic acid for 30 minutes. Following 3 x 10 minute washes in phosphate buffer, slices underwent a series of dehydration steps: 50% acetone for 1 hour and 3x 1 hour in absolute acetone. Slices were then dried in hexamethyldisilazane (HMDS) for 1 hour, placed on filter paper and kept in a dessicator until mounted. Following the mounting of samples they are normally coated with a layer of conductive metal (in this case gold) of around 20-30nm. The coating of the specimen prevents the build up of high voltage charges and prevents heat damage by conducting the heat away from the specimen. The brain slices were gold coated using a Polaron Sputter Coater. The Polaron Sputter Coater creates a vacuum (around 0.1Pa) around the specimen which removes potentially damaging water and oxygen molecules. Once the vacuum has been achieved an inert gas (normally argon) is introduced into the chamber and flow adjusted until the vacuum is maintained at 6-7 Pa. A negatively charged high voltage is then applied and this causes the ionisation of argon into  $\text{Ar}^+$  molecules which strike the gold cathode resulting in the emission of metal atoms which coat the specimen. Following coating the slices were placed in the scanning electron microscope, a vacuum produced, accelerating voltage turned on and image obtained.

Middle cerebral arteries were processed in the same way.

### SEM SPECIMEN PREPARATION

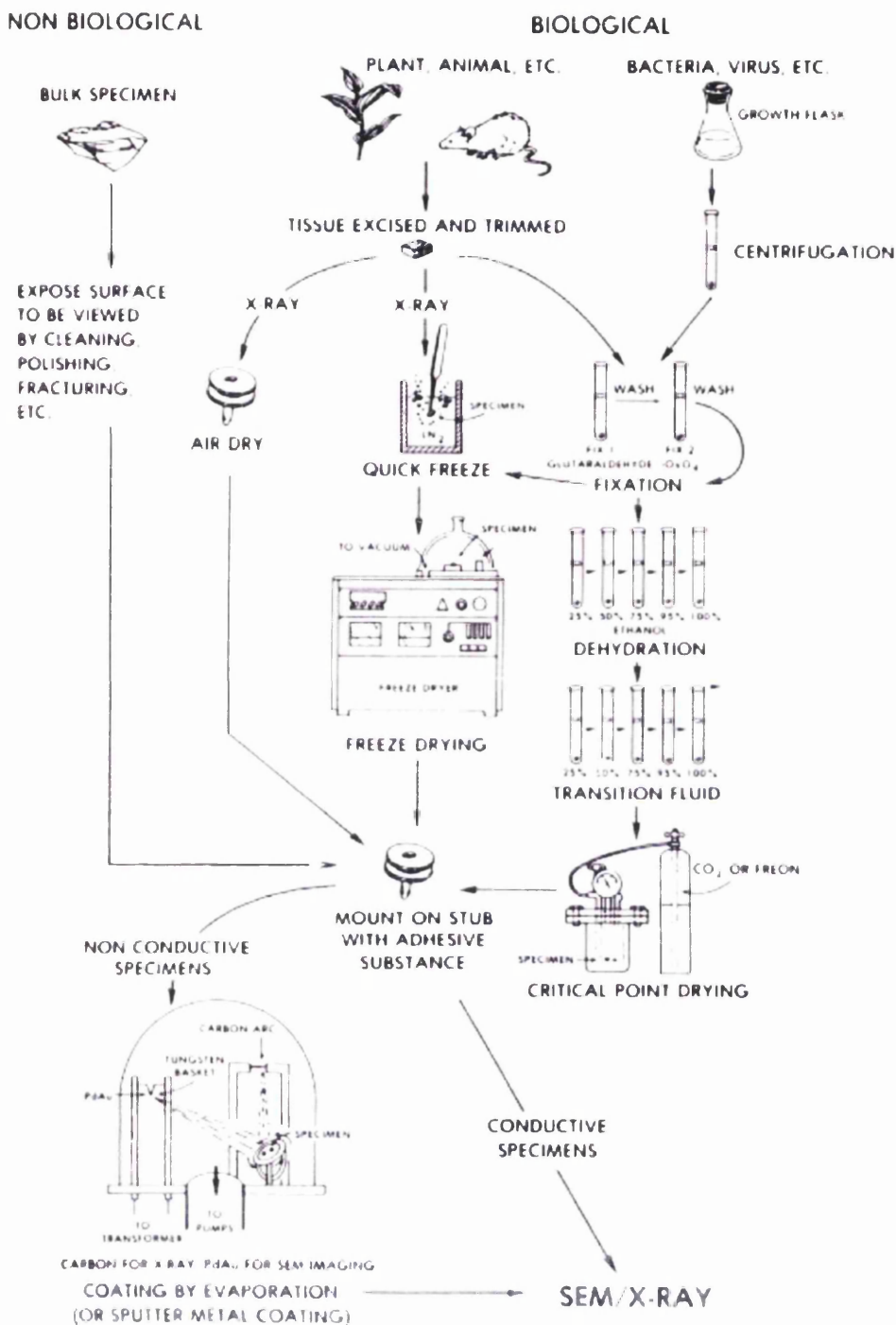


Figure 20. Sequence of events for processing of specimens for SEM. From Bozzola and Russell, 1992.

### **2.4.3 Developing of SEM films**

Images captured on 35mm film from the SEM were developed for 4-7 minutes in Kodak developer (1:3 dilution, 20°C), and then transferred to Kodak fixer (1:4 dilution) for 2-4 minutes. Films were then unwound from their holder and placed in cold running water for 5 minutes then dried and contact prints produced.

## Results: Chapter 3 Microvilli / Neutrophil Study

### 3.1 Introduction

In terms of inflammatory mediated ischaemic damage, previous studies have concentrated on the role of the circulating inflammatory cell, the neutrophil. Neutrophils have the ability to adhere to the endothelium of cerebral blood vessels reducing or completely blocking blood flow. They are also capable of contributing to ischaemic damage indirectly through their ability to release cytotoxic substances. The results of previous studies seem to be divided with some groups reporting a significant early neutrophil accumulation in ischaemic damaged tissue (Chopp *et al.*, 1994; Zhang *et al.*, 1994; Hallenbeck *et al.*, 1986) while others failed to find any significant neutrophil presence in the acute phase (Hayward *et al.*, 1996; Peters *et al.*, 1998; Oruckapten *et al.*, 2000).

In addition to a reported increased presence of neutrophils, other characteristic changes to cerebral blood vessels have been reported following experimental ischaemia. Various morphological changes have been reported using Scanning Electron Microscopy (S.E.M) and Transmission Electron Microscopy (T.E.M), including an increase in the number and distribution of microvilli, astrocytic swelling and ultravascular disruption (Maxwell *et al.*, 1988; Dietrich *et al.*, 1984).

Microvilli are small finger-like projections, which can be found in various parts of the body including the cardiovascular system, the gastrointestinal tract and the cerebrovascular system in the brain. They vary slightly in shape and size depending

on their anatomical position. Within the blood vessels of the brain, microvilli project from endothelial cells for a distance of around  $0.5\mu\text{m}$  in length and  $0.1\mu\text{m}$  in diameter (Fig 21).

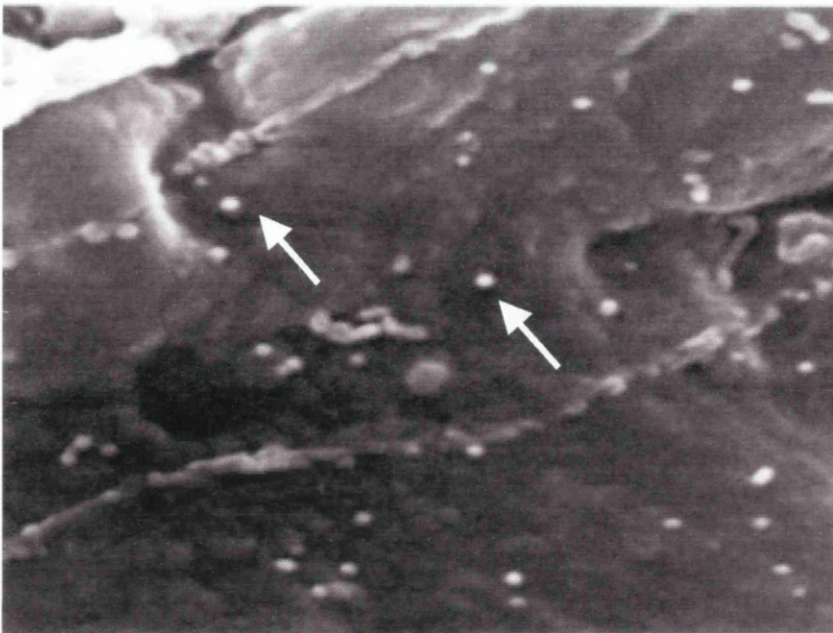


Figure 21. Microvilli in a control non-ischaeamic vessel in the cortex. SEM photograph taken at X 7500. Arrow represents microvilli projecting from endothelial cells of cortical blood vessels.

At present the functional significance of the microvilli and their increased number following ischaemia is not clear. It is possible that they may act as a haemodynamic impediment causing increased vascular resistance and postischaemic hypoperfusion (Dietrich *et al.*, 1984). They may be present to increase the absorption of essential metabolites such as glucose, vitamins etc. (Lossinsky *et al.*, 1989; Tagami *et al.*, 1983). Microvilli have also been shown to express adhesion molecules and so they

may be present to allow the subsequent adhesion and accumulation of inflammatory cells within the vessels of the brain.

The aim of this study was to investigate ultrastructural changes to cerebral blood vessels following intraluminal thread induced middle cerebral artery occlusion and to determine whether there was an increase in neutrophil number and microvilli number, which may result in subsequent inflammatory mediated damage.

## **3.2 Methods**

### **3.2.1 Surgical procedures**

Surgery was carried out with the help of Miss E. Peters.

Male Sprague Dawley rats (n=5) underwent intraluminal thread induced ischaemia using the method of Zealunga *et al* as previously described in section 2.1.2. The thread was inserted into the internal carotid and kept in place for two hours after which the thread was removed and the animal reperfused for a further two hours. Following the period of reperfusion the animals were transcardially perfused with Karnowsky's fixative and the brains and MCA's processed for S.E.M as previously mentioned in section 2.4.2.

Sham animals (n=5) had the thread inserted but removed immediately and the animals were kept under anaesthesia for the same 4 - hour period as the experimental animals.

### **3.2.2 Neutrophil adherence / accumulation**

To determine whether neutrophil adherence was playing a role in intraluminal thrombus induced ischaemic damage, Scanning Electron Microscopy (S.E.M) was used to look for signs of neutrophil adherence or accumulation in cortical blood vessels and in the MCA's. 10 small vessels (<10µm internal diameter (ID)) and 10 large vessels (>10µm internal diameter (ID)) were examined in the fronto-parietal cortex of both the ipsilateral and the contralateral hemispheres and the presence of neutrophils noted and photographed. This process was repeated for ipsilateral and contralateral MCA's in each animal.

### **3.2.3 Ultrastructural changes in parenchymal vessels and MCA's**

Using S.E.M, photographs were taken of 10 small (<10µm ID) and 10 large (>10µm ID) parenchymal cortical blood vessels in both the ipsilateral and contralateral hemispheres and the number of microvilli counted. The vessels were photographed firstly at x1000 to determine the diameter of the vessel and then at x7500 to allow the microvilli counts to be performed.

Microvilli were counted in 3 non-overlapping regions of 25µm<sup>2</sup> in each vessel and the number of microvilli counted and averaged to give microvilli numbers per 25µm<sup>2</sup>.

The photographs were also used to look for signs of damage to the smooth muscle and the endothelium in the ipsilateral hemisphere compared to the contralateral hemisphere and in the sham versus the occluded animals.

### **3.2.4 Statistical analysis**

Data are presented as mean  $\pm$  SEM for the animals used. The significance of differences in physiological variables and microvilli number between ipsilateral and contralateral hemispheres and between sham and occluded animals were determined by a one-way ANOVA followed by an unpaired Student's t-test.

## **3.3 Results**

### **3.3.1 Physiological Variables**

Physiological variables were maintained within normal limits under anaesthesia (Table 7): normocapnia (36-42mmHg), normal physiological pH (7.4), and normal body temperature (36.5-37.5°C). Arterial blood pressure under anaesthesia was similar in both the occluded and the sham animals. A significant difference between body temperature was observed between occluded and sham animals ( $p < 0.01$ ). This difference was of statistical significance but not biological significance as both groups were within the normal physiological range.

	<b>Weight (g)</b>	<b>P<sub>a</sub>CO<sub>2</sub> (mmHg)</b>	<b>P<sub>a</sub>O<sub>2</sub> (mmHg)</b>	<b>pH</b>	<b>MABP (mmHg)</b>	<b>Temp. (°C)</b>
Occluded	285± 12.1	41.1±1.1	153.6±7.1	7.4±.001	85.±2.1	37.1±0.07*
Sham	278±10.21	42.1±4.5	133.7±19.3	7.4±0.03	100.±7.7	36.6±0.16

Table 7. Physiological variables for scanning electron microscopy series using the intraluminal thread model; n=5 in occluded and sham groups. Data represents mean ± SEM. Data analysed by ANOVA followed by unpaired Students t-test. \* p<0.01.

MABP = mean arterial blood pressure.

### 3.3.2 Extent of Ischaemic Damage

The area of ischaemic damage as identified by light microscopy, incorporated both cortical and striatal regions. Figure 22 illustrates the extent of damage achieved with the intraluminal thread model of ischaemia (2 hours of ischaemia followed by 2 hours of reperfusion). The average volume of ischaemic damage was  $62.5 \pm 10.0 \text{ mm}^3$ . No evidence of ischaemic damage was found in any of the sham animals.

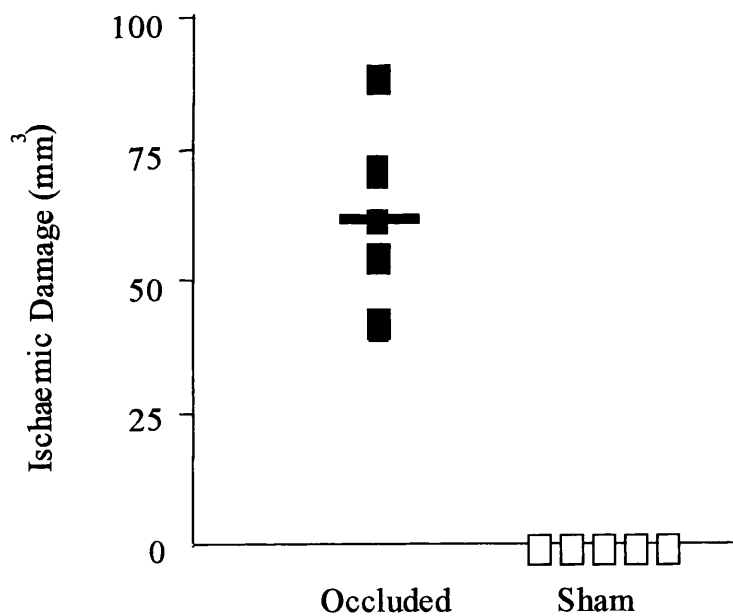


Figure 22. Volume of ischaemic damage ( $\text{mm}^3$ ) for intraluminal thread MCAO, 2 hours of occlusion followed by 2 hours reperfusion.  $n=5$  per group.

### 3.3.3 Neutrophil Adhesion

There were no signs of neutrophil adhesion, as characterised by the appearance of a cell of neutrophil morphology (Fig 23,A), in any of the parenchymal cortical vessels or in the MCAs (Fig 23,B, C) in any of the animals exposed to ischaemia or sham procedures (n=5 per group).

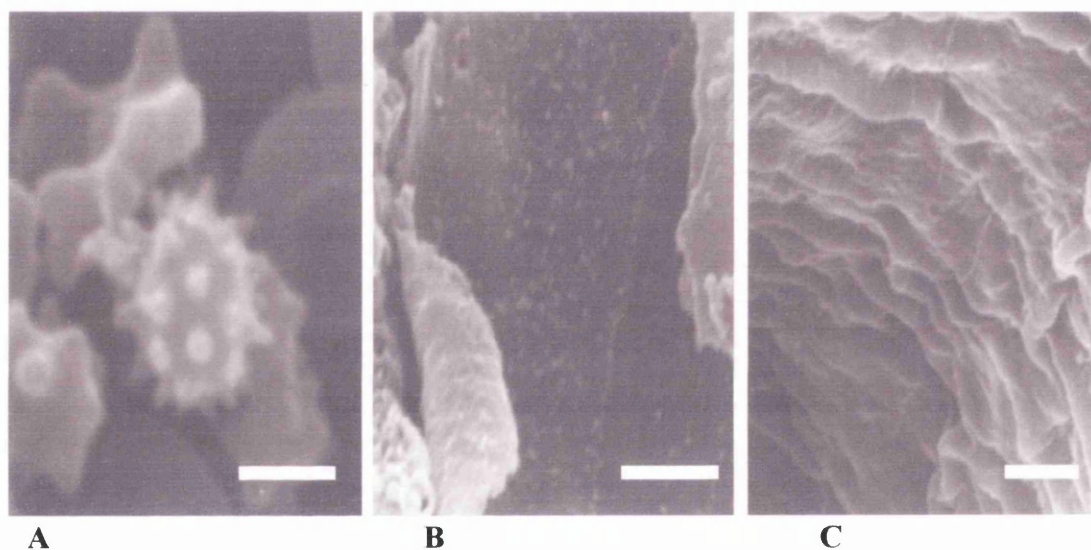


Figure 23 Lack of neutrophil accumulation in parenchymal vessels or MCAs. A. Typical appearance of a neutrophil adhering to the endothelial surface of a cortical blood vessel- taken from a previous study (Peters, 1999) in the Endothelin -1 model of MCAO, B. Lack of neutrophils in parenchymal cortical vessels in the ipsilateral hemisphere of occluded animals, C. Lack of neutrophils in the MCA from the ipsilateral hemisphere of an occluded animal. Photographs taken at X 7500. Scale bar represents 3 $\mu$ m.

### 3.3.4 Microvilli Counts

In both occluded and sham animals, there was a significantly greater number of microvilli present in the blood vessels of the ipsilateral hemisphere when compared to the contralateral hemisphere (For example, in occluded animals, *ipsi* =  $21.45 \pm 1.86$ , *contra* =  $15.33 \pm 0.5$ ,  $p < 0.05$ ; in sham animals, *ipsi* =  $21.01 \pm 0.89$ , *contra* =  $14.85 \pm 0.65$ ,  $p < 0.05$ ) (Figure 24)

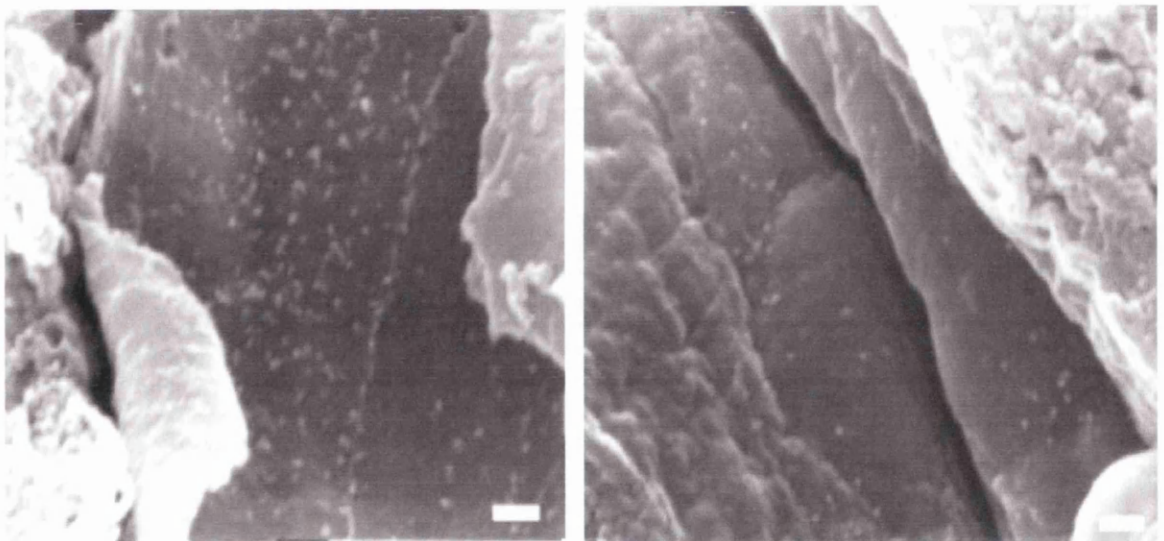
**A****B**

Figure 24. Microvilli in parenchymal cortical vessels. Microvilli were more abundant in the ipsilateral hemisphere (A) of the occluded animals than in the contralateral hemisphere (B). S.E.M photographs taken at X 7500. Scale bar represents  $1\mu\text{m}$ .

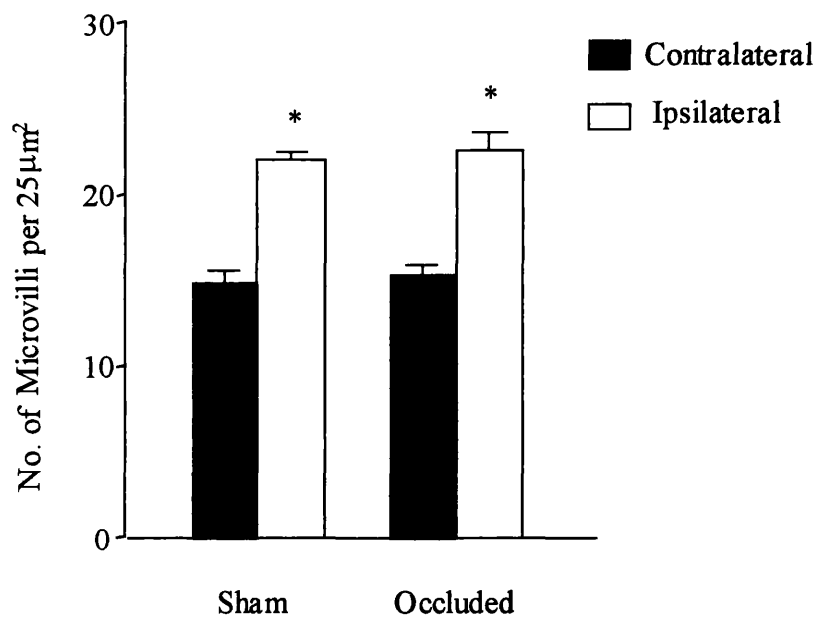


Figure 25. Number of microvilli per  $25\mu\text{m}^2$  in cortical parenchymal blood vessels,  $n=5$  in occluded and sham groups. Data represents mean  $\pm$  SEM and was analysed by ANOVA followed by unpaired Student's  $t$ -test,  $*p<0.05$ .

Microvilli were present in small vessels ( $<10\mu\text{m ID}$ ) and in large vessels ( $>10\mu\text{m ID}$ ) with the larger vessels tending to possess slightly greater numbers of microvilli than the small vessels (For example, in occluded animals, *ipsi*: small =  $20.72 \pm 0.79$  SEM, large =  $22.49 \pm 0.99$  SEM; in sham animals, *ipsi*: small =  $20.63 \pm 0.83$  SEM, large =  $22.72 \pm 2.9$  SEM). (Figure 26)

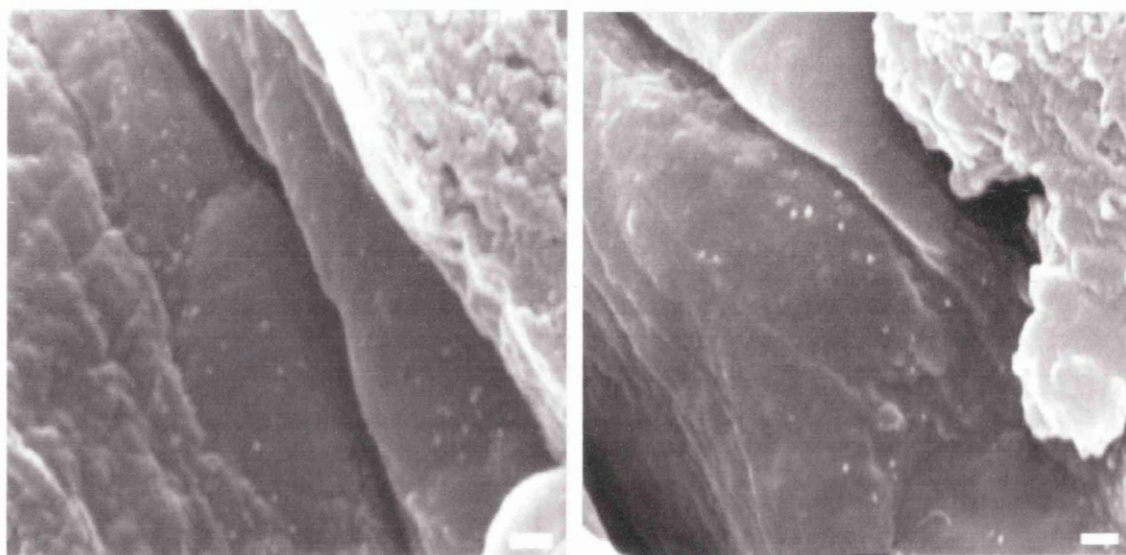
**A****B**

Figure 26. Number of microvilli in small and large vessels. Large vessels (A) ( $>10\mu\text{m ID}$ ) had greater numbers of microvilli than small vessels (B) ( $<10\mu\text{m ID}$ ). The difference did not however achieve statistical significance. Photographs taken at X 7500. Scale bar represents  $1\mu\text{m}$ .

	Small blood vessels (<10 $\mu\text{m}$ ID)		Large blood vessels (>10 $\mu\text{m}$ ID)	
	ipsi	contra	ipsi	contra
Occluded	20.7 $\pm$ 0.79	15.6 $\pm$ 0.53	22.5 $\pm$ 0.99	15.1 $\pm$ 0.47
Sham	20.6 $\pm$ 0.83	13.8 $\pm$ 1.03	22.3 $\pm$ 2.9	15.9 $\pm$ 0.28

Table 8. Number of microvilli per 25 $\mu\text{m}^2$  in intraluminal thread induced ischaemia., n=5 occluded and sham groups. Data represents mean  $\pm$ SEM.

There was no significant difference in the number of microvilli present in the occluded animals when compared to the shams (Figure 27). In sham animals the microvilli tended to be arranged more regimentally and could be seen to form lines along endothelial cell junctions. In occluded animals however, microvilli distribution appeared more random.

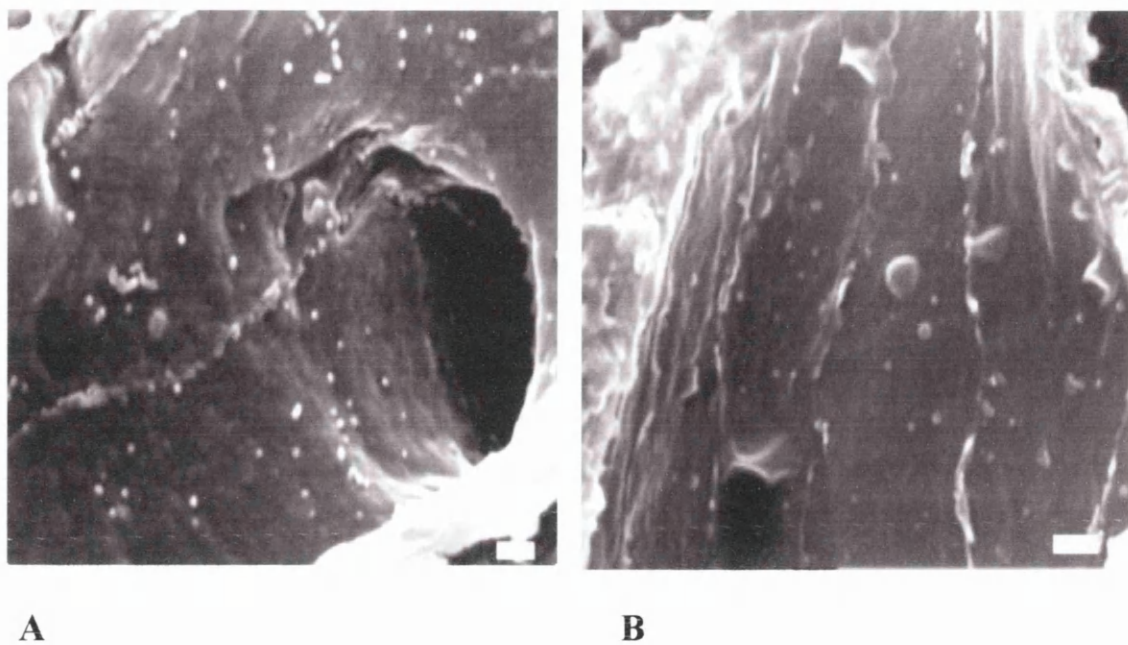


Figure 27. Microvilli distribution and number in parenchymal cortical vessels in A. sham animal and B. occluded animal. S.E.M photograph at X 7500. Scale bar represents  $1\mu\text{m}$ .

There was no evidence of a correlation between volume of ischaemic damage and microvilli number in the occluded group-  $r^2 = 0.137$  (Figure 28)

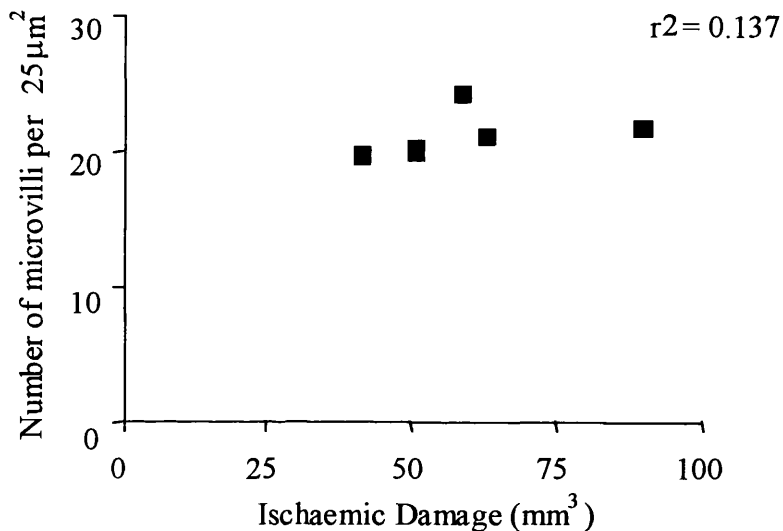


Figure 28. Correlation between the number of microvilli in parenchymal vessels and infarct size following ILT induced ischaemia (2 hours occlusion + 2 hours reperfusion) n=5.

There were very few microvilli present within the MCAs of sham or occluded animals and no obvious differences between the number of microvilli in the MCAs from the ipsilateral hemisphere and the contralateral hemisphere of the occluded animals (occluded- *ipsi*-  $11 \pm 1.5$ , *contra*-  $8 \pm 2.2$ ; sham- *ipsi*-  $9 \pm 0.5$ , *contra*-  $7 \pm 1.6$ ).

### 3.3.5 Ultrastructural Changes to MCA

The appearance of the endothelium of the ipsilateral middle cerebral artery differed slightly between the occluded and the sham animals.

Both sets of MCAs displayed a roughly textured endothelium with a faint corrugated appearance. The endothelium of occluded animals appeared to be slightly rougher in texture than the shams (Figure 29). Few microvilli were present on the endothelium of the MCAs.

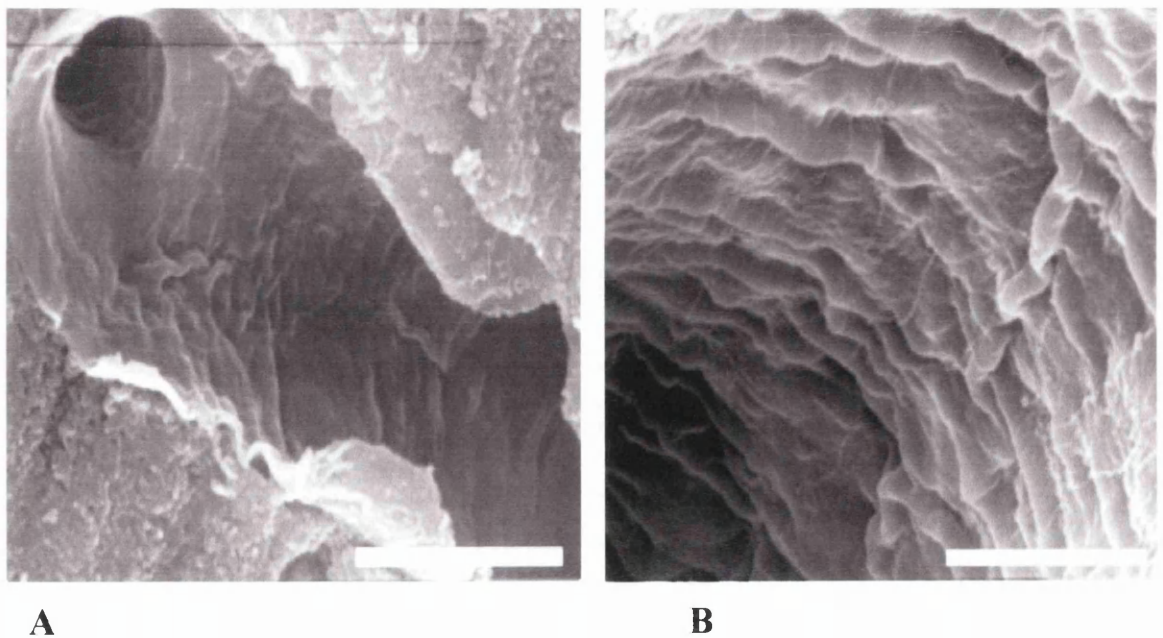


Figure 29. Ultrastructural changes to ipsilateral MCA in A. sham animal and B. occluded animal. S.E.M photographs taken at X 7500. Scale bar represents 10 $\mu$ m.

### 3.4 Discussion

Various changes to the cerebral vasculature have been reported to occur as a result of an ischaemic insult. These include an increase in neutrophil adhesion and an increase in the number of microvilli projecting from the endothelium of cerebral blood vessels (Del Zoppo *et al.*, 1991; Dietrich *et al.*, 1984; Okumura *et al.*, 1994).

#### Neutrophils

The first part of this study considered the role of the neutrophil in ischaemic damage. An increase in neutrophil recruitment following ischaemia can prove detrimental due to the ability of the neutrophil to adhere to the endothelial surface of blood vessels therefore obstructing blood flow through that vessel (Del Zoppo *et al.*, 1991). Once adhered to the endothelium, neutrophils can undergo activation and may release cytotoxic substances and free radicals further potentiating ischaemic damage to the vasculature or parenchyma, if infiltration occurs (Matsuo *et al.*, 1995).

Several groups have investigated the role of the neutrophil in ischaemia but opinion remains divided as to whether it contributes significantly to damage. Studies have shown that administration of antibodies directed against the adhesion molecules involved in the neutrophil – endothelial interaction (e.g. P-selectin, E-selectin, ICAM-1 and CD-18) have successfully attenuated ischaemic damage in a number of species (Chopp *et al.*, 1994; Zhang *et al.*, 1994; Clark *et al.*, 1991). However it has been noted that the reduction in ischaemic damage seen with anti-neutrophil therapies are modest when compared to a 50-75% reduction in ischaemic damage

reported with glutamate antagonists (Hayward *et al.*, 1996). Many of the studies have also indicated that anti-neutrophil therapy may prove more successful in transient MCAO than in permanent MCAO (Zhang *et al.*, 1995) as neutrophil recruitment may contribute greatly to the pathogenesis of reperfusion as compared to non-reperfusion tissue (Prestigiacomo *et al.*, 1999; Matsuo *et al.*, 1994). Increases in neutrophil counts in the blood has been identified in human stroke using the Leukocyte test to measure neutrophil levels in the blood (Silvestrini *et al.*, 1998) with numbers being significantly higher in patients with severe stroke damage. It is therefore important to develop a better understanding of the role of the neutrophil in the pathogenesis of stroke as anti-neutrophil therapy may prove an effective way of reducing damage caused by stroke in a clinical setting. Clinical studies have so far, however, proved unsuccessful in attenuating ischaemic damage. The Enlimomab Acute Stroke Trial (EAST), administered the anti-ICAM-1 antibody R6.5 (Enlimomab) to stroke patients but the results of the study demonstrate that this antibody is not beneficial in improving clinical outcome, with mortality and infarct sizes reported to be greater in the treatment group (Vuorte *et al.*, 1999; Sherman, 1997) than the placebo group. These negative results however cannot rule out an involvement of neutrophils in ischaemic damage as inhibiting ICAM-1 is only one of a number of mechanisms by which one could reduce neutrophil accumulation. Enlimomab was also found to have frequent adverse effects which may have contributed to its failure to improve patient recovery and reduce infarct size (Vuorte *et al.*, 1999).

In addition to the failure of the above clinical trial, various groups have found no evidence for a significant early neutrophil accumulation in experimental models of

ischaemia which is in accordance with the findings of this study in which very few or no neutrophils were found in the parenchymal vessels or MCAs of rats following transient intraluminal thread induced ischaemia (Peters *et al.*, 1998; Hayward *et al.*, 1996). Indeed even in a study inducing neutropenia, the absence of neutrophils had no effect on the size of the infarct (Hayward *et al.*, 1996).

The current study used a transient model of MCAO. If neutrophils were contributing to early reperfusion mediated ischaemic damage one would expect to see evidence of an increase in neutrophil presence in the ipsilateral hemisphere of this model.

However, it could be argued that in this study, a lack of neutrophil accumulation could be attributed to the short duration of reperfusion (2 hours occlusion followed by 2 hours reperfusion) and that if the animals had been reperfused for a longer period of time then neutrophil accumulation may have become apparent. Previous studies have shown neutrophil accumulation following longer periods of reperfusion (24 hours- Matsuo *et al.*, 1994; 46 hours- Chen *et al.*, 1994; 1 week – Zhang *et al.*, 1995). However, previous studies from this laboratory and others have failed to show any evidence for neutrophil accumulation up to 72 hours using both the intraluminal thread and the endothelin-1 models of transient ischaemia in the rat (Peters *et al.*, 1998; Hayward *et al.*, 1996; Dirnagl *et al.*, 1994).

A lack of neutrophil accumulation in this study could also be associated with the processing of the tissue following surgery. In order to preserve the tissue for SEM analysis and for continued storage, the animals were fixed with Karnovsky's fixative. This fixing procedure is standard for .S.E.M and T.E.M studies and involves infusing saline and then the fixative through the blood vessels in order to preserve the brain.

The act of perfusing solutions through the cerebral blood vessels might dislodge any neutrophils which may have been present following the ischaemic insult. However the pressure used to perfuse the animals was no greater than the animals mean arterial blood pressure under anaesthesia. Previous studies using the same method of neutrophil analysis (neutrophil counts in brain slices or blood vessels) in non-fixed brains have reported no evidence of neutrophil accumulation therefore ruling out the possibility of the neutrophils being washed out of the vessels prior to the counting stage (Hayward *et al.*, 1996).

Lastly, the absence of neutrophils following experimental ischaemia may be an indicator of a sterile surgical procedure as neutrophils commonly accompany infection and inflammation which can occur as a result of non- aseptic surgical practice and were found in abundance in the rare cases where an animal had complications of meningitis and abscess formation caused by an infection developing after surgery.

It is clear that neutrophils have the potential to contribute to ischaemic damage either indirectly via the secretion of cytotoxic substances or directly by the plugging of blood vessel and obstruction of flow. However this study failed to provide any evidence for an early significant involvement of neutrophils in the brain damage induced by transient MCA occlusion.

### **Microvilli**

In addition to the role of neutrophils in ischaemic damage, this study also examined potentially pathogenic changes to the vasculature following intraluminal thread induced MCAO and reperfusion.

Microvilli are small bulbous projections from the endothelium of blood vessels which have been shown to increase in number following injury to the brain. An increase in microvilli number has been found to accompany other changes in the cerebral vasculature- astrocytic swelling and general vascular disruption- in models of both global (Dietrich *et al.*, 1984; Kumar *et al.*, 1987; Wisniewski *et al.*, 1995) and transient ischaemia (Okumura *et al.*, 1997; Dietrich *et al.*, 1987).

However, this study showed no significant increase in the number of microvilli in the brains of rats undergoing ILT induced ischaemia when compared to sham animals. Microvilli were identified and counted using scanning electron microscopy (S.E.M), the standard method of identifying microvilli in the studies previously cited.

In both occluded and sham groups, a significantly greater number of microvilli were found to be present in the ipsilateral hemisphere when compared to the contralateral hemisphere ( $p < 0.05$ ) but there was no difference in microvilli number in the ipsilateral hemisphere between sham and occluded animals. An increase in the number of microvilli in the ipsilateral hemisphere of occluded animals would seem to suggest a possible pathogenic link with the development of the ischaemic damage. However, the fact that the hemispheric difference was found in sham animals as well as occluded animals would seem to suggest that the increased microvilli numbers in the ipsilateral hemisphere could be attributed to mechanical damage caused by the insertion of the filament and its subsequent removal from the cerebral vasculature.

Sham animals underwent the same degree of invasive surgery and had the filament inserted to block the origin of the MCA as in the occluded animals. The filament was immediately removed following insertion so no period of ischaemia was induced in the shams. There was no difference in the magnitude of the increase in microvilli

numbers between sham and occluded groups. If ischaemia increased microvilli number one might expect to see a greater increase in the occluded animals representing mechanical stimulation of microvilli and an additional increase attributed to ischaemia which would not be present in the sham animals. This was not the case in this study, and it would appear that insertion of the filament itself may cause sufficient damage to promote maximal microvilli formation.

The number of microvilli counted were not as high as was reported in previous studies from our laboratory using different models of MCAO. For example, in studies using the endothelin-1 method of transient MCAO, microvilli numbers were significantly higher than in this study (around 70 microvilli per  $25\mu\text{m}^2$  in endothelin-1 induced MCAO compared to around 23 microvilli per  $25\mu\text{m}^2$  in ILT induced ischaemia; Gartshore, 1996). If indeed microvilli numbers are primarily increased as a result of mechanical damage associated with a particular model, this could also help to explain the differences in microvilli number observed in the ILT and the endothelin-1 models. The endothelin-1 model as previously discussed (section 1.3.4) involves topical application of the potent vasoconstrictor peptide endothelin-1 directly to the MCA (via a craniectomy) therefore applying a potent force to the smooth muscle and endothelium of the blood vessel causing severe constriction and distortion of the surface of the vessel. One might expect this model therefore to produce a greater degree of mechanical damage than the ILT model where mechanical damage can mainly be attributed to the filament coming into contact with the endothelium of the vessels as it is advanced towards the Circle of Willis and

while it is being removed. The greater degree of physio-mechanical damage in the endothelin-1 model may be contributing to the greater number of microvilli.

Differences in microvilli formation may also depend on the severity of ischaemia associated with the model. The intraluminal thread model produces a more sustained ischaemic insult than the endothelin-1 model (Mean infarct volume  $47.5 \pm 2 \text{ mm}^3$  in Endothelin-1 induced MCAO (From Gartshore, 1996) versus  $67.0 \pm 12 \text{ mm}^3$  in ILT induced ischaemia in this study). It has been reported that energy depletion can affect microvilli formation to such an extent that depleting ATP levels can reduce microvilli formation (Soagabe *et al.*, 1996). Since intraluminal thread induced ischaemia can be said to inflict a more severe insult it could be postulated that this model may cause a greater degree of energy depletion leading to lower numbers of microvilli being present. Intraluminal thread ischaemia could also be expected to cause a greater degree of oxygen deprivation than endothelin-1 induced MCAO since the ischaemia is maintained for 2 hours. A lack of oxygen has been shown to result in reduced microvilli number (Leuschen and Nelson, 1987).

However, the idea that a more severe insult leads to decreased energy and decreased microvilli formation is contradicted by Dietrich and co-workers (1987) who found that prolonged periods of complete ischaemia (4 hours bilateral common carotid artery occlusion) produced greater numbers of microvilli and luminal disruption than 1 hour occlusion and 3 hours reperfusion. It has previously been suggested that reperfusion may cause a reduction in microvilli numbers (Dietrich *et al.*, 1984) and so the differences in microvilli between the ILT model and the endothelin-1 model may be attributed in part to the differences in reperfusion patterns. In the intraluminal

thread model of MCAO, reperfusion occurs immediately on removal of the filament- giving rise to a rapid return of blood. In the endothelin-1 model, however, the vasoconstrictor actions of the peptide wear off gradually over time- leading to a gradual reperfusion. If reperfusion does reduce microvilli formation the quicker, more intense reperfusion in ILT MCAO may help to explain lower numbers of microvilli when compared to the endothelin-1 model.

Another indicator that microvilli presence may not solely be associated with the pathology of ischaemia is that correlation analysis showed no link between the microvilli number and the extent of ischaemic damage ( $r^2 = 0.137$ ). This lack of correlation and the association between increased microvilli number and mechanical damage associated with the experimental models of ischaemia would seem to suggest that microvilli are not major contributors to ischaemic damage but a marker of injury induced by the induction of ischaemia. However it is unwise to rule out a pathogenic role completely as it may be that microvilli are one of many contributors to the damage and may perform a lesser role in ischaemic damage than for example glutamate excitotoxicity or inflammatory mediated damage. It is also possible that microvilli formation may contribute to ischaemic damage at a later time point.

Although an increase in microvilli number in models of MCAO would seem to be associated with the mechanical damage rather than ischaemic damage there may still be a consequence to their increase in number.

There is currently a lack of clarity as to whether microvilli are pathogenic or beneficial following ischaemia and it remains unclear what the function of such endothelial microvilli may be.

It has been proposed that the microvilli are acting to increase the surface area of the blood vessels in an attempt to facilitate the absorption of essential nutrient. Studies have shown that microvilli in other organs, for example the digestive system contribute to the exchange of metabolites and microvilli like tubules have been identified in the injured CNS which have been proposed to be involved in increasing the transport of essential macromolecules to the damaged areas (Lossinsky *et al.*, 1989; Tagami *et al.*, 1983). This would seem even more likely due to the fact that microvilli numbers do not appear to be as high following transient ischaemia as they are following global ischaemia (Dietrich *et al.*, 1987). This may suggest that microvilli are indeed acting to increase the area for absorption to compensate for lack of a normal blood flow. When the blood flow is re-introduced (as in reperfusion models) the supply of nutrients is restored to a greater extent. Therefore an increase in microvilli would no longer be needed. Dietrich *et al.*, 1994 reported that microvilli numbers did indeed decrease towards basal levels on reperfusion. However TEM analysis of microvilli have shown that the microvilli present in the brain do not possess the organelles necessary for nutrient exchange (Dietrich *et al.*, 1984).

Another possible consequence of increased brain endothelial microvilli could be post ischaemic hypoperfusion (Chiang *et al.*, 1968; Dietrich *et al.*, 1984). The numbers of microvilli seen in ischaemic studies appear to be high enough to obstruct normal blood flow and result in a 'no-reflow' phenomenon (Ames *et al.*, 1968). However other studies have failed to provide supporting evidence that numbers of microvilli were high enough, or indeed that microvilli were of sufficient size to significantly affect blood flow (Fischer *et al.*, 1977).

Lastly, an increase in microvilli numbers may well indirectly contribute to ischaemic damage via the promotion of the adherence of inflammatory cells to the vascular endothelium. In addition to increasing the surface area available for neutrophil adherence, microvilli are also present on neutrophils and have been shown to express receptors for adhesion molecules (L & P selectin: Bruehl *et al.*, 1996; Bruehl *et al.*, 1997 and ICAM-1: Sasaki *et al.*, 1998). There may therefore be interactions between the microvilli on the neutrophil and the microvilli on the endothelium of the blood vessels which may aid neutrophil adherence and migration. Brain microvilli in vessels exposed to cancer cells have been shown to express ICAM-1 which may serve to facilitate migration of tumour cells or may facilitate the transport of essential macromolecules to the injured brain (Lossinsky *et al.*, 1995).

In terms of ultrastructural changes to the MCA itself, following ILT induced ischaemia the MCA's appeared rougher in texture than in sham animals. Few microvilli were present on the endothelium of the MCA's. One possibility is that mechanical damage during processing may have resulted in the removal of microvilli from the endothelial surface (Fujimoto *et al.*, 1975)

An increase in the number of folds in the vessels of occluded animals and a general distortion of the regimental alignment of microvilli may occur as a result of ischaemia induced vasospasm (Putz *et al.*, 1991; Naganuma *et al.*, 1990; Wisniewski *et al.*, 1995). However due to the fact that sham animals also possessed a certain degree of transverse ridging and distortion, some form of mechanical damage cannot be ruled out. Disruption of the endothelium of the MCA may also occur as a result of the release of cytotoxic substances during ischaemia.

Free radicals, including nitric oxide are candidates for endothelial damage and the administration of the nitric oxide inhibitor L-arginine methyl ester has been shown to ameliorate damage to the endothelium and reduce microvilli number following brain injury (Katumukache., 1993, MSc thesis). This study has demonstrated an increase in the number of microvilli following experimental ischaemia. Although it cannot be concluded that microvilli are involved in the pathogenesis of ischaemia it can be said that microvilli are markers of the mechanical damage associated with models of experimental ischaemia, independent of whether their presence is beneficial or detrimental. The increase in the number of microvilli and the slight distortion of the endothelium of the MCA were the only sign of acute changes to the ultrastructure of the cerebral vasculature following intraluminal thread induced MCAO, with no evidence of neutrophil or other blood cell adherence to the endothelium.

## **Results: Chapter 4. Matrix metalloproteinase expression following intraluminal thread induced ischaemia.**

### **4.1 Introduction**

Various studies have shown increased expression of certain matrix metalloproteinases in models of both permanent and transient cerebral ischaemia. Elevated levels of MMPs are thought to contribute to inflammatory mediated ischaemic damage by a number of mechanisms including 1) the degradation of the blood brain barrier leading to increased BBB breakdown and oedema, 2) the stimulation of the secretion of cytotoxic substances from inflammatory cells, 3) the facilitation of the migration of inflammatory cells to the site of ischaemic damage and 4) the activation of cytokines.

However, information is currently lacking on the anatomical distribution and cellular localisation of MMPs following cerebral ischaemia. Consequently this study has been carried out in order to develop a better understanding of the ways by which MMPs might contribute to ischaemic damage.

The aims of the study were 1) to map the distribution of MMP-9 (gelatinase B, known to be up regulated following ischaemia) and rat neutrophil collagenase (MMP-8, gifted by British Biotech, Oxford, UK) 24 hours after intraluminal thread induced ischaemia (2 hours ischaemia and 22 hours reperfusion) and 2) to identify the cellular localisation of these two MMPs.

Following experimental ischaemia the blood brain barrier (BBB) can be altered in such a way that its permeability is increased and its role as a regulator of the movement of substances into the brain is compromised.

Various methods are available for the quantification of BBB permeability including Evans Blue, Horseradish Peroxidase and Peroxidase anti-Peroxidase (PAP) staining technique. Studies using these methods, in models of transient ischaemia, would suggest a biphasic opening of the BBB. The period of increased permeability would seem to be associated with the start of reperfusion and could be said to be “haemodynamic” in nature caused by the sudden return of blood through maximally dilated blood vessels (Kuroiwa *et al.*, 1985). This increase in permeability is transient and a second permeability increase occurs some hours later in the reperfusion period. The mechanism of the second opening of the BBB is unclear but is more likely to be related to factors associated with damaged tissue rather than haemodynamic factors.

Matrix metalloproteinases as previously mentioned are thought to play a role in increased BBB permeability due to their ability to degrade components of the extracellular matrix. This study therefore also set out to investigate whether there was evidence of increased BBB permeability associated with intraluminal thrombus induced transient ischaemia and to identify whether this increased BBB permeability correlated with increased MMP expression.

## **4.2 Methods**

### **4.2.1 Surgical procedures.**

All experiments were carried out under licence from the Home Office. Animals were housed under a 12 hour light-dark cycle and were given free access to food and water.

Sprague Dawley rats underwent intraluminal thread induced ischaemia as previously described in section 2.1.2. The filament was inserted into the internal carotid and kept in place for 2 hours after which time the thread was withdrawn and the animals were allowed to recover for 22 hours. Following the recovery period the animals were perfusion fixed with 4% paraformaldehyde in PBS as described in 2.2.1 and brains processed and embedded in paraffin. 6µm sections were collected for H&E staining and for immunohistochemistry.

To ensure that any changes in MMP levels were occurring as a result of ischaemia and not simply as a result of mechanical damage associated with the surgical procedure, sham animals had the filament inserted into the internal carotid but removed again immediately. The sham animals were kept under anaesthesia for the same period of time as animals exposed to focal ischaemia.

#### **4.2.2 Haematoxylin and eosin staining for infarct determination.**

Sections throughout all 8 coronal levels were stained with haematoxylin and eosin and the light microscope used to identify the area of ischaemic damage. The area of damage was then transcribed onto line diagrams using image analysis on a Microcomputer Imaging device or MCID and the volume of infarction calculated by integration (Osborne et al., 1987) as previously described in section 2.2.5.

#### **4.2.3 Western blotting**

Western blotting as described in section 2.3.1 was carried out to determine the specificity of the MMP-9 antibody AB805.

Optical Densities of the bands was measured using the MCID Image analysis program as described in section 2.3.4.

#### **4.2.4 Immunohistochemistry**

Sections throughout all 8 coronal levels were stained with polyclonal antibodies to MMP-9, AB805 (1:100, Chemicon International Plc), MMP-8, SE594 (1:100, British Biotech, Oxford, UK) or MMP-9, C-20 (1:100, Santa Cruz) . Immunohistochemistry was carried out using the polyclonal antibody protocol for paraffin processed material which was described previously in section 2.2.6.3.

The MMP antibodies required pre-treatment involving microwaving in citric acid buffer (1.05g/500mls dH<sub>2</sub>O, pH 6.0) for two periods of five minutes. After the

microwaving the sections were allowed to cool for 30 minutes before proceeding to the washing and blocking stages of the immunohistochemistry protocol.

Immunohistochemistry using the standard polyclonal antibody protocol was also carried out using peroxidase anti-peroxidase (PAP, 1:100, Vector Laboratories, UK) and antibodies to the serum proteins albumin and fibrinogen (rabbit anti-human albumin, 1:1000 and rabbit anti-human fibrinogen, 1:250, DAKO, UK) to investigate any correlation between MMP staining and areas of increased BBB permeability.

#### **4.2.5 Double labelling immunohistochemistry.**

To identify gelatinase B/ rat neutrophil collagenase positive cell types, normal double labelling was carried out with GFAP (Glial Fibrillary Acidic Protein, astrocytic marker, 1:1000, Sigma, UK), mrf-1 (Microglial Response Factor, microglial marker, 1:100, Dr S Tanaka, Hokaido University, Japan) and tau-1 (marker of injured oligodendrocytes, 1:1000, Dr D Hanger, University of London) using DAB (brown chromagen) and SG (grey chromagen) and the standard double labelling technique as described in section 2.2.6.4. This was followed by fluorescence double labelling with confocal microscopy to confirm the results of light microscopy double labelling. Fluorescence double labelling was carried out using the three day protocol described in section 2.2.6.5 using Fluorescein and Texas Red labelled secondary antibodies (1:100, Vector Laboratories, UK).

#### **4.2.6 Blocking peptide protocol for determination of non-specific staining**

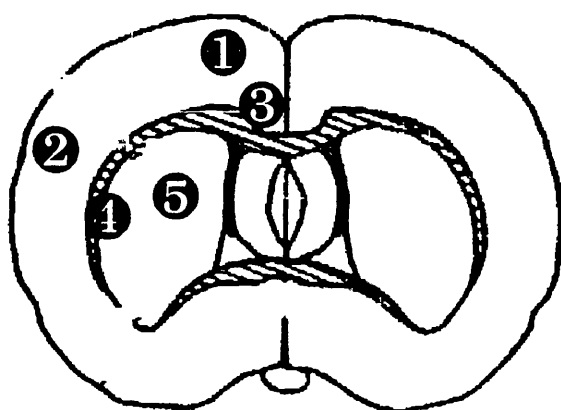
A blocking peptide to the MMP-9 Santa Cruz antibody (C-20) was used in order to determine the specificity of MMP staining patterns (Pollock and Van Noorden, 1997) (blocking peptides were not commercially available for the other MMP antibodies used).

The antibody was diluted 5, 10, 20 and 50 fold with blocking peptide and 100µl of PBS added to each dilution and the solutions placed on a shaker for 3 hours. Solutions were then centrifuged for 15 minutes. After centrifugation, the blocking peptide diluted antibody was diluted as normal (1:100) and applied to the sections as in the normal polyclonal immunohistochemistry protocol (as previously described in section 2.3.6.4). The blocking peptide diluted antibody was run along side the Santa Cruz antibody alone to determine which staining patterns were removed by the presence of the blocking peptide (specific staining) and which patterns remained (non-specific staining). Unfortunately, blocking peptides were not commercially available for the other MMP antibodies used.

#### **4.2.7 Distribution and quantification of staining**

Gelatinase B (MMP-9) and rat neutrophil collagenase (MMP-8) positive cells were identified under the light microscope. Line diagrams featuring the eight coronal levels through the MCA territory were used to produce maps marking the distribution and intensities of MMP-9 and MMP-8 immunohistochemistry.

The cell types showing positive staining were identified by double label immunohistochemistry and any differences in staining patterns between ipsilateral and contralateral hemispheres were noted. The following brain regions were examined in detail.



- 1 Cingulate cortex
- 2 Core of infarct
- 3 Genu Corpus Callosum
- 4 External capsule
- 5 Striatum

#### 4.2.8 Statistical analysis

Data are presented as mean  $\pm$  SEM for the animals used.

The significance of differences in infarct size and physiological variables between groups was determined by ANOVA followed by a two tailed, unpaired Students t-test.

## **4.3 Results**

### **4.3.1 Physiological variables**

Physiological variables were maintained within normal limits under anaesthesia: normocapnia (36-42mmHg), normal physiological pH (7.4) and normal body temperature (36.5-37.5°C). Table 9 illustrates mean  $\pm$  SEM for physiological variables during the surgical procedure. There were no significant differences in any of the above variables between experimental and sham animals.

### **4.3.2 Infarct Size**

The area of ischaemic damage as identified at the light microscopic level incorporated both cortical and striatal regions (Figure 30). The mean infarct size for the occluded animals (n=5) was  $187.14 \pm 10 \text{ mm}^3$  (Figure 30). H&E sections produced from the sham animals (n=5) displayed no evidence of ischaemic damage at any of the coronal levels examined.

	Weight (g)	MABP (mmHg)		PaCO <sub>2</sub> (mmHg)		PaO <sub>2</sub> (mmHg)		pH		Body Temp. (°C)	
		Pre-MCAO	Post-MCAO	Pre-MCAO	Post-MCAO	Pre-MCAO	Post-MCAO	Pre-MCAO	Post-MCAO	Pre-MCAO	Post-MCAO
Occluded	313.6 ± 10.1	75.4 ± 3.5	81.6 ± 4.3	47.3 ± 12.5	42.9 ± 11.7	148.1 ± 17.9	127.4 ± 26.1	7.36 ± 0.1	7.38 ± 0.1	36.7 ± 0.1	36.8 ± 0.1
Sham	310.6 ± 21.5	71.2 ± 1.6	79.9 ± 3.4	39.4 ± 2.7	41.2 ± 3.9	124.9 ± 19.9	127.1 ± 11.9	7.41 ± 0.1	7.39 ± 0.1	36.7 ± 0.31	36.8 ± 0.1

Table 9. Physiological Variables in animals exposed to transient intraluminal thread induced ischaemia. Values represent mean ± SEM. n=5 per group. Pre- MCAO = 15 minutes before ILT occlusion, Post- MCAO = 1 hour after the start of ILT occlusion. Values were analysed using Student's t-Test.

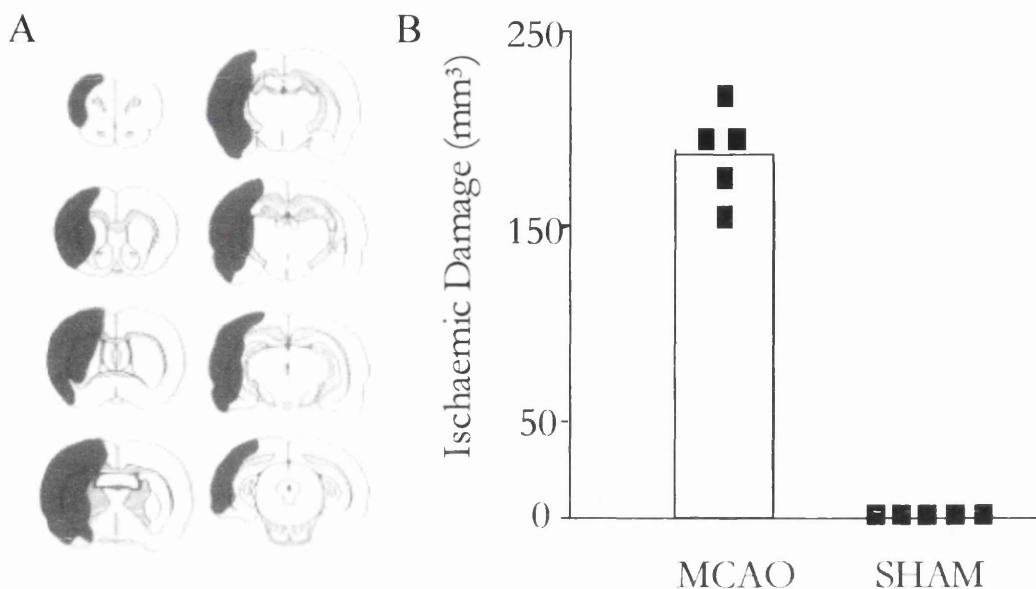


Figure 30. A. Representative line diagram of ischaemic damage following 2 hours  
ILT induced ischaemia plus 22 hours reperfusion. B. Volume of ischaemic damage  
n=5 per group.

#### 4.3.3 Western Blotting- Mini-Gels.

Antibody AB805, is commercially produced as an anti-human MMP-9 antibody. Results have been published involving immunohistochemical studies using AB805 on rodent tissue (Romanic *et al.*, 1998). To confirm that AB805 was detecting the correct protein, mini-blotting was carried out on MCAO rat tissue using the protocol previously described in section 2.3.1.

A standard curve for the Lowry Protein Assay was plotted (Fig 31) to quantify protein concentrations in samples of cortical tissue from the MCA territory of the ipsilateral hemisphere and control tissue from cortical tissue in the contralateral hemisphere from four animals at the 24- hour time point so that  $10\mu\text{g}/\mu\text{l}$  of each sample could be loaded onto the gels. Antibody concentrations of 1:500, 1:1000, 1:2000 and 1:5000 all produced bands which corresponded to the latent (92kDa) and active (88kDa) molecular weights of MMP-9 (Fig 32). In the ipsilateral hemisphere samples, the active band ( $\text{OD}-0.21\pm 0.01$ ) appeared darker in colour than the latent band ( $0.11\pm 0.01$ ) suggesting greater levels of the active form than the latent form (Figure 33). In the contralateral hemisphere, there appeared to be more of the latent form of MMP-9 ( $\text{OD}-0.14\pm 0.01$ ) than the activated form ( $\text{OD}-0.049\pm 0.01$ ) (Figure 33). The Western blot confirmed the specificity of the antibody, ensuring that the antibody was capable of detecting the correct bands for MMP-9 in rat tissue.

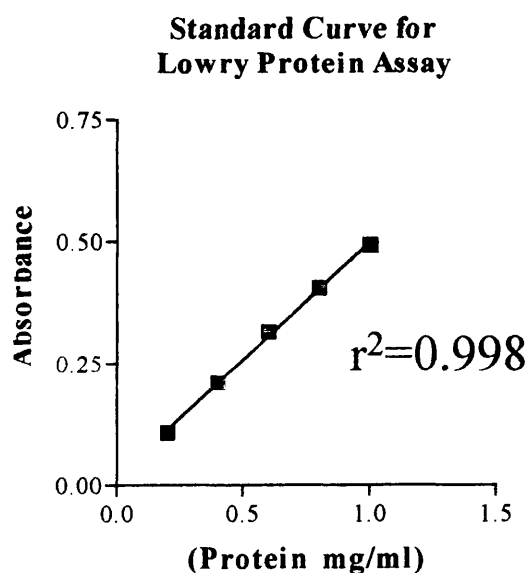


Figure 31. Graph for Lowry Protein Assay.

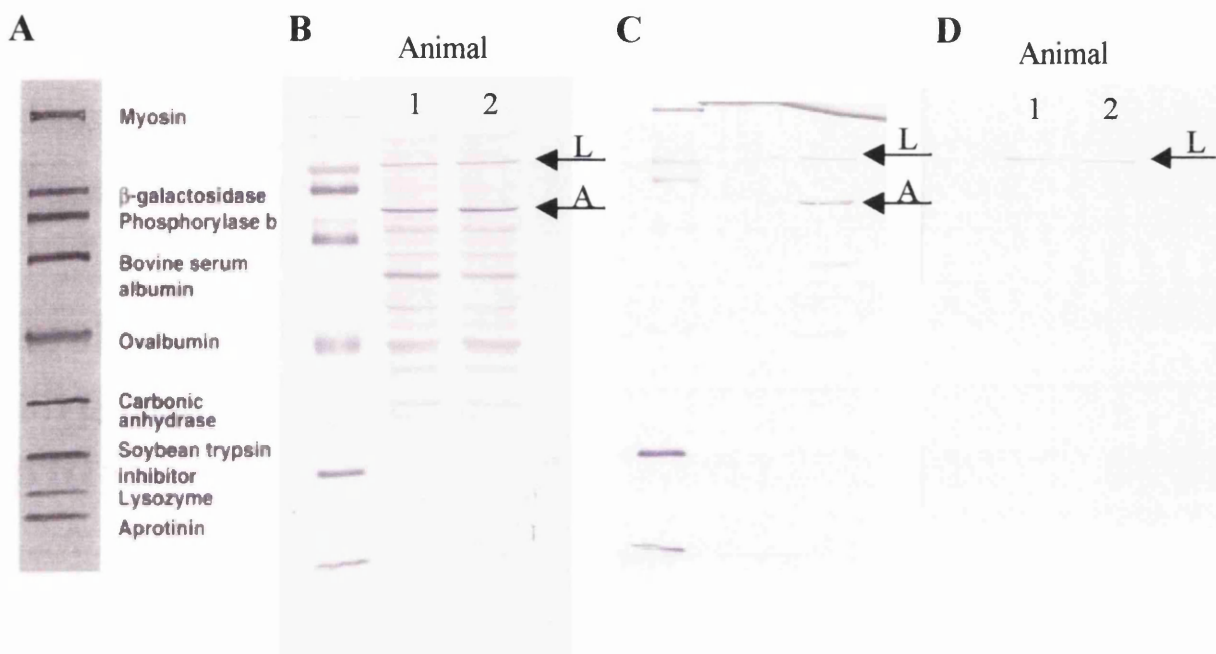


Figure 32. Western Blots for MMP-9 antibody AB805 showing both latent and active bands of the enzyme following 2 hours ILT induced ischaemia plus 22 hours reperfusion.

A. Biotinylated SDS- Page Standard (Broad range),

Myosin = 200 kDa,  $\beta$ - galactosidase = 116 kDa, Bovine serum albumin = 66.2 kDa.

B. Blot of cortical tissue from ipsilateral MCA territory, 1:500 AB805, C. Blot of cortical tissue from ipsilateral MCA territory 1:2000 AB805, D. Blot of MCA territory contralateral hemisphere, 1:2000 AB805. Arrows represent L- latent MMP-9 (92kDa) and A- active MMP-9 (82 kDa).

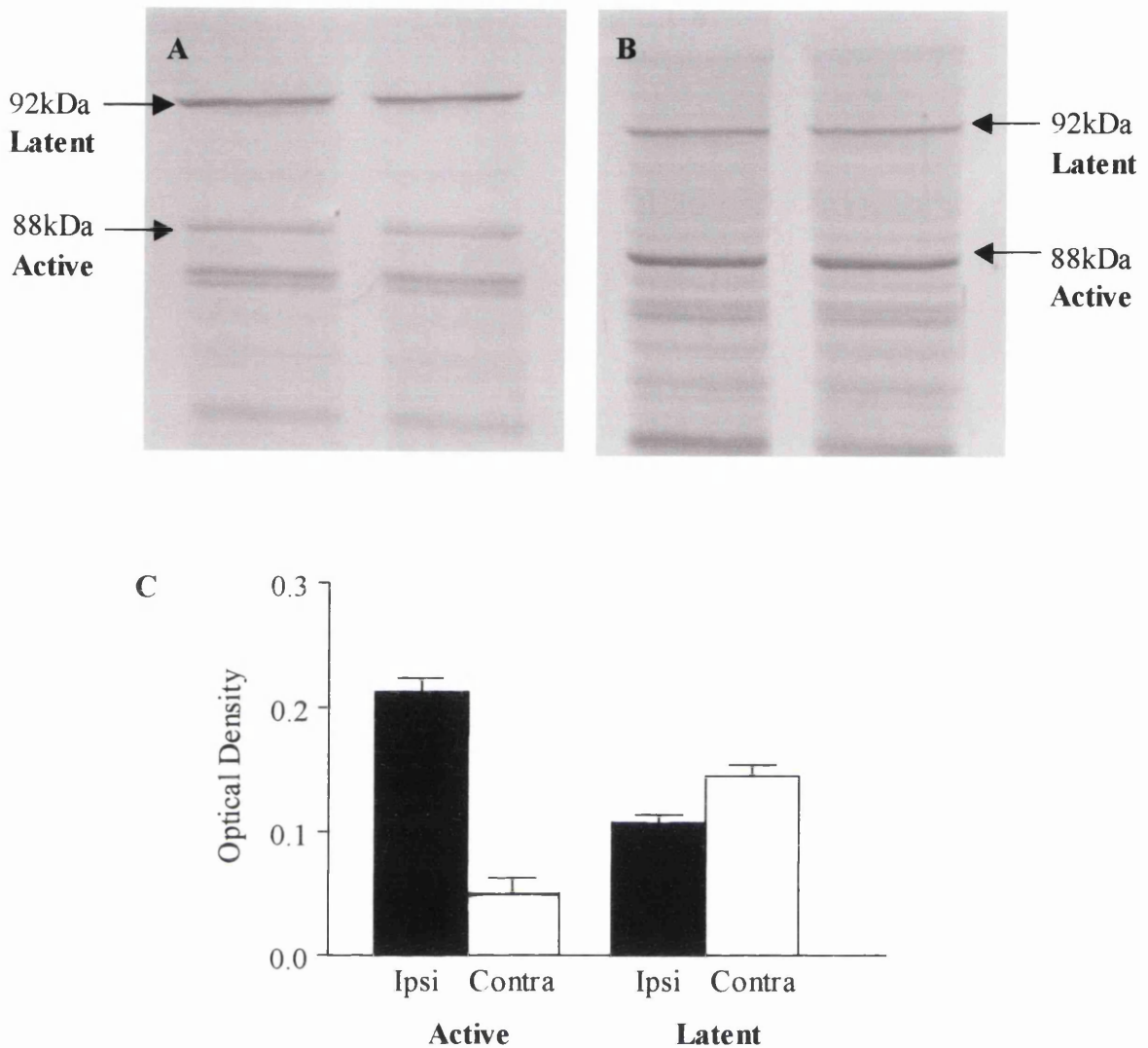


Figure 33. MMP-9 Western Blots captured on MCID. A. Contralateral hemisphere, active and latent bands in cortex of MCA territory, B. ipsilateral hemisphere, active and latent bands in cortex of MCA territory, C. Optical Density in western blots for MMP-9. Data represent mean  $\pm$  SEM, n=2 per group.

#### 4.3.4 Distribution and Cellular Localisation of MMP-9.

Regions of positive staining for MMP-9 (recognised by the presence of immunopositive cells) were drawn onto line diagrams and the boundary of the infarct subsequently superimposed from the H&E sections to determine how the regions of MMP immunoreactivity correlated with the lesion site (Figure 34).

Intense cellular staining was present throughout the infarct but the presence of MMP positive cells also extended beyond the boundary of the infarct into the peri-infarct region in ischaemic animals.

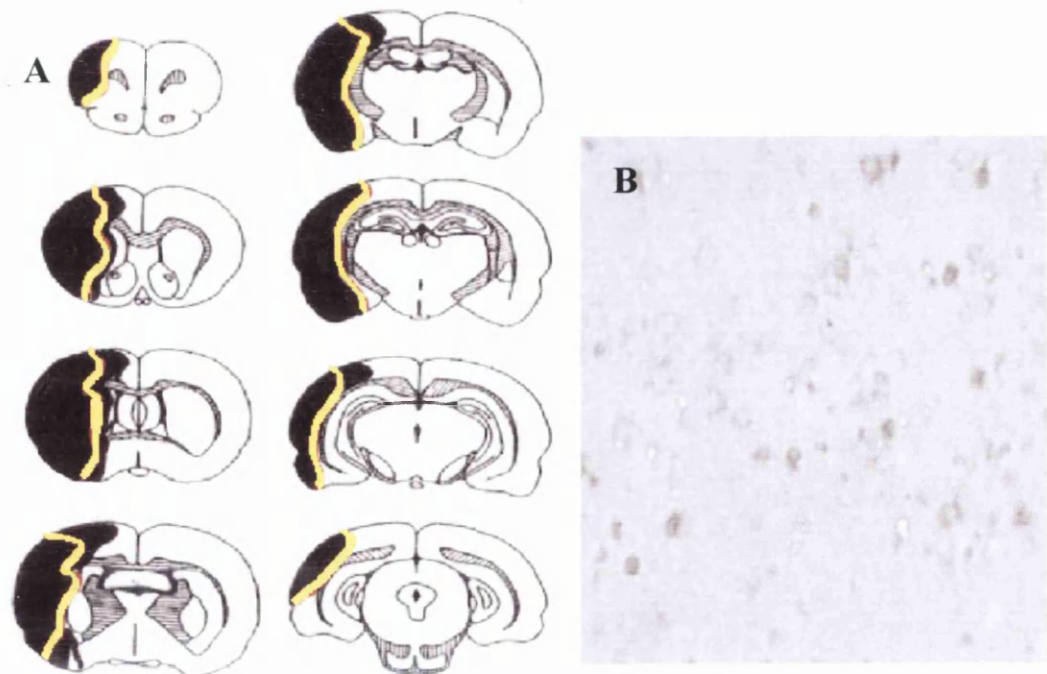


Figure 34. Distribution of MMP-9 staining . A. Representative distribution map for MMP-9 immunoreactivity. The boundary of the lesion is marked in yellow and immunoreactivity in black. B. Representative photo of staining in neurons in the peri-infarct region.

Cells immunopositive for MMP-9 were identified under the light microscope in both the ipsilateral and contralateral hemispheres and were found within the lesion site within the cortex and the striatum. Some of these cells had the appearance of ischaemic neurons being triangular and shrunken in shape. (Figure 35). Blood vessels did not appear immunopositive for MMP-9.

Healthy/non-ischaemic neurons in non-infarcted regions of the ipsilateral hemisphere and in the contralateral hemisphere displayed a less intense and different pattern of staining to that present in ischaemic neurons. Non ischaemic neurons exhibited a cytosolic ‘halo-like’ rim of staining (Figure 36). Sham animals exhibited this halo-like staining of neurons but no other pattern of MMP-9 immunoreactivity.

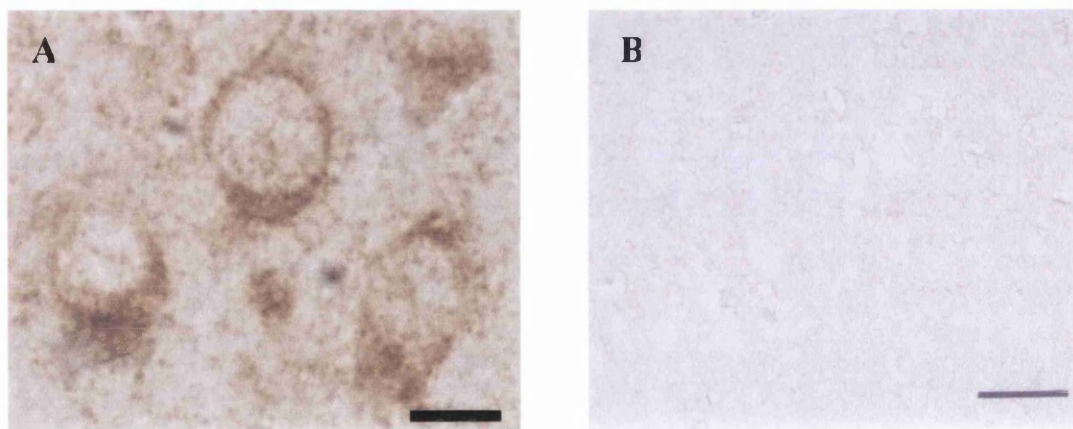


Figure 35. Representative MMP-9 cytosolic staining as present in the contralateral hemisphere of occluded animals and throughout sham sections. A. Staining in neurons of the contralateral hemisphere in occluded animals. B. Negative control for MMP immunohistochemistry. Magnification = X100 in A and X40 in B, scale bar represents 20 $\mu$ m and 50 $\mu$ m respectively.

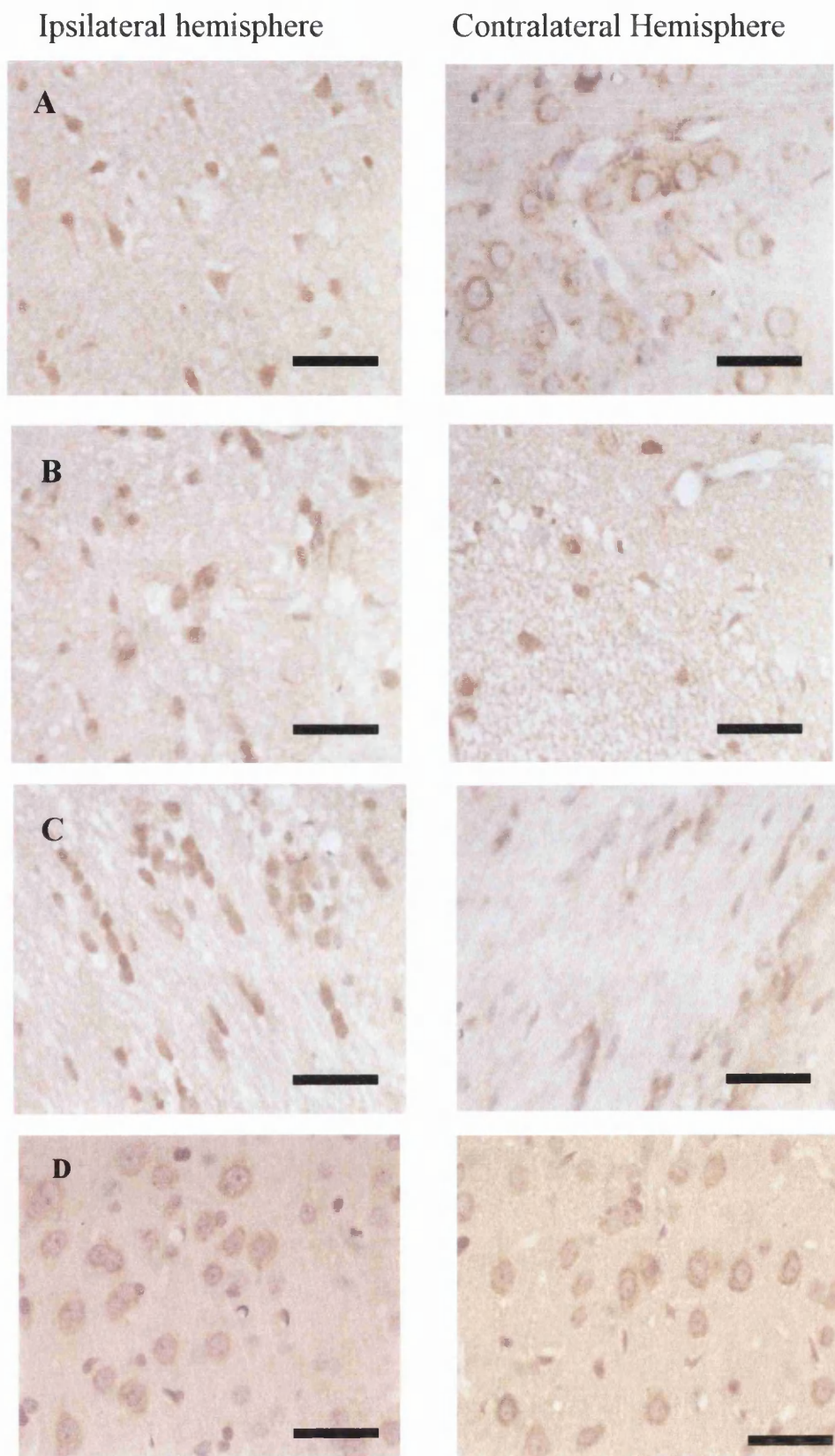


Figure 36. Photographs representing cellular staining of MMP-9 (AB805) in the ipsilateral and contralateral hemispheres of occluded (A-C) and sham (D) animals (n=5). In A. frontal cortex, B. caudate nucleus, C. white matter, D. throughout all regions in sham. Magnification = X40. Scale bar represents 50 $\mu$ m.

Within the white matter tracts of the corpus callosum and external capsule and in axonal tracts within the caudate nucleus, cells with the characteristic morphology of oligodendrocytes exhibited immunoreactivity for MMP-9. Within the genu of the corpus callosum and the external capsule, the positively labelled cells were clearly arranged in lines indicative of oligodendrocytes (Figure 36C).

Other immunopositive cells with a glial appearance were also present within the cortex and caudate of the ipsilateral hemisphere but the staining with DAB alone was insufficient to determine the nature of these MMP-9 positive cell types (Figure 36B).

Due to the fact that microglia and astrocytes have been reported to constitutively express MMPs, double labelling was carried out with DAB (brown) and SG (grey) to identify whether some immunopositive cells were astrocytic or microglial in nature.

Double labelling with MMP-9 and GFAP, appeared to show no double labelling of astrocytes with MMP-9. However double labelling with MMP-9 and mrf-1 (the microglial marker) provided evidence for MMP-9 expressing microglia within the cortex and the striatum of the ipsilateral and contralateral hemispheres of occluded animals (Figure 37). All activated microglia appeared to express MMP-9. Resting microglia expressed little or no MMP-9 as indicated by weak MMP staining (weak brown) or no MMP staining. MMP staining in both activated and resting microglia (when present) appeared to be mainly localised to the cell body rather than the processes.

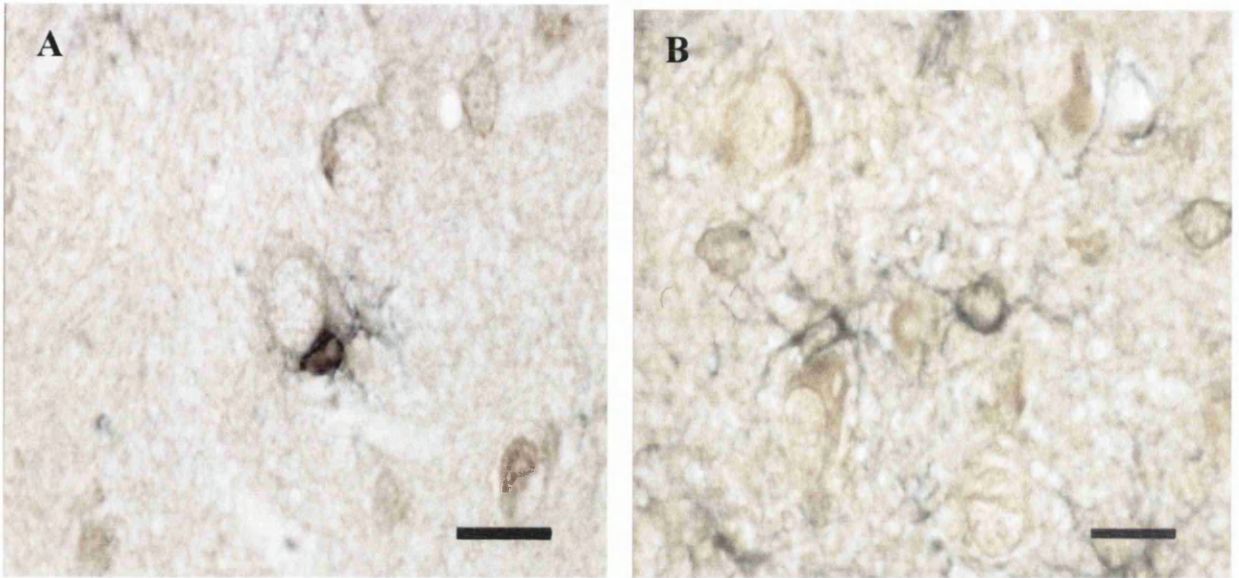


Figure 37. Double labelling with DAB/SG showing A. MMP-9 expressing microglial cell (MMP-9 +ve, mrf-1 +ve) and B. MMP negative astrocyte (MMP-9+ve, GFAP-ve). Magnification = X100. Scale bar represents 20 $\mu$ m.  
= X100, scale bar = 20 $\mu$ m.

Fluorescent double labelling with confocal microscopy was used to confirm whether microglia were indeed expressing MMP-9. Using the confocal microscope activated microglia could clearly be seen to be expressing MMP-9 (Figure 38), with a greater number of fluorescent cells being seen in the ipsilateral hemisphere when compared to the contralateral hemisphere.

At X60 oil objective on the confocal microscope the projections and the cell body of the microglial cell could clearly be seen to be expressing MMP-9.

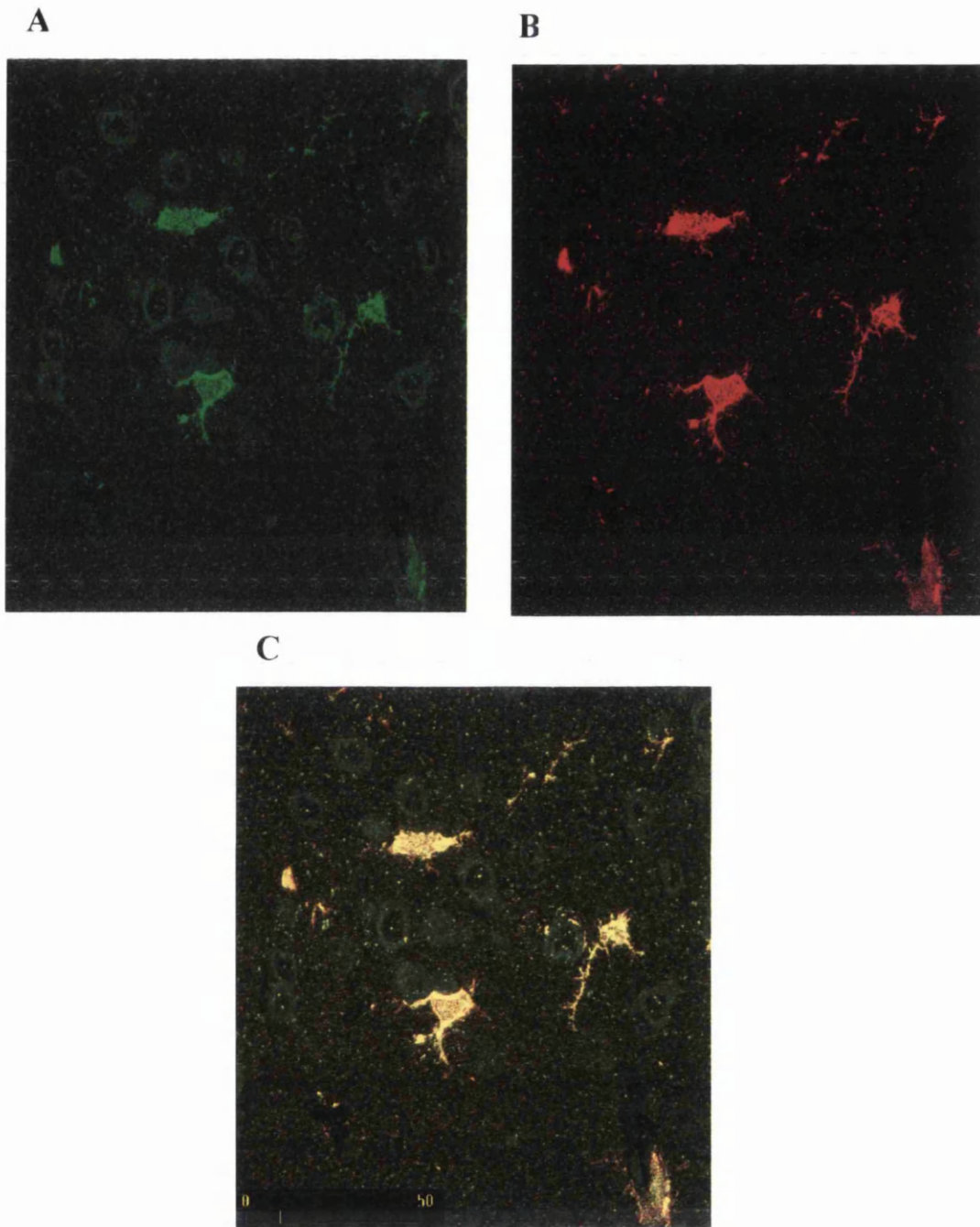


Figure 38. Confocal images (X60 oil objective) representing microglial staining observed with MMP-9. A. Represents MMP immunopositive cells under a fluorescein filter, B. cells are recognised as microglia under a texas red filter (mrf-1 filter) and C. when both images are combined double labelled cells appears as a third colour in this case yellow, indicating microglia are expressing MMP-9 (MMP-8 results (not shown) were almost identical to above images, demonstrating co-localisation of mrf-1 and MMP-8 in activated microglia)

As indicated by light microscopy double labelling, fluorescent double labelling showed both resting and activated microglia were immunopositive for MMP-9 and MMP-8 but the majority of the microglia in the MCA territory were in the activated state as expected following ischaemia. Resting microglia had a much weaker fluorescent signal suggesting lower levels of MMP-9 or MMP-8. Fluorescent double label immunohistochemistry also confirmed that the MMP positive cells in the contralateral hemisphere of occluded animals (identified in earlier single label studies) were activated microglia.

Double label immunohistochemistry with MMP-8 and MMP-9 and tau-1, a marker for ischaemic oligodendrocytes, was also carried out to confirm that oligodendrocytes in the white matter tracts of occluded animals were MMP positive (Figure 39).

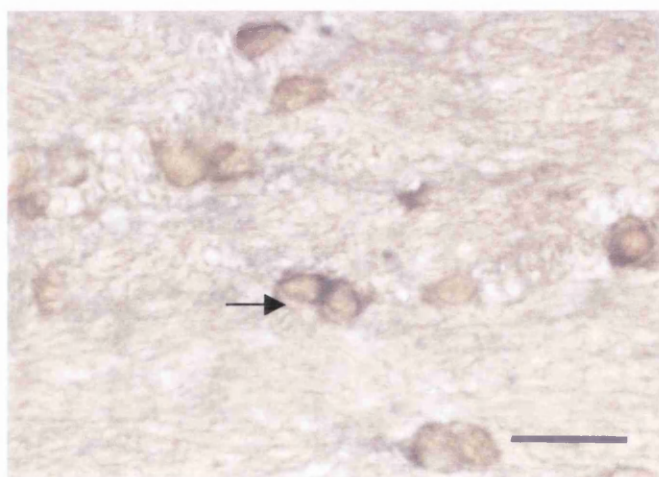


Figure 39 . MMP expression in oligodendrocytes. Double labeling with MMP-9 and Tau-1 in the white matter tract in the ipsilateral hemisphere of an occluded animal. MMP-8 and tau-1 double labeling (not shown) was similar to that seen with MMP-9. Magnification = X40. Scale bar represents 50 $\mu$ m. Arrow represents

#### 4.3.5 Distribution and cellular localisation of MMP-8.

Regions of cellular immunopositive staining for MMP-8 were drawn onto the line diagrams as for MMP-9.

The areas of immunoreactivity with MMP-8 correlated well with the infarcted regions (Figure 40) with further evidence for the spread of MMP immunopositive cells in the peri-infarct region.

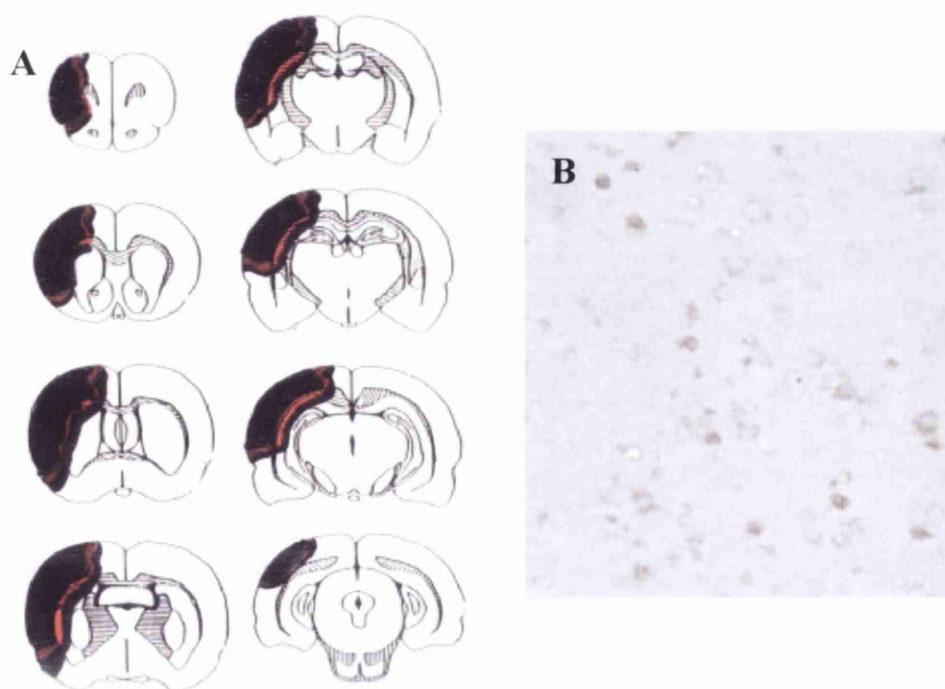


Figure 40. Distribution of MMP-8 staining. A. Representative distribution map for MMP-8 Immunoreactivity. The boundary of the lesion is marked in red and immunoreactivity in Black. B. Representative photo of staining in neurons in the peri-infarct region.

The distribution and the cellular localisation of the MMP-8/ rat neutrophil collagenase was very similar to that of MMP-9/ gelatinase B.

Cells immunopositive for the MMP-8 antibody were found in both the ipsilateral and the contralateral hemispheres with the same neuronal staining patterns being seen as with MMP-9 (Figure 41).

Sham animals once again displayed a cytosolic MMP-8 staining pattern within neurons throughout all region studied.

Oligodendrocytes and glia appeared to be expressing MMP-8 and double labelling followed by fluorescence double labelling and confocal microscopy showed that activated microglia and oligodendrocytes were indeed expressing MMP-8

(Figure 42) but astrocytes were not. As with MMP-9, all activated microglia appeared to express MMP-8 in their cell bodies with resting microglia displaying undetectable or weak MMP-8 staining.

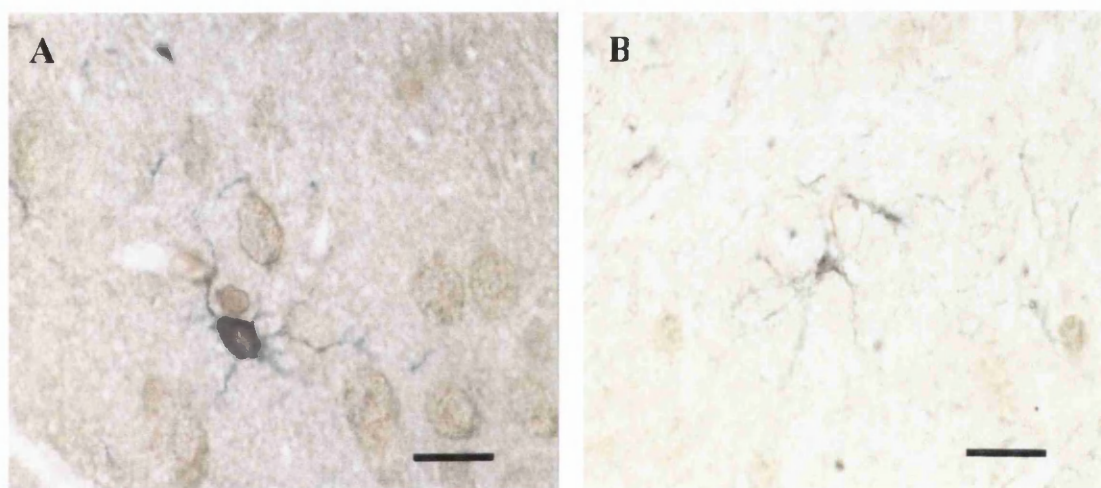


Figure 42. Double labelling with DAB/SG showing A MMP-8 expressing microglial cell (MMP-8+ve, mrf-1+ve) and B. MMP-8 negative astrocytes (MMP-8+ve, GFAP-ve). Magnification = X40. Scale bar represents 50µm.

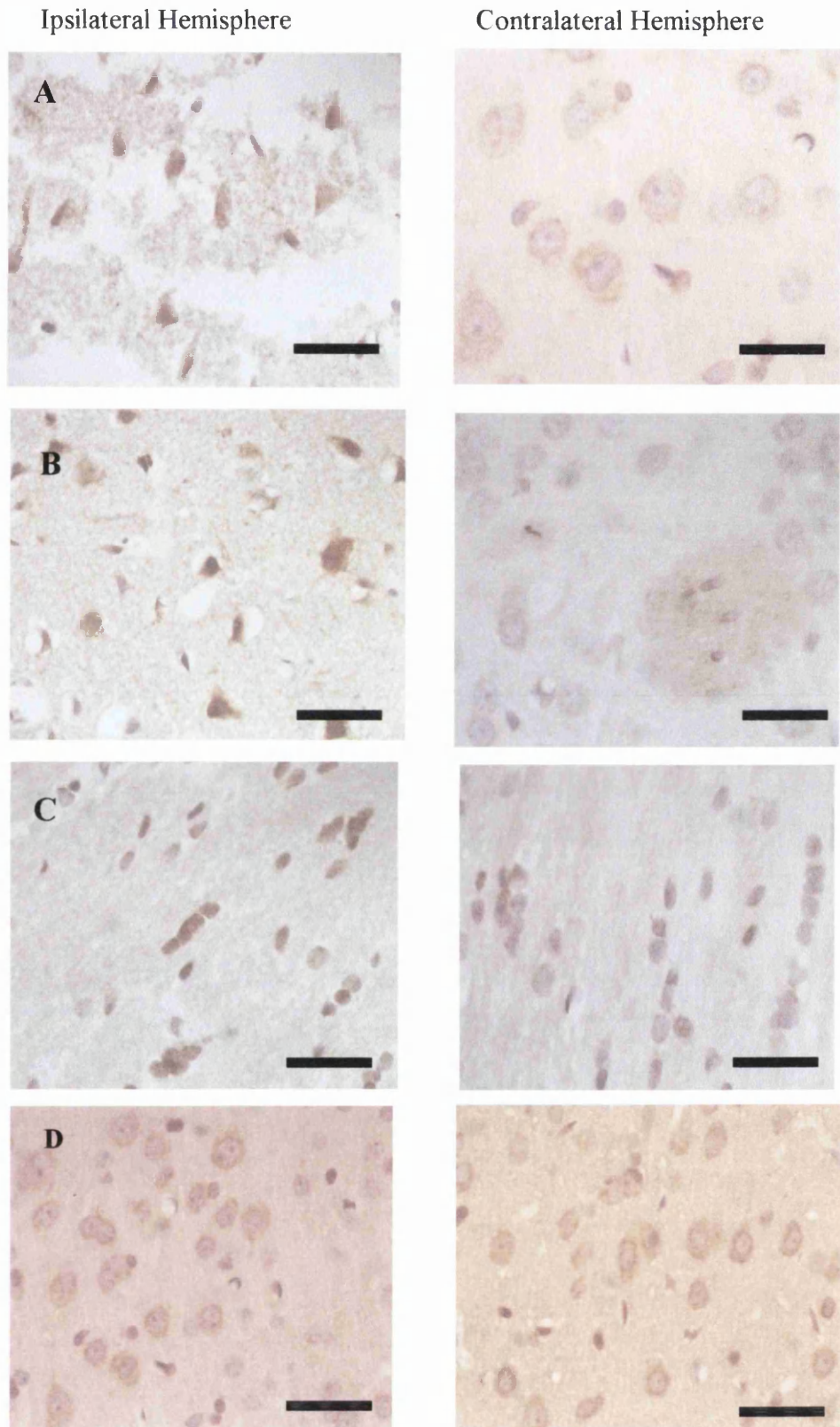


Figure 41. Photographs representing cellular staining of MMP-8 in the ipsilateral and contralateral hemispheres of occluded (A-C) and sham (D) animals (n=5). In A. frontal cortex, B. caudate nucleus, C. white matter and D. throughout all regions in sham.

Magnification = X40. Scale bar represents 50 $\mu$ m.

#### 4.3.6 Specificity of neuronal staining

Due to the possibility that ischaemic neurons could display non-specific staining as a result of their increased stickiness to the antibody, the specificity of the neuronal staining (both in ischaemic neurons and healthy neurons) was later investigated when an MMP-9 antibody with a specific blocking peptide became available. A blocking peptide has the ability to block specific staining patterns so that any immunoreactivity that remains after the use of the blocking peptide is likely to be non-specific.

A blocking peptide was not available for the Chemicon MMP-9 antibody AB805 which was used in this study but one was available for the Santa Cruz MMP-9 antibody C-20. Immunohistochemistry with the polyclonal antibody C-20 (1:100) demonstrated a different pattern of staining to AB805 with immunoreactive blood vessels in addition to staining in ischaemic and healthy neurons (Figure 42). After the addition of the blocking peptide, immunoreactive blood vessels were no longer visible but both types of neuronal staining could still be seen. This would suggest that MMP-9 staining within ischaemic neurons and the cytosolic MMP-9 staining in healthy neurons of both occluded and sham animals may not be specific.

The Santa Cruz antibody did not stain oligodendrocytes or microglia and so no comments can be made in terms of the specificity of these two staining patterns.

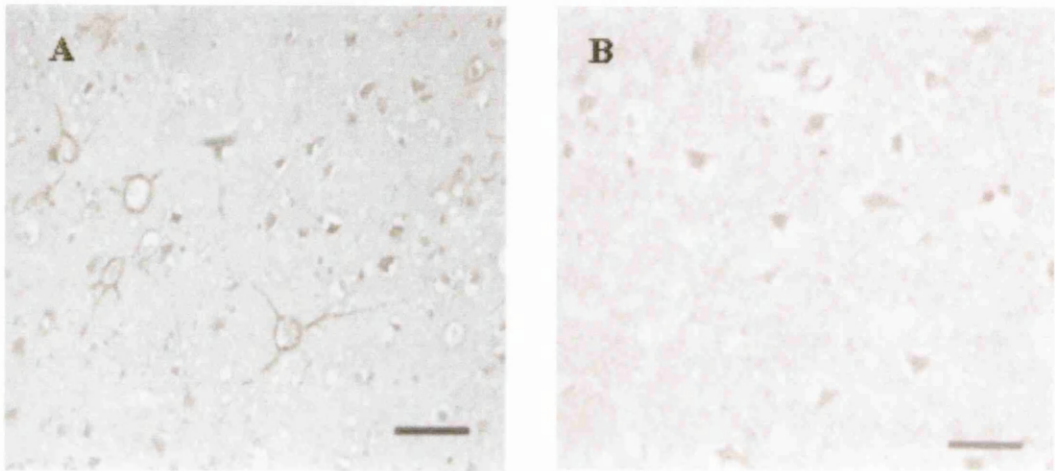


Figure 43. MMP-9 Santa Cruz antibody staining with blocking peptide. A. MMP-9 antibody, B. MMP-9 pre-incubated with blocking peptide. Magnification = X40. Scale bar represents 50 $\mu$ m.

#### 4.3.7 BBB permeability and MMP-9 staining.

PAP immunohistochemistry showed the presence of extravasated proteins within the infarct and showed a characteristic graded pattern of staining with the strongest immunoreactivity in the hypothalamus. Blood vessels within the infarct were also found to be PAP positive (Figure 43) with PAP positive extravasated serum proteins in the surrounding parenchyma.

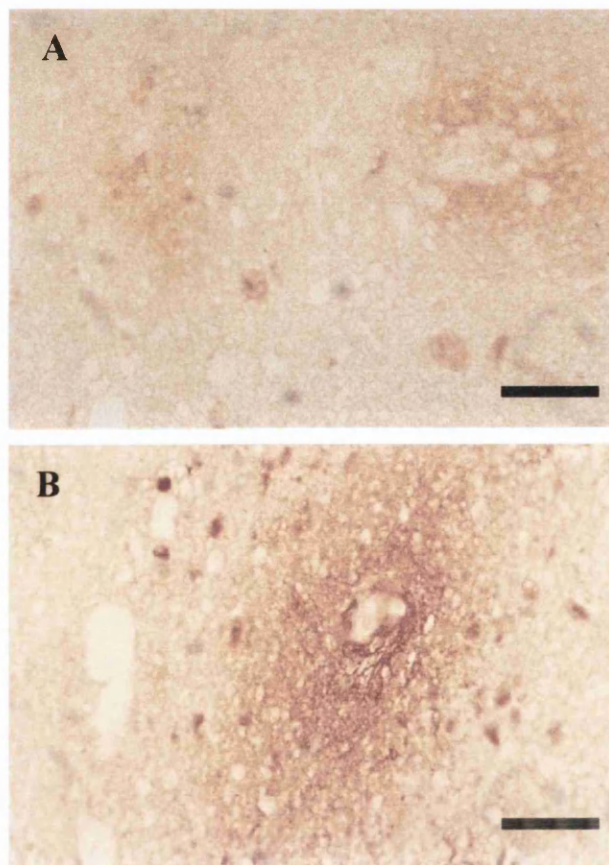


Figure 44. PAP immunoreactivity following ILT induced ischaemia at 24 hours. A. graded staining and B. extravasated serum proteins around an immunopositive blood vessel within the core of the infarct. Magnification =X40. Scale bar represents 50µm.

When the area of PAP immunoreactivity and MMP positive cells in the area of the infarct were compared there was a clear overlap between the regions with MMP positive cells and the region of increased BBB permeability as represented by PAP immunoreactivity. PAP staining was not however consistently found in all animals.

In an attempt to look more specifically at BBB permeability, antibodies to the extracellular proteins albumin and fibrinogen were used to confirm the increase in extravasated proteins occurred following intraluminal thread induced MCA occlusion and to identify any correlation with increased MMP immunoreactivity.

As with PAP immunoreactivity, staining with anti-albumin and anti-fibrinogen was found within and around blood vessels within the infarct (Figure 44). Staining was found in the core of the infarct and in the peri-infarct region and was graded with intense staining at the core of the infarct which became more diffuse as you moved from the core to the boundary of the lesion. Areas of anti-albumin and anti-fibrinogen immunoreactivity correlated with areas of MMP immunoreactivity. However once again the staining was not consistent amongst animals.

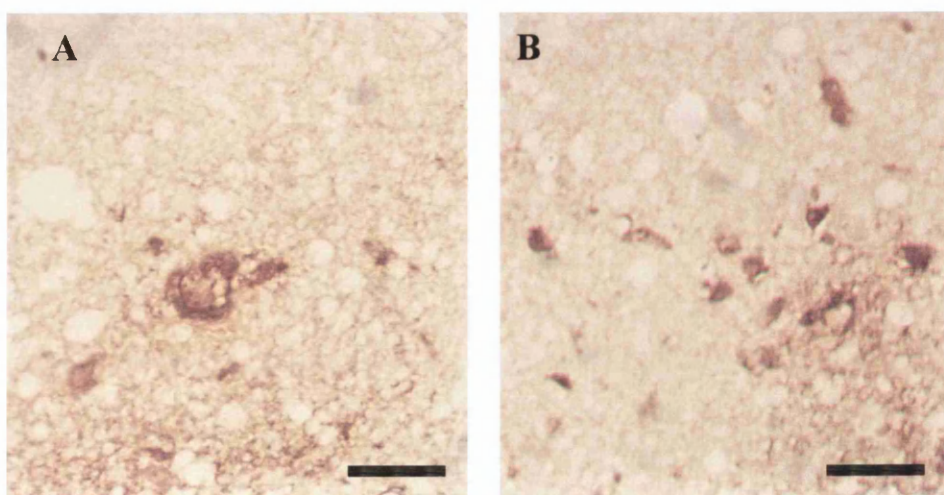


Figure 45. Staining of extravasated serum proteins following ILT induced ischaemia (24 hour time point). A. albumin staining in core of the infarct of an occluded animal, B. fibrinogen staining in the core of the infarct of an occluded animal. Magnification = X40.

#### 4.4 Discussion

Matrix metalloproteinases have been implicated in the pathogenesis of stroke with increases in MMP levels occurring following ischaemia (Rosenberg *et al.*, 1996; Roamanic *et al.*, 1998; Gasche *et al.*, 1999).

Studies using zymography, a form of gel electrophoresis, to measure MMP activity following ischaemia have reported an increase in the activity of gelatinase A (MMP-2) and gelatinase B (MMP-9) (Romanic *et al.*, 1998; Rosenberg *et al.*, 1996) following experimental ischaemia. In some cases an accompanying increase in the levels of members of the TIMP family of naturally occurring MMP inhibitors was also observed suggesting a possible link between the MMP and their inhibitors in the pathogenesis of stroke (Gasche *et al.*, 1999).

The technique of immunohistochemistry has been used by some groups in an attempt to identify MMP expressing cells following ischaemia (Romanic *et al.*, 1998; Gasche *et al.*, 1999). These studies, however, are fewer in number and have not yet conclusively characterized the cellular localization of MMPs and their distribution following ischaemia. Antibodies available for MMPs cannot distinguish between activate and latent forms of the MMP but immunohistochemistry is essential for determining cellular location of the MMPs. The present study therefore set out to investigate which cell types were expressing MMP-8 and MMP-9 along with the anatomic location of MMP staining in order to gain a better understanding of the possible roles of MMPs in ischaemic damage.

In accordance with previous studies, increased levels of MMP-8 (rat collagenase) and MMP-9 (gelatinase B) were found in animals exposed to an ischaemic insult.

Sham animals exhibited only a weak cytoplasmic immunoreactivity of MMP-8 and MMP-9 staining in neurons. In occluded animals, the greatest numbers of immunopositive cells were found in the ipsilateral hemisphere associated with the infarct core and peri-infarct zone supporting a role for MMPs in ischaemic damage.

An important finding of this study was the expression of MMP-8 and MMP-9 in neurons within the peri-infarct zone in animals exposed to 2 hours ILT induced ischaemia and 22 hours reperfusion. It has previously been reported that in the intraluminal thread model of MCAO, following 2 hours occlusion, the infarct is still evolving at the 24 hour time point. Indeed a 62% increase in the volume of ischaemic damage occurs between 24 and 48 hours ( $80 \pm 14\text{mm}^3$  at 24 hours versus  $131 \pm 26\text{mm}^3$  at 48 hours; Peters, 1999). The presence of MMP-8 and MMP-9 in the peri-infarct zone at a time when the infarct is still evolving could implicate the MMPs in the generation of further damage.

As discussed previously, MMPs are believed to contribute to ischaemic damage in a number of ways:

#### **MMPs and BBB breakdown.**

Perhaps the most important potential mechanism of MMP mediated ischaemic damage is the ability of the MMPs to degrade components of the ECM leading to BBB breakdown and oedema. The knock-on effect of this could potentially lead to an increased influx of inflammatory cells and the subsequent release of cytotoxic substances. The degradation of the basal lamina of the ECM by MMPs resulting in a loss of basal lamina integrity is believed to be the main cause of microvascular haemorrhage after focal MCAO (Hamann *et al.*, 1996; Okada *et al.*, 1994) and

studies using synthetic inhibitors of MMPs have reported a decrease in oedema following experimental ischaemia (Mun-Bryce *et al.*, 1999).

This study attempted to investigate the link between BBB permeability and MMP expression and found that following two hours intraluminal thread induced ischaemia and twenty-two hours reperfusion, the serum proteins albumin and fibrinogen, both markers of BBB breakdown, were present in the injured tissue of the ipsilateral hemisphere. Albumin and fibrinogen could be seen around blood vessels in areas with increases in MMP expression. Areas immunopositive for PAP (also used as a marker for BBB breakdown) could also be seen within injured tissue – in the core of the infarct and within the peri-infarct zone and these again correlated with areas of MMP staining in surrounding ischaemic neurons and activated microglial cells. This would support the theory that MMP degradation of ECM components may contribute to BBB breakdown following ILT induced transient ischaemia. This would seem feasible as studies have shown MMP staining of blood vessels following ischaemia (Romanic *et al.*, 1998; Gasche *et al.*, 1999), with blood vessels being the main source of extravasated proteins during increased BBB permeability.

### **MMPs and inflammatory cells.**

MMPs are also believed to contribute to ischaemic damage via their ability to aid the migration of inflammatory cells to the site of damage following MCAO. The tissue degrading properties of the MMPs are well reported and it is feasible that inflammatory cells use MMPs to degrade ECM components to allow their movement through the tissue towards the lesion site. Inflammatory cells such as neutrophils and T cells have been reported to secrete MMPs in order to migrate towards the site of

damage in a number of pathological conditions including Experimental Autoimmune Neuritis (EAN) (Graesser *et al.*, 2000) and experimental MCAO (Heo *et al.*, 1998). Although no neutrophils were identified in the ILT brain sections under the light microscope, another important inflammatory cell- the microglial cell- was found to be immunopositive for MMP-8 and MMP-9. Microglial recruitment is widely accepted to be a major event following ischaemia (Gehrmann *et al.*, 1992) irrespective of whether these microglial cells perform a beneficial (phagocytosis, repair and growth factor secretion) or a detrimental (release of cytotoxic substances and free radicals leading to further tissue damage) role. Previous studies have suggested that microglia may use the white matter tracts to migrate towards the site of tissue damage following ischaemia (Zhang *et al.*, 1997; Peters, 1999) and microglia accumulate in high numbers within the ipsilateral hemisphere within the core and the peri-infarct regions (Peters, 1999; chapters 5 and 6 of this thesis). In this study MMP positive microglia were identified in both grey and white matter in the contralateral and the ipsilateral hemispheres of occluded animals. Sham animals possessed very few activated microglia and a very low level of MMP expression limited to the halo-like cytosolic staining pattern of healthy neurons. The presence of MMP positive microglia in the contralateral hemisphere of occluded animals may suggest a role for the MMPs in aiding the migration of activated microglia in the contralateral hemisphere (the activation is probably stimulated by diaschisis (Seitz *et al.*, 1999) or spreading depression (Kato and Waltz, 2000) to injured regions of the ipsilateral hemisphere where they accumulate in large numbers, in and around the lesion (see chapter 5).

Although no reports of MMP mediated microglial migration have been published, MMPs have been implicated in the migration of neutrophils (Vos *et al.*, 2000; Pugin *et al.*, 1999) and cancer cells giving rise to metastasis. MMPs (commonly MMP-2 and MMP-9) have been reported to aid the movement of cancerous cells/tumorous masses through tissue in various forms of cancer (Liotta *et al.*, 1980; Aoudjit *et al.*, 1998; Tomita *et al.*, 1996). Drugs directed against MMPs have also been shown to slow the progression of cancer metastasis formation in various animal models of cancer (Slavomir *et al.*, 1997; Gomez *et al.*, 1997)

If MMPs are capable of promoting the movement of neutrophils and tumour cells then it is feasible that their presence in microglial cells may indicate a role in the migration of microglia during ischaemia. If this is indeed the case then inhibiting MMP mediated microglial migration may be an important therapeutic strategy in reducing ischaemic damage.

#### **MMPs and increases in cytokines and reactive oxygen species.**

By facilitating the migration of inflammatory cells, MMPs could be said to be indirectly contributing to ischaemic damage by increasing the number of activated microglia present at the lesion site subsequently increasing the levels of cytotoxic substances and reactive oxygen species released by these cells.

A rise in cytotoxic substances (e.g. TNF- $\alpha$ , IL-1 $\beta$ ) and in reactive oxygen species has been reported to occur within hours of an ischaemic insult (Babak *et al.*, 1996).

One of the sources of these substances is believed to be activated inflammatory cells such as neutrophils and microglia. By enabling the neutrophils and microglia to move towards the ischaemic lesion and accumulate within the ipsilateral hemisphere, MMPs could be said to be indirectly increasing the likelihood of the release of cytotoxic substances therefore potentiating ischaemic damage.

It has been reported in various clinical conditions that cytokines and MMPs are closely linked in terms of negative and positive feedback in the inflammatory response to damage. In terms of brain injury IL-1 $\beta$  has been shown to increase the release of MMPs from glial cells (Rosenberg *et al.*, 1996) and in peripheral nerve injury TNF- $\alpha$  and MMP-2 levels correlate well suggesting a role for the TNF- $\alpha$  converting function of MMP-2 in the pathology of this condition (Shubayev *et al.*, 2000). Matrix metalloproteinases have previously been linked to TNF- $\alpha$  production by their ability to cleave the TNF- $\alpha$  precursor to biologically active TNF- $\alpha$  (Gearing *et al.*, 1994; McGeehan *et al.*, 1994). If there was a link between MMP levels and cytokine levels following MCAO, one might expect to see an increase in some of these cytotoxic substances following ischaemia accompanying increases in MMP-8 and MMP-9. To investigate this possibility, this study used an antibody directed against IL-1 $\beta$  to characterise any IL-1 $\beta$  expression following ILT induced ischaemia. No evidence was found for an increase in IL-1 $\beta$  expression in this model of MCAO at the 24-hour time point. However, this was not due to failure of the antibody to identify IL-1 $\beta$  since IL-1 $\beta$  positive microglia could clearly be seen in the positive control tissue which was run along with ischaemic material. If IL-1 $\beta$  were contributing to increases in MMP-8 and MMP-9 leading to increased ischaemic damage one might expect to see some degree of immunoreactivity at 24 hours in this

model as previous studies have shown widespread IL-1 $\beta$  expression in astrocytes, microglia and neutrophils at this time point in models of brain injury and ischaemia (Pearson *et al.*, 1999; Davies *et al.*, 1999; Rothwell *et al.*, 1997; Guilian *et al.*, 1985; Loddick & Rothwell, 1996 ).

Although a number of groups have reported increased IL-1 $\beta$  expression in models of experimental stroke, other studies from this laboratory have also failed to provide evidence for increased IL-1 $\beta$  up to 72 hours following ILT or endothelin-1 induced MCAO in the rat (Peters *et al.*, 1999).

Increased levels of MMPs could therefore result in an increased BBB permeability and an enhanced inflammatory response to ischaemia through a series of cytokine interactions leading to increases in the levels of inflammatory cells and mediators following experimental ischaemia.

### **MMPs and their involvement in the development of the infarct.**

MMPs have been implicated in ischaemic damage and various groups have investigated MMP inhibitors in models of experimental ischaemia in order to determine whether they have the ability to reduce ischaemic damage and/or associated BBB permeability (Asahi *et al.*, 2000; Rosenberg *et al.*, 1998; Romanic *et al.*, 1998).

Romanic and co-workers demonstrated a 30% reduction in infarct size with the systemic administration of an MMP-9 neutralising antibody (monoclonal MMP-9 antibody) 1 hour before MCAO and Asahi and co-workers found that administering the broad spectrum synthetic MMP inhibitor BB-94 at 30 minutes before and 3 hours after the start of a focal ischaemic insult resulted in a significant reduction in

ischaemic volume (around 15%). The presence of MMP-8 and MMP-9 positive cells in the core of the infarct and within the peri-infarct zone in this study would seem to provide further evidence for an MMP role in ischaemic damage and may suggest that an MMP inhibitor/antibody may be a useful therapeutic tool in ischaemic damage.

MMP positive neurons were seen within the core of the infarct suggesting that they may be responsible for ischaemic damage within the core. However due to the sticky nature of ischaemic neurons, the specific nature of the neuronal staining was questioned. The use of a blocking peptide with another MMP-9 antibody (Santa Cruz MMP-9 C-20) confirmed that the neuronal staining observed in ischaemic neurons in the core and the cytosolic halo-like staining observed in healthy neurons in both occluded and sham animals was probably non-specific. However due to the fact that no blocking peptide is currently available for the MMP-9 antibody used in this study (Chemicon, AB805) one cannot completely rule out the possibility that the neuronal staining reported with the Chemicon MMP-9 antibody is specific. Additional evidence that the neuronal staining in ischaemic neurons may be specific is that in the peri-infarct region of the ipsilateral hemisphere of occluded animals MMP positive neurons could be seen which had a more normal morphology and would not have the stickiness of the ischaemic neurons at the core of the lesion. No comments can be made about the specificity of the peri-infarct neuronal staining as the Santa-Cruz antibody alone did not exhibit such staining

If the neuronal staining in the core is non-specific this does not rule out the possibility that MMPs found in other cell types including activated microglia may be contributing to ischaemic damage and or the expansion of the infarct (as suggested

by the presence of MMP expressing activated microglia in the peri-infarct zone). Microglia are widely believed to have a role in ischaemic damage and so their presence in the peri-infarct zone following ILT induced ischaemia may provide evidence for a role in ischaemic damage.

### **Differences in reported MMP immunoreactivity**

In this study MMP-8 and MMP-9 positive microglia, neurons and oligodendrocytes were identified in the occluded animals following ILT induced transient MCAO. In the contralateral hemisphere and throughout both hemispheres in sham animals, a fainter rim of cytosolic staining could be seen around healthy neurons. No studies have previously attempted to characterise MMP-8 cellular localisation but studies using antibodies directed against MMP-9 have reported different results in terms of which cell types exhibited immunoreactivity. Romanic *et al.*, (1998), identified positively stained neutrophils in ischaemic rat tissue while Gasche *et al.*, (1999), identified positively stained neutrophils, blood vessels and a form of extracellular staining in the caudate with MMP-9 antibodies.

Differences in cellular localisation may result from the use of different MMP-9 antibodies from different commercial sources. It could well be that different MMP-9 antibodies are capable of detecting different cellular forms of MMP-9 so while one may be able to detect the microglial form of MMP-9 another may only be able to detect the neutrophil form of MMP-9. This would seem feasible as in this study two different MMP-9 antibodies produced different patterns of staining. The Chemicon MMP-9 antibody (AB805) was found to be expressed in microglia, oligodendrocytes and possibly neurons, while the Santa Cruz MMP-9 antibody (C-20) was

predominantly found in blood vessels suggesting that the two antibodies are detecting different cellular forms of MMP-9. In addition to differences in the antibody used, differences in the model of ischaemia may result in differing degrees of inflammatory mediated damage. Certainly in our model of transient ischaemia very few neutrophils if any were seen in either the experimental or the sham animals. This would explain the lack of neutrophil expression of MMP-8 or MMP-9. Different models may have varying degrees of neutrophil activation depending on the time point examined (see chapter 3). In terms of the neuronal staining of healthy neurons, no such staining has been reported previously. However from the western blots carried out on the ILT tissue, low levels of MMP-9 expression was found within the contralateral hemisphere and studies from other labs using zymography have also reported low levels of MMP expression in the contralateral hemispheres of rat brains (Gasche *et al.*, 1999; Yjanheikki *et al.*, 2000, abstract). However, in the blocking peptide study, all the staining patterns observed in the contralateral hemisphere appeared to be non-specific and the cytoplasmic rim staining of healthy neurons was not apparent with this antibody.

In conclusion, this study has demonstrated an increase in the levels of MMP-8 and MMP-9 following ILT induced transient ischaemia in the rat. Levels of these two MMPs were higher in the ipsilateral hemisphere suggesting that MMPs may contribute to the development of the infarct. The most specific MMP staining was found expressed within activated microglia suggesting a role for MMPs in the migration of these inflammatory cells during ischaemia.

## Chapter 5 SHRSP/WKY Microglia Study

### 5.1 Introduction

Spontaneously hypertensive stroke prone rats (SHRSPs) have a genetically determined increased sensitivity to experimental stroke, displaying greater volumes of cerebral infarction when compared to their normotensive reference strain the Wistar Kyoto (WKY) (Coyle *et al.*, 1983)

One of the main contributory factors to the increased stroke sensitivity of the SHRSP is thought to be a reduced collateral blood supply following middle cerebral artery occlusion. This reduced collateral blood flow may be due to impaired function in anastomotic vessels resulting in reduced supplementary flow from the anterior and posterior cerebral arteries to the middle cerebral artery territory (Coyle *et al.*, 1983).

However it is widely accepted that other factors may also contribute to increased sensitivity to stroke in the SHRSPs. These include an increased release in glutamate following ischaemia (Gemba *et al.*, 1992), genetic hypertension (Yamori *et al.*, 1982) and an increased inflammatory response.

With regard to the inflammatory responses, SHRSP and the related spontaneously hypertensive rat (SHR, the strain from which the SHRSP were derived) have been reported to elicit a greater response to inflammatory stimuli than control strains. In response to a provocative dose of lipopolysaccharide, SHRSP and SHR both produce significantly more tumour necrosis factor (TNF), a mediator of inflammation, in the plasma, than WKY or Sprague Dawley rats (Hallenbeck *et al.*, 1991). Mature SHR have also been reported to have significantly elevated neutrophil, monocyte and

lymphocyte counts in their blood compared to WKY (Del Zoppo *et al.*, 1991), with an abnormal degree of activation of these cells and have been shown to produce higher levels of TNF and platelet activating factor in CSF following i.c.v. lipopolysaccharide (Siren *et al.*, 1992).

Inflammation and inflammatory cells are widely reported to contribute substantially to ischaemic damage. Although it is acknowledged that inflammatory cells in general can aid the repair process at sites of injury it is well established that increases in certain inflammatory cells and inflammatory mediators can lead to increased ischaemic damage.

As previously mentioned, neutrophils in particular have been proposed to contribute to ischaemic damage migrating to sites of injury via a process of slowing, rolling and tethering to the blood vessel wall via the expression of adhesion molecules on their surface and on the endothelium of blood vessels. Once adhered to the vessel wall, neutrophils are capable of damage not only via their physical blockade or “plugging” of vessels, reducing blood flow (no-reflow phenomenon), but also by their activation and release of cytotoxic substances, either at the endothelial surface or following migration into the brain. An increase in the release of cytotoxic substances such as TNF- $\alpha$  (Liu *et al.*, 1994) and certain interleukins (Giulian *et al.*, 1990; Touzani *et al.*, 1991; Loddick *et al.*, 1996) from inflammatory cells such as neutrophils has been shown to potentiate ischaemic damage with the administration of antibodies directed against these inflammatory mediators ameliorating damage in experimental conditions of ischaemia.

In addition to the possible involvement of invading inflammatory cells like neutrophils in inflammatory mediated ischaemic damage, it is also possible that resident inflammatory cells from within the CNS may be contributing to damage.

Microglia, inflammatory cells resident in the brain, have the ability to both prevent further damage by removing debris and aiding neural regeneration and to contribute to ischaemic damage by a variety of mechanisms including the secretion of cytotoxic substances. It is the release of these cytotoxic substances which is thought to be the main cause of microglial mediated damage during and after ischaemia. Cytokines induce lipid peroxidation, excess release of transmitters and hormones, vascular leakage, oedema, necrosis and changes in ion flow. Indeed a rise in cytokine levels occurring 1-2 days following ischaemia (Baback *et al.*, 1996) would seem to correlate well with the timescale for microglial activation. As previously mentioned, an increase in activated microglia has been reported in models of both global and focal experimental ischaemia with the rate of microglial activation being dependent on brain region and duration of the ischaemic insult.

The aim of this study was to investigate the CNS inflammatory response to focal ischaemia in SHRSP and WKY, to determine whether strain differences existed in the number of neutrophils and activated microglia present following experimental ischaemia and to characterise the inflammatory response in relation to evolution of ischaemic damage.

In addition to quantification of microglial numbers in experimental animals, levels were also examined in naïve SHRSP and WKY. SHRSP are known to develop hypertension within weeks of birth resulting in a systolic blood pressure of around 200mmHg maintained throughout life (Yamori *et al.*, 1977). It is possible that this

underlying hypertension could influence the levels of activated microglia under basal conditions. Indeed hypertension in the SHRSP has been shown to predispose the strain to blood brain barrier breakdown (Fredricksson *et al.*, 1985). Damage to the blood brain barrier may act as a stimulus for microglial activation under non-ischaemic conditions with no equivalent activation occurring in the normotensive WKY. Therefore to rule out any influence of potential basal differences between the two strains microglial expression was characterised in naïve animals in addition those undergoing MCAO.

## **5.2 Materials and Methods.**

All experiments were carried out under licence from the Home Office and were subject to The Animals (Scientific Procedures) Act, 1986. Age matched (3-5 month) male rats, were obtained from inbred colonies of SHRSP and WKY held in the Department of Medicine and Therapeutics, University of Glasgow. These colonies were established from a group of 13 SHRSP and WKY rats obtained from inbred colonies held at the University of Michigan as previously described by Davidson *et al.*, 1995.

### **5.2.1 Surgical procedures.**

Middle cerebral artery occlusions were carried out by Dr H.V.O. Carswell.

A 2 mm distal occlusion of the middle cerebral artery (MCA) was carried out via a transorbital approach using a modified version of Tamura *et al.*, 1981 as described previously in section 2.1.3. On completion of the surgery, animals were allowed to recover for 24 hours. Both occluded and naïve animals were perfused with 4% paraformaldehyde in PBS. Brains were then removed, and frozen in isopentane before 30µm sections were cryostat cut, stored in cryoprotectant and mounted onto poly-lysine slides as required for immunohistochemistry, described in section 2.2.6..

### **5.2.2 Infarct Determination.**

Infarcts were transcribed from H&E sections onto line diagrams and infarct area was then measured from the line diagrams using image analysis (MCID, Imaging Research, St Catherines, Ontario) and infarct volume calculated by integration as previously described in section 2.2.5..

Sections from naïve animals were examined at the light microscopic level to look for any evidence of damage or inflammatory responses as a result of any BBB damage.

### 5.2.3 Neutrophil counts.

Neutrophils, easily identified on haematoxylin and eosin stained sections by their morphology and the characteristic segmented or lobular appearance of their nucleus (Figure 46) were counted at coronal levels of the nucleus accumbens, globus pallidus and lateral habenula.

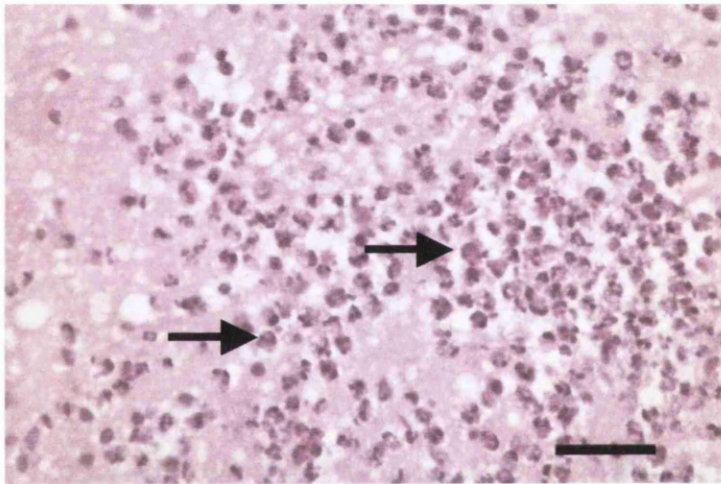


Figure 46. Characteristic neutrophil morphology, showing lobular appearance of the nucleus. Photograph was taken from positive control material for CNS inflammation (infection in an ischaemic animal resulted in massive neutrophil infiltration and meningitis). Scale bar represents 50 $\mu$ m.

#### **5.2.4 Immunohistochemistry**

Sections from 5 of the coronal levels were stained with the monoclonal microglial marker Ox-42 (Serotec, UK, 1:1000) or the polyclonal marker mrf-1 (1:1000 gifted by Dr S. Tanaka and Dr T. Koike, Molecular Neurobiology Laboratory, Hokkaido University). To ensure consistency of staining, SHRSP and WKY sections were always stained in the same immunohistochemistry run with appropriate negative and positive control sections. Negative controls involved the omission of the primary antibody and sections from a rat brain exhibiting signs of meningitis were included as positive control inflammatory tissue. Immunohistochemistry was carried out using protocols described previously in section 2.2.6.

#### **5.2.5 Quantification of inflammatory cell staining.**

Activated microglia, as determined by positive immunostaining, presence of a nucleus and appropriate morphology, were counted in 3 non-overlapping regions (using a 0.25 X 0.25 mm grid at a X 40 magnification) in the following brain regions- cortical infarct core, cingulate cortex, genu of the corpus callosum, external capsule and parietal cortex in the ipsilateral hemisphere and in homotopic regions of the contralateral hemisphere (Figure 47).

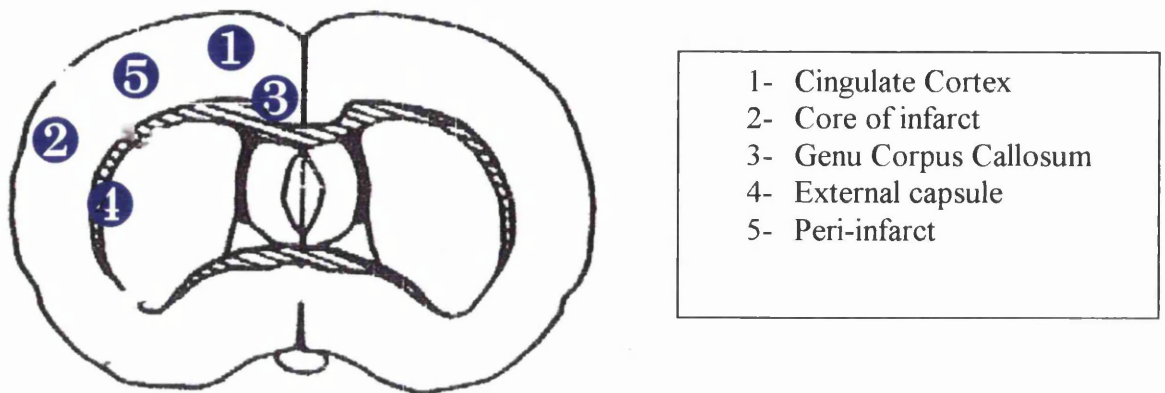


Figure 47. Regions of interest for microglial counts.

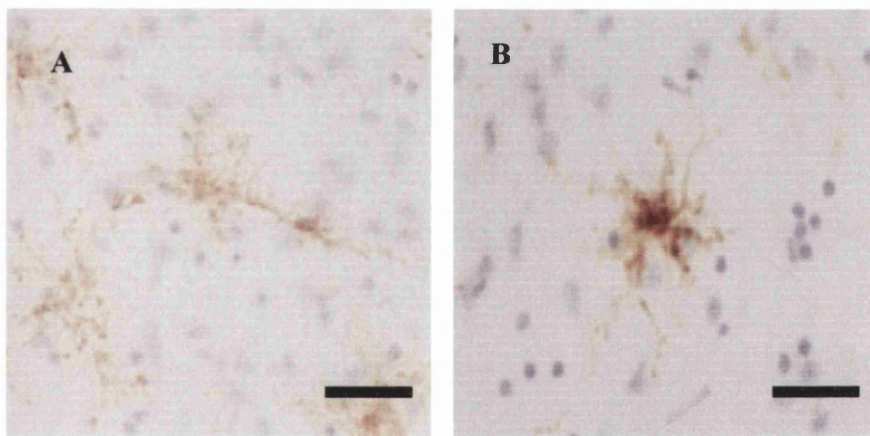


Figure 48. Microglial phenotype. A. Resting and B. Activated phenotype of the microglial cell as stained with Ox-42 antibody in the cortex of an SHRSP animal following distal electrocoagulation of the MCAO. Magnification = X40, scale bar represents 50 $\mu$ m

Values were expressed as activated microglia per mm<sup>2</sup> and graphed.

Staining distribution maps were also produced where areas of increased number of activated microglial displaying intense staining were marked onto line diagrams representing the eight coronal levels.

The diagrams for the five SHRSPs and the five WKYs were superimposed to give an average pattern of distribution for each strain (using an NIH Image program). This involved digitally scanning the line diagrams using a UMAX Powerbook flatbed scanner and importing the images into the NIH program. Diagrams were then aligned to an identical orientation using Alignment software and guided to fiducial markers to produce a single diagram for SHRSP and WKY to indicate number and anatomical distribution of the microglial staining in each strain. The consistency of staining in animals within each group was represented with a grey scale from 0-12 (carried out by Dr J Patterson, Southern General Hospital, Glasgow).

Correlation graphs were plotted for number of activated microglia against infarct size for peri-infarct and core regions.

#### **5.2.6 Statistical analysis.**

Data are presented as mean  $\pm$  SEM. The significance of differences in microglial number, infarct size and physiological variables between strains was determined by ANOVA followed by unpaired, Student's t - test.  $p < 0.05$  was taken as the level of statistical significance.

## **5.3 Results.**

### **5.3.1 Physiological variables**

Physiological variables were maintained within normal limits under anaesthesia (Table 10): normocapnia (36-42mmHg), normal physiological pH (7.4), and normal body temperature (36.5-37.5°C). Brain and body temperature were similar in the two strains, but, as expected, SHRSP exhibited significantly higher mean arterial blood pressure than the normotensive WKY under anaesthesia.

### **5.3.2 Infarct Size**

Ischaemic damage as identified at light microscopic level, was mainly confined to cortical regions as expected with this model of experimental ischaemia.

Infarct volume in SHRSP was  $135 \pm 4.7 \text{mm}^3$  compared to  $102 \pm 4.7 \text{mm}^3$  in WKY ( $p < 0.005$ , unpaired Student's t-test) (Figure 49). When individual coronal levels are examined, SHRSP exhibited a greater degree of damage over all eight coronal levels when compared to WKY (Figure 50)

	Weight (g)	MABP (mmHg)		PaCO <sub>2</sub> (mmHg)		pH		Body Temp (°C)		Brain Temp (°C)	
		Pre-MCAO	Post-MCAO	Pre-MCAO	Post-MCAO	Pre-MCAO	Post-MCAO	Pre-MCAO	Post-MCAO	Pre-MCAO	Post-MCAO
WKY	336 ± 14	78.7 ±5.1	106.3 ±2.4	40.1 ±1.1	42.7 ±3.1	7.41 ±0.1	7.42 ±0.1	37.4 ±0.1	37.3 ±0.2	35.8 ±0.2	36.3 ±0.2
SHRSP	262* ±11	95.6 ±6.2	138.0* ±6.0	37.0 ±2.17	41.4 ±2.3	7.48 ±0.01	7.44 ±0.01	37.1 ±0.1	37.3 ±0.2	35.8 ±0.4	36.6 ±0.3

Table 10. Physiological Variables for 24 hour permanent MCAO by electrocoagulation. Pre-MCAO = 15 minutes before middle cerebral artery occlusion and Post-MCAO = 1 hour after middle cerebral artery occlusion during recovery period. Values represent mean ±SEM. n = 5 per group. Values were analysed using Student's t-Test \*p < 0.05.

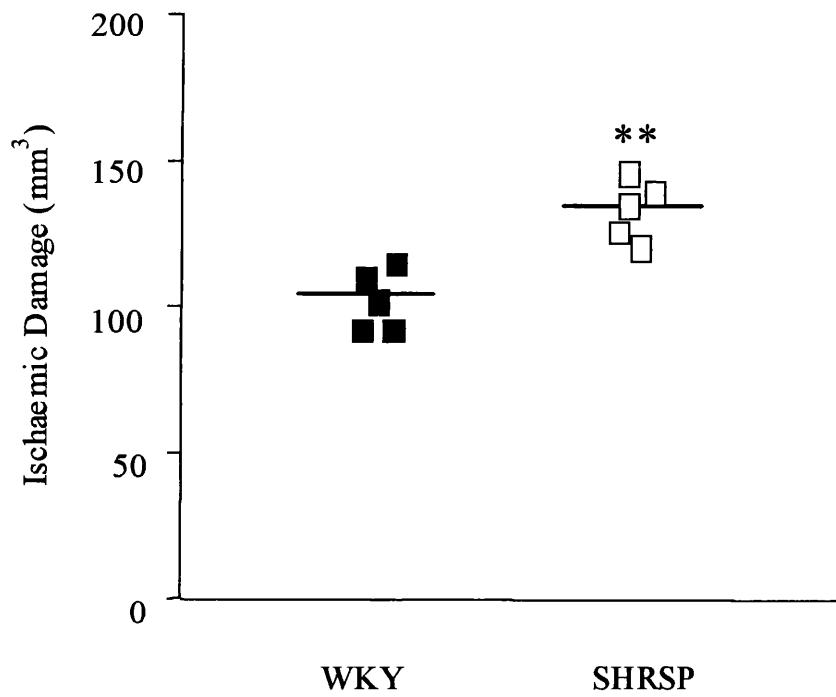


Figure 49. Infarct volume in SHRSP and WKY at 24 hours after distal MCA occlusion. n= 5. Data analysed by Student's t-test, \*\* p< 0.005.

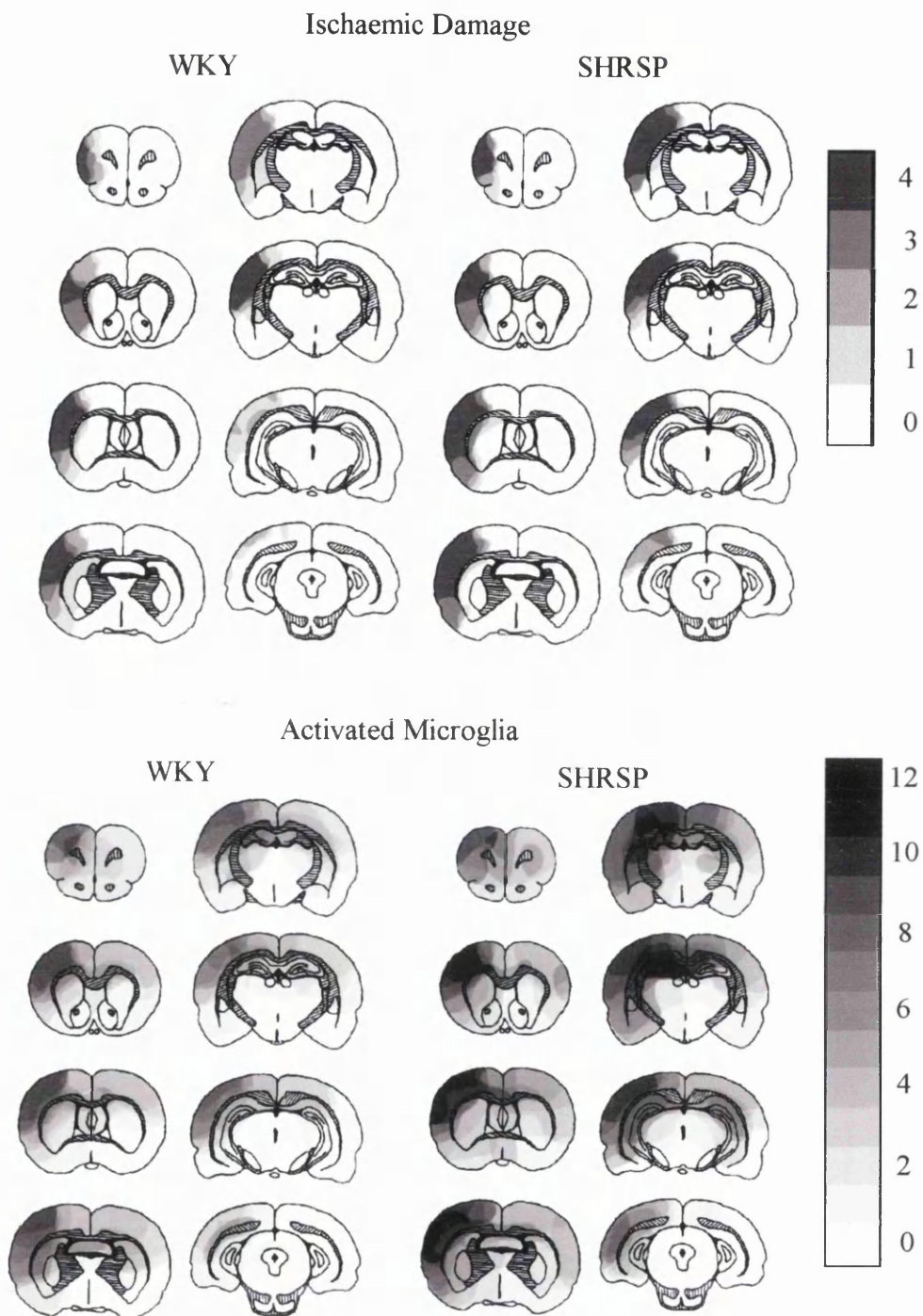


Figure 50. Composite line diagrams of topography of the infarct and of activated microglial densities for WKY (n=5) and SHRSP (n=5). In the top diagram (scale 0 – 4), 4 represents areas that were infarcted in 100% of animals, 3 represents areas infarcted in 75% of animals, 2 represents areas infarcted in 50% of animals and 1 represents areas infarcted in 25% of animals. In the bottom diagram, the scale 0 to 12 represents activated microglia cell densities with 12 representing the greatest density of cells.

### **5.3.3 Neutrophil Counts**

No neutrophils were observed within blood vessels of the MCA territory in either SHRSPs or WKYs in the sections examined. Neutrophils were also extremely rare within the parenchyma. No neutrophils were identified within the parenchyma of any WKY sections examined and only one out of the five SHRSP displayed cells with the morphology of neutrophils. In this animal 3 neutrophils were identified in the cortex at the level of the nucleus accumbens, 2 at the level of the globus pallidus and 4 at the level of the lateral habenula.

### **5.3.4 Characterisation of microglial activation**

The CNS of ischaemic SHRSP and WKY displayed activated microglia as determined by immunopositive staining and morphology under the light microscope. Activated microglia had much shorter projections and more distinct densely stained cell bodies while resting microglia possessed long spindly projections and faintly stained cell bodies.

Distribution of the activated microglia included brain regions in the ipsilateral and the contralateral hemispheres and in both grey and white matter.

As previously reported, the morphology of the microglia differed between grey and white matter, with the grey matter microglia possessing a stellate morphology whilst those in the white matter appeared more bipolar in appearance.

### **5.3.5 Distribution of Microglia**

The composite line diagrams of activated microglial densities and topography of the infarct for each strain (Figure 50) display the greater density of cells and their more widespread distribution in the SHRSP when compared to the WKY. In addition to the distribution of activated microglia was found to be more widespread than the region of ischaemic damage. High concentrations of activated microglia were found within the peri-infarct regions as well as lower concentrations in the contralateral hemisphere. Staining intensity was also greater within the ipsilateral hemisphere and more specifically within the coronal levels nearest to the core of MCA territory (For example at the level of the septal nucleus). The diagrams also show regional microglial distribution within both grey and white matter (Figure 51).

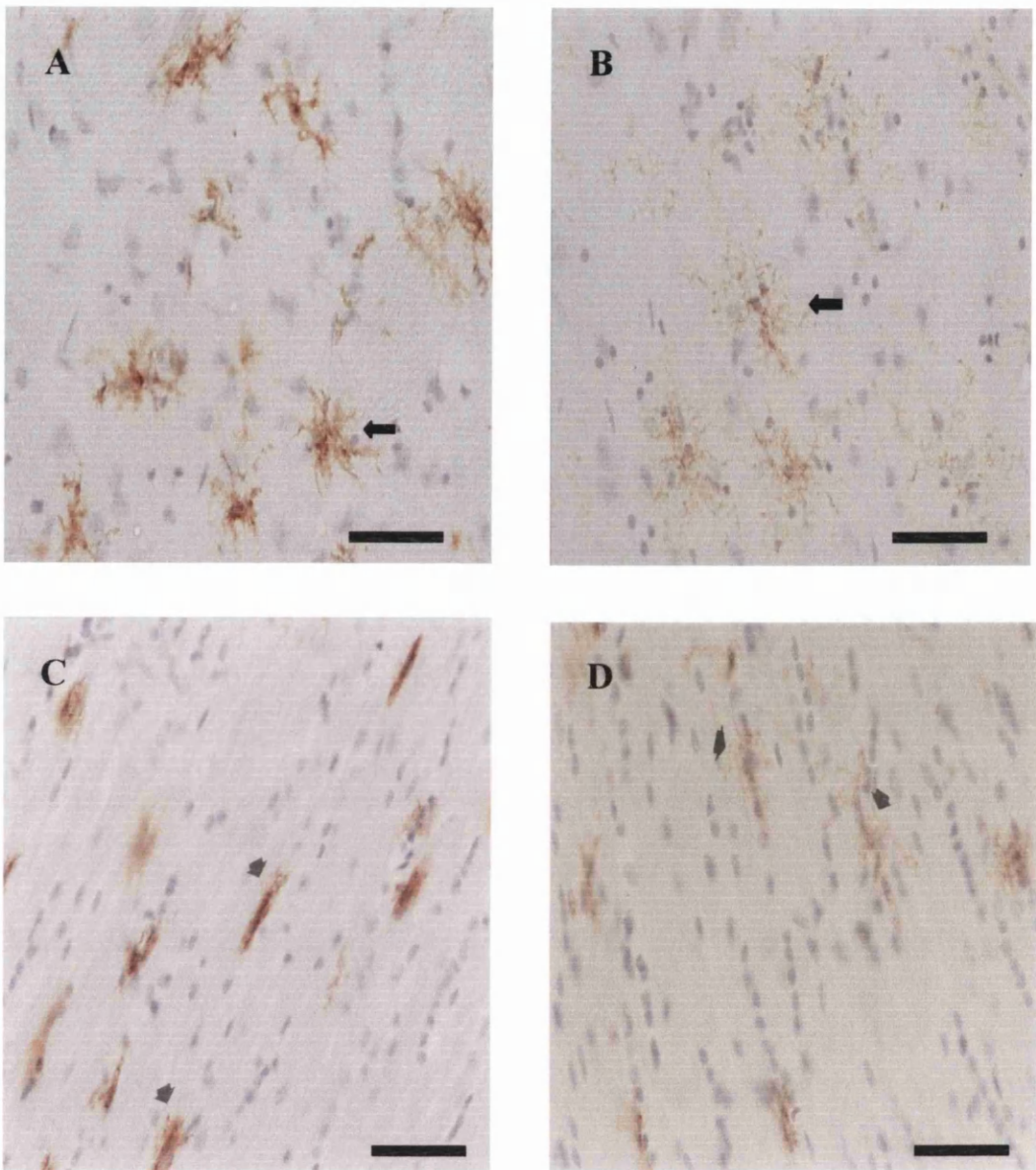


Figure 51. Distribution and morphology of microglial cells in grey and white matter of both hemispheres of SHRSP following distal electrocoagulation of the MCA.

A. Ipsilateral grey matter, B. Contralateral grey matter, C. Ipsilateral white matter, D. Contralateral white matter. Cells stained with Ox-42 antibody. Magnification = X40, scale bar represents 50 $\mu$ m. Arrow represents activated microglia.

### **5.3.6 Microglial Counts**

Significant numbers of activated microglia were evident in both ipsilateral and contralateral hemispheres of both strains within 24 hours of focal cerebral ischaemia with the greatest density of cells being found within the infarct core (Figure 51, 52). The activated and resting microglia did not differ in morphology between the two hemispheres only in their frequency and intensity of staining.

### **5.3.7 Strain differences**

SHRSP exhibited greater numbers of activated microglia than WKY in all 5 brain regions examined in the ipsilateral hemisphere albeit not significant in all regions (Figure 52, 58). The strain difference appeared most significant in the histologically normal, peri-infarct region of the cortex surrounding the infarct (Figure 53), in the adjoining region of the cingulate cortex (Figure 54), also histologically normal, receiving its blood supply from the anterior cerebral artery, and within the infarct core itself (Figure 55). Although activated microglial counts overall were lower in the contralateral hemisphere, a strain difference between SHRSP and WKY was clearly evident. (Figure 53-57).

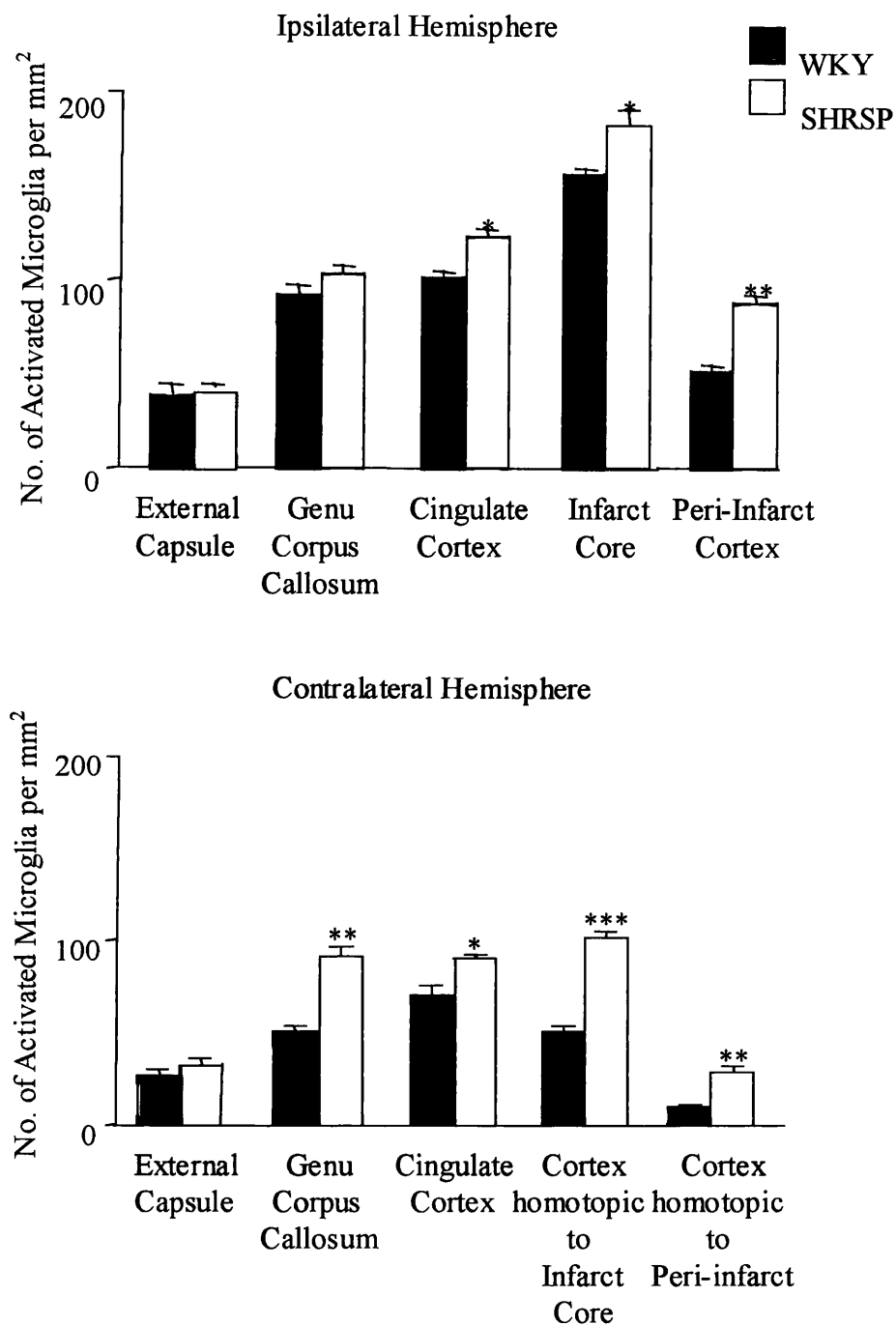


Figure 52. Mean counts of activated microglia per  $\text{mm}^2$  in the brain regions examined in A. ipsilateral and B. contralateral hemispheres. Data analysed using Student's t-test. \* $p < 0.05$ , \*\* $p < 0.005$ , \*\*\* $p < 0.001$ .  $n = 5$  SHRSP,  $n = 5$  WKY.

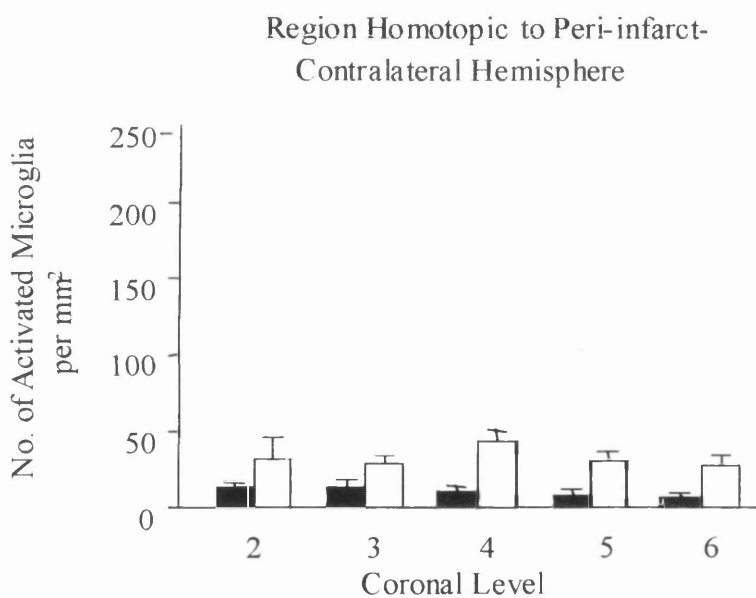
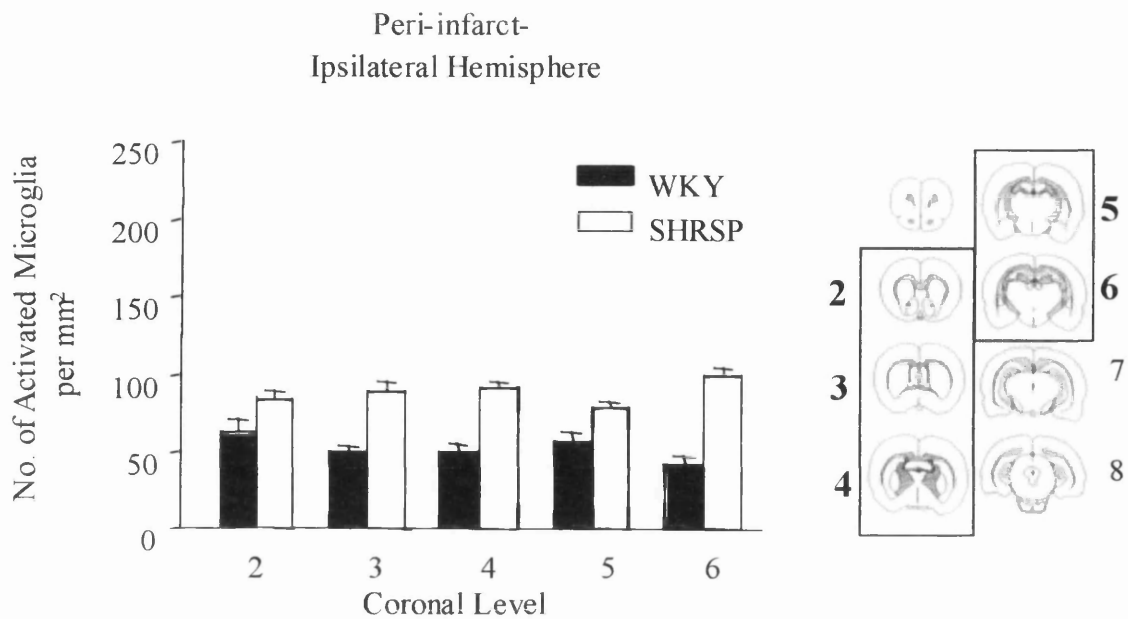


Figure 53. Microglial numbers for peri-infarct region in ipsilateral and equivalent region in contralateral hemispheres, SHRSP Vs WKY, n=5 per group  
Data expressed as mean +/- SEM.

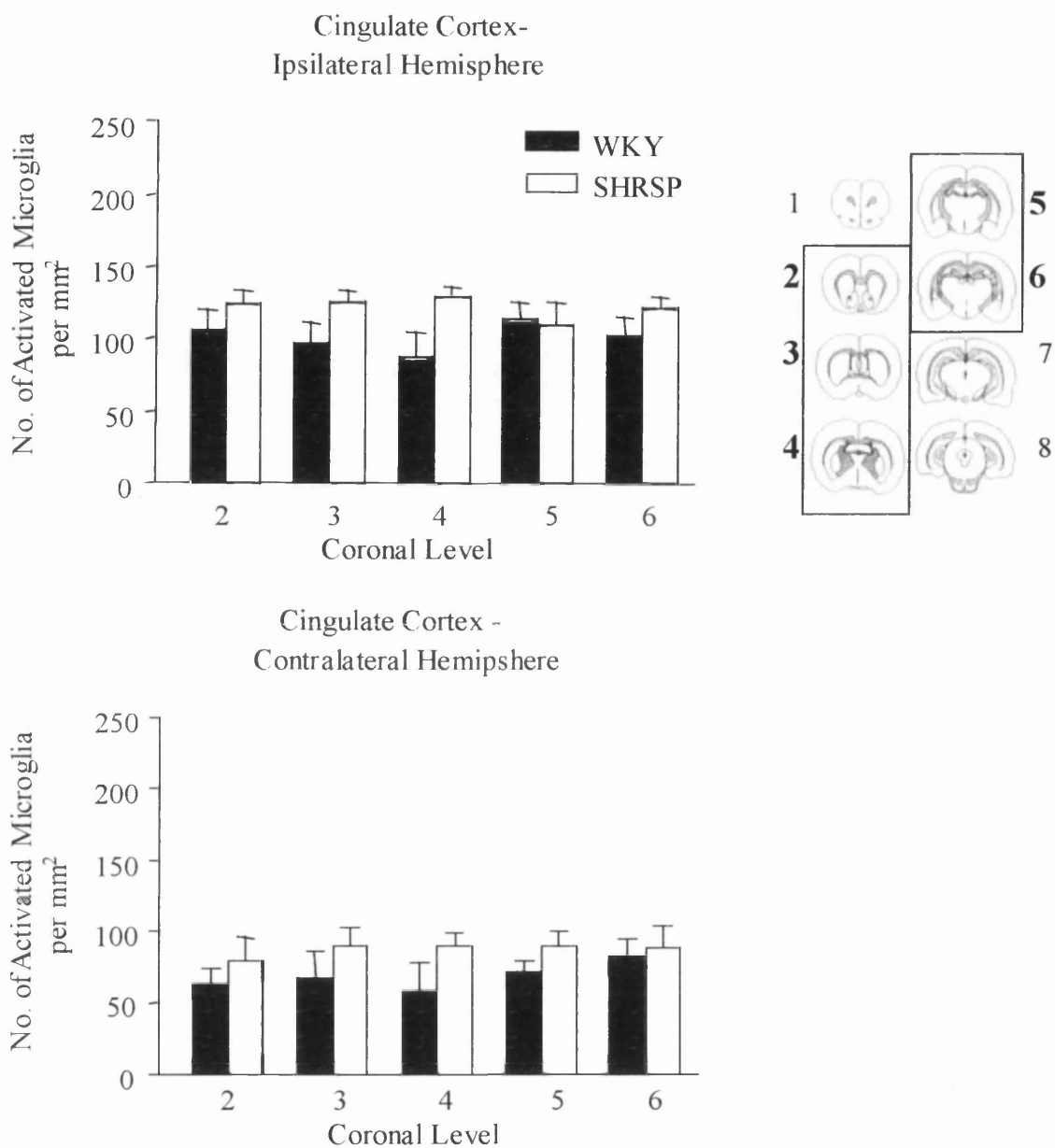


Figure 54. Activated microglial numbers for cingulate cortex region in ipsilateral and in contralateral hemispheres, SHRSP Vs WKY, n=5 per group.

Data expressed as mean  $\pm$  SEM.

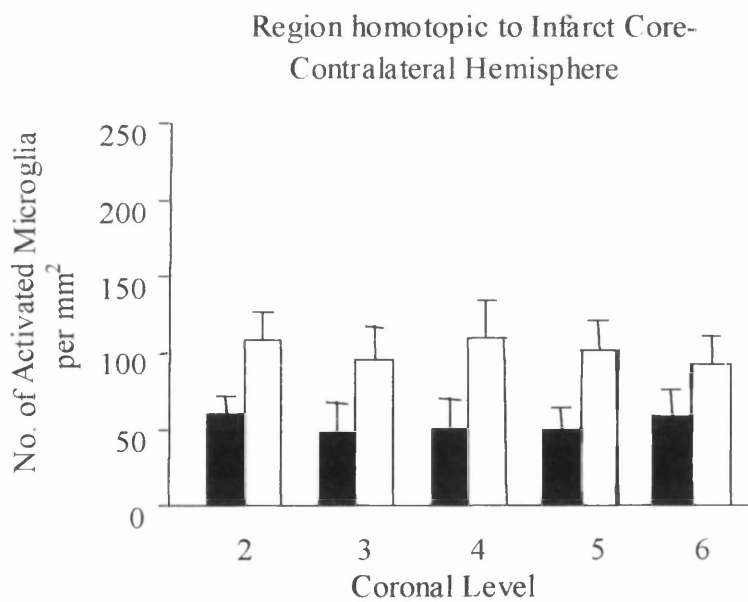
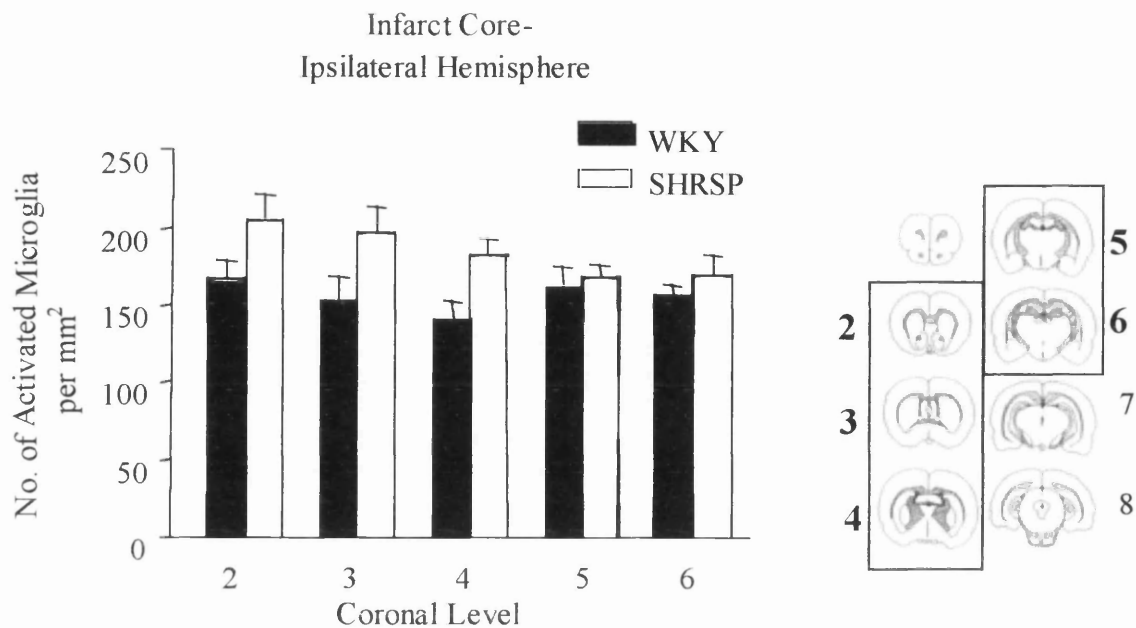
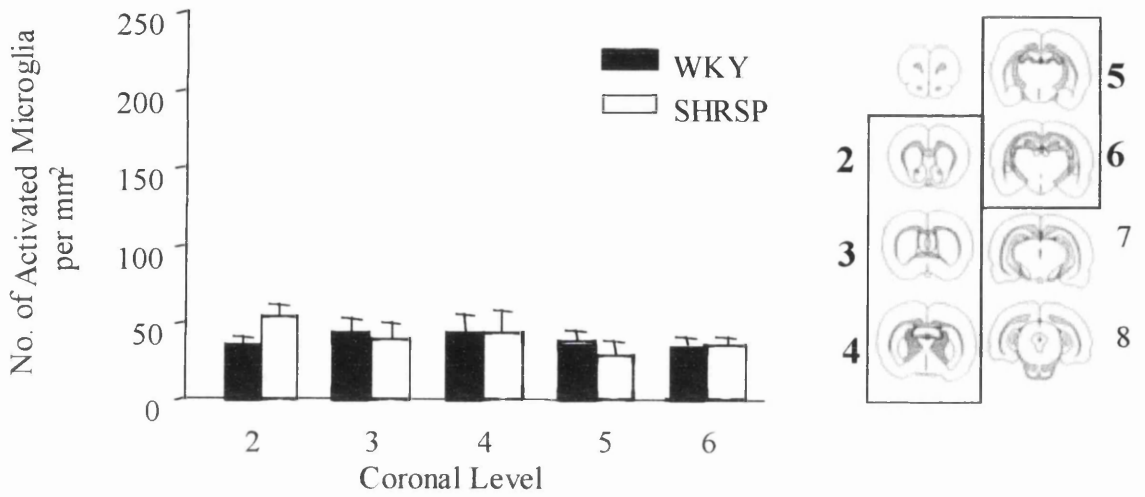


Figure.55. Activated microglial numbers for infarct core region in ipsilateral and equivalent region in contralateral hemispheres, SHRSP Vs WKY, n=5 per group

Data expressed as mean +/- SEM.

External Capsule-  
Ipsilateral Hemisphere



External Capsule-  
Contralateral Hemisphere

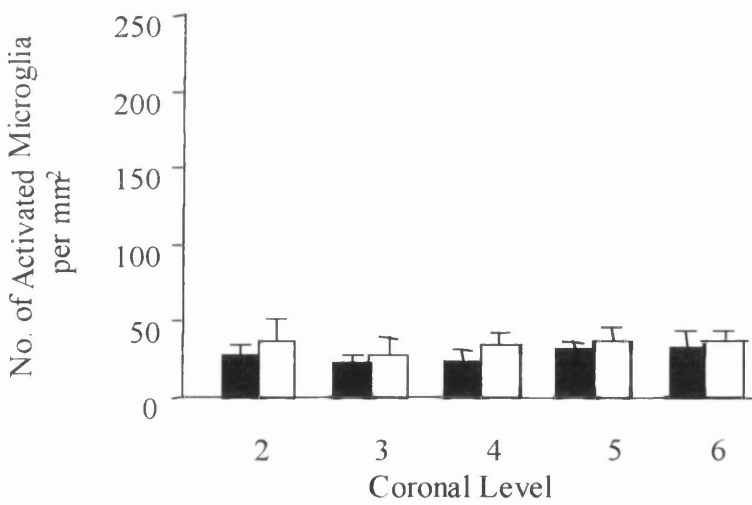
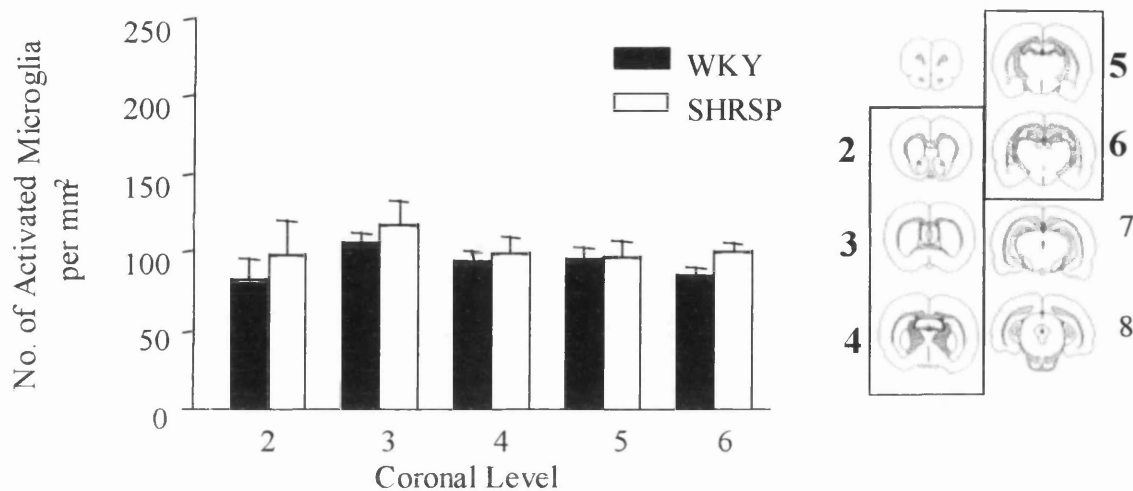


Figure.56. Activated microglial numbers for external capsule region in ipsilateral and in contralateral hemispheres, SHRSP Vs WKY, n=5 per group,

Data expressed as mean +/- SEM.

Genu Corpus Callosum-  
Ipsilateral Hemisphere



Genu Corpus Callosum-  
Contralateral Hemisphere

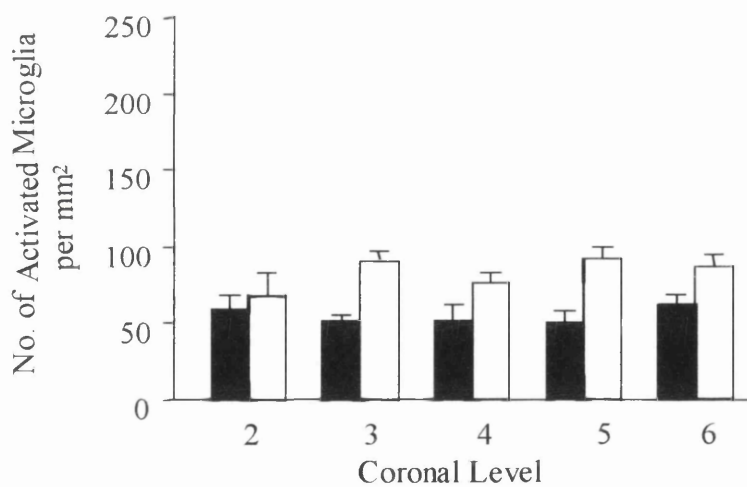


Figure 57. Activated microglial numbers for Genu of Corpus Callosum in ipsilateral and in contralateral hemispheres, SHRSP Vs WKY, n=5 per group.

Data expressed as mean  $\pm$  SEM.

Numbers of activated microglia per  $\text{mm}^2$  are displayed in each of the 5 levels examined in figure 52-56 to reveal any rostro-caudal differences. No differences were apparent over the rostro-caudal extent of MCA territory.

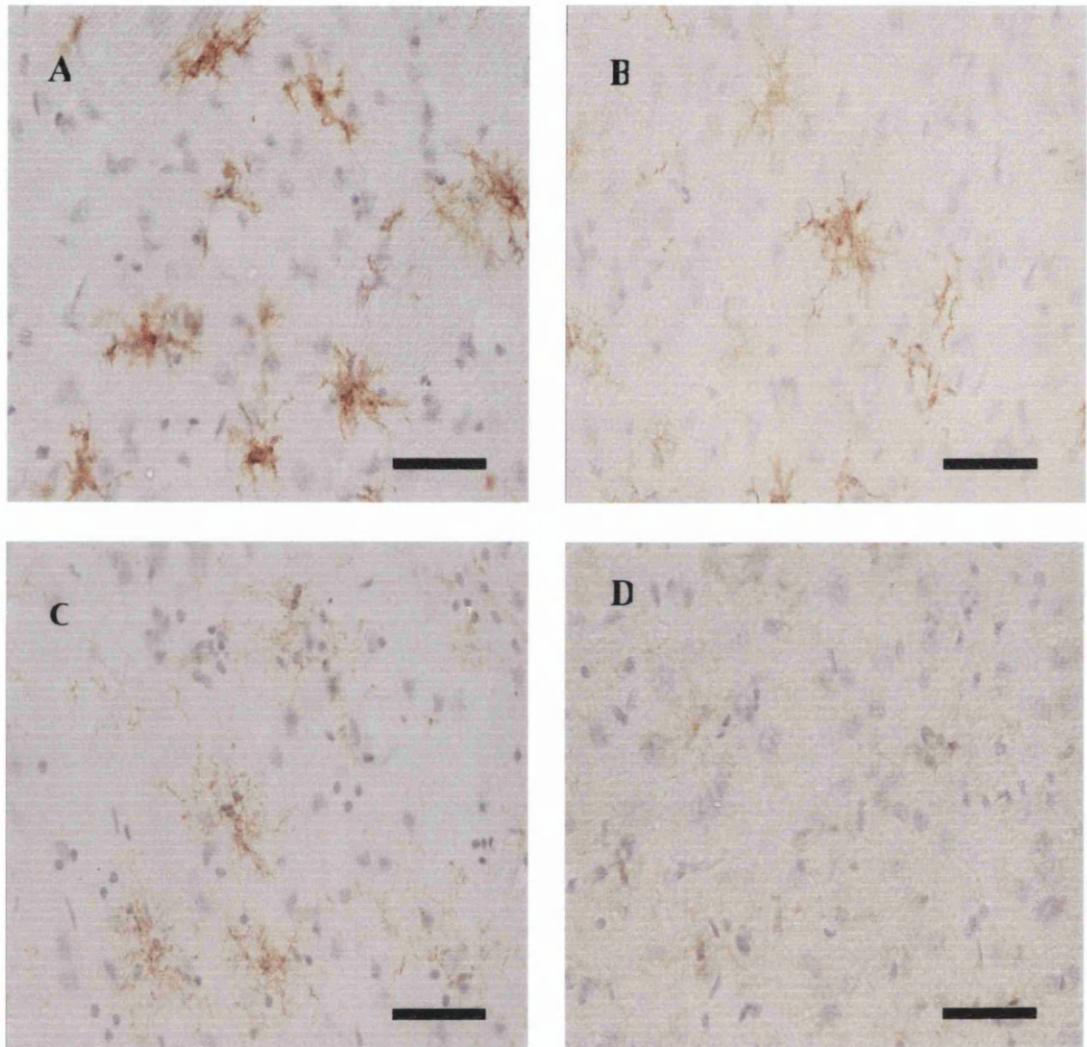


Figure 58. Strain differences between microglial numbers in SHRSP Vs WKY animals. In the cortex of the ipsilateral hemisphere of A. SHRSP and B. WKY and in the contralateral hemisphere of C. SHRSP and D. WKY. Magnification=X40, scale bar represents 50 $\mu\text{m}$ .

### 5.3.8 Correlation graphs

Number of activated microglia in infarct core and peri-infarct regions at the level of the lateral septal nucleus plotted against ischaemic damage showed no evidence for a correlation between number of activated microglia and infarct size (Figure 59) ( $r^2=0.45$ ,  $p=0.214$  for infarct core;  $r^2=0.025$ ,  $p=0.214$  for peri-infarct cortex).

### 5.3.9 Naïve controls

Cells with the morphology of both resting and activated microglia were identified in the CNS of naïve, control SHRSP and WKY animals (Figure 60).

Activated microglia were extremely rare in the MCA territory of naïve control rats of either strain (Figure 61). However, naïve SHRSP brains had higher total numbers of microglia (resting and activated) than WKY in all of the brain regions examined over the eight coronal levels (60).

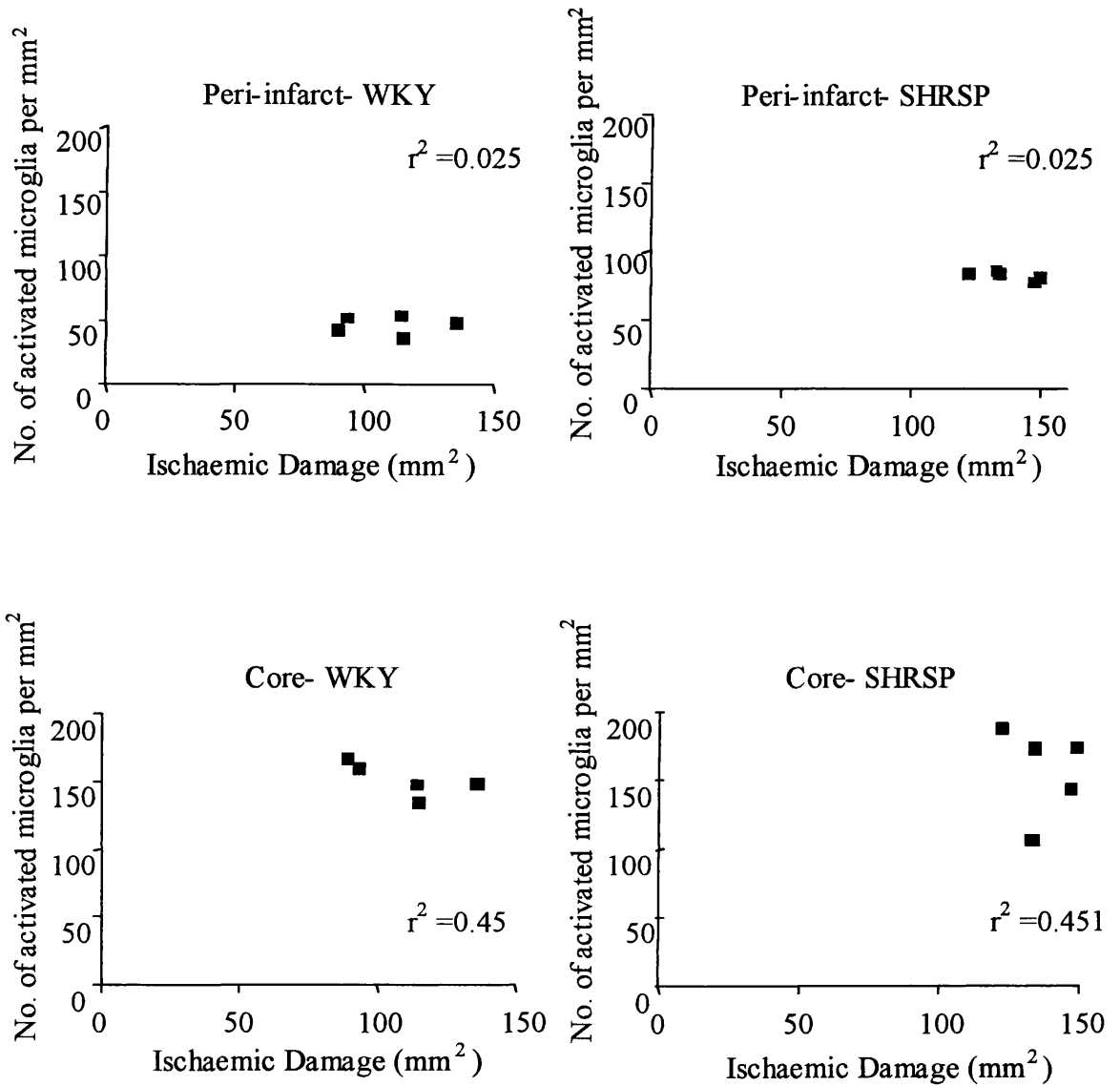


Figure 59. Correlation graphs for SHRSP and WKY - Ischaemic damage versus number of activated microglia at the level of the lateral septal nucleus in the peri-infarct and core regions.  $n = 5$  per group.

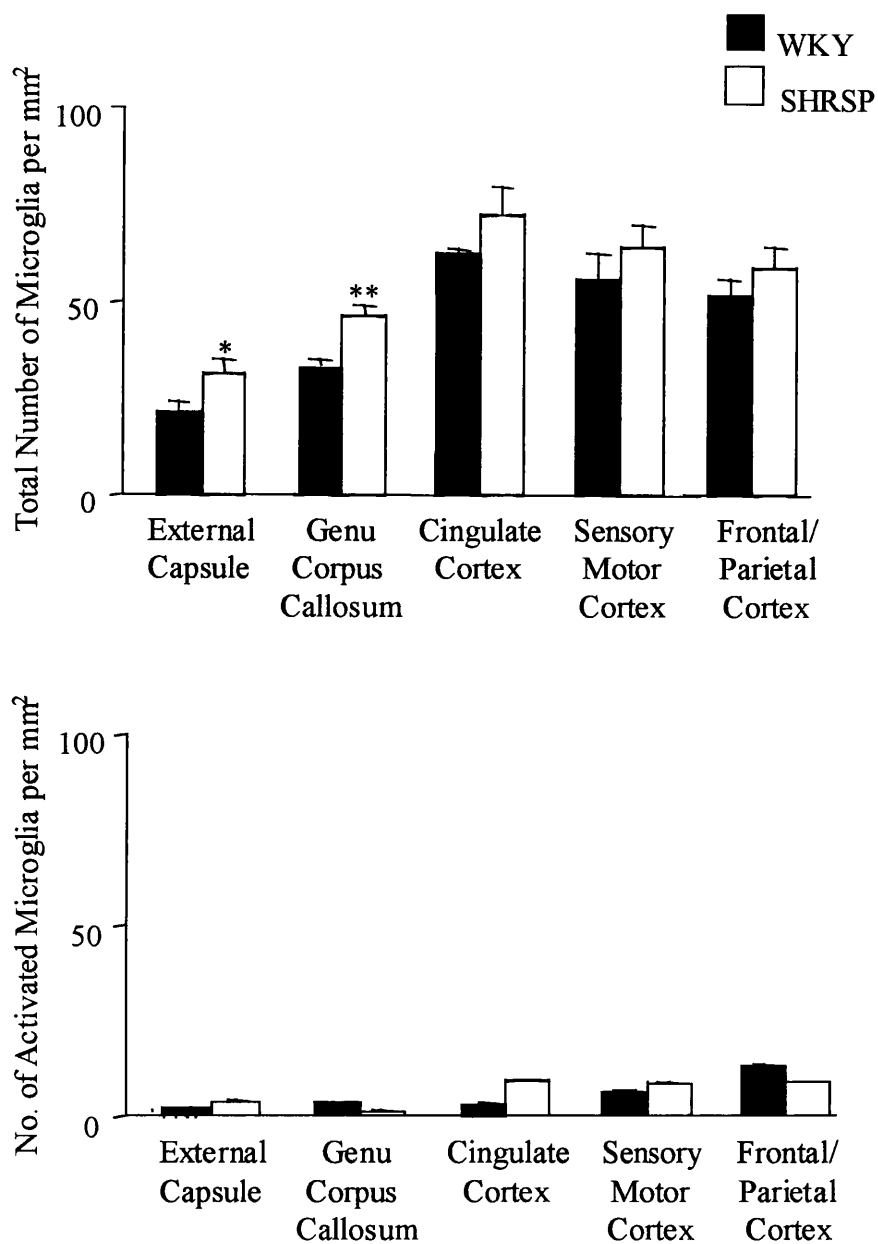


Figure 60. Mean counts of microglia per  $\text{mm}^2$  in the 5 brain regions studied

A. Total number of microglia per  $\text{mm}^2$  and B. number of activated microglia.  $n=5$ .

Data analysed using Student's t-test. \* $p<0.05$ , \*\* $p<0.005$ .

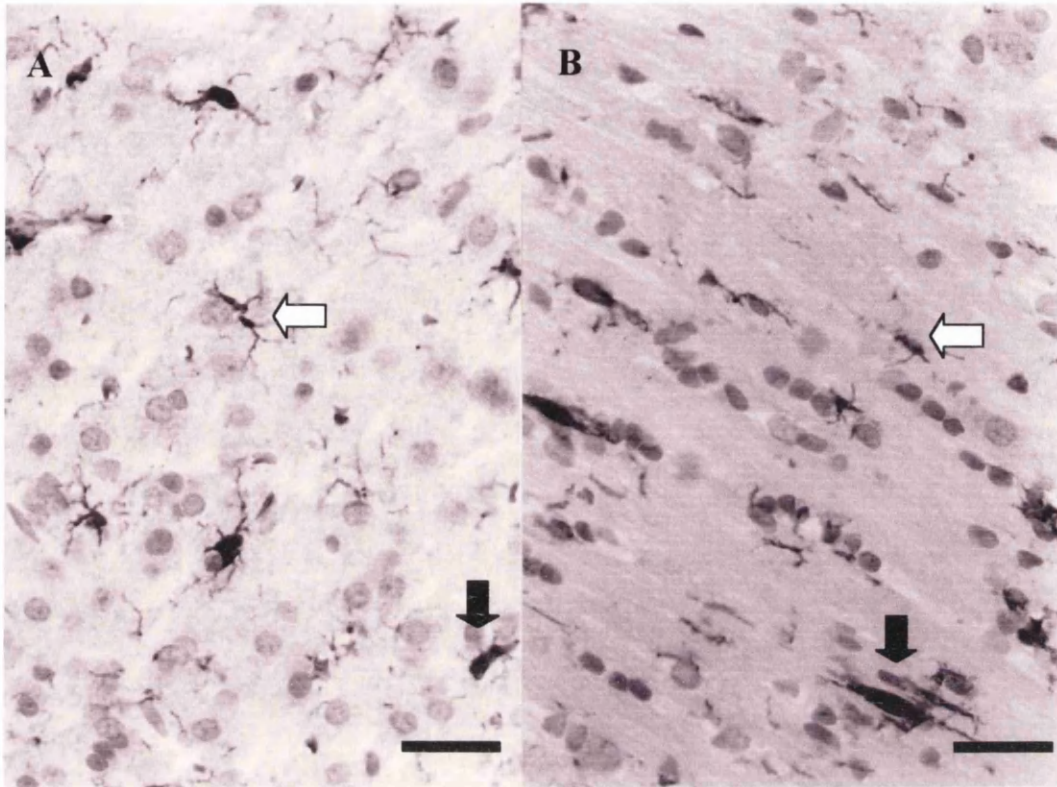


Figure 61. Representative images of activated (  ) and resting (  ) microglia in A. grey and B. white matter of a naive SHRSP rat. Microglia stained with mrf-1 antibody. Magnification =X40, scale bar represents 50 $\mu$ m.

The distribution of microglial cells was similar in both strains. Differences in microglial number between SHRSP and WKY reached statistical significance ( $p < 0.05$ ) in the two white matter regions examined, the external capsule and the genu of the corpus callosum.

## 5.4 Discussion

Quantitative analysis of the inflammatory response to focal cerebral ischaemia in the genetically determined, stroke sensitive SHRSP rat has revealed 3 important results: 1) SHRSP displayed significant increases in the numbers of activated microglia associated with the site of ischaemic injury compared to the WKY reference strain at 24 hours post-ischaemia; 2) there was no evidence for a significant neutrophil involvement in the evolution of the infarct in either strain at 24 hours post- ischaemia and 3) Under normal, non-ischaemic conditions, SHRSP also display a greater density of microglia, especially in white matter tracts, compared to WKY rats. These results are important both in terms of improving our understanding of genetically determined “stroke sensitivity” and of the role of inflammatory cells in focal cerebral ischaemia, two research areas associated with many unresolved questions and opposing views.

Stroke sensitive rat strains such as the SHR and SHRSP have previously been shown to display an elevated inflammatory response to inflammatory stimuli (Hallenbeck *et al.*, 1991; Schmid-Schonbein *et al.*, 1991; Siren *et al.*, 1992) suggesting that an amplified inflammatory response to cerebral ischaemia may be associated with increased stroke sensitivity. This hypothesis was examined in the current study. No significant neutrophil presence was found in cerebral vessels or parenchyma of either SHRSP or WKY animals at 24 hours post-ischaemia which is in accordance with previous studies from this laboratory which have similarly failed to find evidence of neutrophils in acute focal ischaemic damage (Peters *et al.*, 1998) . However, widespread microglial activation was evident within 24 hours of focal ischaemia in

both strains (Figure 52), in agreement with previous studies of global (Gehrmann *et al.*, 1992) and focal (Kato *et al.*, 1996) ischaemia in normotensive rat strains.

SHRSP exhibited greater microglial activation than WKY both in terms of density and distribution of cells (Figure 50), supporting a potential link with increased stroke sensitivity in the SHRSP. However, what is not yet clear is whether the greater microglial activation is *caused by* or might *contribute to* the increased infarct size in the SHRSP. However there was no significant correlation between activated microglial density in either infarct core or peri-infarct cortex and infarct size ( $r^2=0.451$ ,  $p=0.214$  for infarct core;  $r^2=0.025$ ,  $p=0.214$  for peri-infarct cortex). This indicates that the greater microglial activation is probably not simply a direct result of the increased infarct size. The lack of a correlation however does not rule out a contributory role of activated microglia to increase infarct size but if they are involved, they may be one of a number of contributors.

At 24 hours, the infarct is still evolving in the SHRSP (see chapter 6) and tissue in the peri-infarct region (penumbra) is balancing between life and death. Although it is widely believed that the inflammatory response may contribute to ischaemic brain damage, potentiating the destructive effects of ischaemia (Barone and Feuerstein, 1999) , microglia could alternatively have a beneficial influence, representing the brain's attempt to protect itself from further damage as happens in the periphery (Schwartz *et al.*, 1999) (discussed below).

Activated microglia could contribute to ischaemic damage both directly- via synaptic stripping and neurophagia (Nakajima and Kohsaka, 1993) and indirectly- through the release of cytotoxins. These cytotoxins can induce lipid peroxidation, excess release of transmitters and hormones, vascular leakage, oedema, necrosis and

changes in ion flow. Glutamate released from microglia can give rise to excessive NMDA receptor activation (Nakajima and Kohsaka, 1993) resulting in neuronal cell death. High extracellular potassium levels, as found in ischaemic tissue, potentiate glutamate release from microglia which are particularly sensitive to changes in potassium levels due to their lack of a substantial potassium outward current (Banati *et al.*, 1991).

A recent study has suggested that microglia are capable of contributing to the development of the ischaemic infarct at similar time points to the current study (Mabuchi *et al.*, 2000). However, the conclusion was based only on the expression of IL-1 $\beta$  and Bax in microglia within the peri-infarct and infarct areas rather than from the results of an intervention strategy. The definitive experiment, to determine whether microglia contribute to or ameliorate ischaemic injury, would be to selectively block microglial activation without affecting the other inflammatory and deleterious mechanisms in the ischaemic cascade. However, although theoretically feasible, this is not currently achievable as potential drugs and strategies which attenuate microglial activation have significant influences elsewhere in the ischaemic cascade, which would invalidate the interpretation of the results. For example, tetracycline derivatives which block microglial activation also display antagonism of glutamate, cyclo-oxygenase-2, interleukin converting enzyme, inducible nitric oxide synthetase, gelatinase B and superoxide production by leukocytes (Yjranheikki *et al.*, 1998; Yjranheikki *et al.*, 1999).

Some groups would disagree with the idea that microglia are contributing to ischaemic damage and that the early presence of microglial activation preceding neuronal death would seem to suggest a protective role for the microglia (Banati &

Graeber, 1994; Elkabes *et al.*, 1996; He *et al.*, 1997). Indeed the presence of microglial cells next to or even engulfing neurons does not always precede neuronal death and microglial association with neurons which do not subsequently die would seem to provide evidence for a protective role for the inflammatory cells in some circumstances (Kato & Waltz, 2000)

In terms of microglia protecting injured tissue from further damage, following neuronal injury in the periphery, microglia have been reported to participate in neuronal regeneration (Zeev-Brann *et al.*, 1998; Lazarov-Speigler *et al.*, 1998) by performing phagocytosis of debris, for example from permanently degenerated neurons, which then allows neuronal regrowth (Zeev-Brann *et al.*, 1998). Activated microglia, like macrophages, are also recruited into injured brain to remove debris and thereby prevent further damage. In the present study, the highest microglial counts were found in the ipsilateral hemisphere within the infarct in both strains, which would support a phagocytic role.

Microglia also contribute to neuronal regrowth and wound healing via the secretion of growth factors such as TGF-alpha, TGF-beta, bFGF, EGF and IGF (Faber-Elman *et al.*, 1996) which promote migration of glial cells such as astrocytes which are conducive to neuronal regrowth and wound healing (Faber –Elman *et al.*, 1996). As well as stimulating cell migration and/or proliferation, these growth factors may also increase protease activity or alter the expression of extracellular matrix components.

However, the participation of microglia in immune activities and regeneration of neurons within the CNS is much less intense than is seen in cases of peripheral injury. This is possibly due to the presence of inhibitory substances which restrict

their participation (Zeev-Brann *et al.*, 1998; Hirschberg and Schwartz, 1995) and produce an inhospitable growth environment within the CNS (Lazarov-Speigler *et al.*, 1998). In spite of a less pronounced phagocytic response in the CNS, microglia have been reported to perform a beneficial role in CNS injury following viral infection (Bi *et al.*, 1995) and axonal injury (Lazarov-Speigler *et al.*, 1996).

Activation and migration of microglia may be induced by chemokines or cytotoxins released during ischaemia, which would explain the observed increase in numbers of activated microglia in the ipsilateral hemisphere of both strains. A rise in cytokine levels, occurring one to two days following ischaemia (Babak *et al.*, 1996), correlates well with the timescale for microglial activation.

However, significant numbers of activated microglia were also recorded in more distant sites in the contralateral hemisphere in this study and others (Schroeter *et al.*, 1999). Various explanations for contralateral activation of microglia are available for consideration including active recruitment by signals sent from the ipsilateral microglia. A significant increase in the number of activated microglia in the contralateral genu may be representative of migrating microglia which move along the white matter tracts to reach their target site – in this case the area of ischaemic damage. Cytokines secreted from the ipsilateral hemisphere may stimulate activation, proliferation and migration of contralateral resting microglia to the site of damage (Schroeter *et al.*, 1999). Alternatively, contralateral microglia may become activated as a result of diaschisis (Seitz *et al.*, 1999) or waves of ischaemia induced waves of spreading depression (depolarisation) (Stoll *et al.*, 1998). The findings that spreading depression activates astrocytes and microglia (Stoll *et al.*, 1998), and that SHRSP exhibit a greater amount of spreading depression than WKY following

ischaemia (Yasui and Kawasaki, 1994) provide a possible explanation for the greater number of activated microglia in the contralateral hemisphere of SHRSP compared to WKY. Increases in brain swelling and subsequent increases in intracranial pressure represent an alternative stimulus for contralateral activation of inflammatory cells and mediators. In this particular model of ischaemia, brain swelling would be significant at 24 hours in SHRSP but intracranial pressure would not be elevated because of the surgical craniectomy.

Strain differences in the number of activated microglia following ischaemia could be a consequence of differences in basal levels of resting or activated microglia. SHRSP are known to develop hypertension within weeks of birth resulting in a systolic blood pressure of around 200mmHg maintained throughout life (Yamori *et al.*, 1977). It is possible that this underlying hypertension could influence the levels of activated microglia under basal conditions. Indeed hypertension in the SHRSP has been shown to predispose the strain to blood brain barrier breakdown (Fredricksson *et al.*, 1985). Blood brain barrier breakdown could provide changes in the microenvironment which could stimulate microglial activation under non-ischaemic conditions with no equivalent activation occurring in the normotensive WKY. This study showed that numbers of activated microglia within the MCA territory of naïve SHRSP and WKY were extremely small with no significant elevation in the SHRSP. However, microglial counts *per se* (resting and activated combined) were elevated in naïve SHRSP with significantly greater numbers in the two white matter regions studied. The presence of a greater number of basal resting microglia in SHRSP could therefore be a contributory factor in the greater numbers of activated microglia seen in SHRSP following ischaemia.

To conclude, this study has shown evidence of an elevated microglial response to experimental ischaemia in the SHRSP compared to WKY with greater numbers of activated and resting microglia in SHRSP under basal conditions. These results illustrate an increased inflammatory response to focal cerebral ischaemia in the SHRSP and suggest a role for increased microglial activation in “stroke sensitivity”. What remains unclear at present is whether these microglia have a beneficial or detrimental role within the evolving infarct.

## Chapter 6 SHRSP/WKY time course study.

### 6.1 Introduction

The data obtained from the 24-hour microglia study indicated that the SHRSP exhibited a greater degree of microglial activation when compared to the WKY at 24 hours following permanent MCAO. Since it is not known if the infarct is still increasing in size at this time point, a time point study was undertaken with animals undergoing permanent MCAO and recovered for periods of 4,24,48 or 72 hours (n=5 SHRSP, n=5 WKY per time point). The aims of this study were to 1) map the evolution of the infarct in SHRSP Vs WKY, 2) investigate whether strain differences in the number of activated microglia existed at earlier/later time points following permanent MCAO, 3) examine whether microglial activation may precede further development of the infarct (suggesting a role for microglia in the expansion of the ischaemic lesion) and 4) to map the distribution of IL-1 $\beta$ , MMP-8 and MMP-9 to determine whether activated microglia were expressing these mediators of inflammation.

In the previous study in this thesis, microglia were found to express MMP-8 and MMP-9 following 2 hours ILT induced ischaemia plus 22 hours reperfusion (Chapter 4). Levels of MMPs have been shown to be increased following MCAO (Asahi *et al.*, 2000; Rosenberg *et al.*, 1996; Romanic *et al.*, 1998) but what remains unclear is whether their role is solely detrimental. In addition to causing increased BBB breakdown and increased levels of cytotoxic substances, MMPs have been reported

to aid the migration of various cell types via their ability to degrade components of the ECM (Maeda *et al.*, 1996). It is feasible therefore that the presence of MMPs within microglial cells following MCAO may suggest a role for MMPs in the migration of microglia towards the site of damage.

## **6.2 Materials and methods.**

Methods for the time course study were the same as used for the 24 hour study (section 5.2) with additional recovery times of 4, 48 and 72 hours in addition to 24 hours. Brains were paraffin processed and sections used for infarct determination and immunohistochemistry were cut at 6 $\mu$ m on a microtome.

Immunohistochemistry was carried out using antibodies against MMP-8, MMP-9 and IL-1 $\beta$  in addition to microglia as described in section 2.2.6.

### **6.2.1 Assessment of brain swelling**

The influence of brain swelling on measurements of infarct size can be limited by transcribing the area of ischaemic damage onto line scaled drawings as has been presented in this thesis. Over a time course, brain swelling in this model will increase significantly (Barone *et al.*, 1992) Therefore, an assessment of brain swelling was made by measurement of the volume of both ipsilateral and contralateral hemispheres in each animal. It is recognised that this is an assessment rather than an accurate measurement of brain swelling since the tissue processing involved in dehydration and paraffin embedding of the tissue will result in shrinkage of the brain.

Volumes of ipsilateral and contralateral hemispheres was measured from H&E sections over the 8 coronal levels in both strains and over the 4 time points using MCID image analysis. Brain swelling was expressed as a % of the contralateral hemisphere.

$(\text{ipsi-contra} / \text{contra}) \times 100$ .

## **6.3 Results.**

### **6.3.1 Physiological variables**

Physiological variables were maintained within normal limits under anaesthesia (Table 11): normocapnia (36-42mmHg), normal physiological pH (7.4) and normal body temperature (36.5-37.5°C). Body temperature, pH and blood gases were similar in both strains but as expected SHRSPs exhibited a significantly higher mean arterial blood pressure both before and after MCAO when compared to the WKY.

### **6.3.2 Evolution of the infarct over the 72- hour time course.**

Ischaemic damage as identified at the light microscopic level was again mainly confined to cortical regions as expected with this model of MCAO. Very few animals throughout the time course exhibited damage out with the cortex. A small number of SHRSP animals displayed damage to the lateral caudate nucleus. No

	Weight (g)	MABP (mmHg)		PaCO <sub>2</sub> (mmHg)		pH		Body Temp. (°C)		Brain Temp. (°C)	
		preMCAO	postMCAO	preMCAO	postMCAO	preMCAO	postMCAO	preMCAO	postMCAO	preMCAO	postMCAO
<b>4 hour</b>											
WKY	292	76.9	104	41.9	45.1	7.42	7.44	37.2	37.1	35.5	35.8
	±6.1	±3.2	±2.2	±2.1	±0.9	±0.1	±0.1	±0.1	±0.05	±0.2	±0.2
SHRSP	***238	***93.6	***128.2	40.1	44	7.43	7.44	37.08	37.1	35	35.9
	±3.2	±2.3	±3.7	±1.9	±0.6	±0.1	±0.01	±0.1	±0.04	±0.1	±0.2
<b>24 hour</b>											
WKY	290	75.5	101.1	40.7	44.9	7.44	7.44	37.1	37.1	35.6	35.9
	±3.9	±1.8	±3.1	±0.5	±1.2	±0.1	±0.1	±0.1	±0.1	±0.1	±0.1
SHRSP	***242	***89.7	***131	42.3	43.4	7.42	7.45	36.9	37.1	36	35.92
	±2.9	±1.2	±1.2	±1.1	±0.8	±0.1	±0.1	±0.2	±0.1	±0.1	±0.2
<b>48 hour</b>											
WKY	280	73.1	82.6	40	42.8	7.43	7.45	37.5	37.1	35.8	36.1
	±5	±1.6	±19.5	±1.7	±1.1	±0.1	±0.02	±0.35	±0.1	±0.1	±0.1
SHRSP	***237	***87.1	127.3	42.2	42.7	7.44	7.43	37.1	37.1	35.8	35.9
	±2.5	±1.9	±2.4	±1.7	±0.9	±0.1	±0.01	±0.06	±0.1	±0.1	±0.1
<b>72 hour</b>											
WKY	280	73.5	94.2	40.6	45.5	7.44	7.44	37.1	37	35.8	35.9
	±5.2	±1.7	±5.8	±2.8	±1.7	±0.1	±0.001	±0.01	±0.2	±0.3	±0.2
SHRSP	***240	***90.1	*117.7	40.4	42.2	7.45	7.45	36.4	36.8	35.8	35.9
	±0.9	±1.1	±4.9	±3.9	±1.2	±0.1	±0.01	±0.188	±0.2	±0.1	±0.1

Table 11. Physiological variables for time course study of permanent MCAO by electrocoagulation. Values represent mean ± SEM.

n = 5 per group Data analysed using Student's t-test. PreMCAO = 15 minutes prior to MCAO, PostMCAO = 30 minutes post MCAO during recovery from anaesthesia. \*p<0.05, \*\*p<0.01, \*\*\*p<0.001.

damage to the caudate nucleus was observed in WKY. SHRSP displayed a greater degree of ischaemic damage than WKY over all four time points (4,24,48 and 72 hours) (Figure 62) and in some animals, damage was present in the dorsolateral caudate.

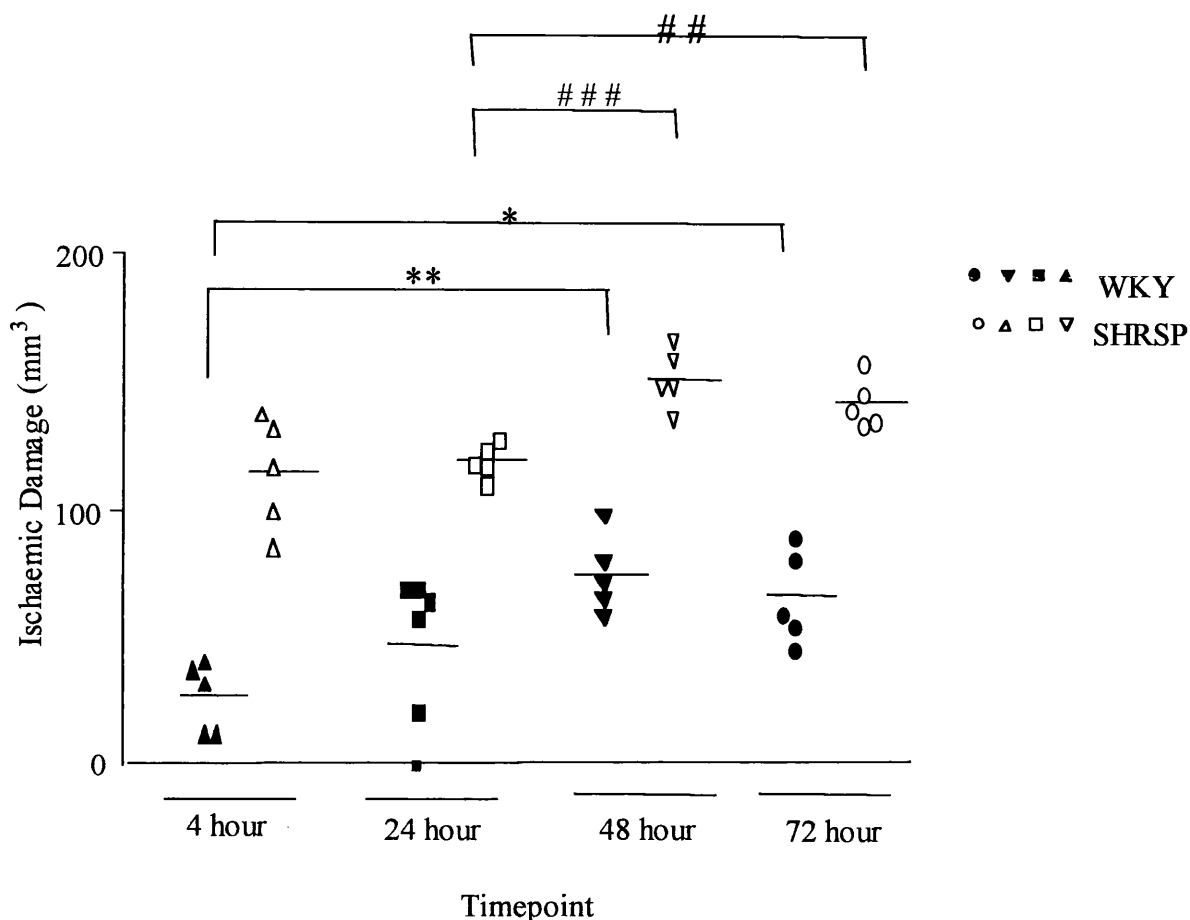


Figure 62. Evolution of the infarct over 72 hours in SHRSP and WKY, n= 5 per group. Data analysed using two-way ANOVA followed by unpaired Student's T-test with a Bonferroni correction for multiple comparisons. SHRSP displayed a significantly greater degree of ischaemic damage compared to WKY at each time point and within each strain the infarct increased with time out to 48 hours.

\*\*p< 0.005, \*p<0.001 comparisons within WKY strain; ### p<0.001, ## p<0.005, comparisons within SHRSP strain.

## Statistics

Data was analysed using ANOVA followed by an unpaired Student's t-test corrected for multiple comparisons.

SHRSP displayed a significantly greater degree of ischaemic damage compared to WKY at all of the 4 time points over the 72 hours ( $p < 0.001$ ).

In SHRSP, the infarct increased in size significantly between 24 and 48 hours ( $p < 0.001$ ) and between 24 and 72 hours ( $p < 0.005$ ).

In WKY, the infarct increased in size significantly between 4 and 48 hours ( $p < 0.005$ ) and between 4 and 72 hours ( $p < 0.05$ ).

From this data it can be said that in both strains, the infarct continued to develop up to 48 hours and then plateaus after this point in both strains. There was no difference in the pattern of change over time in the two strains as indicated by a lack of time/strain interaction in the ANOVA analysis.

### 6.3.3 Tissue Swelling.

As previously reported the SHRSP displayed a significantly greater degree of brain swelling than WKY (Figure 63). Modest brain swelling was evident only at 48 hours in WKY and appeared to have resolved by 72 hours. Significantly more brain swelling was apparent in SHRSP with evidence of significant swelling appearing

earlier (24 hours) in SHRSP than in WKY. This swelling was still evident at 72 hours.

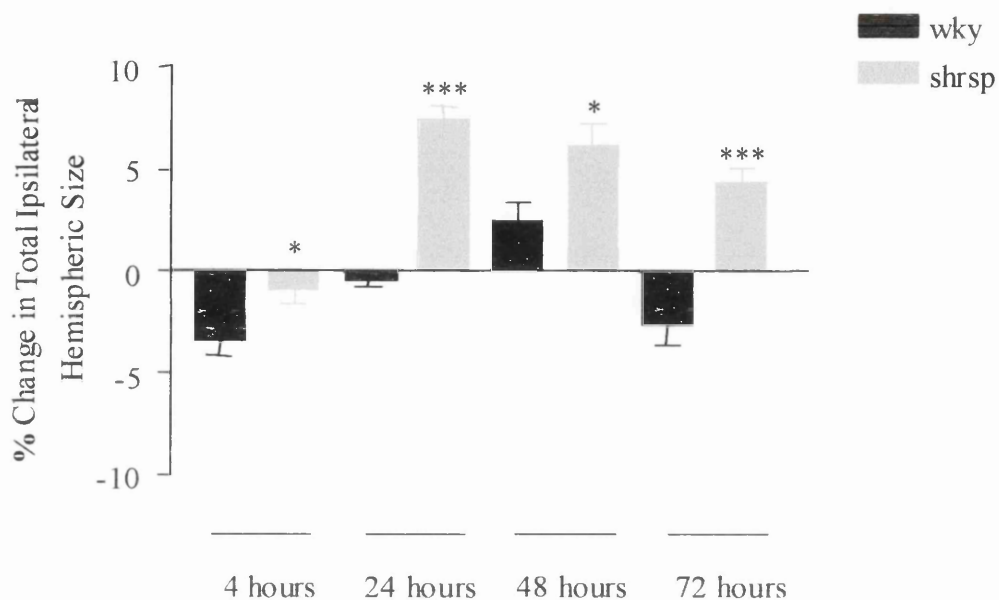


Figure 63. Tissue swelling in SHRSP and WKY over 72 -hour time course. n=5 per group. Data represents mean  $\pm$ SEM and was analysed using 2-way ANOVA followed by Student's t-test. \*p<0.1, \*\*\*p<0.005 comparisons between SHRSP and WKY at each time point.

#### **6.3.4 Microglial counts in specific brain regions over the 72- hour time course.**

Graphs were plotted for each of the 5 brain regions to quantify regional distribution of microglial activation.

The number of activated microglia differed between individual brain regions and between strains.

In both SHRSP and WKY, the number of activated microglia was greater in the ipsilateral hemisphere when compared to the contralateral hemisphere in all five of the regions examined (Figure 64). The numbers of activated microglia changed over time with the greatest numbers of activated microglia observed at the 72-hour time point than in any of the earlier time points.

In terms of strain differences, SHRSP displayed greater numbers of activated microglia than WKY at all the 4 time points in all of the five regions examined (Figure 65-69). These differences were most significant in the peri-infarct region and the two white matter regions - genu of the corpus callosum and the external capsule.

#### **Statistics**

Data were analysed using ANOVA followed by an unpaired Student's t-test with a Bonferroni correction for multiple comparisons.

*Peri-infarct region (Figure 65):* In the ipsilateral hemisphere, SHRSP displayed significantly greater numbers of activated microglia than WKY at 24 hours ( $p < 0.05$ ), 48 hours ( $p < 0.001$ ) and 72 hours ( $p < 0.001$ ). In SHRSP, the number of activated

microglia in the ipsilateral hemisphere increased significantly between 4 and 72 hours ( $p < 0.001$ ), with a step like increase between each time point (significant between 24 and 48 hours,  $p < 0.001$ ; and between 48 and 72 hours,  $p < 0.005$ ). In WKY, numbers of activated microglia also increased significantly between 4 and 72 hours ( $p < 0.05$ ) again with a step like increase between each time point although the differences were not as significant as in SHRSP (significant only between 24 and 72 hours ( $p < 0.001$ )). Numbers of activated microglia were not significantly different between the two strains in the contralateral hemisphere nor was there any significant increase in the number of activated microglia over the 72 - hour time course in either strain.

*Infarct Core (Figure 66):* In the ipsilateral hemisphere, SHRSP displayed significantly greater numbers of activated microglia than WKY at the 24- hour time point only ( $p < 0.05$ ). This was also the case in the equivalent region in the contralateral hemisphere ( $p < 0.05$ ). In SHRSP, numbers of activated microglia in the ipsilateral hemisphere increased significantly between 4 and 72 hours ( $p < 0.001$ ), again with a step like increase between each time point (significant between 4 and 24 hours,  $p < 0.05$  and between 48 and 72 hours,  $p < 0.005$ ). In WKY, there was a significant increase in the number of activated microglia between 48 and 72 hours ( $p < 0.05$ ) only. In the contralateral hemisphere, there was a significant increase in the number of activated microglia between SHRSP and WKY at 24 hours only ( $p < 0.05$ ). In SHRSP numbers of activated microglia increased significantly between 48 and 72 hours ( $p < 0.001$ ) in the contralateral hemisphere. In WKY in the contralateral

hemisphere, there was also a significant increase in numbers of activated microglia between 48 and 72 hours ( $p < 0.05$ ).

*Cingulate cortex (Figure 67):* In the ipsilateral hemisphere, SHRSP displayed greater numbers of activated microglia than WKY at the 48- hour time point ( $p < 0.05$ ). The same was true for the contralateral hemisphere ( $p < 0.05$ ). In the ipsilateral hemisphere, there were significant increases in microglial number between 4 and 72 hours ( $p < 0.005$ ) and between 24 and 72 hours ( $p < 0.005$ ) in SHRSP. No such differences across time existed for WKY microglial numbers. In the contralateral hemisphere, there was a significant increase in the number of activated microglia in SHRSP between 24 and 72 hours ( $p < 0.05$ ) suggesting an increase in number over time. No such changes occurred in the WKY.

*External capsule (Figure 68):* In the ipsilateral hemisphere, there was a significant difference in the number of activated microglia between SHRSP and WKY at 72 hours only ( $p < 0.005$ ). The same was true for the contralateral hemisphere ( $p < 0.05$ ). In the ipsilateral hemisphere, there were also significant increases in the number of activated microglia over time in SHRSP (4 and 72 hours,  $p < 0.005$ ; 48 and 72 hours,  $p < 0.05$ ) In the contralateral hemisphere of SHRSP, there was also a significant increase in the number of activated microglia between 4 and 72 hours ( $p < 0.001$ ) and between 48 and 72 hour ( $p < 0.01$ ). No such differences between time points were evident in the WKY.

*Genu of Corpus Callosum (Figure 69):* In the ipsilateral hemisphere, differences in the number of activated microglia between SHRSP and WKY existed at 48 hours ( $p < 0.05$ ) and 72 hours ( $p < 0.01$ ). In the contralateral hemisphere, differences also existed at the same time points ( $p < 0.05$ ). In the ipsilateral hemisphere, differences in the number of activated microglia existed between 4 and 72 hours ( $p < 0.005$ ); 24 and 48 hours,  $p < 0.01$  and 48 and 72 hours,  $p < 0.05$ ). No such differences over time were present in WKY. In the contralateral hemisphere, differences in activated microglial number were apparent between 4 and 72 hours ( $p < 0.005$ ) again increasing in steps between time points over the time course (significant between 48 and 72 hours,  $p < 0.005$ ). No such increases over time were apparent in the WKY.

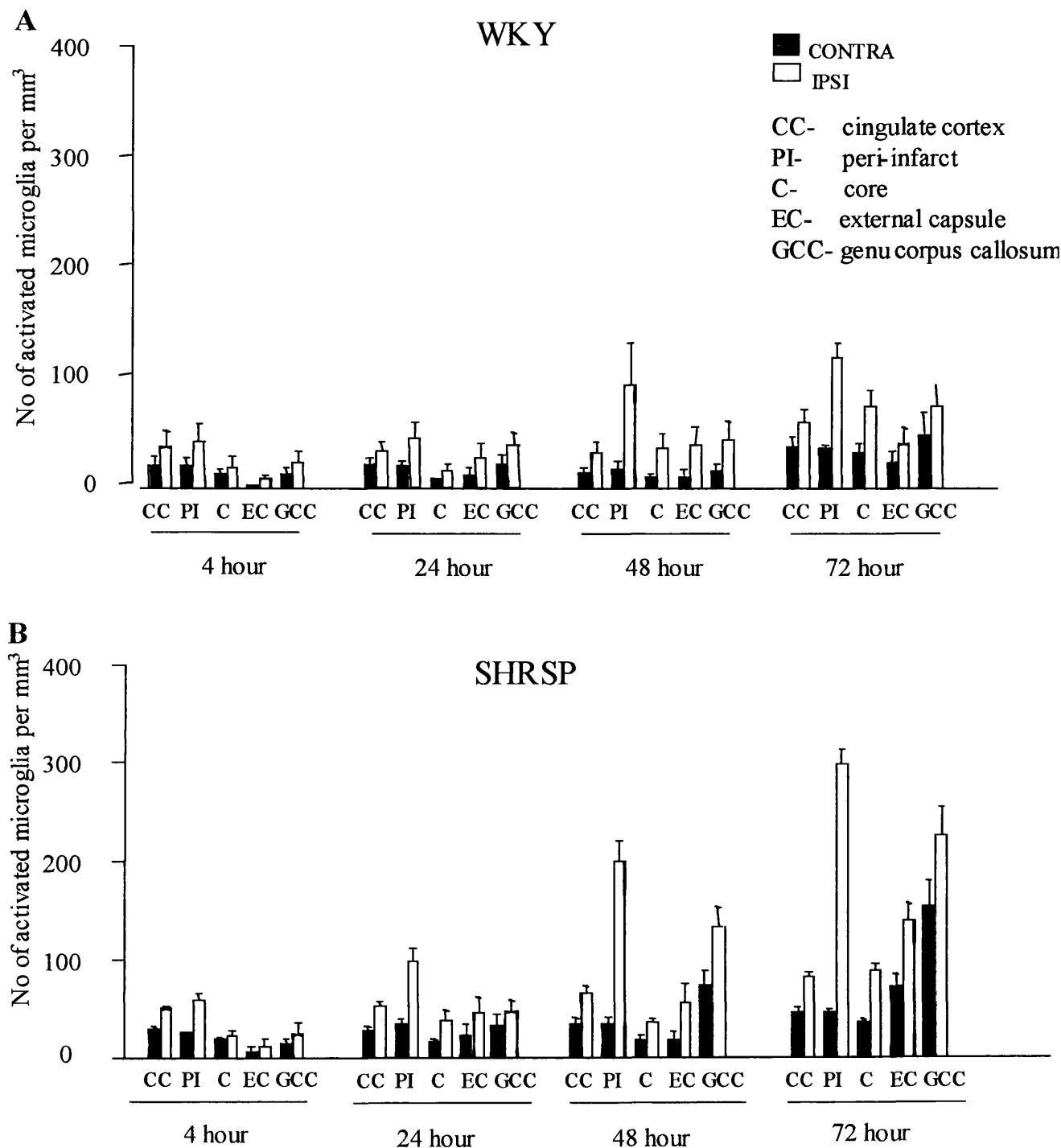


Figure 64. Microglial counts in A. WKY and B. SHRSP over 72 hours.

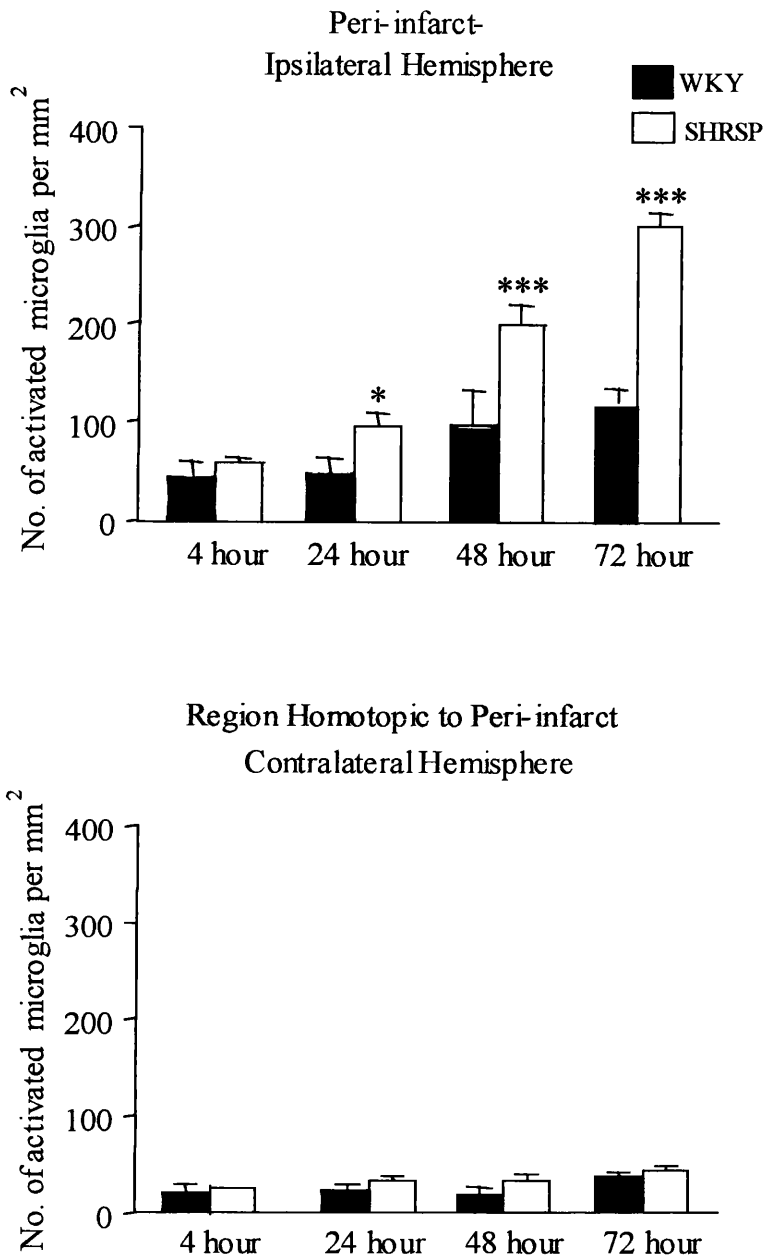


Figure 65. Microglial counts in WKY Vs SHRSP in the Peri-infarct region following permanent MCAO.  $n=5$  per group. Data represent mean  $\pm$ SEM and were analysed using ANOVA followed by Students t-test.

\*  $p < 0.05$ , \*\*\*  $p < 0.001$  for strain differences.

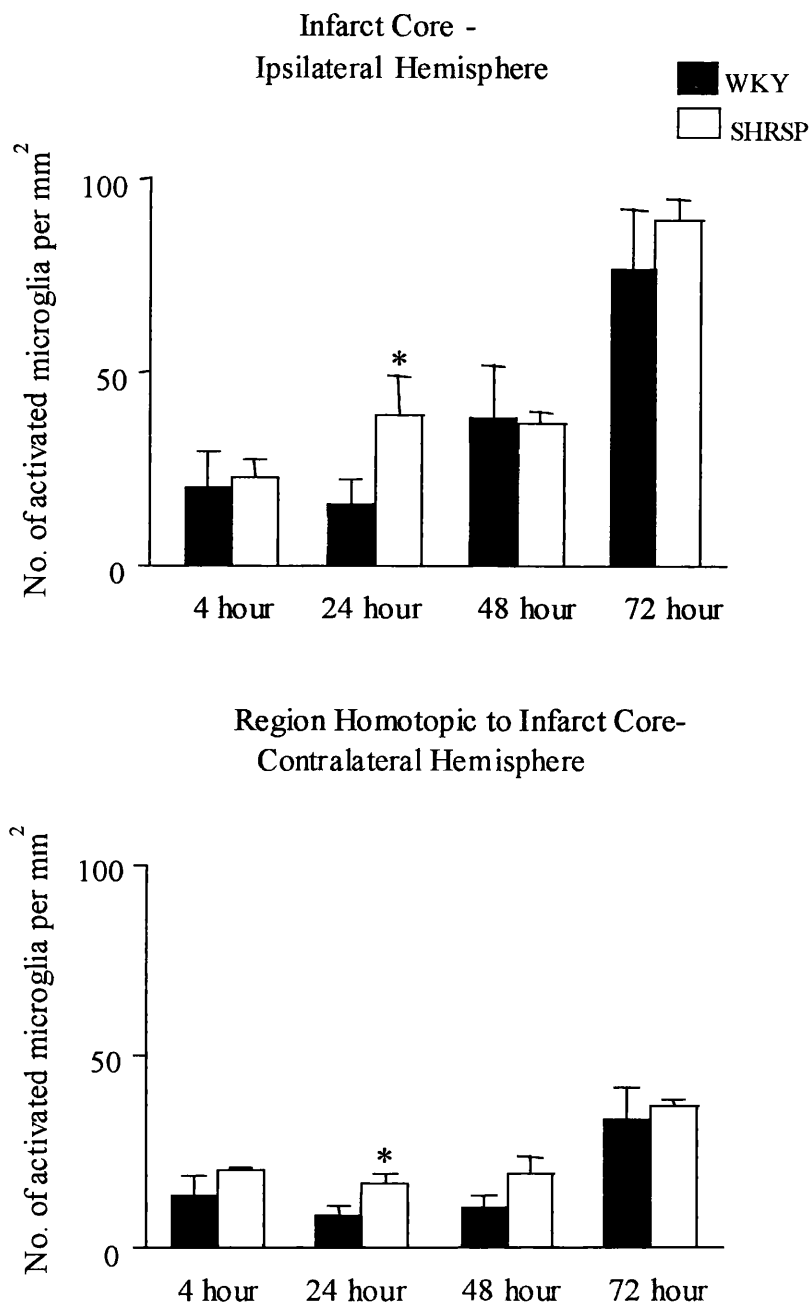


Figure 66. Microglial counts in WKY Vs SHRSP in the infarct core region following permanent MCAO. n=5 per group. Data represent mean  $\pm$ SEM and were analysed using ANOVA followed by Students t-test.

\*  $p < 0.05$  for differences between animals.

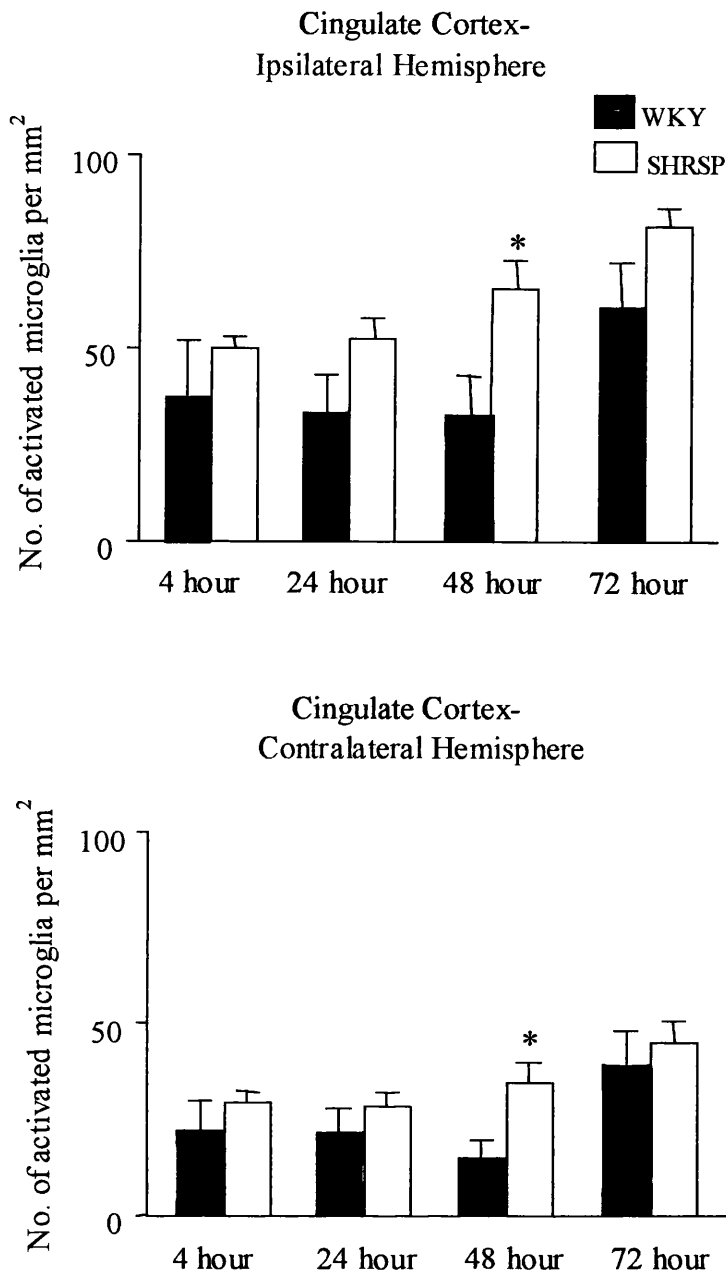


Figure 67. Microglial counts in WKY Vs SHRSP in the cingulate cortex region following permanent MCAO.  $n=5$  per group. Data represent mean  $\pm$ SEM and were analysed using ANOVA followed by Students t-test.

\*  $p<0.05$  for differences between strains.

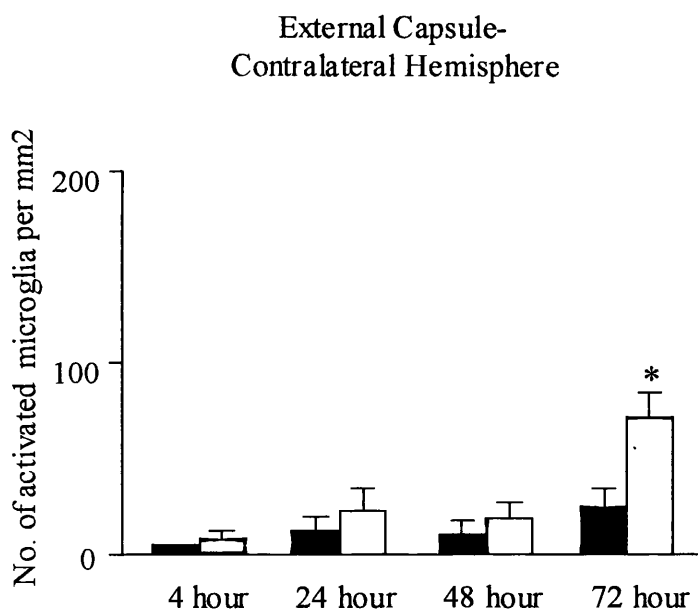
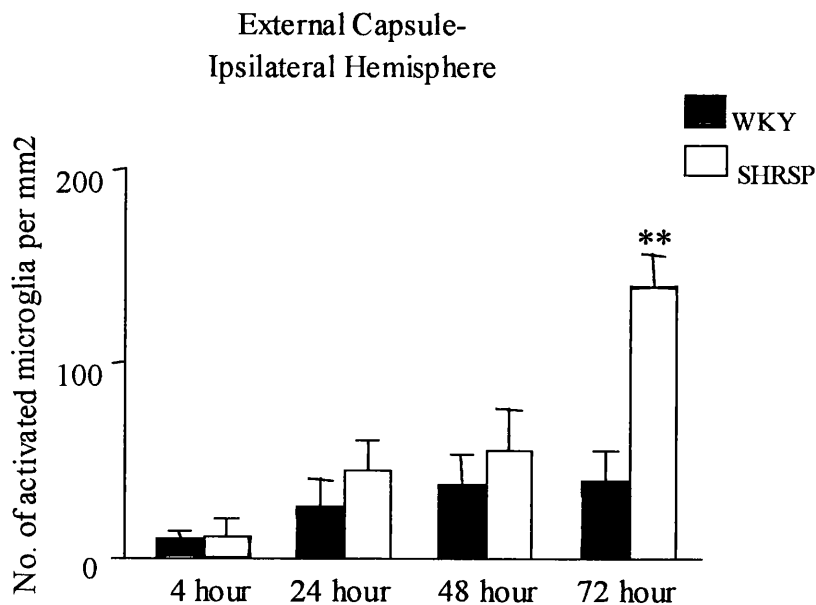


Figure 68. Microglial counts in WKY Vs SHRSP in the external capsule region following permanent MCAO. n=5 per group. Data represent mean  $\pm$ SEM and were analysed using ANOVA followed by Students t-test.

\*  $p < 0.05$ , \*\*  $p < 0.005$  for differences between strains.

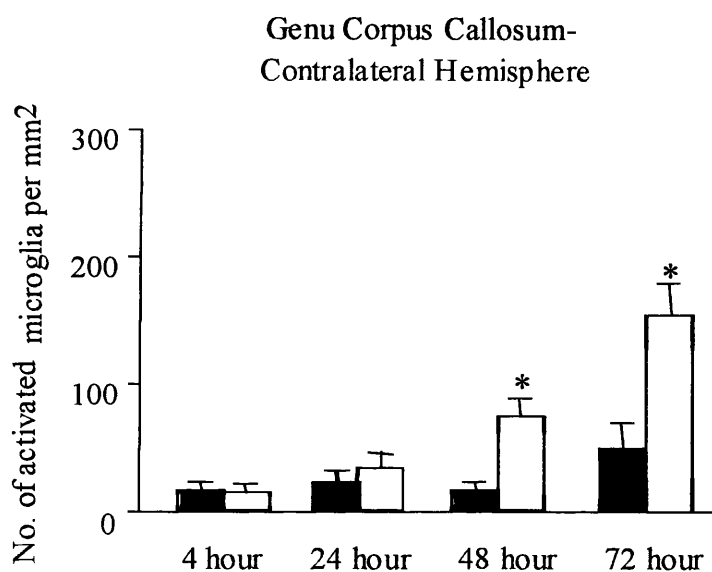
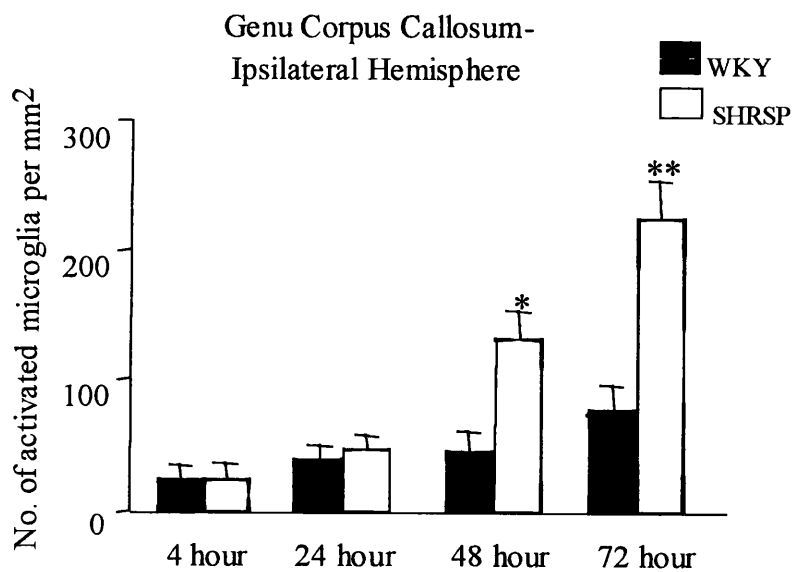


Figure 69 Microglial counts in WKY Vs SHRSP in the genu of corpus callosum following permanent MCAO.  $n=5$  per group. Data represent mean  $\pm$ SEM and were analysed using ANOVA followed by Students t-test. \*  $p, 0.05$ , \*\*  $p<0.01$  for differences between strains.

### 6.3.5 Characterisation of Microglial Response.

At 4 hours post ischaemia, the majority of microglial cells were ramified or resting in appearance (Figure 70) - exhibiting a small cell body and large, fine, spindly projections. Only a few activated microglia (Figure 70) - exhibiting a densely stained cell body and thick shortened projections-, could be identified in both SHRSP and WKY.

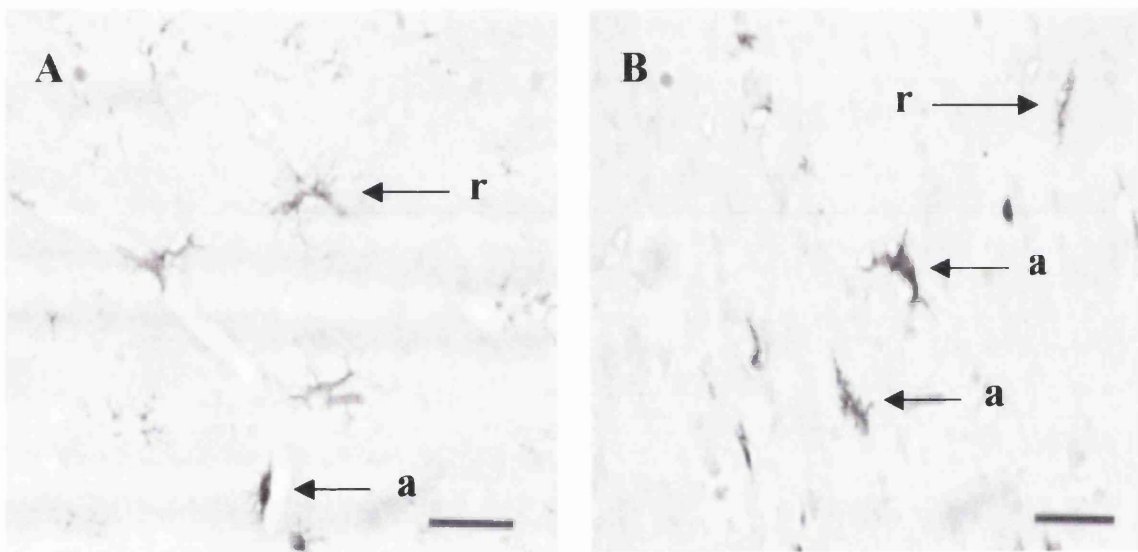


Figure 70. Microglia in the peri-infarct region following 4 hours permanent MCAO in A. WKY and B. SHRSP. Arrows represent: a = activated microglia, r = resting microglia . Magnification = X40. Scale bar represents 50 $\mu$ m.

At 24 hours post ischaemia, an increase in microglia with an activated phenotype could be seen in both SHRSP and WKY with a higher incidence in the ipsilateral hemisphere in both strains. SHRSP displayed a greater density of activated microglia than WKY at 24 hours (Figure 71).

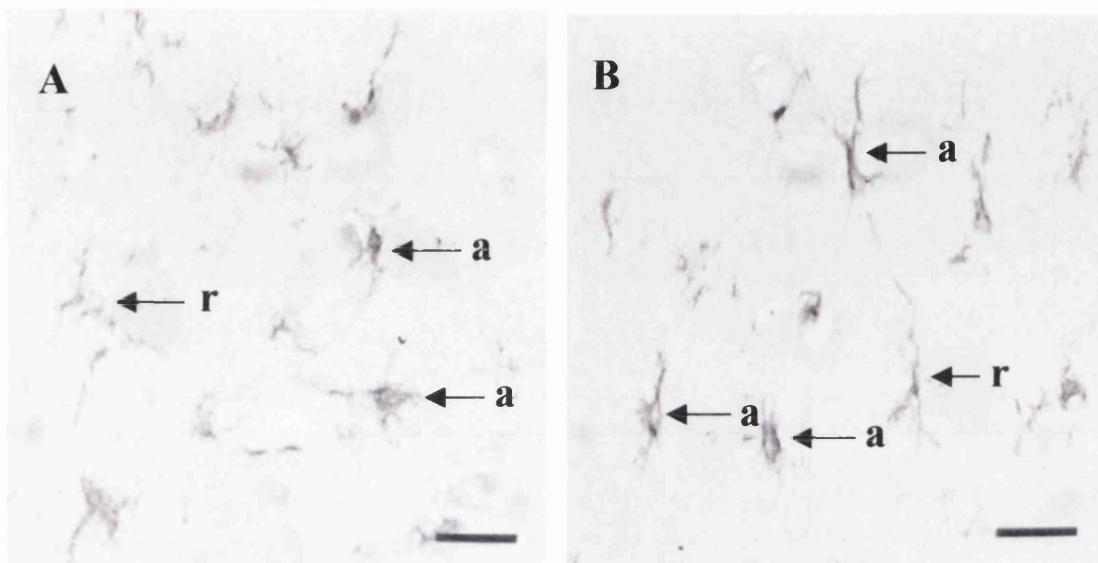


Figure 71. Microglia in the peri-infarct region following 24 hours permanent MCAO in A. WKY and B. SHRSP. Magnification = X40. Scale bar represents 50 $\mu$ m.

Following 48 hours ischaemia a further increase in activated microglia could be seen in both species with SHRSP again displaying a greater increase than WKY (Figure 72). At 48 hours a large number of microglia assumed a phagocytic phenotype-appearing small, round and densely stained.

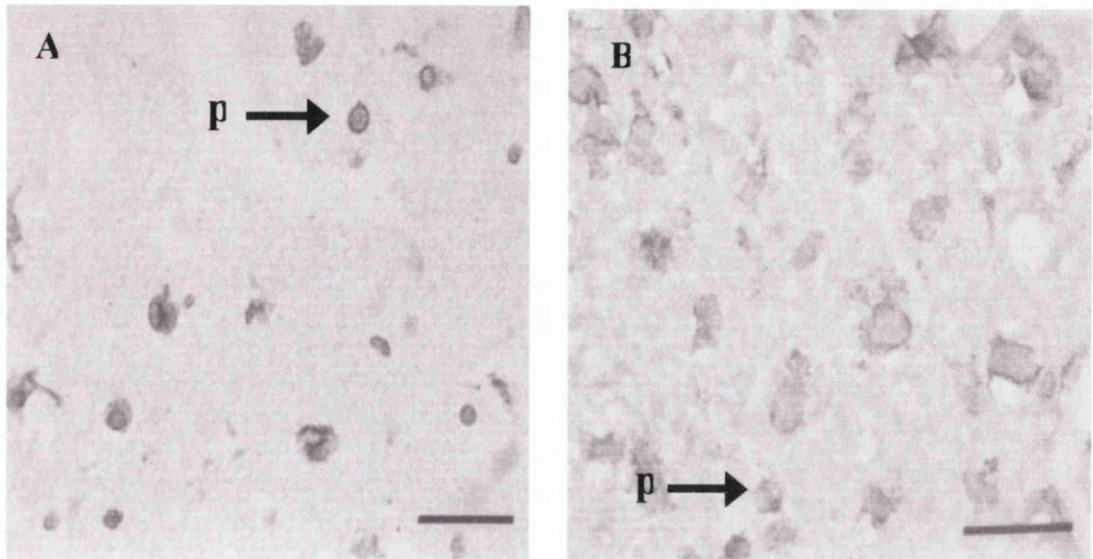


Figure 72. Microglia in the peri-infarct region following 48 hours permanent MCAO in A. WKY and B. SHRSP. p = phagocytic microglia. Magnification = X40. Scale bar represents 50µm.

At 72 hours post ischaemia a further increase in the number of activated and phagocytic microglia could be seen in both strains with SHRSP displaying the greatest increase in staining density (Figure 73).

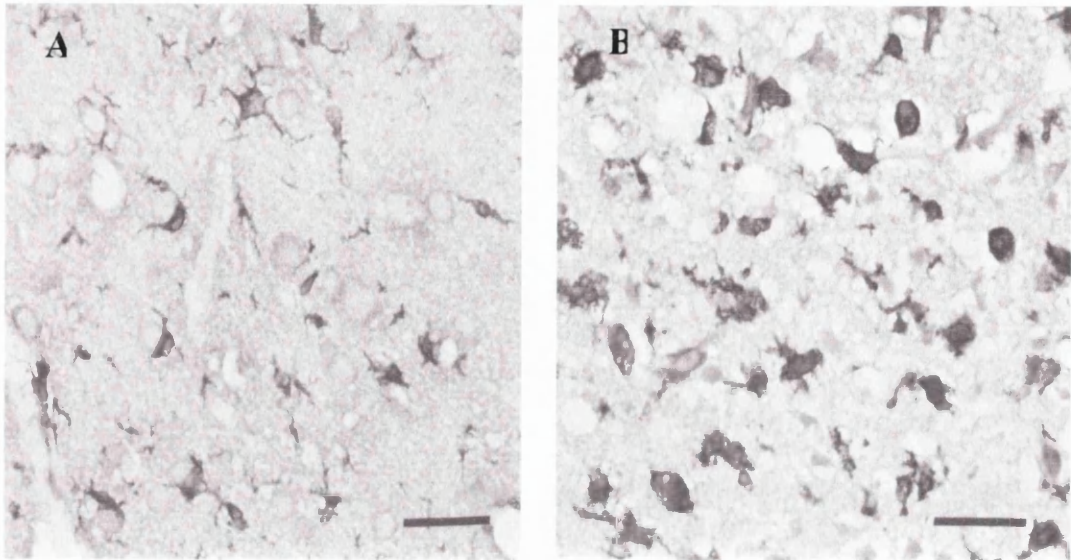


Figure 73. Microglia in the peri-infarct region following 72 hours permanent MCAO in A. WKY and B. SHRSP. Magnification = X40. Scale bar represents 50 $\mu$ m.

### 6.3.6 Microglial Distribution Maps.

The distribution of the activated microglia incorporated all five of the regions Has been studied, with activated microglia being present in both grey and white matter regions at all eight coronal levels (Figure 74-75). At the later time points of 48 and 72 hours, phagocytic microglia could be identified in the peri-infarct region forming a boundary around the ischaemic lesion (Figure 76). A few phagocytic microglia could also be seen in the core of the lesion. Activated microglia could be seen in the white matter tracts of both SHRSP and WKY at all time points although the numbers

increased as the time progressed. This white matter tract expression of activated microglia incorporated both ipsilateral and contralateral hemispheres.

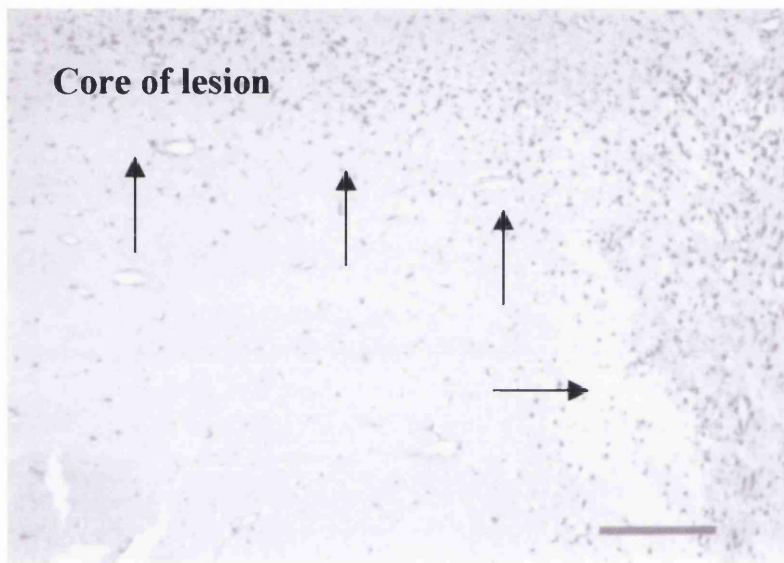


Figure 76. Activated microglia and phagocytic microglia forming a boundary around the infarct. Arrows represent boundary of lesion. Magnification = X20. Scale bar represents 100 $\mu$ m.

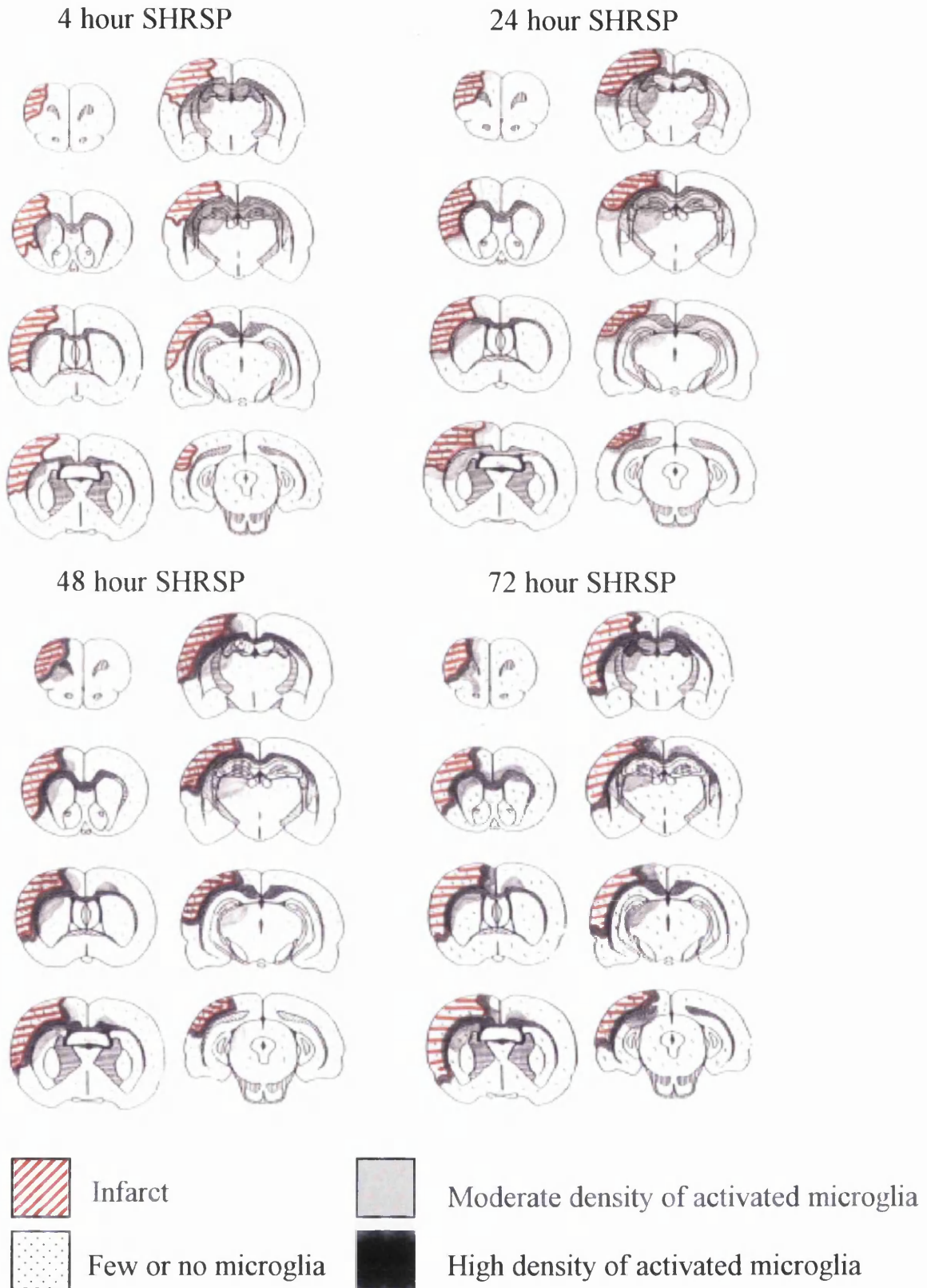


Figure 74. Microglial distribution maps for SHRSP 4- 72 hours



Figure 75. Distribution maps for WKY 4- 72 hours

### 6.3.7 Characterisation of MMP-8 and MMP-9 staining.

MMP positive cells were present over all 4 of the time points in both strains.

At 4 hours, MMP-8 and MMP-9 staining was relatively weak when compared to later time points. Immunopositive cells had the appearance of microglial cells. Both resting and activated microglia were immunopositive for the two MMPs but activated microglia had a more intense MMP staining when compared to resting microglia (Figure 77).

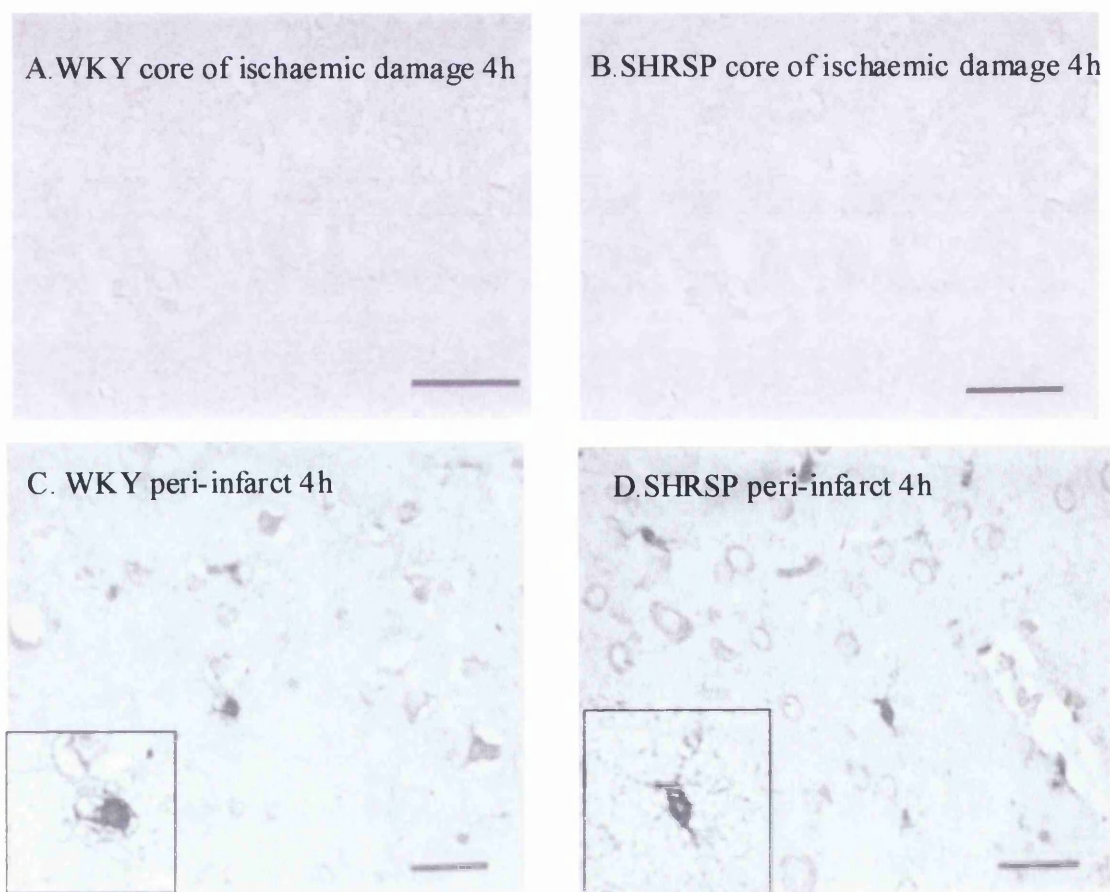


Figure 77. MMP-8 staining 4 hours following permanent MCAO within the region of ischaemic damage in A. WKY and B. SHRSP. Double labelled microglia (MMP-8, brown and mrf-1, grey) in the peri-infarct region of C. WKY and D. SHRSP. Magnification = X40. Scale bar represents 50µm.

Figure 77 represents MMP-8 staining. MMP-9 exhibited very similar staining patterns.

MMP-8 and MMP-9 staining extended over a greater percentage of MCA territory in SHRSP compared to WKY. However there was no real difference in the staining intensity of positive cells in the two strains.

At 24 hours the number of MMP-8 and MMP-9 positive cells increased in accordance with an increase in activated microglia. Most of the immunopositive cells again had the appearance of activated microglia (Figure 78). Figure 78 represents MMP-8 staining, MMP-9 staining was very similar. MMP-8 positive neurons could also be seen within the peri-infarct regions. These neurons had the morphology of salvageable non-ischaemic neurons exhibiting a strong cytosolic staining (Figure 78). MMP-9 staining was also present in neurons within the peri-infarct region at 24 hours but this staining was not as intense as with MMP-8. Again SHRSPs exhibited a greater degree of staining than WKYs due to their larger infarcts but there was no difference in staining intensity between SHRSP and WKY MMP positive cells.

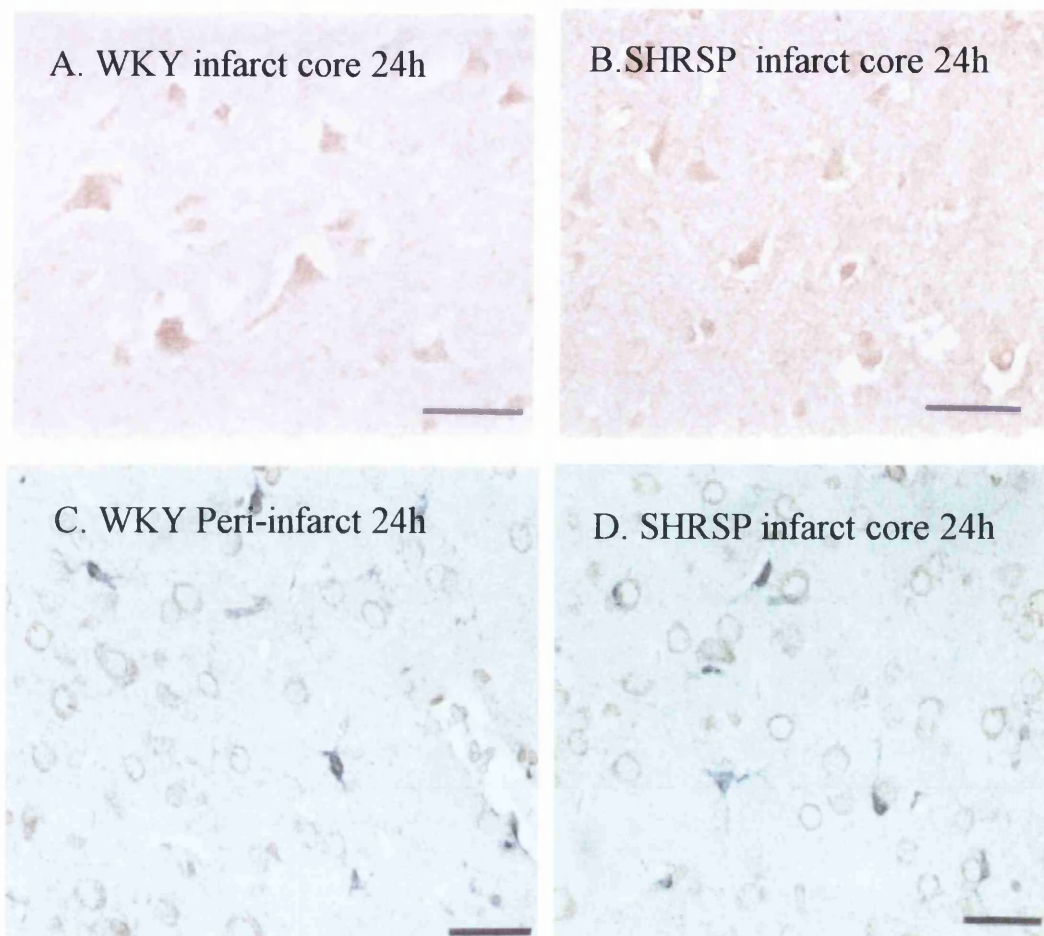


Figure 78. MMP-8 staining 24 hours following permanent MCAO within the infarct in A. WKY and B. SHRSP and double labelled microglia (MMP-8, brown and mrf-1, grey) in the peri-infarct region of C. WKY and D. SHRSP. Magnification = X40, Scale bar represents 50 $\mu$ m (A-D)

At 48 hours the number of MMP positive cells again increased along with the number of activated microglia. Both activated and phagocytic microglia were

positively stained for MMP-8 and MMP-9 (Figure 79) with intense microglial MMP staining within the peri-infarct in both strains. Figure 79 represents MMP-8 double labelling; MMP-9 exhibited similar staining. Once again, cells with a normal morphology (salvageable neurons) could be identified in the peri-infarct zone of the sections stained with MMP-8 and to a lesser extent MMP-9 (Figure 79).

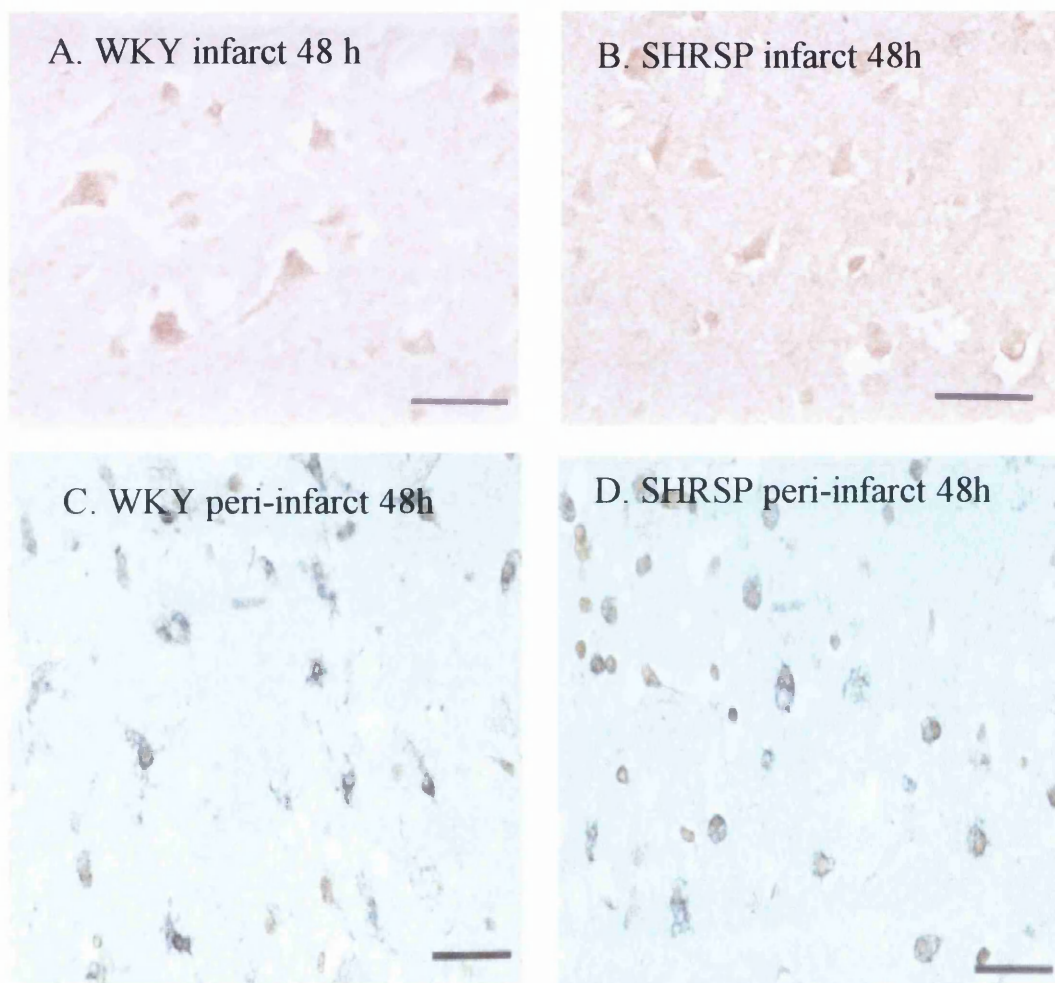


Figure 79. MMP-8 staining 48 hours following permanent MCAO within the infarct in A. WKY and B. SHRSP, and double labelled microglia (MMP-8, brown and mrf-1, grey) in the peri-infarct region of C. WKY and D. SHRSP. Magnification = X40. Scale bar represents 50 $\mu$ m. MMP-9 exhibited similar staining.

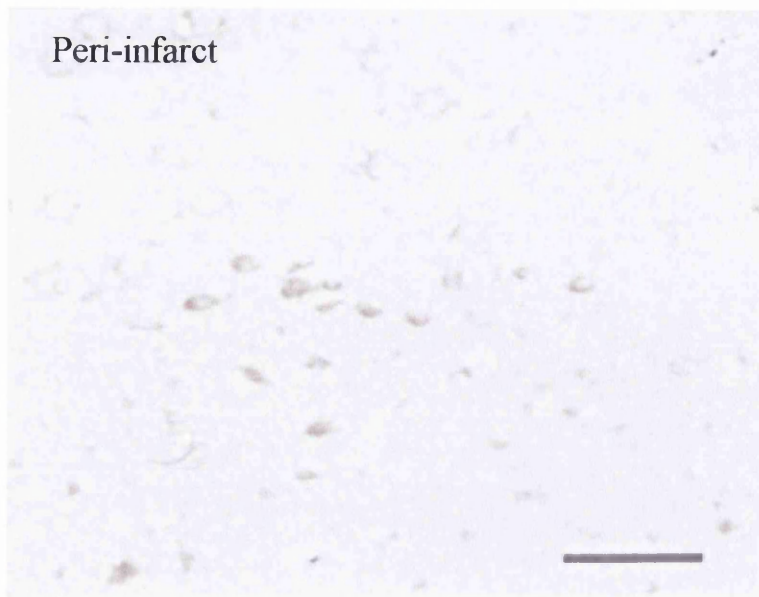


Figure 80. Image representing MMP-8 staining in neurons within the peri-infarct region at following permanent MCAO. Scale bar represents 100 $\mu$ m. Such staining could be seen at 24 and 48 hours in both SHRSP and WKY.

At 72 hours the number of MMP-8 and MMP-9 positive cells increased further, accompanying the increase in the number of activated and phagocytic microglia—particularly around the peri-infarct region in both strains. Activated and some phagocytic microglia were immunopositive for MMP-8 and MMP-9 (Figure 81). Figure 81 represents MMP-8 staining; MMP-9 produced similar staining patterns. At the 72-hour time point, phagocytic microglia appeared to be associated with neurons within the peri-infarct zone, in most cases either surrounding or adjacent to the neuron. There was no evidence of any MMP-8 staining of neurons with a normal morphology within the peri-infarct region in either SHRSP or WKY at this time point. SHRSPs displayed a greater spread of MMP-8 and MMP-9 staining which was linked to their increased infarct size and their increased expression of activated microglia.

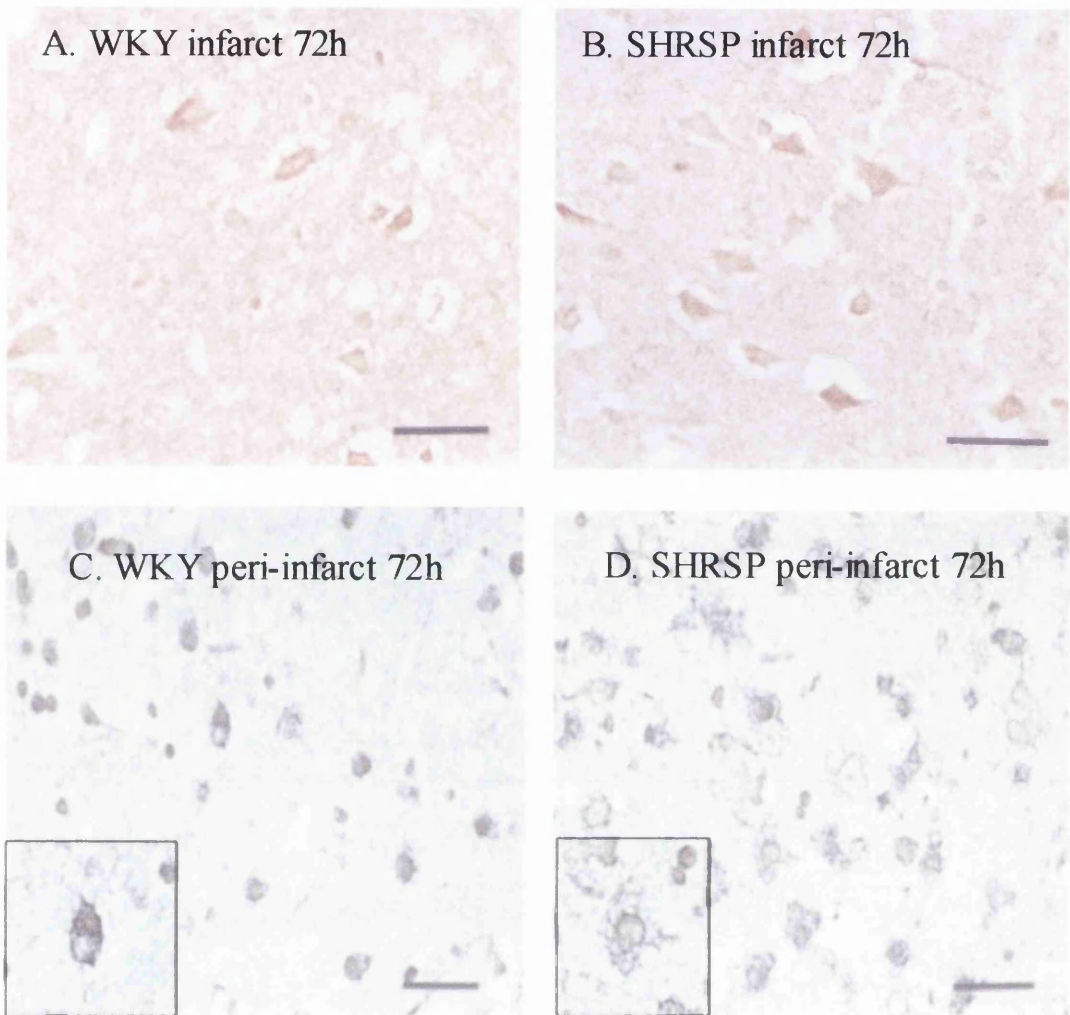


Figure 81. MMP-8 staining 72 hours following permanent MCAO within the infarct in A. WKY and B. SHRSP, and double labelled microglia (MMP-8, brown and mrf-1, grey) in the peri-infarct region of C. WKY and D. SHRSP. Magnification =X40. Scale bar represents 50µm. MMP-9 exhibited very similar staining patterns.

No evidence for astrocytic (Figure 82) or blood vessel MMP-8 or MMP-9 staining was found at any of the 4 time points examined. Oligodendrocytes were found to be immunopositive for both MMP-8 and MMP-9 in the white matter tracts of both SHRSP and WKY following 4-72 hours permanent MCAO. Figure 81 represents MMP-9 staining at 24 hours. MMP-8 staining exhibited similar patterns.

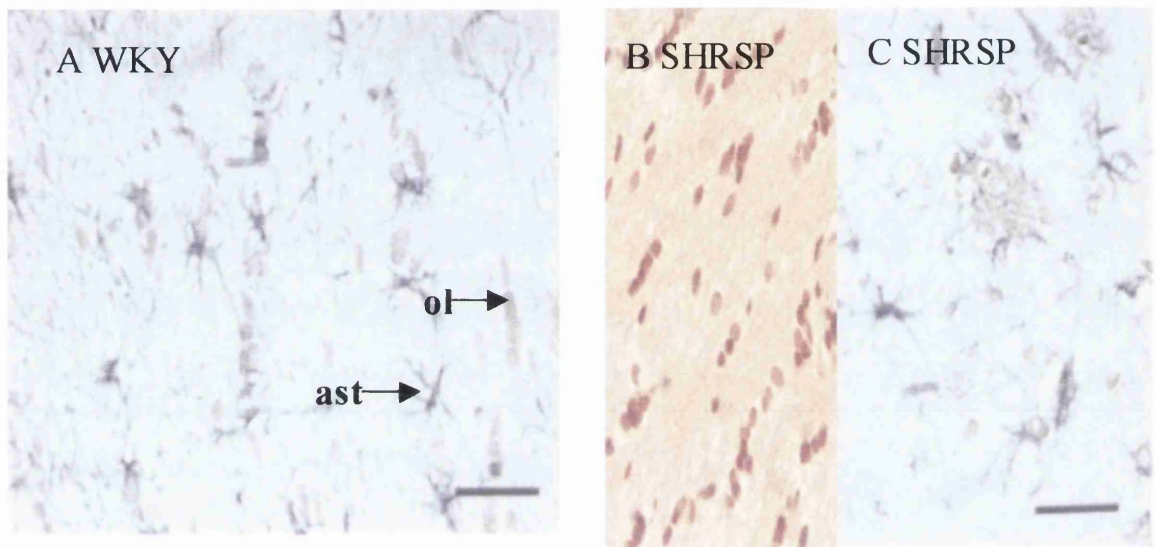


Figure 82. A. Lack of MMP-9 staining in astrocytes (GFAP+ve, MMP-9-ve), and MMP-9 staining in oligodendrocytes in WKY, B. MMP-9 positively stained oligodendrocytes in SHRSP and C. lack of astrocytic MMP-9 staining in SHRSP (GFAP+ve, MMP-9-ve) at 24 hours following permanent MCAO. Ast = astrocyte, ol = oligodendrocyte. Scale bar represents 50 $\mu$ m.

### **6.3.8 Distribution maps for MMP staining.**

MMP-8 and MMP-9 positive cells could be seen in both the contralateral and ipsilateral hemispheres in both SHRSP and WKY (Figures 83-86). More MMP positive cells could be identified in the ipsilateral hemisphere. MMP-8 and MMP-9 positive cells could also be seen in the white matter tracts of both hemispheres although the staining was more intense in the genu of the corpus callosum of the ipsilateral hemisphere. The number of MMP positive cells increased with time over the 72 hours in both strains.

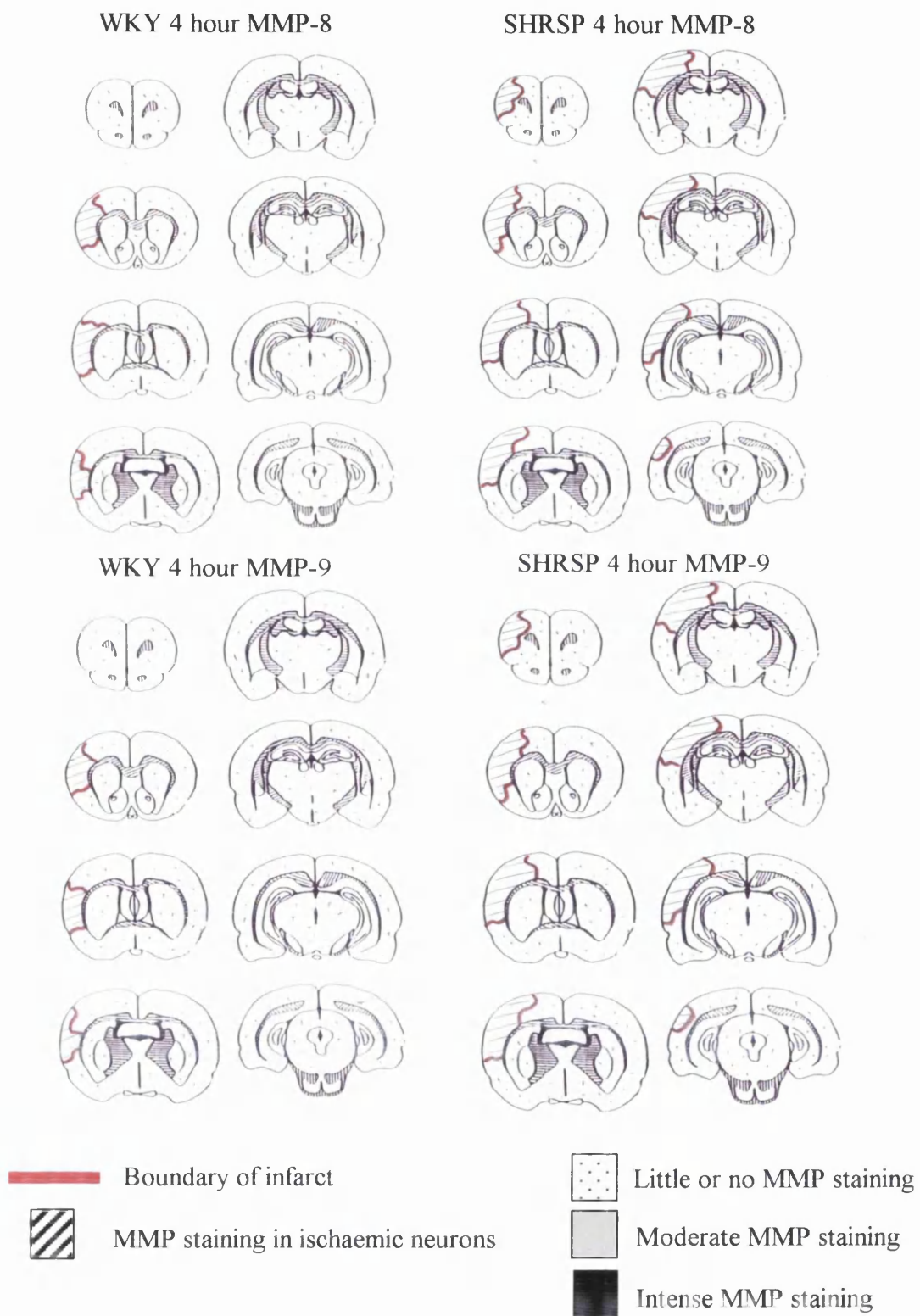


Figure 83. MMP distribution in SHRSP and WKY at 4 hours following permanent MCAO.

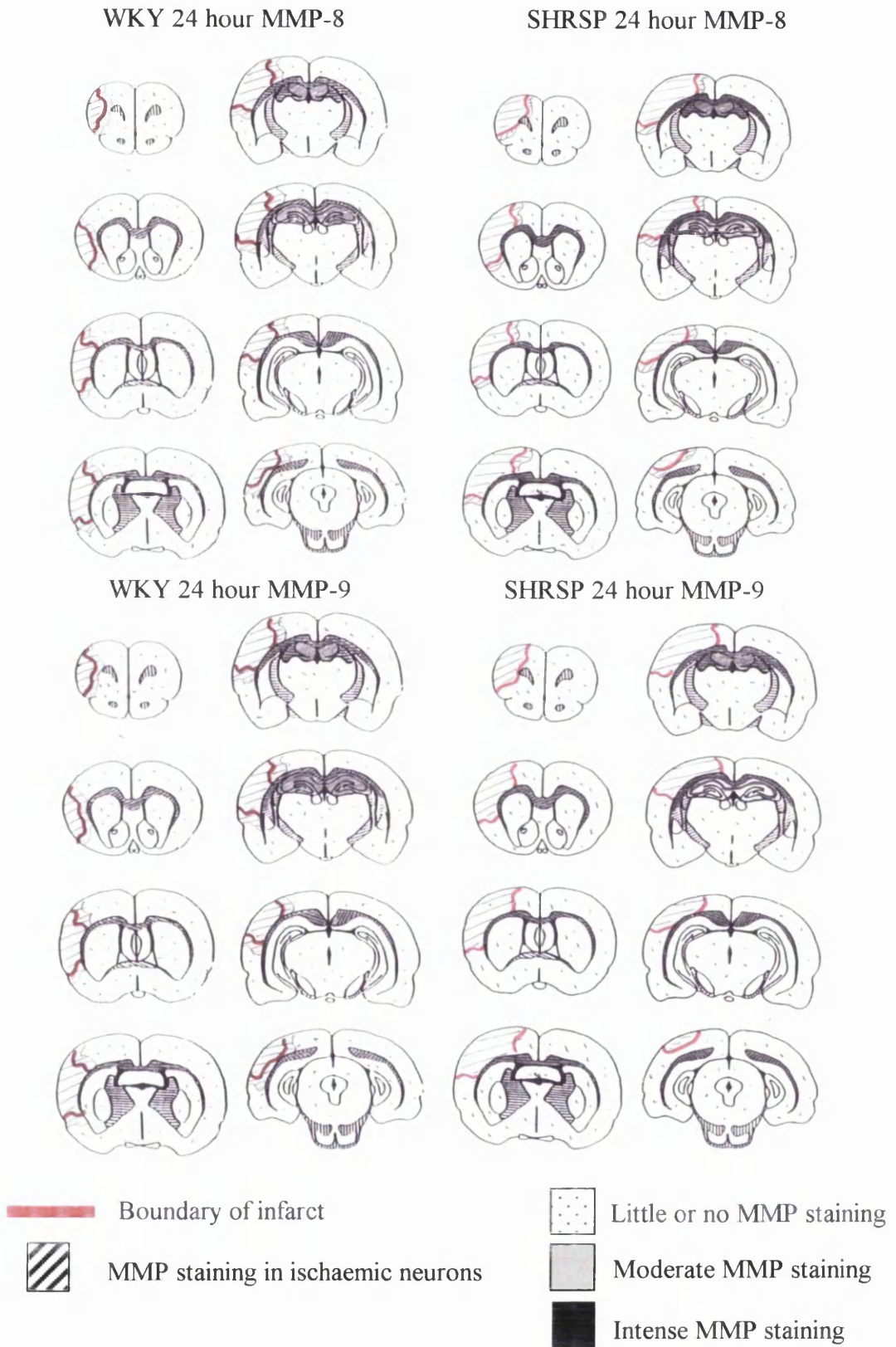


Figure 84. MMP distribution in SHRSP and WKY at 24 hours following permanent MCAO.

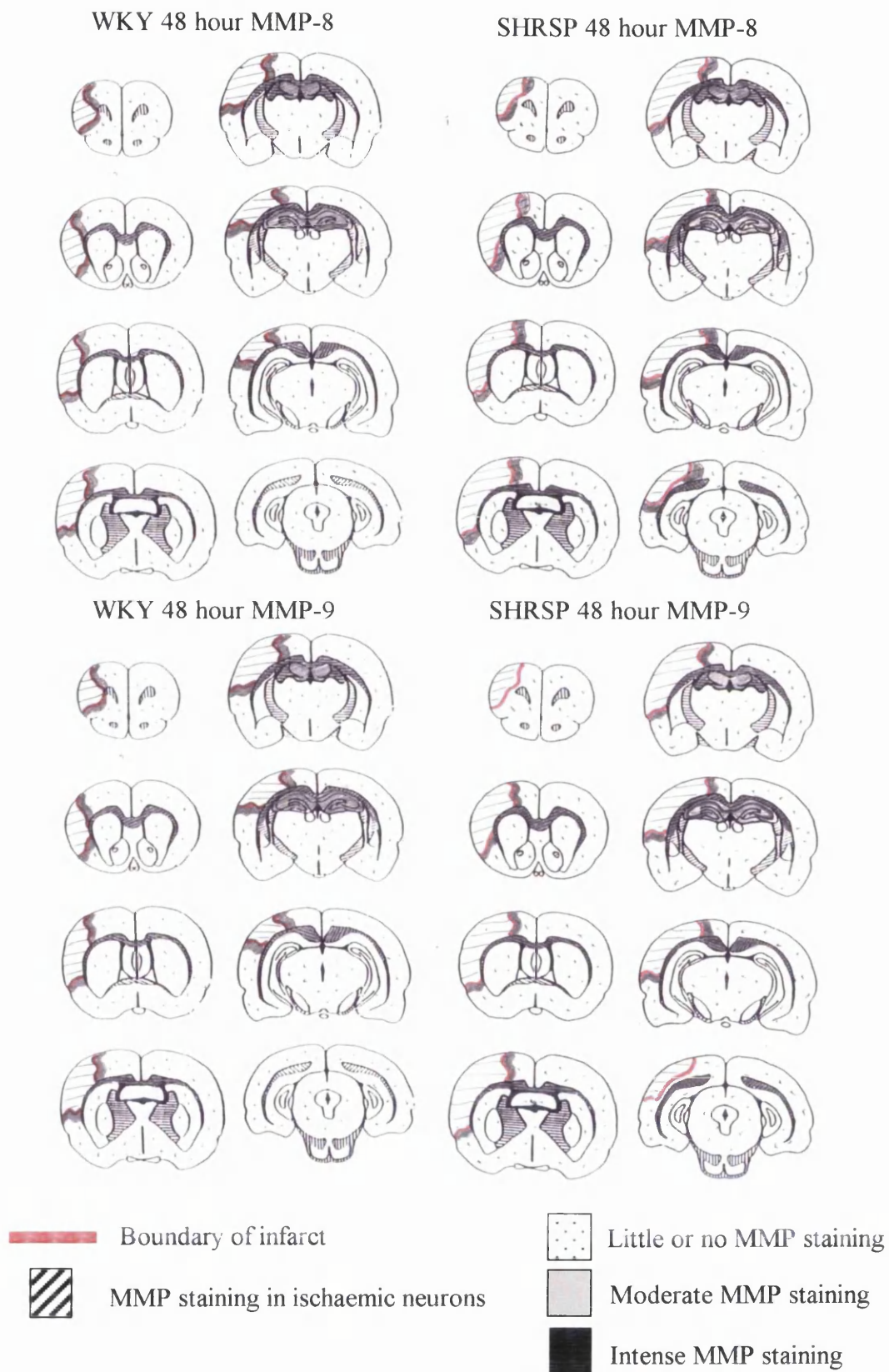


Figure 85. MMP distribution in SHRSP and WKY at 48 hours following permanent MCAO.

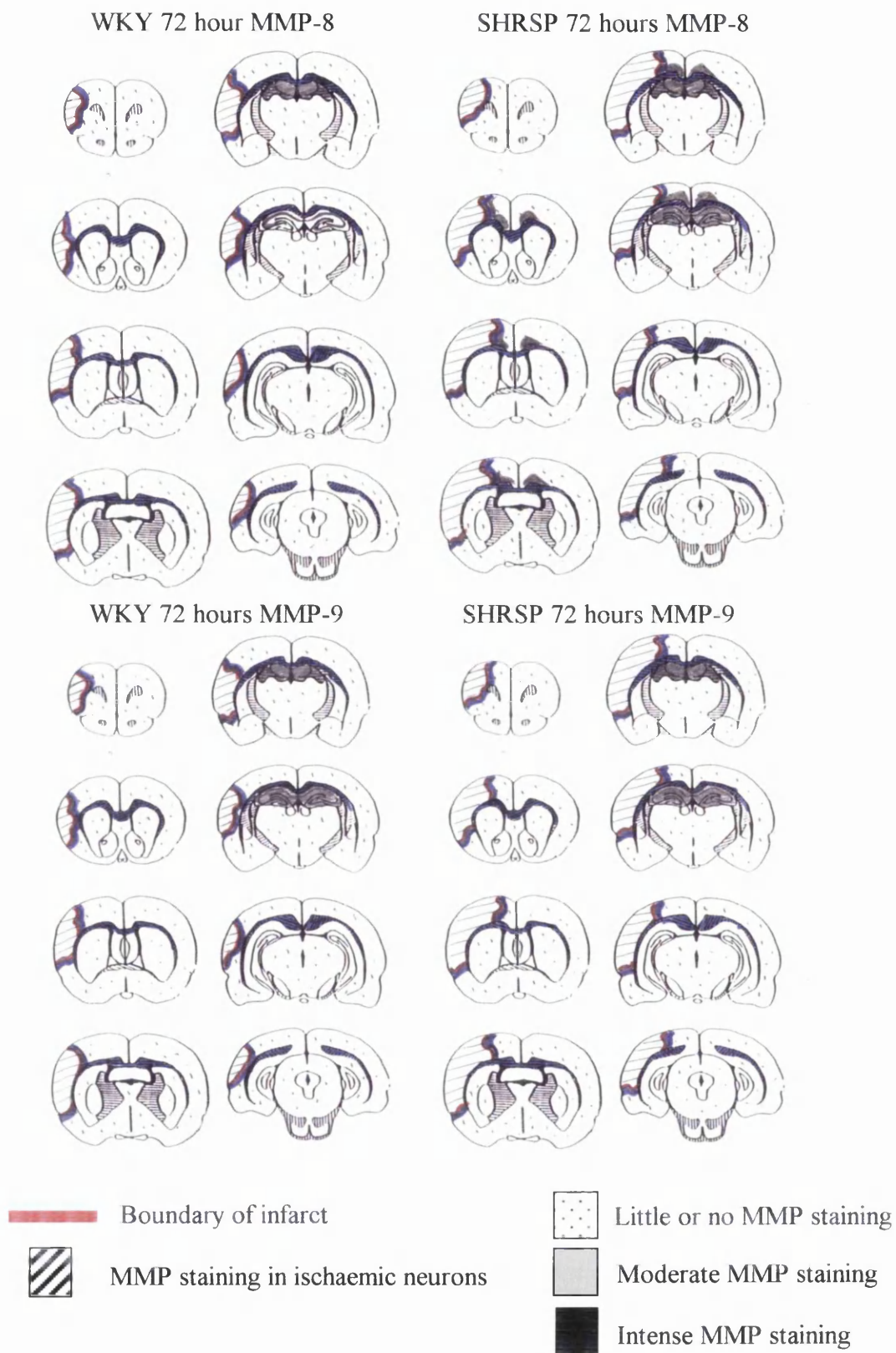


Figure 86. MMP distribution in SHRSP and WKY at 72 hours following permanent MCAO.

### 6.3.9 Characterisation of IL-1 $\beta$ staining.

IL-1 $\beta$  staining was seen in the positive control ischaemic tissue (with meningitis), which was included in each immunohistochemistry run with ischaemic material (Figure 87). However, no cells strongly immunopositive for IL-1 $\beta$  could be seen in either WKY or SHRSP strains over the 72 hours following permanent distal MCAO (Figure 88).

Cells in the positive control material which were immunopositive for IL-1 $\beta$  displayed the characteristic morphology of activated microglia- small dense cell bodies and thick bushy projections.

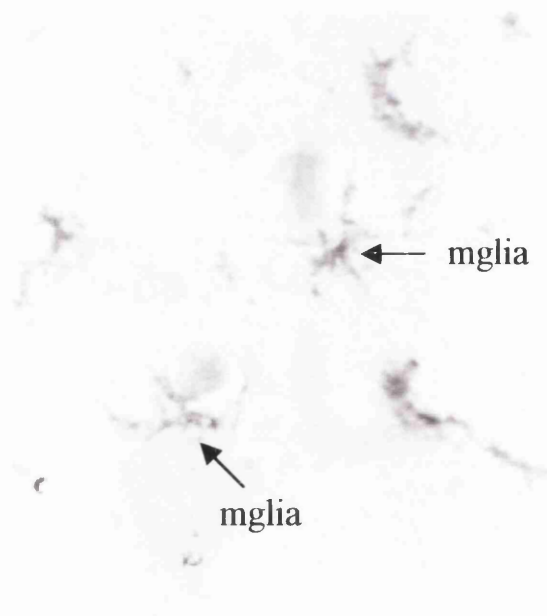


Figure 87. IL-1 $\beta$  staining in positive control material. Arrows represent IL-1 $\beta$  positive microglial cells. Magnification =X40. Scale bar represents 50 $\mu$ m.

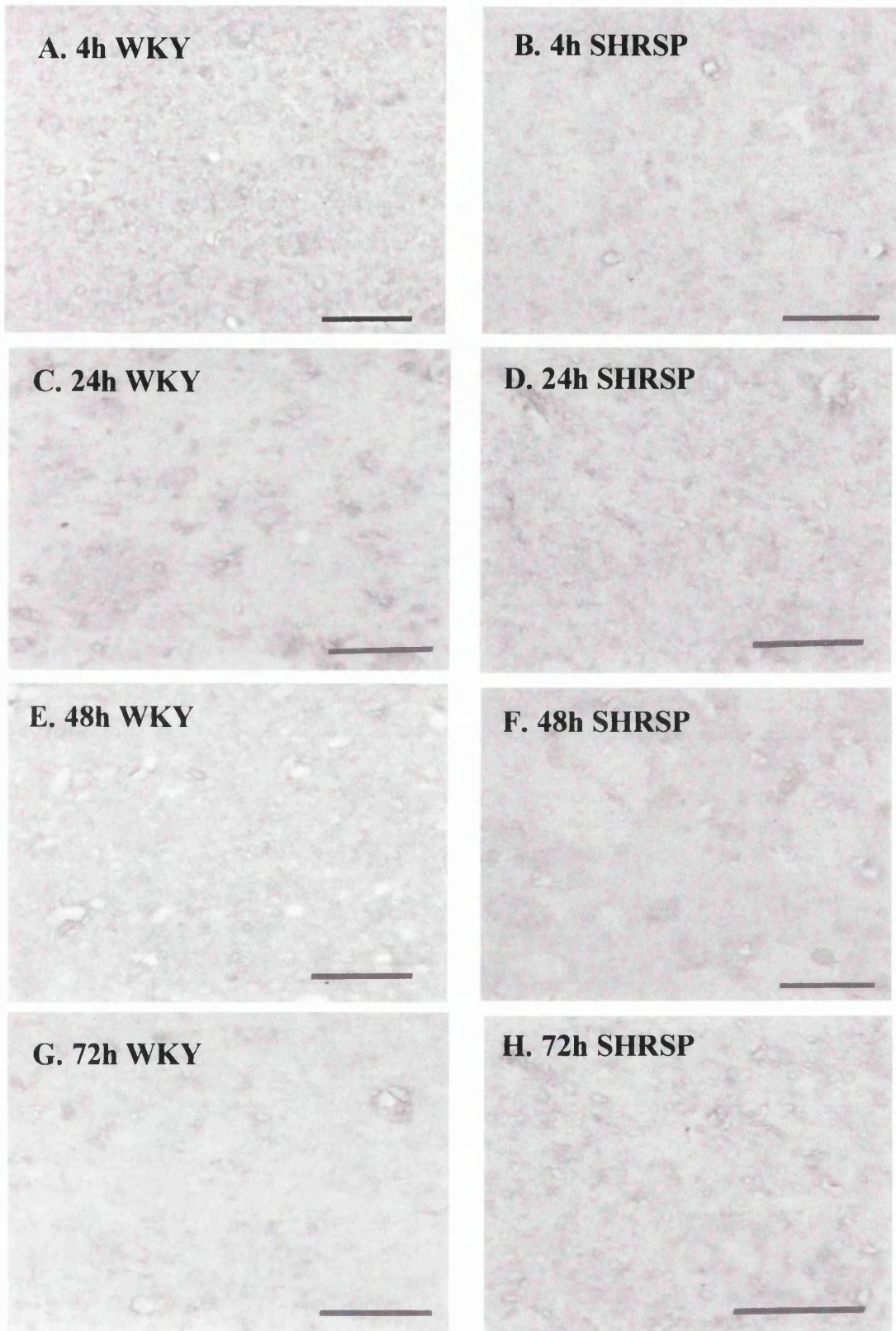


Figure 88. Lack of IL-1 $\beta$  staining in WKY and SHRSP following permanent distal MCAO over 72 hours (A-H). Photographs taken in the caudate region. Magnification = X40. Scale bar represents 50 $\mu$ m.

## 6.4 Discussion

### Evolution of the infarct

This is the first study to investigate changes in the size of the infarct over time in SHRSP and WKY rats.

SHRSPs exhibited a greater degree of ischaemic damage compared to the normotensive WKY over the 4 time points studied ( $p < 0.001$ ), the infarct reaching its maximal size at 48 hours in each strain. The pattern of the evolution (enlargement) of the infarct was very similar in both strains. The greater degree of ischaemic damage in SHRSPs is a finding which is consistent with previous studies which have shown that SHRSP have an increased sensitivity to stroke.

In both SHRSP and WKY, the infarct increased over the first 48 hours in both strains. This is in contrast to previous studies involving **proximal** occlusion of the MCA in Sprague Dawley rats where the infarct attains its maximal size around 4 hours and does not increase in size significantly over the following 68 hours (Dawson, 1993, thesis; Gill, 1992, thesis). The difference in models is the length and position of the MCAO occlusion. In this study only a small segment of the MCA is electrocoagulated (2mm) at a point **distal** to the inferior cerebral vein whilst in models of **proximal** MCA, a much greater extent of the MCA is coagulated (from the lenticulostriate branches to the inferior cerebral vein). One possible explanation for the difference in the time course of damage in the two models is that in occluding only a small portion of the MCA, there is a greater likelihood that collateral blood vessels will still be able to supply the MCA territory giving rise to a certain level of

potential reperfusion injury in turn leading to an increased chance of further damage and possible variation in ischaemic damage with time.

### **Increased microglial activation in SHRSP**

In the time course study, SHRSPs displayed a greater number of activated microglia in all 5 regions examined when compared to WKY. It is not currently clear whether the presence of increased numbers of activated microglia following permanent MCAO is detrimental or beneficial. Microglia are capable of direct tissue damage via synaptic stripping and neurophagia (Nakajima and Kohsaka, 1993) and of indirect damage via the release of cytotoxins such as IL-1 $\beta$  and TNF- $\alpha$ . On the other hand however, microglia may have a beneficial role following ischaemia which may involve participating in neuronal regeneration by performing phagocytosis of debris which then allows neuronal regrowth (Zeev-Brann *et al.*, 1998; Lazarov-Speigler *et al.*, 1998). In the CNS, microglia have been described as the major mononuclear phagocytic participants at the site of injury (Stoll *et al.*, 1989). In a study by Zeev-Brann and co-workers (1998) the phagocytic nature of microglia was investigated *in vitro*. CNS resident microglia isolated from newborn rats were isolated and incubated overnight with either sciatic or optic nerve segments and fluorescent beads. The uptake of fluorescent beads was taken as a measure of the microglial cells phagocytic activity. The microglia were found to possess phagocytic activity in the presence of both types of nerve. However, the phagocytic activity was higher in the presence of the sciatic nerve segments suggesting that phagocytic activity although present in the CNS is being limited by some form of CNS inhibitor substance. Certainly, other

studies have also demonstrated that microglial and macrophage infiltration and accumulation appears to be delayed and restricted when compared to similar responses in the periphery (George & Griffin, 1994; Perry *et al.*, 1987).

In an important recent study, Imai and co-workers (2000, abstract) investigated whether migrating microglia were likely to be contributing to damage by systemically injecting microglia into an ischaemic animal. Although the peripherally injected microglia did migrate into the ischaemic brain, histological analysis and TUNEL staining failed to provide any evidence that these microglia exacerbated ischaemic damage. This study would therefore seem to provide more evidence for a beneficial rather than a detrimental role of microglial in ischaemia.

### **Microglia and progression of the infarct**

If microglia were contributing to the expansion of the infarct, one would expect to see increased microglial activation preceding further development of the infarct.

Although there appears to be a significantly greater degree of ischaemic damage at 4 hours in SHRSP when compared to WKY ( $p < 0.001$ ), there appears to be no significant difference in activated microglial number between the two strains at the 4 hour time point in any of the brain regions studied. This would seem to suggest that certainly at the 4-hour time point, there is little evidence to support a role for activated microglia in increased stroke sensitivity in the SHRSP.

However, the greatest increase in activated microglia between strains, was seen in the peri-infarct region. The presence of activated microglia in the peri-infarct region

of the ipsilateral hemisphere in SHRSP, at a time when the infarct is still evolving (infarct significantly different between 24 and 48 hours in SHRSP,  $p < 0.001$ ) in this model would seem to suggest that activated microglia may be contributing to later increases in ischaemic damage. Indeed activated microglia have been previously associated with increased ischaemic damage (Gehrman *et al.*, 1996; Kato *et al.*, 1992) so it would seem feasible that the microglia may be contributing to neuronal death in the peri-infarct region, (a region containing salvageable neurons capable of either succumbing to ischaemic damage or recovery to normal neuronal function) therefore leading to an expansion of the area of damage.

However, the results of this study could equally support a beneficial role for microglia in ischaemia. The fact that a significant increase in activated microglia in the peri-infarct region also occurs between 48 and 72 hours in SHRSP ( $p < 0.005$ ), and to a lesser extent in the WKY, when there is no accompanying increase in infarct size would seem to suggest the opposite, that an increase in activated microglia may in fact be a protective mechanism occurring in response to damage occurring in the first 48 hours, in an attempt to remove debris and promote re-growth and neuronal regeneration. Microglia are known for their phagocytic properties and their role in neuronal re-growth and regeneration in different forms of injury (Schwartz *et al.*, 1998). Indeed at 72 hours most of the microglia appear phagocytic in appearance. These phagocytic microglia could be seen to be associated with neurons in the peri-infarct and core regions. The microglia appeared to be engulfing neurons or were found adjacent to neurons. This would seem to provide evidence to support the idea that phagocytic microglia may be involved in the removal of dead or irreversibly damaged neurons in the peri-infarct zone allowing subsequent regeneration.

In SHRSP and WKY, a significant increase in the number of activated microglia occurs in the core of the lesion between 48 and 72 hours (SHRSP:  $p < 0.005$ , WKY  $p < 0.05$ ). This would seem to suggest once again that activated microglia present within the core are there not to cause damage but rather to limit and prevent any further damage. Furthermore, there appears to be no significant increase in the number of activated microglia in the core between 24 and 48 hours, suggesting once again that activated microglia may not be contributing to ischaemic damage. However, an increase in activated microglial number in the core of the lesion does occur between 4 and 24 hours ( $p < 0.05$ ) in SHRSP suggesting that they may have a role to play in acute ischaemic damage in this strain. However the fact that there is no significant accompanying increase in ischaemic damage between 4 and 24 hours in either strain may suggest that their activation is stimulated by early ischaemic events in an attempt to prevent further damage.

In addition to an increase in activated microglial numbers in the peri-infarct and the core regions between 48 and 72 hours in the ipsilateral hemisphere in SHRSP, there was also an increase in the number of activated microglia in ipsilateral and contralateral white matter regions: external capsule (ipsi-  $p < 0.05$ ; contra  $p < 0.01$ ) and genu of corpus callosum (ipsi-  $p < 0.05$ ; contra  $p < 0.005$ ) between 48 and 72 hours and also between 24 and 48 hours in the genu of corpus callosum (ipsi-  $p < 0.01$ ). Again this increase would seem to be more likely to be associated with protective rather than detrimental mechanisms as there would appear to be no significant accompanying increase in infarct volume between 48 and 72 hours. It has been suggested that microglia may use the white matter tracts to migrate from distant sites to the region of damage and this would seem to provide a feasible explanation for the

increased numbers of microglia in the white matter tracts. They may be migrating to the lesion site in an attempt to promote regeneration and remove dead or irreversibly damaged neurons.

An additional piece of evidence for a beneficial role for microglia following ischaemia, comes from the lack of IL-1 $\beta$  staining in the microglia. IL-1 $\beta$  is considered to be associated with injury and is often found to be expressed by glia in pathological conditions (Pearson *et al.*, 1999; Loddick *et al.*, 1998). However, lack of IL-1 $\beta$  expression by activated microglia following permanent MCAO would seem to suggest that their presence is not purely detrimental.

### **Pattern of microglial distribution**

The pattern of microglial distribution (Figure 64) indicates that the activated microglia accumulate around the border of ischaemic damage and would seem to migrate towards the infarct over the 72 hour period resulting in a high density of activated and phagocytic microglia in and around the infarct at 72 hours.

In addition to increases in the number of activated microglia in the ipsilateral hemisphere, accompanying increases in microglial number occurred in the contralateral hemisphere would seem to be more pronounced in SHRSP than WKY for all regions suggesting a greater degree of contralateral stimulation possibly by diaschisis (Seitz *et al.*, 1999) or spreading depression (Kato and Waltz, 2000) .

The pattern of microglial distribution within the white matter tracts over the 72 hours suggests that the microglia may be using the white matter tract to migrate towards

the ipsilateral hemisphere as large numbers of activated microglia can be seen to accumulate in the genu of the corpus callosum in the contralateral hemisphere extending into the white matter tracts of the ipsilateral hemisphere. This finding is in accordance with other studies from this laboratory which found similar white matter tract expression of microglia following ischaemia (Zhang *et al.*, 1997; Peters, 1999, thesis). The contralateral activation of microglia would seem to suggest that some form of signalling is being activated across the hemispheres in response to ischaemic damage. Previous studies have shown evidence for spreading depression activating microglia distant from the site of damage (Kato and Waltz, 2000) and the activation of activation of contralateral microglia would seem to support this idea. Alternatively, diaschisis may be another possible activator of contralateral microglia and it has been reported to cause contralateral stimulation in conditions of damage (Seitz, 1999).

### **Microglia and MMP expression**

If indeed the activated microglia are migrating from the contralateral hemisphere to the site of damage in the ipsilateral hemisphere, one would expect to see expression of some of the compounds known to mediate microglial migration. One family of inflammatory mediators known to facilitate the migration of inflammatory cells such as neutrophils and T-cells in CNS injury are the matrix metalloproteinases. Matrix metalloproteinases have been shown to facilitate the migration of neutrophils to the site of damage in lung disease (Gibbs *et al.*, 1999) and to play an important role in metastasis due to their ability to degrade components of the ECM allowing cells to move with ease through tissue (Tomita *et al.*, 1996; Kurschat and Mauch, 2000). If

MMPs were contributing to the migration of the activated microglia one might expect to see MMP expression mirroring the expression of activated microglia. This study found very little or no expression of MMP-8 (neutrophil collagenase) or MMP-9 (gelatinase B) at the 4 hour time point in either SHRSP or WKY. However at the later time points of 24, 48 and 72 hours, MMP-8 and MMP-9 expression mirrored the increase in number of activated microglia and the migration of the microglia towards the lesion site. This suggests that MMPs may play a role in the migration and the effects of microglia on surrounding cells and that expression of MMPs is up regulated with microglial activation. Double labelling using DAB (brown) and SG (grey) confirmed that activated microglia were indeed expressing both MMP-8 and MMP-9 in their cell bodies (Figure 77-81). This included both activated and phagocytic phenotypes.

In addition to the possibility that MMPs are induced to facilitate migration, they may be secreted by microglia contributing to their proposed cytotoxicity and leading to further ischaemic damage. MMPs are known to increase BBB permeability, cause oedema and associated tissue damage and increase the expression of inflammatory mediators such as TNF-alpha. It is therefore feasible that activated microglia may secrete MMP-8 and MMP-9 at some stage during activation providing an explanation for the presence of the two MMPs in the microglial cell body. If on activation, microglia were secreting cytotoxic substances (including MMPs) that were contributing to ischaemic damage, one might expect to see evidence of interleukin production. An increase in IL-1 $\beta$  immunoreactivity has commonly been linked to increased damage following MCAO and one of the

principal cells identified as expressing IL-1 $\beta$  is the microglial cell (Pearson *et al.*, 1999).

No IL-1 $\beta$  positive cells were seen in either SHRSP or WKY at any of the time points over 72 hours. Although many studies have associated an increase in microglial activation with an increase in IL-1 $\beta$  leading to an increase in ischaemic damage (Pearson *et al.*, 1999; Rothwell *et al.*, 1997), it is accepted that activation of microglia does not automatically result in IL-1 $\beta$  expression (Perry, personal communication). Various different stimulants are required for IL-1 $\beta$  expression and it may well be that this model of MCAO does not produce the necessary changes in the micro-environment for stimulation of IL-1 $\beta$  to occur.

### **MMP staining**

In addition to MMP positive microglia, MMP-8 and MMP-9 immunostaining could be seen in ischaemic neurons within the lesion, in neurons with a more normal morphology in the peri-infarct region and in injured (Tau +ve) oligodendrocytes within white matter tracts. The presence of MMP-8 and MMP-9 in the core of the lesion suggests a possible role for the MMPs in ischaemic damage and potentially in the phagocytic process for removal of dead cells. MMP-8 and MMP-9 staining was seen from 24 to 72 hours post- ischaemia but little or no MMP staining was apparent at 4 hours in either SHRSP or WKY. These findings are in accordance with the findings of other (non-quantitative or descriptive) studies reporting MMP-9 expression at 6 hours, peaking at 24 hours following permanent MCAO (Romanic *et al.*, 1998; Rosenberg *et al.*, 1996). The intensity of the MMP staining did not appear

to increase over the 72 hours but the number of immunopositive cells did increase—the majority of them being activated microglia.

The MMP staining of ischaemic neurons was questioned due to the reported stickiness of ischaemic neurons which can lead to non-specific immunostaining (Polack and Van Noorden, 1997). A blocking peptide was used to investigate the likelihood of non-specific neuronal staining within the core of the infarct. Blocking peptide studies showed that staining of ischaemic neurons was still present after the addition of the blocking peptide which would suggest that this staining is likely to be non-specific. However as no blocking peptide was available for the Chemicon MMP-9 antibody used in this study and the results are based on the Santa Cruz MMP-9 antibody, one cannot completely rule out the possibility that the MMP staining of ischaemic neurons is specific (discussed in Chapter 4).

The presence of MMP-8 and MMP-9 in neurons with a more normal morphology in the peri-infarct region at 24 hours and 48 hours, in both strains, may suggest that the neuronal staining (at least in these cells) may be specific. The staining in the peri-infarct region appeared strongest for MMP-8. The presence of MMP positive neurons in the salvageable area of the lesion may suggest that MMPs may be contributing to the expansion of the lesion. Indeed MMP expression would appear to precede expansion of the infarct over the first 48 hours.

MMP-8 and MMP-9 positive oligodendrocytes were seen in the white matter tracts of both SHRSP and WKY. Oligodendrocyte MMP expression has previously been reported in the literature but was associated with process outgrowth and myelination by oligodendrocytes in culture (Luke *et al.*, 1999). This would seem to suggest that

MMP-9 expression associated with oligodendrocytes may not be pathological but may be associated with an attempt to repair damage and promote regeneration and remyelination in damaged ischaemic tissue.

Although astrocytes have been reported to express MMPs (including MMP-9) constitutively and in conditions of acute and chronic MS (Maeda *et al.*, 1996). However this study showed no evidence for MMP-8 or MMP-9 expression in astrocytes in any of the brain region studied. There appears to be variation in reported cellular location of MMPs in models of experimental ischaemia and other pathological conditions (e.g. MS, EAN). These differences in MMP positive cell types could be caused by different MMP antibodies detecting different cellular forms of MMP. The MMP-9 antibody used in this study may detect the microglial form of MMP-9 while other commercially available antibodies detect the astrocytic or neutrophilic form of the enzyme (discussed further in chapter 4). Due to the difference in antibody specificity, one cannot rule out the possibility that astrocytes may express MMP-8 and or MMP-9 in the permanent model of MCAO only that the Chemicon MMP-9 or Santa Cruz MMP-9 antibody did not detect any astrocytic expression of MMP-9.

## Chapter 7 General Discussion

### 7.1 Introduction

The search for a therapeutic agent with the ability to reduce the damage associated with clinical stroke is an extremely important area for scientific research as stroke is not only one of the biggest killers throughout the world but also one of the largest causes of disability and reduced quality of life (Bamford *et al.*, 1988; Forbes, 1993).

The factors contributing to stroke are numerous and no one factor can be said to be the sole cause of the damage. The downstream consequences of cerebral ischaemia include excitotoxicity, oxidative stress, changes in gene expression, waves of spreading depolarisation and inflammation ultimately leading to necrosis, programmed cell death and brain swelling. All of these components are being investigated in order to gain a better understanding of how we can reduce the severity of a clinical stroke.

Although a number of cells and substances have been implicated in inflammatory mediated ischaemic damage, it remains unclear in many cases, whether their presence is detrimental or beneficial to the brain's recovery.

In this thesis, different models of experimental stroke, different rodent strains (including stroke sensitive strains) and time course studies have been employed to increase our knowledge of inflammation and stroke.

## **7.2 The role of neutrophils and microvilli in ischaemic damage.**

### **Lack of evidence for a neutrophil involvement in acute ischaemic damage.**

No evidence was found for a significant neutrophil accumulation in either parenchyma or blood vessels at 4 hours or 24 hours after intraluminal thread induced ischaemia (2 hours occlusion + 2 hours or 22 hours reperfusion) in Sprague Dawley rats (chapters 3 and 4) or at 4-72 hours after diathermy induced MCA occlusion (chapters 5 and 6). This suggests that neutrophils may not be contributing to acute ischaemic damage and therefore anti-neutrophil therapy in the early stages of ischaemia may not significantly ameliorate ischaemic damage. At early time points, therapies should perhaps concentrate on other components of the inflammatory response.

As widely discussed (chapter 3), neutrophils are believed by many to have the ability to block cerebral blood vessels and obstruct blood flow during ischaemia. It has also been suggested that they may contribute to ischaemic damage indirectly via the secretion of cytotoxic substances such as cytokines (IL-1 $\beta$ , TNF- $\alpha$ ), proteases (MMP-2, MMP-9) and free radicals (superoxide anion, hydroxyl radical) (Del Zoppo *et al.*, 1991; Groggaard *et al.*, 1989; Hallenbeck *et al.*, 1988). In terms of the contribution of neutrophils to ischaemic damage, experimental studies have shown varied results. Some groups have found that inhibiting neutrophil accumulation with antibodies directed against adhesion molecules reduces infarct size (Chopp *et al.*, 1994; Zhang *et al.*, 1994; Clark *et al.*, 1991) while others have found no evidence for

significant neutrophil accumulation in models of experimental cerebral ischaemia (Hayward *et al.*, 1996; Peters *et al.*, 1998; Oruckaptan *et al.*, 2000).

In addition to studies in experimental animal models of ischaemia, neutrophil accumulation has been studied in conditions of clinical stroke, with Silvestrini and co-workers (1998) reporting significantly higher numbers of neutrophils in patients with severe stroke damage. However phase 3 clinical studies using inhibitors of neutrophil adhesion have reported no beneficial clinical outcome after administration (EAST trial of Enlimomab) (Sherman and Polmar, 1997). This would seem to suggest that neutrophils are not major contributors to inflammatory mediated ischaemic damage.

Although this study would seem to suggest that neutrophils do not play a major role in inflammatory mediated ischaemic damage, one cannot entirely rule out a neutrophil contribution to ischaemic damage. If the study had been extended to include later time points, one may have seen a greater degree of neutrophil accumulation. Certainly of those studies reporting significant neutrophil accumulation in experimental cerebral ischaemia, most used late time points- Matsuo and co-workers, 24 hours; Chen and co-workers, 48 hours and Zhang and co-workers, 1 week). In spite of these findings, in this thesis where ischaemic damage was investigated over time (Chapter 6) no significant neutrophil presence was evident prior to or including the time point where the infarct reached its maximal size. Previous studies from this laboratory and others have also reported no evidence of a neutrophil contribution to ischaemia as late as 72 hours post ischaemic damage (Peters *et al.*, 1998; Hayward *et al.*, 1996).

### **Lack of evidence for microvilli contribution in acute ischaemic damage.**

This thesis found no evidence to support a microvilli contribution to ischaemic damage. Rather, microvilli would appear to be useful markers of a general perturbation to the cerebrovasculature induced by the occluding device associated with intraluminal thread induced ischaemia (2 hours occlusion + 2 hours reperfusion) as both occluded and sham animals exhibited almost identical numbers of microvilli (chapter 3, section 3.3.4;  $21.61 \pm 0.89$  in occluded animals Vs  $21.45 \pm 1.86$  in sham animals). Also no correlation was found between number of microvilli and infarct size ( $r^2 = 0.137$ ).

Various studies have suggested that an increase in microvilli number may prove a useful marker of ischaemic damage (Dietrich *et al.*, 1984; Dietrich *et al.*, 1996; Okumara *et al.*, 1997, previously discussed in Chapter 3) with an increase in microvilli number accompanying astrocytic swelling and general vascular disruption in models of transient focal (Dietrich *et al.*, 1986; Okumura *et al.*, 1997) and global (Dietrich *et al.*, 1984) experimental ischaemia.

Although this study would seem to rule out a major role for microvilli in ischaemic damage, as with neutrophil accumulation, one cannot rule out entirely a role for microvilli based on the results of this thesis. If the study had been extended to later time points, a role for microvilli in ischaemic damage may have been observed as it has been postulated that microvilli may have the ability to express receptors for

adhesion molecules therefore allowing them to participate in the migration and accumulation of inflammatory cells such as neutrophils (Lossinsky *et al.*, 1995).

Once again it can be said that it appears unlikely that microvilli are contributing to acute ischaemic damage and that acute inflammatory mediated damage must be associated with another component or components of the inflammatory response to ischaemia.

### **7.3 The role of microglia in inflammatory mediated ischaemic damage.**

Microglia are known to become activated in conditions of experimental ischaemia with this activation occurring within minutes to hours of the ischaemic insult (Morioka *et al.*, 1991; Gehrmann, 1992; Kato *et al.*, 1994). Although activated microglial numbers increase following ischaemia it is not entirely clear whether this increase serves to protect the brain from further damage or contribute to ischaemic damage.

In this thesis (Chapters 5,6) numbers of activated microglia were found to be increased following diathermy MCAO in SHRSP and WKY rats (chapter 6, section 6.3.4). This increase was apparent from 4 hours to 48 hours in a time course study extending out to 72 hours. Numbers of activated microglia were significantly greater in the SHRSP, a strain known to exhibit an increased sensitivity to stroke, which may in part be due to an enhanced inflammatory response to ischaemia. The presence of significantly greater numbers of activated microglia in the SHRSP when compared to

the normotensive WKY would at first glance appear to suggest that the microglia may be contributing to the greater degree of ischaemic damage in the SHRSP over the 72 hour time course (chapter 6, section 6.3.2). Further evidence to support a role for activated microglia in ischaemic damage comes from the observation that the most significant increases in activated microglia occurred in the peri-infarct region—the region where the infarct can expand over time. It would seem feasible therefore that the presence of activated microglia in the peri-infarct region may suggest a role for these cells in the expansion of the infarct. However, when numbers of activated microglia were studied in relation to the development of the infarct, a significant increase in activated microglia (chapter 6, section 6.3.4,  $p < 0.005$ ) occurred at a time when there was no accompanying increase in infarct size (between 48 and 72 hours, chapter 6, section 6.3.2). In addition, there was no correlation between the number of activated microglia and infarct size at 24 hours in the SHRSP in the core ( $r^2 = 0.45$ ) or the peri-infarct region ( $r^2 = 0.025$ ) (chapter 5, section 5.3.8). An alternative hypothesis is that rather than contributing to ischaemic damage, the microglia may become activated in an attempt to prevent further damage and promote repair and neuronal regeneration, a role which macrophages appear to perform in the periphery (Chen et al., 1995; Faber –Elman et al., 1996; Zeev-Brann et al., 1998). Certainly at the later time points of 48 and 72 hours, microglia had a phagocytic phenotype both in the peri-infarct and in the core of the lesion (chapter 6, section 6.3.5) suggesting that they are present to remove cellular debris and encourage repair. In addition to this another piece of evidence to support a role for microglia in regeneration and repair may be the observation that phagocytic microglia appeared to be closely

associated with neurons in the peri-infarct region at later time points (chapter 6, section 6.3.7). At the 72 hour time point when there is a massive accumulation of microglia in the peri-infarct and core regions, there is no increase in infarct size compared to the 48 hour time point (chapter 6, section 6.3.4 + 6.3.2), suggesting that the microglia have halted the progression of damage.

Further evidence for a protective rather than destructive role for the microglia comes from the fact that the activated microglia do not appear to be secreting IL-1 $\beta$ , one of the main cytotoxic substances believed to be involved in indirect microglial mediated ischaemic damage (Rothwell *et al.*, 1997; Pearson *et al.*, 1999). Lack of IL-1 $\beta$  would seem to suggest that their role is not purely one of destruction (chapter 6, section 6.3.9).

Activated microglial cells were found to be expressing MMP-8 and MMP-9, two members of the matrix metalloproteinases family. Although MMPs are reported to contribute to ischaemic damage, their presence in microglial cells should not be associated purely with damage. MMPs have the ability to aid the migration of a number of cells including T-cells, neutrophils and cancer cells (Graesser *et al.*, 2000; Vos *et al.*, 2000; Auodjit *et al.*, 1998). Their presence in activated microglia could therefore be in a capacity to aid the migration of the microglia to the site of damage in order that they can then perform their phagocytic role.

#### **7.4 The role of MMP-8 and MMP-9 in inflammatory mediated ischaemic damage.**

In this study, elevated numbers of immunopositive cells for MMP-8 and MMP-9 were found following intraluminal thread induced ischaemia, (2 hours occlusion + 22 hours reperfusion ,Chapter 4) and following diathermy induced permanent mCA occlusion (Chapter 5, 6 ) which suggests an MMP involvement in inflammation associated with ischaemia. MMP-8 and MMP-9 immunopositive cells could clearly be seen in the peri-infarct region in addition to the core of the lesion (chapter 6, section 6.3.8-diathermy MCAO; chapter 4, section 4.3.4 + 4.3.5—ILT induced ischaemia) at a time when the infarct was still evolving in both models (24 hours) .

Double label immunohistochemistry with mrf-1 (microglial marker) and MMP-8 and MMP-9 antibodies confirmed that the majority of the MMP-8 and MMP-9 positive cells in the peri-infarct region were activated microglia.

Increased numbers of MMP-8 and MMP-9 positive activated microglia occurred at a time when there was no accompanying increase in infarct size (48-72 hours) (chapter 6, section 6.3.4) in the diathermy model of MCAO. If MMP-8 and MMP-9 were contributing significantly to ischaemic damage one would expect to see an increase in infarct size accompanying the increase in MMP-8 and MMP-9 expression. This would seem to suggest that the MMPs may not have a purely destructive role in ischaemia and that their presence in microglia, as previously discussed, may be for migration to the site of damage.

MMPs are believed to play a role in ischaemic damage due to their ability to degrade the brain matrix tissue leading to increased BBB permeability and the subsequent influx of inflammatory cells. Various studies have reported increases in the levels of MMPs, primarily MMP-2 and MMP-9 following experimental ischaemia (Rosenberg *et al.*, 1998; Romanic *et al.*, 1998; Gasche *et al.*, 1999) and some have shown that administration of an MMP inhibitor has the ability to reduce infarct size and oedema (Rosenberg *et al.*, 1998; Romanic *et al.*, 1998; Asahi *et al.*, 2000). This study did show MMP expression following experimental ischaemia but did not provide strong evidence for a pathologic role for MMPs in inflammatory mediated ischaemic damage

### **7.5 General conclusions.**

The studies undertaken in this thesis have shown the complicated nature of the inflammatory response to ischaemia. It is clear that in response to cerebral ischaemia, a complex inflammatory response is initiated. However, this study provides evidence that not all the components of this inflammatory response are necessarily detrimental to the brain with responses such as microglial activation possibly acting to prevent further damage. One must also consider the fact that the inflammatory response to ischaemia may differ significantly in different species and models of ischaemia. One must, therefore, consider this possibility when considering new therapies which block such components of the inflammatory

response and weigh up the risks of attenuating beneficial effects against the benefits of attenuating the destructive effects.





## References

Abe, K., Kogniek, K., Yamamota, H. (1987) Mechanism of arachidonic acid liberation during ischaemia in gerbil cortex. Journal of Neurochemistry, 44, 168-172.

Abraham, H. and Lazar, G. (2000) Early microglial reaction following mild forebrain ischaemia induced by common carotid artery occlusion in rats. Brain Research, 862, 63-73.

Ames, A., Wright, L.W., Kowade, M., Thurston, J.M, Majors, G. (1968) Cerebral Ischaemia: II. The no-reflow phenomenon. American Journal of Pathology, 52, 437-453.

Anthony, D.C., Ferguson, B., Matyak, M.K., Miller, K.M., Esiri, M.M. and Perry, V.H. (1997) Differential matrix metalloproteinase expression in cases of multiple sclerosis and stroke. Neuropathology and Applied Neurobiology, 23, 406-415.

Aoudjit, F., Potworowski, E.F., St Pierre, Y. (1998) Bi-directional Induction of Matrix Metalloproteinase-9 and Tissue Inhibitor of Matrix Metalloproteinase-1 During T Lymphoma/ endothelial Cell Contact: Implication of ICAM-1. The Journal of Immunology, 160,2967-2973.

Aronowski, J., Strong, R., Grotta, J.C. (1997) Reperfusion Injury: Demonstration of Brain Damage Produced by Reperfusion After Transient Focal Ischaemia in Rats. Journal of Cerebral Blood Flow and Metabolism, 17, 1048-1056.

Asahi, M., Asahi, K., Jung, J.C., Del Zoppo, G.J., Fini, M.E., Lo, E.H. (2000) Role for Matrix Metalloproteinase 9 After Focal Cerebral Ischemia: Effects of Gene Knockout and Enzyme Inhibition With BB-94. Journal of Cerebral Blood Flow and Metabolism, Vol.20, No.12, 1681-1690.

Babak, A. (1996) The role of inflammation and cytokines in brain injury. Neuroscience and Biobehavioural Reviews, Vol. 20, No.3, 445-452.

Backstrom, J.R. (1996) Matrix metalloproteinase-9 (MMP-9) is synthesised in neurons of the human hippocampus and is capable of degrading the amyloid-beta peptide (1-40). Journal of Neuroscience, 16(24),7910-7919.

Backstrom, J.R., Miller, C.A., Tokes, Z.A. (1992) Characteristics of neutral proteinases from Alzheimer affected and control brain specimens: identification of calcium dependent metalloproteinases from the hippocampus. Journal of Neurochemistry, 58(3), 983-992.

Baker, J.R. (1968) in Principles of Biological Microtechnique-A study of fixation and dyeing. Methuen & Co.

Bamford, J., Sandercock, P., Dennis, M., Warlaw, C., Jones, L., McPherson, K., Vessey, M., Fowler, G., Molyneux, A., Hughes, T., Burn, J., Wade, D. (1988) A prospective study of acute cerebrovascular disease in the community; the Oxfordshire Community Stroke Project 1981-1986. I. Methodology, demography and incident of cases of first ever stroke. Journal of Neurology, Neurosurgery and Psychiatry, 51, 1373-80.

Bamford, J., Sandercock, P., Jones, L., Warlow, C. (1987) The natural history of lacunar infarction: the Oxford 1987 Community Stroke Project. Stroke, 18, 545-51.

Banati, R.B., Gehrman, J., Schubert, P., Kreutzberg, G.W. (1993) Cytotoxicity of Microglia. Glia, 7, 111-118.

Banati, R.B., Gottmann, K., Kreutzberg, G.W., Kettenberg, H (1991) A subpopulation of bone marrow derived macrophages –like cells shares a unique ion channel pattern with microglia. Journal of Neuroscience Research, 30, 593-600.

Banyai, L., Tordai, H., Patthy, L. (1994) The gelatin- binding site of human 72 kDa type IV collagenase (gelatinase A). Biochemistry Journal, 1, 298(2), 403-7.

Barone, F.C., Price, W.J., White, R.F., Willette, R.N., Feuerstein, G.Z. (1992) Genetic Hypertension and Increased Susceptibility to Cerebral Ischemia. Neuroscience and Biobehavioural Reviews, Vol.16, 219-233.

Barone, F.C. and Feuerstein, G.Z. (1999) Inflammatory mediators and stroke: new opportunities for novel therapeutics. Journal of Cerebral Blood Flow and Metabolism, 19(8), 819-34.

Barron, K.D. (1995) The microglial cell. A historical review. Journal of the Neurological Sciences, 134, (suppl), 57-68.

Bauer, E.A., Stricklin, G.P., Jeffrey, J.J., Eisen, A.Z. (1975) Collagenase production by human skin fibroblasts. Biochemical and Biophysical Research Communications, 64, 232-240.

Beamer, N.B., Coull, B.M., Clark, W.M., Hazel, J.S., Silberger, J.R. (1995) Interleukin-6 and Interleukin-1 receptor antagonists in acute stroke. Annals of Neurology, 37, 800-804.

Beckett, R.P., Davidson, A.H., Drummond, A.H., Huxley, P., Whittaker, M. (1998) Recent advances in matrix metalloproteinase inhibitor research. Drug Discovery Today, Vol.1, No.1, 16-26.

Bederson, J.B., Pitts, L.H., Tsuji, M., Nishimura, M.C., Davis, R.L., Bartkowski, H. (1996) Rat Middle Cerebral Artery Occlusion: Evaluation of the Model and Development of a Neurologic Examination. Stroke, Vol 17, No.3, 472-476.

Beetsch, J.W., Park, T.S., Dugan, L.L., Shah, A.R., Gidday, J.M. (1998) Xanthine oxidase derived superoxide causes reoxygenation injury of ischaemic cerebral endothelial cells. Brain Research, 786(1-2) 89-95.

- Bi, Z., Barna, M., Komatsu, T., Reiss, C.S. (1995) Vesicular Stomatitis Virus Infection of the Central nervous System Activates both Innate and Acquired Immunity. Journal of Virology, 6466-6472.
- Boya, J., Carbonell, A.L., Calvo, J.L., Borraron, A. (1991) Microglial cells in the central nervous system of the rabbit and rat: cytochemical identification using two different lectins. Acta Anatomica, 140(3), 250-3.
- Bozzola, J.J. and Russell, L.D. (1992) in Electron Microscopy, Chapter 3 Specimen Preparation for Scanning Electron Microscopy, p43. Jones and Bartlett Publishers Inc.
- Bruehl, R.E., Springer, T.A., Bainton, D.F. (1996) Quantification of L-selectin distribution on human leukocyte microvilli by immunogold labelling and electron and microscopy. Journal of Histochemistry and Cytochemistry, 44(8), 835-44.
- Bruehl, R.E., Moore, K.L., Lorant, D.E., Borregaard, N., Zimmerman, G.A., McEver, R.P., Bainton, D.F. (1997) Leukocyte activation induces surface redistribution of P-selectin glycoprotein ligand-1. Journal of Leukocyte Biology, 61 (4), 489-99.
- Butterfield, J.D. and McGraw, C.P. (1978) Free Radical Pathology. Stroke, Vol 9, No 5, 443-444.
- Buttini, M., Sauter, A., Boddehe, H.W.G.M. (1994) Induction of interleukin-1beta mRNA after focal cerebral ischaemia in the rat. Molecular Brain Research, 23, 126-134.
- Carswell, H.V., Anderson, N.H., Morton, J.J., McCulloch, J., Dominiczak, A.F., Macrae, I.M. (2000) Investigation of estrogen status and increased stroke sensitivity on cerebral blood flow after focal ischaemic insult. Journal of Cerebral Blood flow and Metabolism, 20(6), 931-6.

Carrieri, P.B. (1994) The role of cytokines in the pathogenesis of multiple sclerosis. Int MSJ, 1, 53-59.

Carswell, H.V.O., Anderson, N.H., Clark, J.S., Graham, D., Jeffs, B., Dominiczak, A.F., Macrae, I.M. (1999) Genetic and Gender Influences on Sensitivity to Focal Cerebral Ischaemia in the Stroke-Prone Spontaneously Hypertensive Rat. Hypertension, 33, 681-685.

Chen, D.F., Jhaveri, S., Schneider, G.E. (1995) Intrinsic changes in developing retinal neurons result in regenerative failure of their axons. Proceedings of the National Academy of Science of the United States of America, Vol.92, 7287-7291.

Chen, H., Chopp, M., Zhang, R.L., Bodzin, G., Chen, Q., Rusche, J.R., Todd, R.F. (1994) Anti-CD11b monoclonal antibody reduces ischaemic damage after transient focal cerebral ischaemia in the rat. Annals of Neurology, 35, 458-463.

Chiang, J., Kowada, M., Ames, A., Wright, R.L., Majno, G. (1968) Cerebral Ischaemia. III. Vascular changes. American Journal of Pathology, 52, 455-76.

Chopp, M., Zhang, R.L., Chen, H., Li, Y., Jiang, N., Rusche, J.R. (1994) Postischaemic administration of an anti-MAC-1 antibody reduces ischaemic cell damage after transient middle cerebral artery occlusion in the rat. Stroke, 25, 869-876.

Clark, I.M. and Cawston, T.E. (1989) Fragments of human fibroblast collagenase. Purification and characterisation. Biochemistry Journal, 263, 201-206.

Clark, W.M., Madden, K.P., Rothelin, R., Zivin, J.A. (1991) Reduction of central nervous system ischaemic injury by monoclonal antibody to intercellular adhesion molecule. Journal of Neurosurgery, 75, 623-627.

Corbett, D. and Thornhill, J. (2000) Temperature modulation (hypothermic and hyperthermic conditions) and its influence on histological and behavioural outcomes following cerebral ischemia. Brain Pathology, 10(1), 145-52.

Coyle, P. and Heistad, D.D. (1991) Development of collaterals in the cerebral circulation. Blood Vessels, 28, 183-189.

Coyle, P. and Jokelainen, P.T. (1993) Differential outcome to middle cerebral artery occlusion in spontaneously hypertensive stroke-prone rats (SHRSP) and Wistar-Kyoto (WKY) rats. Stroke, 14, 605-611.

Crabbe, T., Ioannou, C., Docherty, A.J.P. (1993) Human progelatinase A can be activated by autolysis at a rate that is concentration dependent and enhanced by heparin bound to the C-terminal domain. European Journal of Biochemistry, 218, 431-438.

Cross, J. and Lapiere, C.M. (1962) Collagenolytic activity in amphibian tissue: a tissue culture assay. Proceedings of the National Academy of Science of the United States of America, 48, 1014-1022.

Damoiseaux, J.G.M.C., Dopp, E.A., Calame, W., Chao, D., MacPherson, G.G., Dijkstra, C.D. (1994) Rat macrophage lysosomal membrane antigen recognised by monoclonal antibody ED1. Immunology, 83, 140-147.

Davidson, A.O., Schork, N., Jaques, B.C., Kelman, A.W., Sutcliffe, R.G., Reid, J.L., Dominiczak, A.F. (1995) Blood pressures in genetically hypertensive rats: influence of the Y chromosome. Hypertension, 26, 452-459.

Davies, C.A., Loddick, S.A., Toulmond, S., Stroemer, R.P., Hunt, J., Rothwell, N.J. (1999) The progression and topographic distribution of interleukin-1 beta expression following permanent middle cerebral artery occlusion in the rat. Experimental Neurology, 154 (1), 199-212.

Davis, E.J., Foster, T.D., Thomas, W.E. (1994) Cellular Forms and Functions of Brain Microglia. Brain Research Bulletin, Vol. 34, No.1, 73-78.

Dawson, D.A. (1993) An investigation into the pathophysiology of a new model of transient focal cerebral ischaemia in the rat. PhD thesis, University of Glasgow.

Dawson, T.M., Dawson, V.L., Snyder, S.H. (1992) A novel neuronal messenger molecule in the brain: the free radical, nitric oxide. Annals of Neurology, 32, 297-311.

Del Zoppo, G.J., Schmid-Schonbein, G.W., Mori, E., Copeland, B.R., Chang, C-M. (1991) Polymorphonuclear leukocytes occlude capillaries following middle cerebral artery occlusion and reperfusion in baboons. Stroke, 22,1276-1283.

Derouesne, C., Cambon, H., Yelnik, A., Duydaerts, C., Hauw, J.J. (1993) Infarcts in the middle cerebral artery territory. Acta Neurologica Scandinavica, 87, 361-6.

Dickson, D.W., Mattiace, L.A., Kure, K., Hutchins, K., Lyman, W.D., Brosnan, C.F. (1991) Biology of Disease. Microglia in human disease, with an emphasis on acquired immune deficiency syndrome. Laboratory Investigation, 64, 135-155.

Dickson, D.W., Lee, S.S., Mattiace, L.A., Yen, S.C., Brosnan, C. (1993) Microglia and cytokines in Neurological disease, with special references to AIDS and Alzheimer's disease. Glia, 7, 75-83.

Dietrich, W.D., Busto, R., Ginsberg, M.D. (1984) Cerebral Endothelial Microvilli: Formation Following Global Forebrain Ischemia. Journal of Neurophology and Experimental Neurology, Vol.43, No.1, 72-83.

Dietrich, W.D., Busto, R., Yoshida, S., Ginsberg, M.D. (1987) Histopathological and hemodynamic consequences of complete versus incomplete ischemia in the rat. Journal of Cerebral Blood Flow and Metabolism, 7, 3,300-8.

Dietrich, W.D., Nakayam, H., Watson, B.D., Karemistu, H. (1989) Morphological consequences of early reperfusion following thrombotic or mechanical occlusion of the rat MCA. Acta Neuropathologica, 78, 605-14.

Dirnagl, U., Niwa, K., Villringer, A. (1994) Cortical hypoperfusion after global forebrain ischemia in rats is not caused by microvascular leukocyte plugging. Stroke, 25,5,1028-38.

Duverger, D. and MacKenzie, E. (1988) The quantification of Cerebral Infarction Following Focal Ischaemia in the Rat: Influence of Strain, Arterial Pressure, Blood Glucose Concentration, and Age. Journal of cerebral blood Flow and Metabolism, Vol.8, No.4, 449-461.

Elkabes, S., DiCicco-Bloom, E.M., Black, I.B. (1996) Brain microglia/macrophages express neutrophins that selectively regulate microglial proliferation and function. Journal of Neuroscience, 16, 2508-2521.

Elkof, B. and Siesjo, B. (1972) The effect of bilateral carotid ligation upon the blood flow and energy state of the rat brain. Acta Physiologica Scandinavica, 86, 155-165.

Esiri, M.M and McGee, J.O. (1986) Monoclonal antibody to macrophages (EMB/11) labels macrophages and microglial cells in human brain. Journal of Clinical Pathology, 39(6), 615-621.

Faber-Elman, A., Solomon, A., Abraham, J.A., Marikovsky, M., Schwartz, M. (1996) Involvement of Wound-associated Factors in Rat brain Astrocyte Migratory Response to Axonal Injury: In Vitro Simulation. Journal of Clinical Investigation, 97,162-171.

Fabian, R.H. and Kent, T.A. (1999). Superoxide anion production during reperfusion is reduced by an antineutrophil antibody after prolonged cerebral ischaemia. Free Radical, Biology and Medicine, 26(3-4), 355-61.

Fischer, E.G., Ames, A., Hedley-Whyte, E.T., O’Gorman, S. (1977) Reassessment of cerebral capillary changes in acute global ischaemia and their relationship to the “no-re-flow phenomenon”. Stroke, 8, 36-9.

Forbes, J.F. (1993) Cost of Stroke. Scottish Medical Journal ,38, S4-5.

Frackowiak, J., Wisniewski, H.M., Weigiel, J., Merz, G.S., Iqbal, K., Wang, K.C. (1992) Ultrastructure of the microglia that phagocytose amyloid and the microglia that produce  $\beta$ -amyloid fibrils. Acta Neuropathologica, 84:225-235.

Fredricksson, K., Auer, R.N., Kalimo, C., Norborg, C., Johansson B.B. (1985) Cerebrovascular Lesions in Stroke-prone Spontaneously Hypertensive Rats. Acta Neuropathologica (Berl), 68, 284-294.

Fujimoto, S., Yamamoto, K., Takeshige, Y. (1975) Electron Microscopy of Endothelial Microvilli of Large Arteries. Anatomical Record, 183, 259-266.

Garcia, J.H. and Kamijyo, Y. (1974) Cerebral infarction: Evolution of histopathological changes after occlusion of a middle cerebral artery in primates. Journal of Neuropathology and Experimental Neurology, 33,408-421.

Gartshore, G. (1996) The consequences of reperfusion on cerebral ischaemic damage. PhD thesis, University of Glasgow.

Gasche, Y., Fujimura, M., Morita-Fujimura, Y., Copin, J-C., Kawase, M., Massengale, J., Chan, P.H (1999) Early Appearance of Activated Matrix Metalloproteinase-9 After Focal Cerebral Ischemia in mice: A Possible Role in Blood –Brain Barrier Dysfunction. Journal of Cerebral Blood Flow and Metabolism, 19, 1020-1028.

Gearing, A.J., Beckett, P., Christodoulou, M., Churchill, M., Clements, J., Davidson, A.H., Drummond, A.H., Galloway, W.A., Gilbert R. (1994) Processing of tumour necrosis factor-alpha precursor by metalloproteinases.

Nature, 18, 370(6490), 555-7.

Gebicke-Haerter, P.J., Calkner, D.V., Norenberg, W., Illes, P. (1996) Molecular mechanisms of microglial activation. A. Implications for regeneration and neurodegenerative diseases. Neurochemistry International, Vol.29, No.1, 1-12.

Gehrmann, J. (1992) Immunocytochemical study of an early microglial activation in ischaemia. Journal of Cerebral Blood Flow and Metabolism, 12, 1257-1269.

Gehrmann, J. (1996). Microglia : a sensor to threats in the nervous system. Research in Virology, 147, 79-88.

Gehrmann, J., Yamashita, K., Back, T., Kreutzberg, G.W., Wiessner, C. (1995) The microglial reaction in focal ischaemia: An early and generalised response not attenuated by post-ischaemic pharmacological intervention. Journal of Cerebral Blood Flow and Metabolism, 15, S5353.

Gemba, Y., Matsunga, K., Ueda, M. (1992) Changes in extracellular concentration of amino acids in the hippocampus during cerebral ischaemia in stroke-prone SHR, stroke resistant SHR and normotensive rats. Neuroscience Letters, 135, 184-188.

Gibbs, D.F., Shanley, T.P., Warner, R.L., Murphy, H.S., Varani, J., Johnson, K.J. (1999) Role of Metalloproteinases in Models of Macrophage – Dependent Acute Lung injury. American Journal of Respiratory and Cellular Molecular Biology, 20, 1145-1154.

Gill, R. (1992) The pharmacology of excitatory amino acid antagonists in focal cerebral ischaemia in the rat. PhD thesis, University of London.

- Giulian, D. and Lachman, L.B. (1985) Interleukin-1 stimulation of astroglial proliferation after brain injury. *Science*, 228 (4698), 497-9.
- Giulian, D. (1987) Ameboid microglia as effectors of inflammation in the central nervous system. *Journal of Neuroscience Research*, 18:155-171.
- Giulian, D. (1990) Microglia, Cytokines, and Cytotoxins: Modulators of Cellular Responses after Injury to the Central Nervous System. *Journal of Immunology and Immunopharmacology*, Vol.10, No.1, 15-20.
- Giulian, D., Li, J., Bartel, S., Broker, J., Li, X., Kirkpatrick, J.B. (1995) Cell Surface Morphology Identifies Microglia as a Distinct Class of Mononuclear Phagocyte. *The Journal of Neuroscience*, 15(11), 7712-7726.
- Golub, L.M., Lee, H.M., Lehrer, G., Nemiroff, A., McNamara, T.F., Kaplan, R., Ramamurthy, N.S. (1983) Minocycline reduces gingival collagenolytic activity during diabetes. Preliminary observations and a proposed new mechanism of action. *Journal of Periodental Research*, 18, 516-526.
- Gomez, D.E., Alonso, D.F., Hitoshi, Y., Thorgeirsson, U.P. (1997) Tissue inhibitors of metalloproteinases: structure, regulation and biological functions. *European Journal of Cell Biology*, 74, 111-122.
- Gong Chao, C., Qin, Z., Betz, A.L., Liu, X.H., Yang, G.Y. (1998) Cellular Localisation of tumor necrosis factor alpha following focal cerebral ischaemia in mice. *Brain Research*, 801,1-8.
- Graeber, M.B., Streit, W.J., Kreutzberg, G.W. (1998) Axotomy of the rat facial nerve leads to increased CR3 complement receptor expression by activated microglial cells. *Journal of Neuroscience Research*. 21:18-24.

- Greene, J., Wang, M., Liu, Y.E., Raymond, L.A., Rosen, C., Shi, Y.E. (1996) Molecular cloning and characterisation of human tissue inhibitor of metalloproteinases 4. Journal of Biological Chemistry, 271, 30375-30380.
- Greenfield, J.G. (1992) in Greenfield's Neuropathology (5<sup>th</sup> Edition), Hume-Adams, J. editor. Edward Arnold, London.
- Grogaard, B., Schurer, L., Gerdin, B., Arfors, K.E. (1989) Delayed hypoperfusion after incomplete forebrain ischaemia in the rat: The role of polymorphonuclear leukocytes. Journal of Cerebral Blood Flow and Metabolism, 9, 500-505.
- Grotta, J.C., Pettigrew, L.C., Rosenbaum, D., Reid, C., Rhoades, H., McCandless, D. (1988) Efficacy of action of a calcium channel blocker after global cerebral ischaemia in rats. Stroke, 19, 447-454.
- Hallenbeck, J.M., Dutka, A.J., Tanishima, T., Kochanek, P.M., Kumaroo, K.K., Thompson, C.B., Obrenovitch, T.P., Contreras, T.J. (1986) Polymorphonuclear leukocyte accumulation in brain regions with low blood flow during the early postischaemic period. Stroke, 17, 246-253.
- Hallenbeck, J.M., Dutka, A.J., Kochanek, P.M., Siren, A., Pezeshkpour, G.H., Feuerstein G. (1988) Stroke risk Factors Prepare Rat Brainstem tissues for Modified Local Schwarzman Reaction. Stroke, 19, 863-869.
- Hallenbeck, J.M. and Dutka, A.J. (1990) Background Review and Current Concepts of Reperfusion Injury. Archives of Neurology, Vol. 47, 1245-1254.
- Hallenbeck, J.M., Dutka, A.J., Vogel, S.N., Heldman, E., Doron, D.A., Feuerstein, G. (1991) Lipopolysaccharide- induced production of tumor necrosis factor activity in rats with and without risk factors for stroke. Brain Research, 541, 115-120.
- Halliwell, B. and Grutteridge, J.M.C. (1985) Oxygen Radicals and the Nervous System. Trends in Neuroscience, 8, 22-26.

Hamann, G.F., Okada, Y., Del Zoppo, G.J. (1996) Hemorrhagic transformation and microvascular integrity during focal cerebral ischemia/reperfusion.

Journal of Cerebral Blood Flow and Metabolism, 16(6),1373-8.

Hayward, N.J., Elliott, P.J., Sawyer, S.D., Bronson, R.T., Bartus, R.T. (1996) Lack of Evidence for Neutrophil Participation during Infarct Formation Following Focal Cerebral Ischaemia in the Rat. Experimental Neurology, 139, 188-202.

He, B.P., Tay, S.S., Leong, S.K. (1997) Do microglial cells have a neuroprotective function? Journal Hirnforsch, 38, 309-315.

Helps, S.C. & Gorman, D.F. (1991) Air embolism of the brain in rabbits pre-treated with mechloroethamine. Stroke, 22, 351-354.

Heo, J.H., Lucero, J., Abumiya, T., Koziol, J.A., Copeland, B.R., Del Zoppo, G.J. (1999) Matrix Metalloproteinases Increase Very Early During Experimental Focal Cerebral Ischemia. Journal of Cerebral Blood Flow and Metabolism, 19, 624-633.

Hirschberg, D.L. and Schwartz, M. (1995) Macrophage recruitment to acutely injured central nervous system is inhibited by a resident factor: A basis for an immune-barrier. Journal of Neuroimmunology, 61, 89-96.

Htain, W.W., Leong, S.K., Ling, E.A. (1994) A comparative Mac-1 immunocytochemical and lectin histochemical study of microglial cells in the normal and athymic mice. Glia, 12 (1), 44-51.

Hunter, A.J., McKay, K.B., Rogers, D.C. (1998) To what extent have functional studies of ischaemia in animals been useful in the assessment of potential neuroprotective agents? Trends in Pharmacological Sciences, Vol 19, 59-65.

Jeffs, B., Clark, J.S., Anderson, N.H., Gratton, J., Brosnan, M.J., Gaugier, D., Reid, J. L., Macrae, I.M., Dominiczak, A.F. (1997) Sensitivity to cerebral ischaemic insult in a rat model of stroke is determined by a single genetic locus: possible analogy to human ischaemic stroke. Nature Genetics, 16, 364-367.

- Kato, H. and Waltz, W. (2000) The Initiation of the Microglial Response. Brain Pathology, 10, 137-1443.
- Kato, H., Kogure, K., Araki, T., Itoyama, Y. (1994) Astroglial and microglial reactions in gerbil hippocampus with induced ischaemic tolerance. Brain Research, 664, 69-76.
- Kato, H., Kogure, K., Araki, T., Itoyama, Y. (1995) Graded expression of immunomolecules on activated microglia in the hippocampus following ischaemia in a rat model of ischaemic tolerance. Brain Research, 694, 85-93.
- Kato, H., Kogure, K., Liu, X.H., Araki, T., Itoyama, Y. (1996) Progressive expression of immunomolecules on activated microglia and invading leukocytes following focal cerebral ischaemia in the rat. Brain Research, 734(1-2), 203-212.
- Keane, R.W. and Hickey, W.F. (Editors). (1997) Immunology of the Nervous System. Chapters 5,7,11, Oxford University Press.
- Kinouchi, H., Epstein, C.J., Mizui, T., Carlson, E.J., Chen, S.F., Chan, T. (1991) Attenuation of focal cerebral ischaemia injury in transgenic mice overexpressing CuZn superoxide dismutase. Proceedings of the National Academy of Science of the United States of America, 88,11158-11162.
- Kinuta, Y., Kimura, M., Yoshinori, I., Mastsune, J., Kituchi, H. (1989) Changes in xanthine oxidase in ischaemic rat brain. Journal of Neurosurgery, 71,417-420.
- Koizumi, J., Yoshida, Y., Nakazawa, T., Oonedda, G. (1986) Experimental studies of ischaemic brain edema: 1. A new experimental model of cerebral embolism in which recirculation can be introduced in the ischaemic area. Japanese Journal of Stroke, 8, 1-8.
- Konstantopoulos, A. (1996) Microvascular responses to an ischaemic insult. SHHD Summer student report, University of Glasgow.

Koroshetz, W.J. and Moskowitz, M.A. (1996) Emerging treatments for stroke in humans. Trends in Pharmacological Sciences, Vol. 17, 227-233.

Korthuis, R.J., Granger, D.N., Townsely, M.I., Taylor, A.E. (1985) The role of oxygen derived free radicals in ischaemia induced increases in canine skeletal muscle. Circulation Research, 57,599-629.

Kumar, K., White, B., Krause, G., Garritano, A.M., Koestner, A. (1987) Cerebral endothelial microvilli following global brain ischemia in dogs. Brain Research, 421, 309-314.

Kuroiwa, T., Ting, P., Martinez, H., Klatzo, I. (1985) The Biphasic Opening of the Blood Brain Barrier to Proteins Following Temporary Middle Cerebral Artery Occlusion. Acta Neuropathologica, 68, 122-129.

Kurschat, P. and Mauch, C. (2000) Mechanisms of metastasis. Clinical and Experimental Dermatology, 25, 482-489.

LASA report 1999.

Lauffenburger, D.A. and Horwitz, A.F. (1996) Cell Migration: A Physically Integrated Molecular Process. Cell, Vol. 84, 359-369.

Lazarov-Spiegler, O., Rapalino, O., Agranov, G., Schwartz, M. (1998) Restricted inflammatory reaction in the CNS: a key impediment to axonal regeneration. Molecular Medicine Today, 4, 337-342.

Lazarov-Spiegler, O., Solomon, A., Zeev-Brann, A.B., Hirschberg, D.L., Lavie, V., Schwartz, M. (1996) Transplantation of activated macrophages overcomes central nervous system regrowth failure. FASEB Journal, 10, 1296-1302.

Lee, J-M., Zipfel, G.J., Choi, D.W. (1999) The changing landscape of ischaemic brain injury mechanisms. Nature, Vol. 399, supp, A7-A13.

- Lee, R.M.K.W. (1995) Morphology of Cerebral Arteries. Pharmacology and Therapeutics, Vol. 66, 149-173.
- Leuschen, M.P. and Nelson, R.M. (1987) Effects of asphyxia on telencephalic microvessels of premature beagle pups. Journal of Perinatology, 7,2, 93-9.
- Levine, S. and Marvine, K. (1960) Ischaemic infarction and swelling in the rat brain. Archives of Pathology, 69, 76-85.
- Linas, S.L., Whittenburg, D., Repine, J.E. (1990) Role of xanthine oxidase in ischaemia/ reperfusion injury. American Journal of Physiology, 258(3 Pt 2), F711-F716.
- Linn, G.P., Russell, M.J., Cullen, M.J., Tokes, Z.A. (1997) MMPs in dogs brains exhibiting Alzheimer-like characteristics. Journal of Neurochemistry, 68(4),1606-1611.
- Liotta, L.A., Tryggvasan, K., Garbisa, S., Hart, I., Foltz, C.M., Shtie, S. (1980) Metastatic potential correlates with enzymatic degradation of basement membrane collagen. Nature, 284 (5791), 67-8.
- Liu, T., McDonnell, P.C., Young, P.R., White, R.F., Siren, A.L., Hallenbeck, J.M., Feuerstein, G.Z. (1993) Interleukin-1 beta mRNA expression in the ischaemic rat cortex. Stroke, 24,1746-1751.
- Loddick, S. A. and Rothwell, N.J. (1996) Neuroprotective effects of human recombinant interleukin-1 receptor antagonist in focal cerebral ischaemia in the rat. Journal of Cerebral Blood Flow and Metabolism, 16(5), 932-40.
- Longa, E.Z., Weinstein, P.R., Carlson, B.S., Cummins, R. (1989) Reversible Middle Cerebral Artery Occlusion Without Craniectomy in Rats. Stroke, 20, 84-91.

Lossinsky, A.S., Mossakowski, M.J., Pluta, R., Wisniewski, H.M. (1995) Intercellular Adhesion Molecule-1 (ICAM-1) Upregulation in Human Brain Tumors as an Expression of Increased Blood Brain Barrier Permeability. Brain Pathology, 5, 339-344.

Lossinsky, A.S., Song, M.J., Wisniewski, H.M. (1989) High voltage electron microscopic studies of endothelial cell tubular structures in the mouse blood-brain barrier following brain trauma. Acta Neuropathologica, 77, 480-488.

Lovejoy, B., Cleasby, A., Hassell, A.M., Longley, K., Luther, M.A., Weigl, D., McGeehan, G., McElroy, A.B., Drewry, D., Lambert, M.H. (1994) Structure of the catalytic domain of fibroblast collagenase complexed with an inhibitor. Science, 263, 403-407.

Lowry, O.H., Rosenborough, N.J., Farr, A.L., Randall, R.J. (1951) Protein measurement with the folin phenol reagent. Journal of Biological Chemistry, 193, 265-275.

Luke, Y.S., Larsen, P.H., Krekoski, C.A., Edwards, D.R., Donovan, F., Werb, Z., Yong, V.W. (1999) Matrix Metalloproteinase-9/ Gelatinase B Is Required for Process Outgrowth by Oligodendrocytes. The Journal of Neuroscience, 19(19), 8464-8475.

Mabuchi, T., Kitagawa, K., Ohtsuki, T., Kuwabara, K., Yagita, Y., Yanagihara, T., Hori, M., Matsumoto, M. (2000) Contribution of Microglia/Macrophages to Expansion of Infarction and Response of Oligodendrocytes After Focal Cerebral Ischemia in Rats. Stroke, 31, 1735.

Macrae, I.M., Robinson, M.J., Graham, D.I., Reid, J.L., McCulloch, J. (1993) Endothelin-1 induced reductions in cerebral blood flow: dose dependency, time

course, and neuropathological consequences. Journal of Cerebral Blood Flow and Metabolism, 13, 276-84.

Maeda, A. and Soebel, R.A. (1996) Matrix Metalloproteinases in Normal Human Nervous System, Microglial Nodules, and Multiple Sclerosis Lesions. Journal of Neuropathology and Experimental Neurology, Vol. 55, No.3, 300-309.

Male, D., Cooke, A., Owen, M., Trowsdale, J., champion, B. (1996) in Advanced Immunology, Chapter 1: The immune system. Mosby.

Massova, I. (1998) Matrix metalloproteinases: structures, evolution and diversification. FASEB Journal, 12,1075-1095.

Matsuo, Y., Kihara, T., Ikeda, M., Ninomiya, M., Onodera, H., Kogure, K. (1995) Role of neutrophils in radical production during ischaemia and reperfusion of the rat brain: effect of neutrophil depletion on extracellular ascorbyl radical formation . Journal of Cerebral Blood Flow and Metabolism, 15, 941-947.

Mattiace, L.A., Davies, P., Yen, S.H., Dickson, D.W. (1990) Microglia in cerebellar plaques in Alzheimer's disease brains. Acta Neuropathologica, 80, 493-498.

Maxwell, W., Irvine, A., Adams, J.H., Graham, D.I., Gennarelli, T.A. (1988) Response of Cerebral Microvasculature to Brain Injury. Journal of Pathology, 155, 327-335.

McAuley, M.A. (1995) Rodent Models of Focal Ischaemia. Cerebrovascular and Brain Metabolism Reviews,7,153-180.

McDonald, J.W., Althomsons, S.P., Hyrc, K.L., Choi, D.W., Goldberg, M.P. (1998) Oligodendrocytes from forebrain are highly vulnerable to AMPA/kainite receptor mediated excitotoxicity. Nature Medicine, 4, 291-297.

- McGee, J.O.D., Isaacson, P.G., Wright, N.A. (1992) in Oxford Textbook of Pathology, Vol 1, Principles of Pathology, p524. Oxford University Press.
- McGeer, P.L., Itagaki, S., Boyes, E., McGeer, E.G. (1988) Reactive microglia are positive for HLA-DR in the substantia nigra of Parkinson's and Alzheimer's disease brains. Neurology, 38:1285-1291.
- McGeehan, G.M., Becherer, J.D., Bast, R.C., Boyer, C.M., Champion, B., Connolly, K.M., Karp, S., Kidaos, S. (1994) Regulation of tumour necrosis factor-alpha processing by a metalloproteinase inhibitor. Nature, 370 (6490), 558-61.
- Meyer, J.S., Obara, K., Muramastu, K. (1993) Diaschisis. Neurol Res, 15, 362-266.
- Moore, S. and Thanos, S. (1996) The concept of microglia in relation to central nervous system disease and regeneration. Progress in Neurobiology, Vol.48, 441-460.
- Mori, T., Asaro, T., Matsui, T., Muramatsu, H., Ueda, M., Kamiya, T., Karayama, Y., Abe, T. (1999) Intraluminal increase of superoxide anion following transient focal cerebral ischaemia in rats. Brain Research, 816 (2), 350-7.
- Morioka, T., Baba, T., Black, K.L., Streit, W.J. (1992) Immunophenotypic analysis of infiltrating leukocytes and microglia in an experimental rat glioma. Acta Neuropathol, 83,590-597.
- Mun-Bryce, S. and Rosenberg, G.A. (1998) Gelatinase B modulates selective opening of the blood brain barrier during inflammation. American Journal of Physiology, 274, R1203-R1211.
- Mun-Bryce, S. and Rosenberg, G.A. (1998) Matrix metalloproteinases in cerebrovascular disease. Journal of Cerebral Blood Flow and Metabolism, 18 (11), 1163-72.

Muzylak, M. and Maslinska, D. (1995) Ultrastructure of Brain Vessel in Vincristine Treated Rabbits. Folia Neuropathology, 33, 261-264.

Naganuma, Y. (1990) Changes of the cerebral microvascular structure and endothelium during the course of permanent ischemia. Kero Journal of Medicine, 39(1), 26-31.

Nakajima, K. and Kohsaka, S. (1998) Functional Roles of Microglia in the Central Nervous System. Human cell, 11(3), Vol.11, No.3, 141-155.

Nakashima, M., Niwa, M., Iwai, T., Vematsu, T. (1999) Involvement of free radicals in cerebral vascular reperfusion injury evaluated in a transient focal cerebral ischaemia model of rat. Free Radical Biology and Medicine, 26 (5-6), 722-9.

Nakayami, H., Ginsberg, M.D., Dietrich, W.D. (1988) (S-emopamil), a novel calcium channel blocker and serotonin S2 antagonist, markedly reduces infarct size following middle cerebral artery occlusion in the rat. Neurology, 38, 1667-1673.

National Stroke Association, NSA homepage ‘ [www.stroke.org](http://www.stroke.org) ‘

Nikawa, S., Li, Y., Huang, T.T., Carlson, E., Chen, S., Kondo, S., Murakami, K., Epstein, C.J., Chan, P.H. (1995) Cerebral infarction is exacerbated in mitochondrial manganese dismutase (SOD) knockout mutant mice after focal cerebral ischaemia & reperfusion. Society of Neuroscience Abstract, 21,1268.

Nishino, T. (1994) The conversion of xanthine dehydrogenase to xanthine oxidase and the role of the enzyme in reperfusion injury. Journal of Biochemistry, 116(1),1-6.

Okada, Y., Copeland, B.R., Mori, E., Tung, M-M., Thomas, W.s., Del Zoppo, G.J. (1994) P-Selectin and Intercellular Adhesion Molecule-1 Expression After Focal Brain Ischemia and Reperfusion. Stroke, 25,202-211.

Okamoto, K., Yamori, Y., Nagaoka, A. (1974) Establishment of the SHRSPs (SHR). Circulation Research, 34, (suppl I), I-1-153.

Okumura, K., Sakaki, T., Hiramatsu, K., Tominaga, M., Yabuno, T. (1997) Microvascular Changes Associated with Postischaemic Hypoperfusion in Rats. Acta Neurochir (Wein), 139, 670-677.

Oruckaptan, H.H., Caner, H.H., Kilnic, K., Ozgen, T. (2000) No apparent role for neutrophils and neutrophil-derived myeloperoxidase in experimental subarachnoid haemorrhage and vasospasm: a preliminary study. Acta Neurochir (Wien), 142 (1), 83-90.

Osborne, K.A., Shigeno, T., Balarsky, A.M., Ford, I., McCulloch, J., Teasdale, G.M., Graham, D.I. (1987) Quantitative assessment of early brain damage in a rat model of focal cerebral ischaemia. Journal of Neurology, Neurosurgery and Psychiatry, 50: 402-410.

Pantani, L., Sarti, C., Inzitari, D. (1998) Cytokines and cell adhesion molecules in cerebral ischaemia: experimental bases and therapeutic perspectives. Arteriosclerosis, Thrombosis and Vascular Biology, 18,(4),503-13.

Patt, A., Harkes, A.H., Burton, L.K., Rodell, T.C., Piermattei, D., Schorr, W.J., Parker, N.B., Berger, E.M., Horsch, J.R., Terada, L.S. *et al.*, (1988) Xanthine oxidase derived hydrogen peroxide contributes to ischaemia reperfusion induced oedema in gerbil brains. Journal of Clinical Investigation, Vol, 81, 1556-1562.

Paxinos, G.(editor) (1995) in The Rat Nervous System (2<sup>nd</sup> Edition ) Chapter 1- Cerebral Vascular System.p3-35. Academic Press.

Pearson, V.L., Rothwell., N.J., Toulmond., S. (1999) Excitotoxic Brain Damage in the Rat Induces Interleukin-1 $\beta$  Protein in Microglia and astrocytes: Correlation With the Progression of Cell Death. Glia, 25, 311-323.

Penar, P.L. A model of embolic cerebral ischaemia in the rat. (1987) Experimental Neurology, 96, 393-405.

Perry, V.H., Hume, D.A., Gordon, S. (1985) Immunohistochemical localisation of macrophages and microglia in the adult and developing mouse brain. Neuroscience, 15, 313-326.

Peters, E.E., Gartshore, G., Maxwell, W.L., Macrae, I.M. (1998) Lack of evidence for early leukocyte adhesion in a model of transient focal cerebral ischaemia. Neuropathology and Applied Neurobiology, 24, 154.

Peters, E.E., Marks, L., Gartshore, G., Maxwell, W.L., Graham, D.I., Macrae, I.M. (1999) No evidence for significant leukocyte involvement in transient focal ischaemia. Journal of Cerebral Blood Flow and Metabolism, 19, S574.

Peters, E.E. (1999) Inflammatory Responses and Cerebral Ischaemia. PhD thesis, University of Glasgow.

Peterson, J.N. and Evans, J.P (1937) The anatomical end results of cerebral artery occlusion. Trans Am Neurol Assoc, 67, 394-398.

Phillis, J.W., Estevez, A.Y., O'Regan, M.H. (1998) Protective effects of the free radical scavengers dimethyl sulfoxide and ethanol, in cerebral ischaemia in gerbils. Neuroscience Letters, 244(2), 109-111.

Pluta, R., Lossinsky, A.S., Mossakowski, M.J., Faso, L., Wisniewski, H.M. (1991) Reassessment of a new model of complete cerebral ischemia in rats. Acta Neuropathologica, 83, 1-11.

Polack, J.M. and Van Noorden, S. (1997) In Introduction to Immunocytochemistry (2<sup>nd</sup> Edition), Chapter 3. Bios Scientific Publishers.

Pozzilli, C., Lenzi, G.L., Argentino, C., Carolei, A., Rasula, M., Signore, A., Bozzao, L. & Pozzilli, P. (1985) Imaging of leukocytic infiltration in human cerebral infarcts. Stroke, 16,251-255.

Prestigiacomo, C.J., Kim, S.C., Connolly, E.S., Liao, H., Yan, S., Pinsky, D.J. (1999) CD18-Mediated Neutrophil Recruitment Contributes to the Pathogenesis of Reperused but not Nonreperused Stroke. Stroke, 30,1110-1117.

Pugin, J., Widner, M.C., Kossodo S., Liang, C.M., Preas, H.L., Suffredini, A.F. (1999) Human neutrophils secrete gelatinase B in vitro and in vivo in response to endotoxin and proinflammatory mediators. American Journal of Respiratory and Cellular Molecular Biology, 20(3), 458-64.

Pulsinelli, W.A. and Brierly J.B. (1979) A new model of bilateral hemispheric ischaemia in the unanaesthetised rat. Stroke 10, 267-272.

Rang, H.P., Dale, M.M., Ritter, J.M. (1995) in Pharmacology (3<sup>rd</sup> Edition). Churchill Livingstone.

Rauvich, G., Bluethmann, H., Kreutzberg, G.W. (1996) Signalling Molecules and Neurological Activation in the Injured Central Nervous System. Keio J Med, 43(3), 239-247.

Raynes, J.G., Clarke, F.A., Anderson, J.C., Fitzpatrick, R.J., Dobson, H. (1988) Collagenase inhibitor concentration in cultured cervical tissue of sheep is increased in late pregnancy. Journal of Reproduction and Fertility, 83, 893-900.

Repine, J.E. (1990) Role of Xanthine oxidase in ischaemia/reperfusion injury. American Journal of Physiology, 258(3 pt 2), F711-F716.

Rieske, E., Graeber, M.B., Tetzlaff, W., Czlonkowska, A., Streit, W., Kreutzberg, G.W. (1989) Microglia and microglia-derived brain macrophages in culture: Generation from axotomized rat facial nuclei, identification and characterisation in vitro. Brain Research, 492:1-14.

Rio-Hortega, P. (1932) Microglia. In Cytology and cellular pathology of the nervous system, Penfield, W., editor, 481-584, New York: Hoeber.

Robinson, A.P., White, T.M., Mason, D.W. (1986) Macrophage heterogeneity in the rat as delineated by two monoclonal antibodies MRC OX-41 and MRC OX-42, the latter recognizing complement receptor type 3. Immunology, 57, 239-247.

Robinson, R.G. and McCulloch, J. (1990) Contractile responses to endothelin in feline cortical vessels in situ. Journal of Cerebral Blood Flow and Metabolism, 10, 285-9.

Robinson, R.G., Shoemaker, W.J., Schlumpf, M., Valk, T., Bloom, F.E. Effect of experimental cerebral infarction in rat brain on catecholamines and behaviour. Nature, 225, 332-4.

Romanic, A.H., Raymond, F., White, B.S., Arleth, A.J., Ohlstein, E.H. and Barone, F.C. (1998) Matrix metalloproteinase expression increases after cerebral focal ischaemia in rats. Stroke 29, 1020-1030.

Romanic, A.M. and Madri, J.A. (1994) The induction of 72kDa Gelatinase in T-cells upon Adhesion to Endothelial Cells is VCAM-1 Dependent. The Journal of Cell Biology, Vol. 25, 1165-1178.

Rosenberg, G.A. (1994) Injury induced 92kDa gelatinase and urokinase expression in the rat brain. Lab Invest. 71, 417-422.

Rosenberg, G.A., Dencoff, J.E., McGuire, P.G., Liotta, L.A., Stetler-Stevenson, W.G. (1994) Injury-induced 92 kDa gelatinase and urokinase expression in the rat brain. Laboratory Investigation, 71, 417-422.

Rosenberg, G.A., Navratil, M., Barone, F.C., Feuerstein, G. (1996) Proteolytic Cascade Enzymes Increase in Focal Cerebral Ischaemia in the Rat. Journal of Cerebral Blood Flow and Metabolism, 16, 360-366.

Rosenblum, W.I. (1986) Biology of Disease- Aspects of Endothelial Malfunction and Function in Cerebral Microvessels. Laboratory Investigation, Vol.55, No.3, 252-267.

Ross, B., Dawson, D., Dewar, D., Macrae, M., McCulloch, J. (1993) Effects of post-mortem delay on high affinity forskolin binding sites and adenylate cyclase activity in rat and human striatum and cerebral cortex. Brain Research, 629(2), 225-30.

Rothlin, R. (1997) Overview of leukocyte adhesion. Neurology, 49, (suppl 4), S3-S4.

Rothwell, N.J., Allan, S., Toulmond, S. (1997) The role of interleukin-1 $\beta$  in acute neurodegeneration and stroke: pathophysiological and therapeutic implications. Journal of Clinical Investigation, 100, 2648-2651.

Rutka, J.T., Apodaca, G., Stern R. and Rosenblum, M. (1988) The Extracellular Matrix of the Central and Peripheral Nervous Systems: Structure and Function. Journal of Neurosurgery, 69,155-170.

Sasaki, K., Okouchi, Y., Rothkoter, H.J., Pabst, R. (1998) Three dimensional distribution of intercellular adhesion molecule-1 on lymphocytes in the high endothelial venule analysed by backscatter electron imaging. Acta Anatomica, 162 (1), 33-9.

Sauter, A. and Rudin, M. (1995) Strain dependent drug effects in rat middle cerebral artery occlusion model of stroke. Journal of Pharmacology and Experimental Therapeutics, 274, 1008-1013.

Schmid -Elsaesser, R., Hungerhuber, E., Zausinger, S., Baethmann, A., Reulen, H.J. (1999) Neuroprotective efficacy of combination therapy in two different anti-oxidants in rats subjected to transient focal ischaemia. Brain Research, 816(2), 471-9.

Schmid- Schonbein , G.W., Seiffge, D., DeLano, F.A., Shen, K., Zweifach, B.W. (1991) Leukocyte Counts and Activation in Spontaneously Hypertensive and Normotensive Rats. Hypertension, 17, 323-330.

Schroeter, M., Jander, S., Witte, O.W., Stoll, G. (1999) Heterogeneity of the microglial response in photochemically induced focal ischaemia of the rat cerebral cortex. Neuroscience, Vol. 89, No.4, 1367-1377.

Schwartz, M., Cohen, I., Lazarov-Spiegler, O., Moalem, G., Yoles, E. (1999) The remedy may lie in ourselves: prospects for immune cell therapy in central nervous system protection and repair. Journal of Molecular Medicine, 77, 713-717.

Siegel, G.J., George, J.A., Wayne, R.W.R. (1976) Editors, Basic Neurochemistry (2<sup>nd</sup> Edition), Mass, Little & Brown, Boston.

Seitz, R.J., Azari, N.P., Knorr, U., Binkofski, F., Herzog, H., Freund, H-J. (1999) The Role of Diaschisis in Stroke Recovery. Stroke, 30, 1844-1850.

Sharkey, J., Ritchie, I.M., Kelly, P.A.T. (1993) Perivascular application of endothelin-1: a new model of focal cerebral ischaemia in the rat. Journal of Cerebral Blood Flow and Metabolism, 13, 865-71.

Sharkey, J., Kelly, J.S. and Butcher, S.P. (1996) Inflammatory Responses to Cerebral Ischaemia; Implications for Stroke Treatment in Clinical Pharmacology of Cerebral Ischaemia, Horst, G.J. and Korf, J. (editors), Humana Press.

Sheng, H., Bart, R.D., Oury, T.D., Pearlstein, R.D., Crapo, J.D., Warne, D.S. (1999) Mice overexpressing extracellular superoxide dismutase have increased resistance to focal cerebral ischaemia. Neuroscience, 88(1), 185-91.

Sherman, D. and Polmar, S. (1997) The Enlimomab Acute Stroke Trial: Final results. Neurology, 48 (suppl), A270.

Shigeno, T., Teasdale, G.M., McCulloch, J., Graham, D.I. (1985) Recirculation model following MCA occlusion in rats. Journal of Neurosurgery, 63, 272-277.

Shubayev, V.I. and Myers, R.R. (2000) Upregulation and interaction of TNF $\alpha$  and gelatinases A and B in painful peripheral nerve injury. Brain Research, 7,855(1), 83-9.

Siddiqi, F.A., Darakchiev, B.J., Cohen, S.M., Hariri, R.J., Fantini, G.A. (1996) Free radicals, anti-oxidants and reperfusion injury in the CNS. Ballieres Clinical Anaesthesiology, Vol 10, No 3, 497-509.

Silvestrini, M., Pietroiusti, A., Troisi, E., Franceschelli, L., Piccolo, P., Magrini, A., Bernardi, G., Galante, A. (1998). Leukocyte count and aggregation during the evolution of cerebral ischemic injury. Cerebrovascular Disease, 8(6), 305-9.

Simon, R.P., Swan, J.H., Griffiths, T., Meldrum, B.S. (1984) Blockade of N-methyl D-aspartate receptors may protect against ischaemic damage in the brain. Science, 226, 850-852.

Siren, A.L., Heldman, E., Doron, D., Lysko, P.G., Yue, T-L., Liu, Y., Feuerstein, G., Hallenbeck, J.M. (1992) Release of Proinflammatory and Prothrombotic Mediators in the Brain and Peripheral Circulation in Spontaneously Hypertensive and Normotensive Wistar- Kyoto Rats. Stroke, 23, 1643-1651.

Slavomir, M., Wojtowicz-Praga, Dickson, R.B., Hawkins, M.J. (1997) Matrix Metalloproteinase Inhibitors. Investigational New Drugs, 15, 61-75.

Soagabe, K., Roeser, N.F., Davis, J.A., Nurko, S., Venkatachalam, M.A., Weinberg J.M. (1996) Calcium dependence of integrity of the actin cytoskeleton of proximal tubule cell microvilli. American Journal of Physiology, 271(2 Pt 2), F292-303.

Soriano, S.G., Lipton, S.A., Wang, Y.F., Xiao, M., Springer, T.A., Gutierrez-Ramos, J-C., Hickey, P.R. (1996) Intercellular Adhesion Molecule-1-deficient Mice are Less Susceptible to cerebral Ischemia-Reperfusion Injury. Annals of Neurology, 39, 618-624.

Sornas, R., Ostlund, H., Muller, R. (1972) Cerebrospinal fluid cytology after stroke. Archives of Neurology, 26, 489-501.

Springman, E.B., Angleton, E.L., Birkdale- Hanson, H., Van-Wart. (1990) Multiple models of activation of latent human fibroblast collagenase: evidence for the role of a Cys active site zinc complex in latency and a 'cysteine switch' mechanism for activation. Proceedings of the National Academy of Sciences of the United States of America, 87, 364-368.

STAIR report 1999.

Stoll, G., Jander, S., Schroeter, M. (1998) Inflammation and Glial Responses in Ischemic Brain Lesions. Progress in Neurobiology, Vol.56, 149-171.

Tagami, M., Kubota, A., Sunaga, T., Maezawa, H., Kihara, M., Nara, Y., Yamori, Y. (1983) Increased transendothelial channel transport of cerebral capillary endothelium in stroke-prone SHR. Stroke, 14, 591-596.

Takamatsu, H., Kondo, K., Ikeda, Y., Umemura, K. (1998) Hydroxyl radical generation after the third hour following ischaemia contributes to brain damage. European Journal of Pharmacology, 352(2-3), 165-9.

Takasago, T., Peters, E.E., Graham, D.I., Masayatsu, H., Macrae, I.M. (1997) Neuroprotective efficacy of ebselen, an anti-oxidant with anti-inflammatory actions, in a rodent model of permanent middle cerebral artery occlusion. British Journal of Pharmacology, 122 (6), 1251-6.

Tamura, A., Graham, D.I., McCulloch, J., Teasdale, G.M. (1981) Focal Cerebral Ischaemia in the Rat: 1. Description of Technique and Early Neuropathological

Consequences Following Middle Cerebral Artery Occlusion. Journal of Cerebral Blood Flow and Metabolism, Vol.1, No.1, 53-60.

Tanaka, S., Suzuki, K., Watanabe, M., Matsuda, A., Tone, S., Koike, T. (1998) Upregulation of a new microglial gene, mrf-1, in response to programmed cell death and degeneration. Journal of Neuroscience, 18, 6358-6369.

Tarkowski, E., Rosengreen, L., Blomstrand, C., Wikketso, C., Jensen, C., Ekholm, S., Tarkowski, A. (1995) Early intrathecal production of IL-6 predicts the size of brain lesions in stroke. Stroke, 26, 1393-1398.

Tarlton, J.F., Vickey, C.J., Leaper, D.J., Bailey, A.J. (1997) Postsurgical wound progression monitored by temporal changes in the expression of matrix metalloproteinase-9. British Journal of Dermatology, 137(4), 506-16.

Tomita, T. and Iwata, K. (1996) Matrix Metalloproteases and Tissue Inhibitors of Metalloproteinases in Colonic Adenomas- Adenocarcinomas. Dis Colon Rectum, 39: 1255-1264.

Touzani, O., Boutin, H., Chuquet, J., Rothwell, N.J. (1999) Potential mechanisms of interleukin-1 involvement in cerebral ischaemia. Journal of Neuroimmunology, 100, 203-215.

Traystman, R.J., Kirsch, J.R., Koehler, R.C. (1991) Oxygen radical mechanisms of brain injury following ischaemia and reperfusion. Journal of Applied Physiology, 71, 1185-1195.

Trengove, N.J., Stacey, M.C., MacAuley, S., Bennett, N., Murphy, G., Schultz, G. (1999) Analysis of the acute and chronic wound environments: the role of proteases and their inhibitors. Wound Repair and Regeneration, 7(6), 442-52.

Ulvestad, E., Williams, K., Mork, S., Antel, J., Nyland, H. (1994) Phenotypic Differences between Human Monocytes/Macrophages and Microglial Cells Studied *In Situ* and *In Vitro*. Journal of Neurophthology and Experimental Neurology, Vol. 53, 492-501.

Van-Wart, H.E. and Birkdale- Hansen, H. (1992) The cysteine switch: a principle of regulation of metalloproteinase activity with potential applicability to the entire matrix metalloproteinase gene family. The Proceedings of the National Academy of Science of the United States of America, 87(14), 5578-82.

Vos, C.M., Gartner, S., Ransohoff, R.M., McArthur, J.C., Wahl, L., Sjulson, L., Conant, K. (2000) Matrix metalloproteinases-9 release from monocytes increases as a function of differentiation: implications for neuroinflammation and neurodegeneration. Journal of Neuroimmunology, 109(2), 221-7.

Vuorte, J., Lindsberg, P.J., Kaste, M., Meri, S., Jansson, S.E., Rothlein, R., Repo, H. (1999) Anti-ICAM-1 monoclonal antibody R6.5 (Enlimomab) promotes activation of neutrophils in whole blood. Journal of Immunology, 15,162(4),2353-7.

Watson, B.D., Dietrich, W.D., Prado, R, *et al.*, (1987) Argon laser-induced arterial photothrombosis. Journal of Neurosurgery, 66, 748-54.

Wee Yong, V., Kretoski, C.A., Forsyth, P.A., Bell, R. and Edwards, D.R. (1998) Matrix Metalloproteinases and Diseases of the CNS. Trends in Neurological Sciences, 21,75-80.

Wieloch, T. (1985) Hypoglycemia-induced neuronal damage prevented by an N-methyl D-aspartate antagonist. Science, 230, 681-683.

Wisniewski, H.M., Pluta, R., Lossinsky, A.S., Mossakowski, M.J. (1995) Ultrastructural studies of cerebral vascular spasm after cardiac arrest-related global cerebral ischemia in rats. Acta Neuropathologica, 90, 432-440.

Woessner, J.F and Nagase, H. (2000) in Matrix Metalloproteases and TIMPs, Oxford University Press.

Wysocki, A.B., Kusakabe, A.O., Chang, S., Tuant, L. (1999) Temporal expression of urokinase plasminogen activator, plasminogen activator inhibitor and gelatinase-B in chronic wound fluid switches from a chronic to acute wound profile with progression to healing. Wound Repair and Regeneration, 7(3), 154-165.

Yang, G-Y. and Betz, L. (1994) Reperfusion- Induced Injury to the Blood Brain Barrier After Middle Cerebral Artery Occlusion in Rats. Stroke, 25, 1658-1665.

Yamori, Y. and Horie, R. (1977) Developmental course of hypertension and regional cerebral blood flow in stroke-prone spontaneously hypertensive rats. Stroke, 8(4), 456-61.

Yamori, Y. (1982) Physiopathology of the various strains of spontaneously hypertensive rats. In Hypertension, Genest, J., Kurchel, O., Hamet, P., Cantin, M (editors), McGraw Hill, New York, 556-581.

Yashuda, H., Kishiro, K., Izumi, N. (1985) Biphasic liberation of arachidonic acid and stearic acids during cerebral ischaemia. Journal of Neurochemistry, 45, 168-172.

Yasui, M and Kawasaki, K. (1994) Vulnerability of CA1 neurons in SHRSP hippocampal slices to ischaemia and its protection by Ca<sup>2+</sup> channel blockers. Brain Research, 642, 146-152.

Yin, H.Z., Turetsky, D., Choi, D.W., Weiss, J.H. (1994) Cortical neurons with Ca<sup>2+</sup> permeable AMPA/kainite channels display distinct receptor immunoreactivity and are GABAergic. Neurobiology of Disease, 1, 43-49.

Yrjanheikki, J., Keinanen, R., Pellikka, M., Hokfelt, T., Koistinaho, J. (1998) Tetracyclines inhibit microglial activation and are neuroprotective in global brain ischaemia. Proceedings of the National Academy of Sciences of the United States of America, Vol.95, 15769-15774.

Yrjanheikki, J., Tikka, T., Keinänen, R., Goldsteins, G., Chan, P.H., Koistinaho, J. (1999) A tetracycline derivative, minocycline, reduces inflammation and protects against focal cerebral ischaemia with a wide therapeutic window. Proceedings of the National Academy of Sciences of the United States of America, 23, 13496-13500.

Zea-Longa, Z., Weinstein, P.R., Carlson, S., Cummins, R. (1989) Reversible middle cerebral artery occlusion without craniectomy in rats. Stroke, 84-91.

Zeev-Brann, A.B., Lazarov-Spiegler, O., Brenner, T., Schwartz, M. (1998) Differential Effects of Central and Peripheral Nerves on Macrophages and Microglia. Glia, 23, 181-190.

Zhang, R.L., Chopp, M., Jiang, N., Tang, W.X., Probst, J., Manning, A.M., Anderson, D.C. (1995) Anti-Intercellular Adhesion Molecule-1 Antibody reduces Ischemic Cell Damage After Transient But Not Permanent Middle Cerebral Artery Occlusion in the Wistar Rat. Stroke, 26, 1438-1443.

Zhang, R.L., Chopp, M., Li, Y., Zaloga, C., Jiang, M., Jones, M., Miyasaka, M., Ward, P. (1994) Anti-ICAM-1 antibody reduces ischaemic cell damage after transient middle cerebral artery occlusion in the rat. Neurology, 44, 1747-1751.

Zhang, Z., Chopp, M., Powers, C. (1997) Temporal profile of microglial response following transient (2h) middle cerebral artery occlusion. Brain Research, 744, 189-198.

Zivin, J., De Girolami, U., Lyden, P., Kochhar, A., Mazzarella, V., Hemenway, C., Henry, M. (1987) A model for quantitative evaluation of embolic stroke therapy. Brain Research, 435, 305-8.

## Publications

### Abstracts:

Marks, L., Peters, E.E., Gartshore, G., Maxwell, W.L., Macrae, I.M. (1999)

Ultrastructural changes to the cerebrovasculature in two models of cerebral ischaemia. Journal of Cerebral Blood Flow and Metabolism, 19, S728.

Marks, L., Carswell, H.V.O., Peters, E.E., Jafar, I., Graham, D.I., Dominiczak, A.F., Macrae, I.M. (1999) Elevated microglial response to ischaemia in spontaneously hypertensive stroke prone rats (SHRSPs). Journal of Cerebral Blood Flow and Metabolism, 19, S660.

Marks, L., Macrae, I.M., Graham, D.I. (2001) Characterisation of matrix metalloproteinases expression following transient and permanent middle cerebral artery occlusion (MCAO) in rodents. Neuropathology and Applied Neurobiology, 100<sup>th</sup> Meeting of the British Neuropathological Society, abstract booklet, p6.

Peters, E.E., Marks, L., Gartshore, G., Maxwell, W.L., Graham, D.I., Macrae, I.M. (1999). No evidence for significant leukocyte involvement in transient focal ischaemia. Journal of Cerebral Blood Flow and Metabolism, 19, S574.

**Papers:**

Marks, L., Carswell, H.V.O., Peters, E.E., Graham, D.I., Patterson, J., Dominiczak, A.F., Macrae, I.M. Characterisation of the Microglial Response to Cerebral Ischaemia in the Stroke Prone Spontaneously Hypertensive Rat (SHRSP). Accepted by Hypertension, Dec 2000.

Peters, E.E., Marks, L., Gartshore, G., Maxwell, W.L., Graham, D.I., Macrae, I.M. The post ischaemic inflammatory response involves microglia but not neutrophils (in preparation)

Peters, E.E., Marks, L., Gartshore, G., Maxwell, W.L., Graham, D.I., Macrae, I.M. Ultrastructural alterations in the cerebrovasculature following transient focal cerebral ischaemia (in preparation)

## APPENDICES

### Appendix A: Solutions.

#### PVP (Polyvinylpyrrolidone)

25g of PVP in 50mls of sterile saline + 10,000 units of heparin.

Solution was stirred for 2-3 hours and stored at -4°C.

#### 50mM phosphate buffer

For 1L:

38mls of  $\text{Na}_2\text{PO}_4$  + 162mls of  $\text{Na}_2\text{HPO}_4$  + 7.2g NaCl were added to 800mls of  $\text{dH}_2\text{O}$  and the solution mixed and stored at -4°C.

#### 200mM phosphate buffer

For 1L:

190mls of  $\text{NaH}_2\text{PO}_4$  + 810mls of  $\text{Na}_2\text{HPO}_4$  .

#### PAM Fixative (4% paraformaldehyde in 50mM phosphate buffer)

For 1L:

500mls  $\text{dH}_2\text{O}$  heated to 65°C. 40g of paraformaldehyde were added and the solution mixed. A few drops of 1M NaOH were added to aid dissolution. The solution was filtered and 250mls of 200mM phosphate buffer added and the solution made up to 1L with  $\text{dH}_2\text{O}$  and stored at -4°C.

### Karnovsky's Fixative (2% gluteraldehyde, 2% formaldehyde)

For 1L:

400mls of dH<sub>2</sub>O heated to 65°C and 20g paraformaldehyde added. A few drops (2-4) of NaOH were added to aid dissolution. 80mls of gluteraldehyde (25% solution) were added followed by 500mls of 50mM phosphate buffer and 4mls of 0.5% CaCl<sub>2</sub>. The solution was made up to 1L with dH<sub>2</sub>O and pH adjusted to 7.4 and stored at -4°C.

### Cryoprotectant

For 1L:

1.57g of NaH<sub>2</sub>PO<sub>4</sub> + 5.46g Na<sub>2</sub>HPO<sub>4</sub> were dissolved in 400mls dH<sub>2</sub>O. 300mls glycerin and 300mls ethylene glycol were added to the solution and the solution mixed for 1 hour and stored at -20°C.

### Poly-L-lysine coating of slides

Slides were racked and placed in 10% poly-L-lysine solution for 5 minutes. Slides were then placed into an oven at 40-50°C overnight to dry.

## **Solutions for western blotting**

### Hepes Buffer

For 250mls:

0.2975g of 5mM Hepes

27.38g of 0.32M sucrose

1.2mls of 5mM benzamide

43.75 $\mu$ l of  $\beta$ -mercaptoethanol

0.285g EGTA

0.03075g of  $MgSO_4$

2.5mls of 10 $\mu$ M sodium vandate

200 $\mu$ l of 0.1mM phenylmethyl-sulphonyl fluoride

500 $\mu$ l of Leupeptin

1.25mls Pepstatin A

500 $\mu$ l of Aprotinin.

pH to 8.0.

### Solutions for Lowry assay

2% copper sulphate solution in  $H_2O$ , 2% potassium sodium tartrate in  $H_2O$  and 2% sodium carbonate in 0.1 Molar NaOH.

Mixture A: 500 $\mu$ l copper sulphate + 500 $\mu$ l potassium sodium tartrate + 50mls sodium carbonate.

Folins: 1ml of mix A + 25 $\mu$ l of sample + 100 $\mu$ l Folins. Mix and allow to stand at room temperature for 20-30 minutes.

Standard Curve dilutions: BSA :0.2mg/ml- 20 $\mu$ l H<sub>2</sub>O/5 $\mu$ l BSA.  
0.4mg/ml- 15 $\mu$ l H<sub>2</sub>O/10 $\mu$ l BSA  
0.6mg/ml- 10 $\mu$ l H<sub>2</sub>O/15 $\mu$ l BSA  
0.8mg/ml- 5 $\mu$ l H<sub>2</sub>O/20 $\mu$ l BSA  
1.0mg/ml- 25 $\mu$ l BSA

For samples: 12.5 $\mu$ l of sample + 12.5 $\mu$ l H<sub>2</sub>O.

### Laemmli Buffer

0.1M Tris HCL pH8

0.1% bromophenol blue

5M urea

5% DTT

5% SDS

aliquot and store at -20°C.

### Solution 1 (for resolving gel)

0.75M Tris-base , pH 8.8

0.2% SDS

(per 100mls- 9.1g Tris -base + 0.2g SDS)

store at room temperature

### Solution 2 (for stacking gel)

0.25M Tris-base, pH 6.8

0.2% SDS

(per 100mls- 3.03g Tris-base + 0.2g SDS)

store at room temperature

Resolving gel

6mls Solution 1

4.02 mls acrylamide

1.98 mls distilled water

60 $\mu$ l 10% APS

15 $\mu$ l TEMED

Stacking gel

0.562 mls acrylamide

2.44mls Solution 2

1.94 mls distilled water

50 $\mu$ l 10% APS

10 $\mu$ l TEMED

Running buffer

72g glycine

15g Tris

50 mls SDS

Incubation buffer (T-TBS-M)

TBS + 5% Tween 20 (T-TBS)

+ 5% Marvel (T-TBS-M)

## Appendix B: Paraffin processing

Station Number	Time (Hours)	Temperature (°C)	Solution
1	2	35	70% alcohol
2	3	35	80% alcohol
3	4	35	95% alcohol
4	4	35	100% alcohol 1
5	5	35	100% alcohol 2
6	5	35	100% alcohol 3
7	6	35	100% alcohol 4
8	4	35	100%
9	5	35	alcohol/Xylene
10	5	35	Xylene 1
11	5	60	Xylene 2
12	5	60	Wax 1
13	6	60	Wax 2 Wax 3

Processing carried out using an automated tissue processor.

The process comprises a 60 hour cycle- 59 hours processing + 1 hour turnover.

Pressure and a vacuum are maintained at each stage over the 60 hour cycle.

### Appendix C: Antibody details

Antibody	Target	Tissue	Dilution	Blocker	Secondary	Source
OX-42	Microglia	Fixed, Frozen	1:1000	Normal Horse Serum	Anti-mouse raised in horse	Serotec, Ltd. UK
MRF-1	Microglia	Fixed, Paraffin Processed	1:100	Normal Goat Serum	Anti-rabbit raised in goat	Dr Tanaka Hokkaido Uni, Japan
GFAP	Astrocytes	Fixed, Paraffin Processed	1:1000	Normal Horse Serum	Anti-mouse raised in horse	Sigma Ltd. UK
MMP-9 (AB805)	MMP-9	Fixed, Paraffin Processed	1:100	Normal Goat Serum	Anti-rabbit raised in goat	Chemicon, Ltd, UK
MMP-8 (SE594)	MMP-8	Fixed, Paraffin Processed	1:100	Normal Goat Serum	Anti-rabbit raised in goat	British Biotech, UK
IL-1 $\beta$ (S328)	IL-1 $\beta$	Fixed, Paraffin Processed	1:100	Normal Donkey Serum	Anti sheep raised in donkey	NISBC, UK
Fibrinogen	Fibrinogen	Fixed, Paraffin Processed	1:100	Normal Goat Serum	Anti-rabbit raised in goat	Dako Ltd, UK
Albumin	Albumin	Fixed, Paraffin Processed	1:100	Normal Goat Serum	Anti-rabbit raised in goat	Dako Ltd, UK
Tau-1	Oligo- dendrocytes	Fixed, Paraffin Processed	1:1000	Normal Horse Serum	Anti-mouse raised in horse	Dr S Hanger University of London

